State of Florida
Department of Transportation
BE702 Final Report

July 2021

National Center for Asphalt Technology
NCAT
at AUBURN UNIVERSITY

Design and Performance of Open-Graded Friction Course (OGFC) Mixtures Containing Epoxy Asphalt

ncat.us

Design and Performance of Open-Graded Friction Course (OGFC) Mixtures Containing Epoxy Asphalt

FDOT Contract No. BE702

Final Report

Submitted to

Florida Department of Transportation

By

National Center for Asphalt Technology
Auburn University

July 2021

DISCLAIMER

This research was performed in cooperation with the Florida Department of Transportation (FDOT) and the Federal Highway Administration (FHWA). The opinions, findings, and conclusions expressed in this publication are those of the authors and not necessarily those of the State of Florida Department of Transportation.

TECHNICAL REPORT DOCUMENTATION PAGE

<table>
<tr><td colspan="2">1. Report No.
N/A</td><td>2. Government Accession No.
N/A</td><td colspan="2">3. Recipient's Catalog No.
N/A</td></tr>
<tr><td colspan="3" rowspan="2">4. Title and Subtitle
Design and Performance of Open-Graded Friction Course (OGFC) Mixtures Containing Epoxy Asphalt</td><td colspan="2">5. Report Date
July 2021</td></tr>
<tr><td colspan="2">6. Performing Organization Code
N/A</td></tr>
<tr><td colspan="3">7. Author(s)
Fan Yin, Anurag Anand, Raquel Moraes, Nam Tran, Randy West, Fan Gu</td><td colspan="2">8. Performing Organization Report No.
N/A</td></tr>
<tr><td colspan="3" rowspan="2">9. Performing Organization Name and Address
National Center for Asphalt Technology
277 Technology Parkway
Auburn, AL 36830</td><td colspan="2">10. Work Unit No.
N/A</td></tr>
<tr><td colspan="2">11. Contract or Grant No.
BE702</td></tr>
<tr><td colspan="3" rowspan="2">12. Sponsoring Agency Name and Address
Florida Department of Transportation
605 Suwannee Street, MS 30
Tallahassee, FL 32399</td><td colspan="2">13. Type of Report and Period Covered
Final Report
February 2019 – July 2021</td></tr>
<tr><td colspan="2">14. Sponsoring Agency Code
N/A</td></tr>
<tr><td colspan="5">15. Supplementary Notes
N/A</td></tr>
<tr><td colspan="5">16. Abstract
The objective of this study was to determine the viability of using epoxy-modified asphalt (EMA) to improve the long-term durability and life span of open-graded friction course (OGFC) mixtures in Florida. To that end, a comprehensive literature review and laboratory experimental plan were conducted. The laboratory test procedure combining the storage stability test and Soxhlet asphalt extraction as well as the fluorescence microscopy were effective in evaluating the chemical compatibility of EMA binders. Low-dosage epoxy modification showed an overall stiffening effect on the base asphalt binders, but its improvement in their rheological properties was not as pronounced as styrene-butadiene-styrene modification. EMA OGFC mixtures showed improved raveling resistance and durability as the epoxy dosage rate (EDR) increased between 15% and 40%. Based on the results, 30% was recommended as the optimum EDR regarding material cost and mixture performance properties. After extended long-term aging, the EMA mixtures at 30% EDR and HP mixtures showed significantly better raveling resistance and durability than the PMA mixtures. All OGFC mixtures had acceptable Tensile Strength Ratio (TSR) test results regardless of the type of asphalt binder used. Two EMA mixtures exhibited high severity stripping failures in the Hamburg Wheel Tracking Test (HWTT), which was possibly due to of the lack of cohesive strength of the not fully cured EMA binder. Performance testing of dense-graded asphalt mixtures containing different types of artificial RAP materials suggested that EMA OGFC mixtures could be successfully recycled as RAP into new asphalt mixtures. Finally, recommendations for future research and implementation activities are provided.</td></tr>
<tr><td colspan="3">17. Key Words
Open-graded friction course, epoxy-modified asphalt, polymer-modified asphalt, chemical compatibility, rheology characterization, FC-5 mix design, raveling resistance, durability, mixture performance testing, recyclability</td><td colspan="2">18. Distribution Statement
No restrictions</td></tr>
<tr><td>19. Security Classification (of this report)
Unclassified</td><td>20. Security Classification (of this page)
Unclassified</td><td>21. No. of Pages
180</td><td colspan="2">22. Price
N/A</td></tr>
</table>

Form DOT F 1700.7 (8-72) Reproduction of completed page authorized

ACKNOWLEDGEMENTS

This project was conducted in cooperation with FDOT and FHWA. The authors would like to express their gratitude to FDOT project manager Ahmad Chami and members of the FDOT project committee: Howard Moseley, Bouzid Choubane, Greg Sholar, and Wayne Rilko. The authors would also like to acknowledge the material suppliers, including but not limited to: ChemCo Systems, Inc., Taiyu Kensetsu Co., Ltd., Gardner Asphalt, Associated Asphalt, Hunt Refining, CWR Contracting, Anderson Columbia, Martin Marietta Materials, Midsouth Aggregates, and White Rock Quarries. Finally, acknowledgements extend to Nathan Moore, Pamela Turner, Adam Taylor, Jason Moore, Vickie Adams, Aung Moe, and Mariah Langan of the National Center for Asphalt Technology (NCAT) for their assistance with the laboratory-related activities.

EXECUTIVE SUMMARY

The Florida Department of Transportation (FDOT) requires open-graded friction course (OGFC) on all multilane roadways where the design speed is 50 mph or higher, except for curb and gutter areas. Over the last two decades, the performance of Florida's OGFC mixtures has greatly improved due to the use of polymer-modified asphalt (PMA). However, these mixtures are still prone to raveling and last five years less on average than dense-graded friction courses. Therefore, FDOT is constantly looking for innovative technologies to reduce the raveling of OGFC mixtures. One such technology is epoxy-modified asphalt (EMA), which claims to have superior aging resistance to oxidative aging and mix embrittlement. Over the last few years, low-dosage EMA has been successfully used in OGFC and stone matrix asphalt (SMA) mixtures as a cost-effective alternative to traditional PMA binders in New Zealand and the Netherlands.

The objective of this study was to determine the viability of using EMA to improve the long-term durability and life span of OGFC mixtures in Florida. To that end, a comprehensive literature review was conducted to synthesize existing studies on the state-of-the-practice on use of OGFC, OGFC mix design and performance testing, performance characterization of EMA binders and mixtures, and production and construction of EMA mixtures. Furthermore, informal communications with asphalt researchers, epoxy material suppliers, and international agency and industry representatives were made to gather information about their experiences with the design, production, and performance of OGFC mixtures containing EMA binders.

Based on the information collected, a systematic experimental plan was developed and executed to explore the use of EMA for OGFC applications. The experimental plan consisted of five supplementary laboratory experiments. Experiment 1 was to select suitable asphalt binders for epoxy modification based on the chemical compatibility evaluation of EMA binders. Experiment 2 was to determine the optimum epoxy dosage rate (EDR) with respect to material cost and OGFC performance properties. Experiment 3 focused on developing a method of designing OGFC mixtures containing EMA binders. Experiment 4 was to characterize the performance properties of OGFC mixtures prepared with EMA *versus* PG 76-22 PMA and high polymer (HP) binders. Finally, Experiment 5 aimed at the recyclability evaluation of EMA OGFC mixtures for use as reclaimed asphalt pavements (RAP) in dense-graded asphalt mixtures.

Major findings of the study are summarized as follows:

- The laboratory test procedure combining the storage stability test and Soxhlet asphalt extraction, as well as the fluorescence microscopy, were effective in qualitatively and quantitatively evaluating the compatibility of EMA binders prepared with different sources of epoxy materials and base binders. A reasonable correlation was observed between the saturates, aromatics, resins and asphaltenes (SARA) fractions of the base binders and the chemical compatibility of the resultant EMA binders. Among the four base binders, binders Z and C were found the most suitable for modification with the epoxy materials from a foreign source and domestic source, respectively.
- The rotational viscosity test was effective in characterizing the curing behavior of EMA binders. As temperature increased, the viscosity of EMA binders decreased, and the time required to achieve a fully cured stage became shorter. Epoxy modification had an overall stiffening effect on the performance grades of the base binders. In most cases, the EMA

binders at 15% and 25% EDRs had better Multiple Stress Creep Recovery (MSCR) test results in terms of creep compliance and percentage recovery than the base binders, but the improvement due to epoxy modification was not as pronounced as with styrene-butadiene-styrene (SBS) modification. The Linear Amplitude Sweep (LAS) test results indicated that the HP and PMA binders had better fatigue resistance than the base and EMA binders. Based on the Glover-Rowe (*G-R*) aging index results, the HP and low-dosage EMA binders were most resistant to oxidative aging in PAV, followed by the PMA binder, and then the unmodified base binders. Finally, it was found that epoxy and SBS modification could significantly affect the shape of the master curve of asphalt binders, decreasing its slope and altering the time-dependency of the material response in a specific frequency range.

- The Binder Bond Strength (BBS) test results indicated that the type and chemical characteristics of the aggregates greatly affected the bond strength of PMA, HP, and EMA binders. The asphalt-aggregate systems with the least susceptibility to moisture damage were the "HP + GRN1" and "U15C + GRN2" combinations.
- As the EDR increased between 15% and 40%, the EMA OGFC mixtures had reduced Cantabro loss, increased indirect tensile (IDT) strength, and increased IDT fracture energy (G_f) results, indicating improved raveling resistance, tensile strength, and fracture resistance. Furthermore, the U-EMA mixtures (i.e., EMA mixtures prepared with the base binder C and epoxy materials from a domestic source) exhibited the best aging resistance, followed by the J-EMA mixtures (i.e., EMA mixtures prepared with the base binder Z and epoxy materials from a foreign source), and then the PMA mixtures. Based on these results, 30% was selected as the most cost-effective EDR for OGFC applications. At this EDR, the estimated material cost of EMA OGFC mixtures is approximately 3.5 to 5 times higher than those containing a PG 76-22 PMA binder.
- A mix design procedure for designing OGFC mixtures containing EMA binders at 30% EDR was developed. This procedure is essentially consistent with FDOT's current practice for mix design approval of OGFC mixtures containing a PMA or HP binder but requires additional pie plate and Cantabro testing of the EMA OGFC mixture. The procedure was successfully validated with four FDOT-approved FC-5 mix designs and has the potential of designing EMA OGFC mixtures with adequate raveling resistance before aging and minimal potential for asphalt draindown during production.
- Overall, OGFC mixtures prepared with the HP binder had the best Cantabro test results and thus, are expected to have the best raveling resistance at both the short-term aging and extended long-term aging conditions (i.e., compacted specimen aging for 20 days at 85°C). In most cases, the EMA mixtures at 30% EDR and HP mixtures had similar Cantabro loss values after extended long-term aging, which were significantly lower than those of the PMA mixtures. These results highlight the potential of using HP or EMA binders in improving the long-term raveling resistance and extending the life span of OGFC mixtures in Florida.
- The IDT and Tensile Strength Ratio (TSR) results indicated that the EMA mixtures had enhanced tensile strength and fracture resistance over the PMA and HP mixtures, but all the mixtures showed acceptable moisture resistance regardless of the type of asphalt binder. Different from the other mixtures, the U-EMA mixtures had considerably higher wet strength than dry strength in the TSR test. This increase in the tensile strength is

likely attributable to the accelerated curing of the EMA binder when the mixture was conditioned in a 60°C water bath for moisture conditioning.

- The Hamburg Wheel Tracking Test (HWTT) results of OGFC mixtures were highly dependent on the FC-5 mix design and type of asphalt binder used. All mixtures prepared with the GRN1 and LMS mix designs had acceptable HWTT results with minimum rutting and no signs of stripping. For the GRN2 and GRN3 mix designs, the J-EMA mixtures had the best HWTT results in terms of rutting resistance and moisture resistance. The PMA and HP mixtures prepared with the GRN2 mix design showed low to medium severity stripping failures, while the U-EMA mixtures prepared with both the GRN2 and GRN3 mix designs exhibited early, high severity stripping failures. It is speculated that the U-EMA mixtures exhibited early failure in HWTT when tested at the short-term aging condition because the EMA binder was still at the early stage of its curing process and had not gained sufficient cohesive strength to resist the severe condition of HWTT.
- Solvent extraction using trichloroethylene was not effective in extracting asphalt binders from the laboratory-aged artificial RAP materials prepared with EMA OGFC mixtures at 30% EDR. Therefore, the cured EMA binders could not be accurately tested for performance grading because of the solvent extraction issues.
- Dense-graded FC-12.5 and SP-12.5 asphalt mixtures prepared with different types of artificial RAP materials containing PMA, HP, J-EMA, and U-EMA binders had similar HWTT and Indirect Tensile Asphalt Cracking Test (IDEAL-CT) results and thus, are expected to have equivalent rutting resistance and intermediate-temperature cracking resistance. These results seem to suggest that EMA OGFC mixtures, upon reaching their service lives, could be successfully recycled as RAP into new asphalt mixtures.

Based on the test results and findings of this study, it is recommended that FDOT conduct a heavy vehicle simulator (HVS) experiment to evaluate the post-compaction curing behavior of U-EMA OGFC mixtures prepared with the GRN2 and GRN3 mix designs. It is also suggested that FDOT construct a field demonstration project to identify the challenges, if any, associated with the production and construction of EMA OGFC mixtures. Finally, future research on field-to-laboratory aging correlation analysis, life-cycle cost analysis, and additional HWTT testing of OGFC mixtures is recommended.

TABLE OF CONTENTS

LIST OF FIGURES

LIST OF TABLES

LIST OF ACRONYMS

ARB	Asphalt Rubber Binder
ATR	Attenuated Total Reflectance
BBR	Bending Beam Rheometer
BBS	Binder Bond Strength
BPT	British Pendulum Tester
BYET	Binder Yield Energy Test
CAI	Cantabro Aging Index
CAPTIF	Canterbury Accelerated Pavement Testing Indoor Facility
CII	Colloidal Instability Index
COV	Coefficient of Variation
CT_{index}	Cracking Tolerance Index
DCT	Disc-shaped Compact Tension
DFT	Dynamic Friction Tester
DSC	Differential Scanning Calorimetry
DSR	Dynamic Shear Rheometer
E'	Storage Modulus
EDR	Epoxy Dosage Rage
EMA	Epoxy-modified Asphalt
FDOT	Florida Department of Transportation
FHWA	Federal Highway Administration
FI	Flexibility Index
FTIR	Fourier Transform Infrared
|G*|	Complex Modulus
G_f	Fracture Energy
G-R	Glover-Rowe
GRN	Granite
HP	High Polymer
HVS	Heavy Vehicle Simulator
HWTT	Hamburg Wheel Tracking Test
IDEAL-CT	Indirect Tensile Asphalt Cracking Test
IDT	Indirect Tensile
I-FIT	Illinois Flexibility Index Test
IP	Institute of Petroleum
JAA	Japanese Asphalt Association
JMF	Job Mix Formula

J_{nr}	Non-recoverable Creep Compliance
LAS	Linear Amplitude Sweep
LMS	Limestone
LTA	Long-term Aging
LTPP	Long-Term Pavement Performance
LVDT	Linear Variable Differential Transformer
MSCR	Multiple Stress Creep Recovery
NCAT	National Center for Asphalt Technology
N_{design}	Design Gyration Level
N_f	Number of Cycles to Failure
NMAS	Nominal Maximum Aggregate Size
NTZA	New Zealand Transport Agency
OBC	Optimum Binder Content
OECD	Organization of Economic Cooperation and Development
OGFC	Open-graded Friction Course
OT	Overlay Test
PA	Porous Asphalt
PAV	Pressure Aging Vessel
PEM	Permeable European Mix
PFC	Porous Friction Course
PG	Performance Grade
PMA	Polymer-modified Asphalt
POTS	Pull-off Tensile Strength
PWT	Pine Wheel Tester
RAP	Reclaimed Asphalt Pavements
RTFO	Rolling Thin Film Oven
SARA	Saturates, Aromatics, Resins, and Asphaltenes
SBS	Styrene-Butadiene-Styrene
SCB	Semi-Circular Bending
SGC	Superpave Gyratory Compactor
SIP	Stripping Inflection Point
SMA	Stone Matrix Asphalt
SST	Superpave Shear Tester
STA	Short-term Aging
TCE	Trichloroethylene
T_g	Glass-transition Temperature

TSR	Tensile Strength Ratio
TSRST	Thermal Restrained Specimen Test
UV	Ultraviolet
VCA	Voids in Coarse Aggregate
VMA	Voids in Mineral Aggregate
δ	Phase Angle
σ	Tensile Strength

CHAPTER 1. INTRODUCTION

1.1 Background

Open-graded friction course (OGFC) is a special asphalt surface layer that provides significant safety and environmental benefits, including reduced risk of hydroplaning, reduced splash and spray from vehicle tires, and improved visibility. OGFC has been widely used by state highway agencies in the southeast United States. The Florida Department of Transportation (FDOT) requires OGFC on all multi-lane roadways where the design speed is 50 mph or greater, except for curb and gutter areas. Over the last two decades, the performance of Florida's OGFC (or FC-5) mixtures has been improved by using polymer-modified asphalt binders. However, these mixtures are still prone to raveling and last five years less on average than dense-graded friction courses. It has been reported that FDOT spends an average of $67 million annually on the OGFC resurfacing program. Thus, the agency is constantly looking for new technologies to reduce the raveling of OGFC mixtures.

Epoxy-modified asphalt (EMA) binder is a premium asphalt material that is modified with thermosetting polymers. Compared to asphalt binders containing thermoplastic elastomers, EMA binder has better thermal stability, rigidity, and resistance to deformation. The real breakthrough of EMA binder is its superior resistance to oxidative aging and embrittlement, which are two major contributors to the raveling of OGFC mixtures, among other factors. Therefore, EMA binder has a potential to improve the long-term durability and extend the life span of OGFC mixtures. Over the last few years, low-dosage EMA binders have been successfully used in OGFC and stone matrix asphalt (SMA) mixtures in New Zealand and the Netherlands (Herrington et al., 2007; Herrington, 2010; Wu et al., 2017; Zegard et al., 2019). Field trials of EMA OGFC mixtures in New Zealand have been performing well. However, it remains unknown whether EMA binders can be successfully used in OGFC mixtures with Florida materials and conditions.

1.2 Objectives

The overall objective of this study was to determine the viability of using EMA binders to improve the durability and life span of OGFC mixtures in Florida. Specifically, this study sought to (1) select the optimum EDR for asphalt binder modification with respect to material cost and mixture performance properties, (2) develop an effective mix design procedure for OGFC mixtures containing EMA binders, (3) characterize the performance properties of OGFC mixtures with EMA binders and SBS-modified asphalt binders, and (4) assess the recyclability of EMA OGFC mixtures as reclaimed asphalt pavements (RAP) for use in dense-graded asphalt mixtures.

1.3 Research Approach

Figure 1 illustrates the research approach that was followed to accomplish the objectives of the study. First, a thorough literature review was conducted to synthesize existing studies on EMA binders and mixtures. Review topics of special interests were the comparisons in laboratory test results and field performance of OGFC mixtures containing EMA binders *versus* unmodified, SBS-modified, and rubber-modified binders. The literature review also included mix design procedures and laboratory conditioning and performance testing of OGFC mixtures. In addition,

informal communications with asphalt researchers, epoxy material suppliers, and international agency and industry representatives were made to gather information about their experiences with the design, production, and performance of OGFC mixtures containing EMA binders.

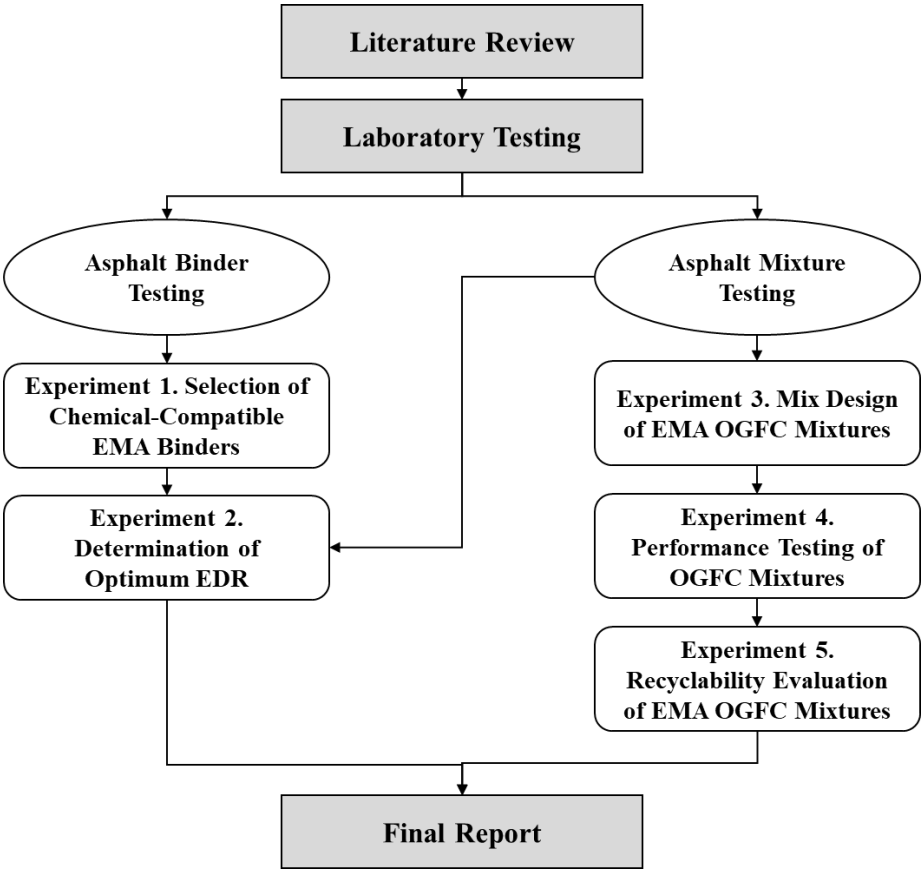

Figure 1. Graphical Illustration of Research Approach

Based on information collected from the literature review, a comprehensive experimental plan was developed and executed, which included five supplementary laboratory experiments. Experiment 1 was to screen base asphalt binders from different sources for epoxy modification. A laboratory test procedure combining the storage stability test and Soxhlet asphalt extraction test was conducted to evaluate the colloidal stability of EMA binders prepared with different sources of epoxy materials and base binders. Furthermore, fluorescent microscopy analysis was performed to characterize the chemical compatibility of EMA binders and quantify the network formation of epoxy resin in the modified binder. For each source of epoxy materials, the base binder that yielded the most chemically compatible EMA binders was selected for further evaluation in the study.

The objective of Experiment 2 was to determine the optimum EDR with respect to material cost and mixture performance properties. This experiment consisted of two sub-experiments focusing on binder performance testing and mixture performance testing, respectively. The binder testing experiment sought to evaluate the curing behavior, aging characteristics, rheological properties, cohesive and adhesive properties, and moisture susceptibility of EMA binders. Because of the thermosetting behavior of EMA binders at high EDRs, the traditional Superpave asphalt binder

tests using the Rotational Viscometer, Dynamic Shear Rheometer (DSR), and Bending Beam Rheometer (BBR) were conducted on EMA binders at 15% and 25% EDRs only to avoid the risk of damaging the test devices. Data analysis was conducted to determine if the low-dosage EMA binders had enhanced rheological properties over a PG 76-22 polymer-modified asphalt (PMA) binder and a high polymer (HP) binder as control. The mixture testing experiment focused on evaluating the raveling resistance, tensile strength, and fracture resistance of OGFC mixtures containing EMA binders at various EDRs *versus* a PG 76-22 PMA binder using the Cantabro and Indirect Tensile (IDT) tests. Both tests were conducted under three mix aging conditions to account for the impact of asphalt aging on the mixture performance properties. Finally, the optimum (i.e., most cost-effective) EDR was selected based on the Cantabro and IDT test results as well as the material cost of OGFC mixtures with EMA binders at various EDRs.

Experiment 3 was to determine an effective method of designing OGFC mixtures containing EMA binders. Following FDOT's current mix design procedure for FC-5 mixtures containing PMA or HP binders, a similar procedure was proposed to design EMA OGFC mixtures based on the pie plate and Cantabro tests. Several modifications to the pie plate test procedure in FM 5-588 were made to accommodate the curing and thermosetting behavior of EMA binders at the optimum EDR determined in Experiment 2. The proposed mix design procedure was preliminarily validated with EMA OGFC mixtures prepared with four FDOT approved FC-5 mix designs.

Experiment 4 focused on the performance characterization of OGFC mixtures containing EMA binders at the optimum EDR *versus* PMA and HP binders. Four FC-5 mix designs were included, which corresponded to three sources of granite and one source of limestone. The Cantabro, IDT, modified Tensile Strength Ratio (TSR), and Hamburg Wheel Tracking Test (HWTT) tests were conducted to evaluate the raveling resistance, tensile strength, fracture resistance, moisture resistance, and rutting resistance of OGFC mixtures prepared with different types of asphalt binders. Test results were analyzed to determine if the use of EMA binders could improve the long-term durability and extend the life span of OGFC mixtures in Florida.

Experiment 5 was to evaluate the recyclability of EMA OGFC mixtures as RAP in dense-graded asphalt mixtures. Four sets of heavily aged artificial RAP materials were prepared in the laboratory using OGFC mixtures containing two EMA binders, one PMA binder, and one HP binder. Attempts were made to extract and recover asphalt binder from the EMA RAP materials but were not totally successful. Two sets of dense-graded mixtures (one friction course and one structural course) were prepared using the four artificial RAP materials and tested in the HWTT and Indirect Tensile Asphalt Cracking Test (IDEAL-CT) to evaluate their rutting resistance and intermediate-temperature cracking resistance, respectively. Performance diagram analysis was conducted to determine the effects of different artificial RAP materials on the performance properties of dense-graded asphalt mixtures as an indirect approach of assessing the recyclability of OGFC mixtures containing EMA binders *versus* PMA and HP binders as RAP.

Finally, this report was prepared to summarize the test results, key findings, and conclusions of the study as well as to provide recommendations for future research and implementation of research findings.

1.4 Organization of the Report

This report consists of eight chapters. Chapter 1 provides a description of the background, objectives, and research approach of the study. Chapter 2 summarizes the literature review findings on topics of state-of-the-practice on use of OGFC, OGFC mix design and performance testing, characterization of EMA binders and mixtures, and production and construction of EMA mixtures. Chapters 3 through 7 present detailed discussions of the experimental plan, test results, and findings of the five laboratory experiments discussed above. Finally, Chapter 8 summarizes the key findings and conclusions of this study and provides recommendations for future research and implementation.

CHAPTER 2. LITERATURE REVIEW

This chapter summarizes the literature review on the topics of state-of-the-practice on use of OGFC, OGFC mix design and performance testing, EMA binders and mixtures, and production and construction of EMA mixtures. The following sections provide detailed discussions on each topic followed by a summary of key literature review findings.

2.1 State of the Practice on Use of OGFC

OGFC is a gap-graded asphalt mixture that contains a high percentage of air voids (typically between 15% and 22%) (Alvarez et al., 2006). It is also known as Permeable European Mix (PEM), Porous Friction Course (PFC), and Porous Asphalt (PA), which has been widely used in Europe, Asia, and the United States for decades (Alvarez et al., 2011). OGFC is usually paved as the final riding surface on roadways because of the safety and environmental benefits associated with this mixture. Despite the benefits, the use of OGFC has diminished over the years mainly due to durability and service life issues. The durability issues are generally evidenced by raveling, and once the distress begins, it progresses rapidly (Watson et al., 1998). A survey of state highway agencies conducted in 1998 showed that 22 states had discontinued use of OGFC (Kandhal and Mallick, 1998). A more recent survey conducted in 2015 showed that only half of the 41 responding agencies were using OGFC (Watson et al., 2018). As shown in Figure 2, most of the agencies using OGFC are in the southeast and western United States. For example, FDOT requires OGFC mixtures on all multi-lane roadways where the design speed is 50 mph or greater, except for curb and gutter areas. The 2015 survey also revealed that agencies not using OGFC were concerned about the durability and cost-effectiveness of OGFC mixtures.

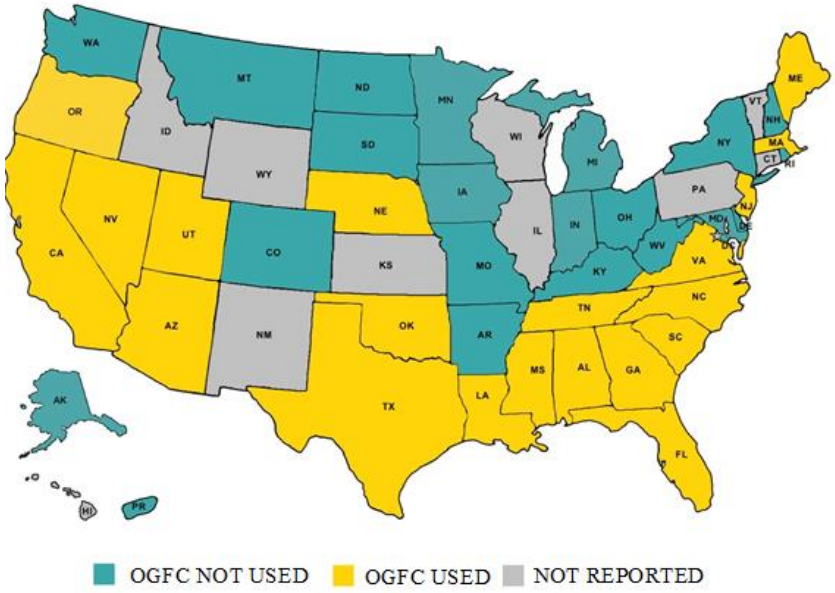

Figure 2. Use of OGFC Mixtures by State Highway Agencies in 2015 (Watson et al., 2018)

The safety and environmental benefits of OGFC have been documented in many studies. Regarding safety, one of the obvious abilities of OGFC mixtures is to channel water through the pavement structure. The reduction in water standing or flowing across the pavement surface during wet weather is a significant improvement over the performance of dense-graded pavement

surfaces (Chen et al., 2017; Geng et al., 2017; Chen et al., 2018). Thereby, the use of OGFC as a surface layer is effective in improving the friction resistance of the pavement in wet weather, reducing splash and spray from surrounding vehicles, reducing glare from on-coming headlights during rainy conditions, and enhancing the visibility of pavement markings. Because of these safety benefits, OGFC has been shown to lower wet weather vehicle crashes or accident rates and reduce the economic costs of accidents. Shimeno and Tanaka (2010) conducted a traffic study in Japan and found that OGFC significantly reduced the fatality rate in rainy weather by 4.6% when compared to conventional dense-graded pavement surfaces. Hernandez-Saenz et al. (2016) reported that these safety-related benefits were the main reason for using OGFC in the United States. However, some studies challenged that the safety effectiveness of OGFC was limited and inconclusive (Elvik and Greibe, 2005; Buddhavarapu et al., 2015). These studies claimed that the road user usually drives faster on OGFC surfaced pavements, which could result in a higher accident rate as compared to conventional dense-graded pavements.

In terms of environmental benefits, OGFC has been found effective in reducing the tire/pavement noise and improving the water runoff quality. The majority of highway noise comes from the pavement-tire interaction, especially when the traffic speed is above 45 mph. The noise can become an annoyance to human beings, which leads to negative impacts on the quality of life. It can also have an economic impact on real estate by keeping properties from being developed or sold (Donavan, 2007). Because of its high interconnected air void content, OGFC acts as a resonant cavity structure that efficiently absorbs sound energy generated from the tire-pavement interface. Existing studies showed that the use of OGFC reduces the tire/pavement noise by 3 to 6 dBA, which is equivalent to diminishing the traffic volume by 50% or comparable to the construction of a noise barrier wall (Bernhard and Wayson, 2004). Due to the noise reduction benefit, OGFC has been used as a strategic means of meeting environmental noise regulations in Europe. In addition, a few studies pointed out that the water runoff generated from OGFC surface was of better quality than that from conventional dense-graded pavement surfaces (Barrett, 2008; Roseen et al., 2012). According to these studies, the water runoff from OGFC had a significant lower concentration of total suspended solids, total metals, and phosphorus. This benefit of OGFC is attributed to the reduction of splash and spray that reduces the amount of pollutants derived from the bottoms of vehicles, as well as a large number of pores in the surface layer that are able to retain these pollutants.

Despite the safety and environmental benefits, the use of OGFC is also associated with several shortcomings, such as its high material cost. The material cost of OGFC mixtures is usually 20% to 40% higher than that of conventional dense-graded asphalt mixtures. Winter maintenance is another issue for OGFC pavements. Compared to conventional dense-graded pavements, OGFC pavements have earlier and more frequent frost and ice formations due to their low thermal conductivity caused by the porous void structure (Partl et al., 2010). To maintain a desirable ride quality in winter, OGFC pavements typically require more deicing agents and more frequent maintenance activities, resulting in an increase in pavement maintenance cost. In addition, OGFC mixtures are often associated with poor long-term performance or durability issues. As compared to dense-graded mixtures, OGFC mixtures are more susceptible to raveling due to oxidation of the binder, which results in a reduced service life for OGFC pavements.

2.2 OGFC Mix Design and Performance Testing

In 1974, the Federal Highway Administration (FHWA) developed an OGFC mix design procedure, but it was less than satisfactory (Watson et al. 2003). As a result, state highway agencies continued using a wide variety of mix design methods to design OGFC, which led to inconsistency in the reported field performance of the friction courses. In 1999, NCAT recommended a new-generation OGFC mix design procedure based on existing research studies, field performance of in-place OGFC pavements in Georgia, and experience in Europe (Kandhal and Mallick 1999). Later on, ASTM D7064 and AASHTO PP 77 documented the standard practice for OGFC materials selection and mix design. These two standards are slightly different in terms of materials selection and performance criteria. FDOT specifies OGFC (FC-5) mix design under Section 337 of the Standard Specifications for Road and Bridge Construction, where the optimum binder content is determined using the pie-plate method per Florida Method of Test FM 5-588. In general, OGFC mix design requires three parts: selecting suitable materials, selecting a well-designed gradation, and determining the optimum binder content.

Selection of Suitable Materials[1]

OGFC mixtures typically consist of aggregates, asphalt binders, stabilizing agents (i.e., fibers), and anti-stripping agents. A detailed description of the selection of these materials is presented as follows.

Aggregates

In the United States, the most commonly used aggregate types are granite, limestone, gravel, and sandstone. Some state highway agencies also allow the use of traprock, steel slag, and blast furnace slag for OGFC mixtures. The aggregate characteristics typically considered for OGFC mix design include durability, polish resistance, angularity, shape, cleanliness, abrasion resistance, and absorption. Table 1 summarizes the requirements of these aggregate characteristics in the existing mix designs for OGFC. FDOT allows four types of coarse aggregates for use in FC-5 mixtures, which are granite, granite gneiss, limestones having a minimum of 12% residue from the acid insoluble test, FM 5-510, and shell rock.

Asphalt Binders

Although unmodified asphalt binders had been used in OGFC mixtures for many years, the use of modified binders has become more prevalent since these binders are more effective in preventing asphalt draindown and improving the durability of OGFC mixtures. In the United States, the most commonly used binder modifiers for OGFC mixtures are styrene-butadiene-styrene (SBS) polymer and rubber (e.g., crumb rubber modifier and ground tire rubber). These modifiers provide a stiffer asphalt binder for OGFC mixtures, which leads to increased cohesion in aggregate stone skeleton. For this reason, OGFC mixtures with polymer or rubber modified binders usually have higher resistances to rutting, cracking, and raveling damage, and exhibit better durability in the field. Table 2 presents the requirements of different state highway agencies for the use of asphalt binders in OGFC mixtures.

[1] Reprinted with revisions from a previous NCAT study by Watson et al. (2018).

Table 1. Aggregate Requirements for OGFC Mix Designs

Test Description	Method	ASTM 7064	AASHTO PP 77	FDOT
Coarse Aggregate				
Los Angeles Abrasion, % Loss	AASHTO T 96	Max 30	Max 30	Max 45
Flat or Elongated, % (5 to 1)	ASTM D 4791	Max 10	Max 10	Max 10
Sodium Sulfate	AASHTO T 104	-	Max 10	Max 12
Magnesium Sulfate		-	Max 15	-
Uncompacted Voids	AASHTO T 326	-	Min 45	-
Fine Aggregate				
Sodium Sulfate	AASHTO T 104	-	Max 10	-
Magnesium Sulfate		-	Max 15	-
Uncompacted Voids	AASHTO T 304	Min 40	Min 45	-
Sand Equivalent	AASHTO T 176	Min 45	Min 50	-

Table 2. Requirements of Asphalt Binders Used in OGFC Mixtures

State	Asphalt Binder Requirement
Florida	PG 76-22 PMA, HP, PG 76-22 asphalt rubber binder (ARB)
Alabama	PG 76-22
Arizona	PG 64-16
California	PG 58-34, PG 64-16 (rubber modified)
Mississippi	PG 76-22
New Jersey	PG 64E-22, PG 64-22R, PG 58-28R
New Mexico	PG 70-28
North Carolina	PG 76-22, PG 64-22
South Carolina	PG 76-22
Texas	PG 76-XX (low temperature found in Superpave PG procedure)
Virginia	PG 70-28

Stabilizing Agents

Stabilizing additives are often used to improve the durability of OGFC mixtures by preventing asphalt draindown and by increasing mixture tensile strength. When draindown occurs during the production and transportation of OGFC mixtures, part of the mixture has a reduced asphalt content, which reduces its durability and resistance to premature raveling or cracking distresses (Cooley et al., 2009). The asphalt that drained from part of the mixture can saturate another part of the mixture resulting in flushed areas on the pavement. FDOT recommends using either cellulose or mineral fiber as stabilizing additive, which is typically added at a rate of 0.2 to 0.5 percent by total weight of the mixture.

Anti-stripping Agents

Anti-stripping agents are recommended for use in OGFC mixtures to improve the bond between aggregates and asphalt binders and mixture resistance to moisture damage. Anti-stripping agents commonly used in FDOT OGFC mixtures are hydrated lime and liquid anti-stripping agents.

Selection of Design Gradation[2]

With suitable materials selected, trial gradations with initial asphalt contents should then be established. The rules of thumb for the gradation design are to establish a coarse aggregate skeleton with stone-on-stone contact and ensure high interconnected air voids content. Currently, there is no nationally accepted gradation band for OGFC mixtures in the United States. Table 3 lists the aggregate gradations for OGFC mixtures that are specified by different state highway agencies. As shown, these agencies primarily use a 12.5 to 19.0 mm maximum aggregate size with the majority of aggregates occurring between the 9.5 mm sieve and the 4.75 mm sieve. To achieve an open gradation, OGFC mixtures typically have less amount of fine aggregates than conventional dense-graded mixtures.

Table 3. Aggregate Gradations for OGFC Mixtures Specified by Highway Agencies

State	Sieve Size							
	19 mm	12.5 mm	9.5 mm	4.75 mm	2.36 mm	1.18 mm	0.6 mm	0.075 mm
FL	100	85-100	55-75	15-25	5-10	-	-	2-5
AL	100	85-100	55-65	10-25	5-10	-	-	2-4
GA 1	-	100	85-100	20-40	5-10	-	-	2-4
GA 2	100	85-100	55-75	15-25	5-10	-	-	2-4
GA 3	100	80-100	35-60	10-25	5-10	-	-	1-4
LA 1	-	100	90-100	25-50	5-15	-	-	2-5
LA 2	100	85-100	55-75	10-25	5-10	-	-	2-4
MS	-	100	80-100	15-30	10-20	-	-	2-5
NC	-	100	75-100	25-45	5-15	-	-	1-3
SC	100	85-100	55-75	15-25	5-10	-	-	0-4
TN	100	85-100	55-75	10-25	5-10	-	-	2-4
TX 1	100	80-100	35-60	1-20	1-10	-	-	1-4
TX 2	100	95-100	50-80	0-8	0-4	-	-	0-4

Determination of Optimum Binder Content

Once the design gradation is selected, the optimum binder content (OBC) is determined. In this step, three or four trial asphalt binder contents are selected with a 0.5 percent increment above and below the initial asphalt content. There are three approaches to determine the OBC of OGFC mixtures: absorption calculation, visual determination, and compacted specimen evaluation.

- The absorption calculation method utilizes the oil absorption capacity and the apparent specific gravity of aggregates to empirically estimate the OBC of OGFC mixtures. One limitation of this method is that it fails to consider the influence of binder type and aggregate type; thus, it cannot always ensure the satisfactory field performance of OGFC mixtures.
- The visual determination method is often referred to as to the pie-plate or Pyrex bowl test, which is adopted by FDOT as FM 5-588. In this method, approximately 1,200 g of uncompacted OGFC mixture is placed in a glass pie plate. The plate is then placed in an over for one hour at 160°C. After that, the pie plate is allowed to cool at room temperature. Finally, the plate is inverted for visual inspection of the bottom surface. The

[2] Reprinted with revisions from a previous NCAT study by Watson et al. (2018).

asphalt content that displays sufficient bonding between the mixture and the bottom of the plate without evidence of excessive asphalt draindown is considered the OBC. A limitation of this method is that the visual determination can be subjective and requires an experienced technician to judge the results. To overcome this limitation, Pernia et al. (2016) employed an image analysis technique to quantitatively determine the OBC of OGFC mixtures.

- The compacted specimen evaluation method directly targets the performance of OGFC mixtures to determine the OBC. A set of specimens are compacted with either 50 gyrations using a Superpave gyratory compactor (SGC) or 50 blows per each side using a Marshall compactor. The following properties of the compacted specimens are then evaluated:
    - Air voids and permeability to ensure mixture permeability;
    - Voids in coarse aggregate (VCA) of the dry-rodded aggregate (VCADRC) and VCA of the mix (VCAMIX) to ensure stone-on-stone contact;
    - Cantabro loss to evaluate mixture durability; and
    - TSR to evaluate mixture moisture susceptibility.
    - Additionally, asphalt draindown test (ASTM D6390) is often conducted on an uncompacted OGFC sample to evaluate its draindown potential during mix design and field production.

Table 4 summarizes three sets of performance test criteria for determining the OBC of OGFC mixtures (Kandhal, 2002). In general, these criteria are in good agreement with each other. Compared to the absorption calculation and visual determination methods, the compacted specimen evaluation method is considered a better approach to selecting the OBC because it provides assessments of the performance concerns of OGFC mixtures. However, this method still cannot always ensure the satisfactory field performance of designed OGFC mixtures. Several studies reported that OGFC mixtures designed with the compacted specimen evaluation method still had premature distresses including raveling, shoving, and excessive rutting (Gu et al. 2018; Watson et al. 2018). Therefore, these studies recommended that other engineering properties such as cracking resistance and rutting resistance should also be addressed in the OGFC mix design method.

Table 4. Optimum Asphalt Content Properties for OGFC Mixes

Mix Property	NCHRP 640	ASTM D7064	NAPA Series 115
Air Voids (%)	18 – 22	≥18	≥18
Unaged Cantabro Loss (%)	≤15.0	≤20.0	≤20.0
VCA_{MIX} (%)	$<VCA_{DRC}$	$\leq VCA_{DRC}$	$\leq VCA_{DRC}$
Tensile Strength Ratio	≥0.70	≥0.80	≥0.80
Draindown at Production Temperature (%)	≤0.30	≤0.30	≤0.30
Permeability (m/day)	100	100	100

Performance Testing of OGFC Mixtures

Watson et al. (2018) developed a balanced mix design approach for designing OGFC mixtures, which requires the use of performance tests to assess mixture permeability, durability, cracking,

and cohesiveness of asphalt mixtures. Each of the performance tests selected are elaborated as follows.

Permeability Test

The permeability of OGFC specimens is tested according to FM 5-565, Florida Method of Test for Measurement of Water Permeability of Compacted Asphalt Paving Mixtures. The falling head permeability apparatus for 15-cm specimens is used to determine the coefficient of permeability (k). For conditioning, the specimens are submerged in a container and allowed to soak a minimum of one hour prior to testing. Equation 1 is used to calculate the permeability of OGFC specimens.

$$k = \frac{aL}{At} ln\left(\frac{h_1}{h_2}\right) \quad \text{Equation 1}$$

Where,

k = coefficient of permeability (cm/s);
a = inside cross-sectional area of the standpipe (cm^2);
L = lift thickness of asphalt mixture;
A = base area of the permeameter (cm^2);
t = elapsed time between h1 and h2 (s);
h_1 = initial head (cm); and
h_2 = final head (cm).

Cantabro Test

The Cantabro test is used to determine the durability of OGFC mixtures. ASTM D7064 allows the use of either unaged specimens or specimens aged for seven days at 60°C. During testing, the OGFC specimens are individually placed in the Los Angeles Abrasion machine and tested for 300 revolutions at a rate of 30 to 33 revolutions per minute. The loose material is discarded, and the final specimen weight is recorded. The percent mass loss is calculated for each specimen using Equation 2. According to ASTM D7064, the maximum acceptable amount of mass loss is 20% for unaged specimens and 30% for aged specimens.

$$CL = \frac{A - B}{A} * 100 \quad \text{Equation 2}$$

Where,

CL = Cantabro Loss, %;
A = Initial weight of test specimen; and
B = Final weight of test specimen.

Tensile Strength Ratio Test

TSR is defined as the ratio of the tensile strength of water-conditioned specimens to the tensile strength of unconditioned specimens, which is shown in Equation 3.

$$TSR = \frac{S_2}{S_1} * 100 \quad \text{Equation 3}$$

Where,

S_1 = the average tensile strength of unconditioned specimen; and
S_2 = the average tensile strength of conditioned specimen.

To accommodate OGFC mixtures, the AASHTO T 283 test procedure is modified in terms of specimen preparation and conditioning. In the modified procedure, the OGFC specimens are compacted to the design gyration level (N_{design}) instead of the target height (i.e., 95 mm). The specimens are saturated at 660.4 mm Hg below atmospheric pressure for 10 minutes and then frozen in plastic concrete cylinder molds. The specimens are kept submerged under water while freezing to keep the interior voids filled with water. Specimens are then conditioned in a hot water bath at 60°C for 24 hours and then put in a 25°C water bath according to AASHTO T 283 prior to breaking. Finally, the specimens are tested for indirect tensile strength at a rate of 51 mm per minute. The tensile strength of the mixture is determined by using the peak load recorded on the device and the specimen dimensions.

Hamburg Wheel Tracking Test

HWTT per AASHTO T 324 is used to determine the rutting resistance and moisture susceptibility of compacted asphalt mixtures. The test is normally used to evaluate dense-graded mixtures. For OGFC mixtures, the specimens should be compacted to an air void content consistent with the in-place air void content of the layer in the field. The specimens are submerged and conditioned in a 50°C water bath for 30 minutes prior to testing. The water bath maintains a constant temperature for the duration of the test (20,000 passes). All data output of the linear variable differential transformer (LVDT) attached to each arm is recorded by a computer and analyzed to determine the total rut depth and stripping inflection point (SIP) of the mixture. There is currently no nationally accepted criterion for the maximum allowable HWTT rut depth. Watson et al. (2018) recommended the following criteria based on the virgin binder grade:

- PG 64 or lower, no less than 10,000 passes before reaching 12.5-mm rut depth;
- PG 70, no less than 15,000 passes before reaching 12.5-mm rut depth; and
- PG 76 or higher, no less than 20,000 passes before reaching 12.5-mm rut depth.

Illinois Flexibility Index Test

The Illinois Flexibility Index Test (I-FIT) is used to discriminate asphalt mixtures with different cracking potentials at an intermediate test temperature (Al-Qadi et al., 2015). Each 150-mm diameter, 61-mm thick specimen is first cut in half to create two semi-circular specimens, and a notch is then cut along the axis of symmetry at 15 mm in depth and 1.5 mm in width. A monotonic load is applied along the vertical radius of the specimen with a constant displacement rate of 50 mm/min. Most research with the I-FIT has been conducted at 25°C. The flexibility index (FI), defined as the fracture energy divided by the slope at the inflection point of the post peak load *versus* displacement curve (Equation 4 and Equation 5), is used to evaluate the load-related cracking resistance of OGFC mixtures.

$$G_f = \frac{W_f}{A} = \frac{\int (P) d(\Delta)}{A} \quad \text{Equation 4}$$

$$FI = \frac{G_f}{|m|} \times 0.01 \quad \text{Equation 5}$$

Where,

G_f = fracture energy;
W_f = work of fracture;
P = vertical load;
Δ = load-line displacement;
A = specimen ligament area; and
m = slope at the inflection point of the post-peak load *versus* displacement curve.

Indirect Tensile Asphalt Cracking Test

Another cracking test that can potentially be used to evaluate the intermediate-temperature load-related cracking resistance of OGFC mixtures is the IDEAL-CT per ASTM D8225-19. The test was developed by Zhou et al. (2017) and has gained great popularity among several state highway agencies and the asphalt industry due to its simplicity, practicality, and ease of implementation. The test is similar to the I-FIT test except for the testing of cylinder specimens instead of notched semi-circular specimens. As shown in Figure 3(a), during the test, a monotonic load is applied along a cylinder specimen at a constant displacement rate of 50 mm/min. The most commonly used test temperature is 25°C. For data analysis, the load-displacement curve is analyzed to determine the work of fracture, which refers to the total area under the curve, and the slope of the curve at 25% reduction from the peak load. The cracking parameter CT_{Index} is then calculated by dividing the work of fracture by the slope [Figure 3(b)]. Asphalt mixtures with better resistance to cracking are expected to have a higher CT_{Index} value than those that are more susceptible to cracking.

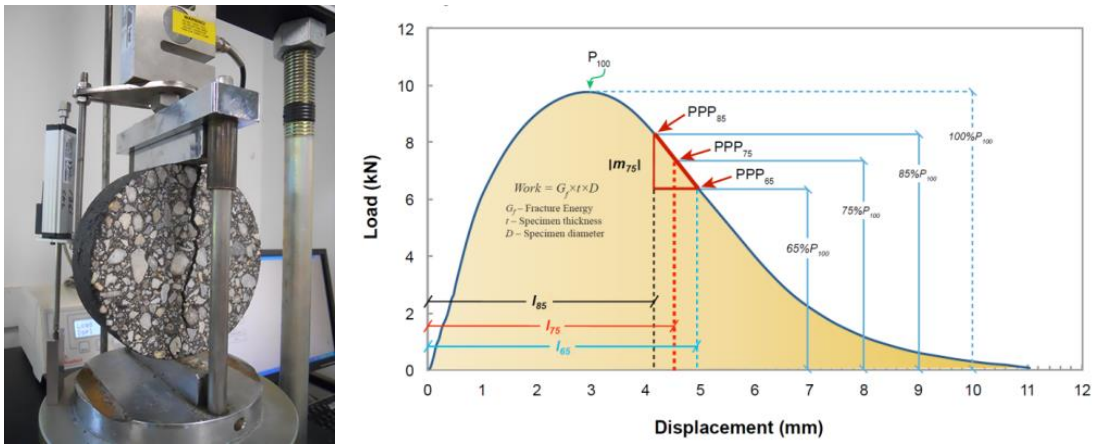

(a) (b)

Figure 3. Indirect Tensile Asphalt Cracking Test: (a) Test Device, (b) Data Analysis (Zhou et al., 2017)

The applicability and suitability of the above-mentioned performance tests (except the IDEAL-CT) and criteria were determined through evaluation of six OGFC mixtures with known good and poor performance in the field. Watson et al. (2018) found that the air voids content of OGFC mixtures was directly related to their permeability and recommended a minimum permeability rate of 50 meters per day and a design air void content range of 15 to 20%. The Cantabro test proved to be a good indicator of mixture durability and resistance to raveling, and a maximum mass loss of 20% was recommended for unconditioned OGFC specimens. The indirect tensile

strength test, based on a modified version of AASHTO T 283, was identified as a good indicator of mixture cohesiveness. The peak load of the I-FIT test was shown to be a good measure of resistance to cracking. Finally, the study concluded that higher P200 contents (percent passing the No. 200 sieve) improved the durability of OGFC mixtures with high air voids, high Cantabro loss, and low tensile strength.

2.3 Epoxy-modified Asphalt (EMA) Binders

Epoxy Resin for Asphalt Modification

A few research studies have shown that the properties of asphalt binders can be significantly improved by adding epoxy resins (i.e., thermosetting polymers) (Youtcheff et al., 2006; Cong et al., 2011; Cong et al., 2016). Thermosetting polymers are produced by blending two components, one containing a resin and the other a hardener (i.e., curing agent). The process of curing an epoxy resin converts the initially low molecular weight resin into its thermoset form, which is a space network or three-dimensional chemical structure. The prefix "thermo" implies that the cross-linking proceeds through the influence of heat energy input, and "setting" indicates that an irreversible reaction has occurred on a macro scale (Peng and Riedl, 1995). The term "epoxy resin" refers to both the uncured and the cured forms of the resin.

Epoxy groups are characterized by reactivity towards both nucleophilic and electrophilic species and are receptive to a wide range of curing agents. Curing agents may be either catalysts or hardeners. An exothermic curing reaction (i.e., chemical reaction that releases energy through heat) can be induced at room or elevated temperatures or, in the presence of appropriate catalysts, can be initiated by ultraviolet (UV) radiation. Therefore, the specific curing procedure required to produce a cured epoxy resin of optimized performance characteristics depends on the precise combination of resin, curing agent and/or catalyst (Hodd, 1989). Compared with thermoplastic elastomers, epoxy resins have (Massingill and Bauer, 2000):

- Excellent chemical resistance, particularly to alkaline environments;
- Outstanding adhesion to a variety of substrates;
- Very high tensile, compressive, and flexural strengths;
- Low shrinkage on cure;
- Excellent electrical insulation properties and retention thereof on aging or exposure to difficult environments;
- Remarkable resistance to corrosion;
- A high degree of resistance to physical abuse;
- Ability to cure over a wide range of temperatures; and
- Superior fatigue strength.

On the other hand, epoxy resins are more expensive and harder to process, thus limiting their use in asphalt modification. Since the cost of EMA binder can be two to four times more expensive than traditional polymer-modified asphalt binders, a cost-effective solution to reduce the material cost is to dilute EMA binder with unmodified asphalt binders, and the dilution process is depicted in Figure 4.

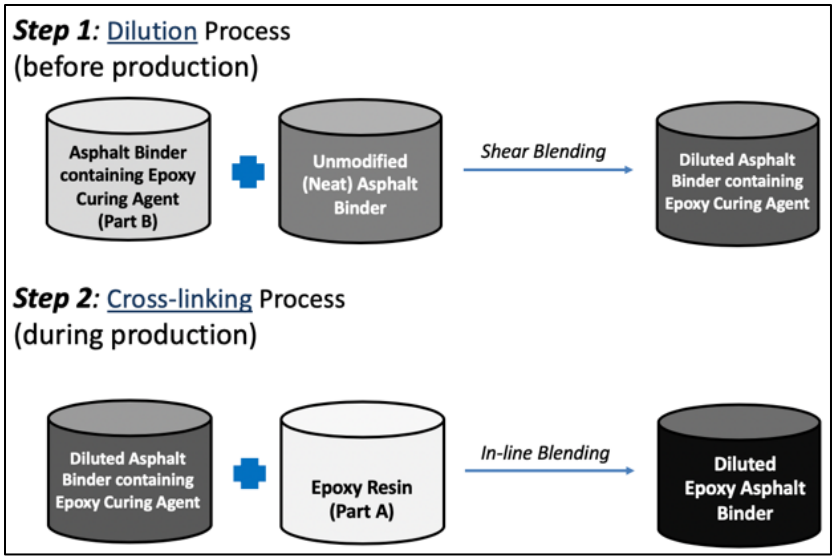

Figure 4. Diluted EMA Binder Preparation Process

The epoxide resins are characterized by having more than one 1,2-epoxy group (Figure 5) per molecule. The three-membered epoxy ring is reactive to many substances by a rearrangement polymerization type of reaction.

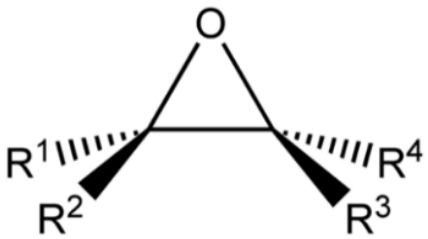

Figure 5. Structure of the Epoxide Group

Epoxy asphalt is a two-phase chemical system in which the continuous phase is a liquid epoxy resin (i.e., Part A) and the discontinuous phase is a blend of asphalt binder and epoxy curing agent (i.e., Part B). Usually, the liquid epoxy resin is obtained when either bisphenol-A or bisphenol-F and epichlorohydrin are combined in a chemical reaction producing diglycidyl ether of bisphenol (Figure 6). As for curing agents, polyamides and polyamines are often used. When added to the binder, the epoxide rings in the asphalt binder system react with long chain hardener components to form dense flexible crosslinks that block nucleophilic sites where asphalt oxidation occurs (McGraw, 2018). Regarding the mechanisms of interaction between EMA binders and mineral aggregates, the epoxy resin during the polymerization reaction is capable of forming covalent bonds with silicon monoxide (Si-O) molecules on the surface of silicon oxide containing aggregates, which are highly resistant to UV exposure and stripping. Furthermore, one of many advantages of epoxy asphalt is the absence of solvent, which makes the EMA binder 100% non-volatile.

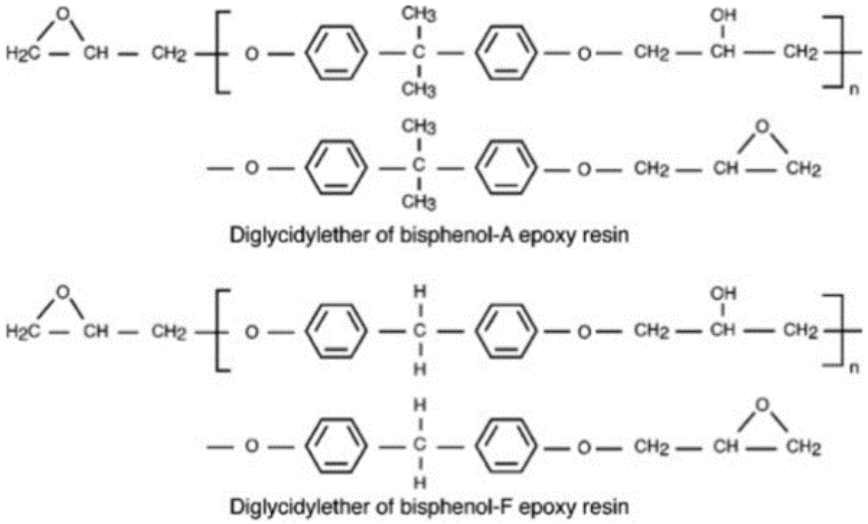

Figure 6. Diglycidyl Ether of Bisphenol-A and Diglycidyl Ether of Bisphenol-F Epoxy Resin

Some manufacturers that produce epoxy resin for asphalt modification provide the epoxy resin and the curing agent as separate components, while others provide the epoxy resin and a blend of asphalt binder with epoxy curing agent. Figure 7 shows two EMA samples from one domestic source and one foreign source. The domestic epoxy materials [Figure 7(a)] are produced with an acid-based epoxy curing agent and have an EDR, as defined in Equation 6, of approximately 40%. Table 5 presents the recommended component proportions of EMA binders produced with an amine-based epoxy curing agent [Figure 7(b)]. Regardless of the manufacturer selected, when the Part A and Part B of epoxy materials are fully blended with asphalt binder, the EMA binder will behave more like a modified thermosetting polymer rather than asphalt (Dinnen, 1991).

$$Epoxy\ Dosage\ Rate = \frac{Epoxy\ Resin + Curing\ Agent}{Epoxy\ Resin + Curing\ Agent + Asphalt\ Binder} \qquad \text{Equation 6}$$

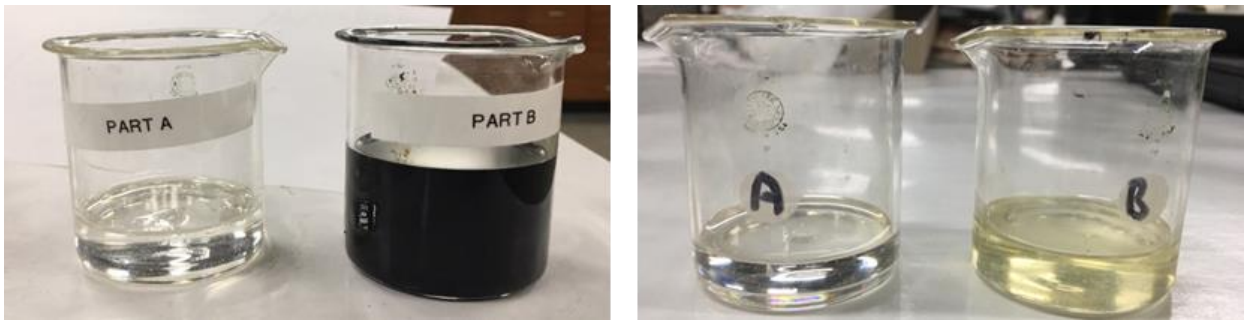

(a) (b)

Figure 7. Epoxy Material Samples from Two Different Sources: (a) Domestic Source – *Part A:* Liquid Epoxy Resin, *Part B:* Blend of Asphalt Binder and Curing Agent, (b) Foreign Source – *Part A:* Liquid Epoxy Resin, *Part B:* Curing Agent

Table 5. Recommended Component Proportions of EMA Binders Prepared with Epoxy Materials from a Foreign Source

Application	Component Proportion (% weight)			Epoxy Dosage Rate
	Epoxy Resin	Curing Agent	Asphalt Binder	
SMA	12.2	7.8	80	20%
Airfield Pavement	18.3	11.7	70	30%
OGFC	24.4	15.6	60	40%
Steel Bridge Deck	30.5	19.5	50	50%

Chemical and Rheological Evaluation of EMA Binders

Table 6 presents a list of laboratory tests that have been used to investigate the chemistry and rheology of EMA binders. The description of the most common used tests is included as follows.

Table 6. Testing Procedures to Investigate Chemistry and Rheology of EMA Binders

Property	Test Type	Research Parameter	Reference
Curing Behavior	Rotational Viscometer Softening Point	Viscosity Melting temperature	Cong et al., 2019; Xu et al., 2018; Motamedi et al., 2017; Cong et al., 2016.
Compatibility	Storage Stability	Polymer separation	Cong et al., 2016; Motamedi et al., 2017.
Morphology	Fluorescence Microscopy Atomic Force Microscopy	Network formation Microstructure characteristics	Apostolidis et al. 2019; Cong et al., 2019; Xu et al., 2018; Cong et al., 2016; Wei and Zhang, 2012.
Cohesive and Adhesive Properties	Binder Bond Strength	Pull-off tensile strength	Youtcheff et al., 2005.
Chemical Characterization	Differential Scanning Calorimetry FTIR Spectroscopy	Glass-transition temperature Structural functions	Apostolidis et al. 2019; Cong et al., 2019; Apostolidis et al., 2018; Xu et al., 2018; Motamedi et al., 2017; Xin et al., 2016; Wei and Zhang, 2012; Herrington and Alabaster, 2008.
Rheological Characterization	Dynamic Shear Rheometer Dynamic Mechanical Analysis	$\lvert G^* \rvert$, δ, J_{nr}, N_f, Yield Energy Storage modulus (E') and loss factor (tan δ)	Apostolidis et al. 2019; Zegard et al., 2019; Apostolidis et al., 2018; Holleran et al., 2017; Motamedi et al., 2017; Cong et al., 2015; Kang et al., 2015; Youtcheff et al., 2006.
Oxidative Aging	Rolling Thin Film Oven Pressure Aging Vessel	Rheological performance after aging	Apostolidis et al. 2019; Zegard et al., 2019.

<u>Curing Behavior of EMA Binders</u>

The effect of viscosity on the workability of asphalt binders is important for selection of proper mixing and compacting temperatures. Unlike thermoplastic asphalt, EMA binder is a

thermosetting material. Because the epoxy resin is cross-linked chemically (i.e., irreversibly), it cannot be melted or placed in solution for analysis and characterization. Thus, when the two components in a thermosetting binder are mixed, there is limited "shelf life" for the material. The amount of time available with the workable binder depends on the material temperature and the curing rate of the epoxy resin. The curing behavior of epoxy binders is most commonly evaluated with a simple viscosity test. Studies have shown that the viscosity of an EMA binder increases during curing, and both temperature and epoxy resin content of the EMA binder affect the viscosity and curing behavior of the modified asphalt (Xu et al., 2018; Cong et al., 2019). Cong et al. (2016) showed that asphalt content has a significant effect on the viscosity of an EMA binder. As can be seen in Figure 8(a), in the initial stage of curing, the viscosity of the EMA binder increases as the epoxy resin dosage rate is decreased. The initial viscosities are 120, 170, 198, 200, and 210 mPa·s for the EMA binders containing 45, 55, 65, 75, and 85% by weight of asphalt, respectively. As the curing process continues, the viscosity increases rapidly with higher epoxy resin dosage rates. The effect of temperature on the viscosity of an EMA binder is illustrated in Figure 8(b). At the start of the curing process, higher temperatures lower the viscosity of EMA binders, but the viscosity increases rapidly for 10 to 40 minutes and ultimately the higher temperatures drive the rate of curing, causing a higher viscosity.

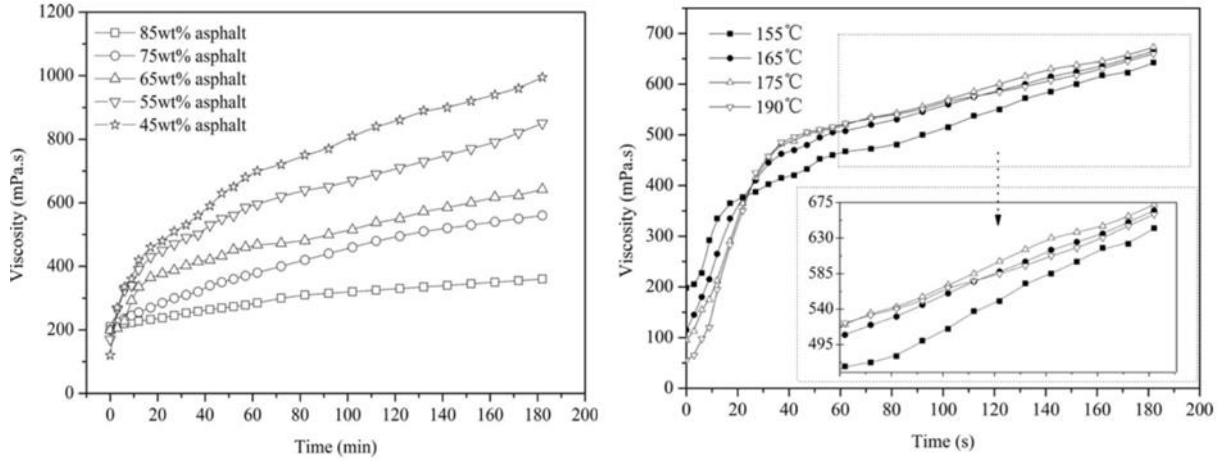

(a) (b)

Figure 8. (a) Effect of Epoxy Dosage Rate on the Viscosity of EMA Binders at 165°C: (b) Effect of Temperature on the Viscosity of EMA binders containing 65% by Weight of Asphalt (Cong et al., 2016)

Compatibility of EMA Binders

Blends of asphalt with polymers form multiphase systems. Because of the lack of compatibility of some modifiers with asphalt, once the modifier is dispersed into the asphalt phase, the resultant modified asphalt binder will undergo phase separation when the binder is stored. As a result, the properties of the modified asphalt binders depend on the concentration and type of polymer used for modification. A key behavior of polymer modification is, therefore, the formation of a thermodynamically unstable but kinetically stable mixture. To investigate the compatibility between epoxy resins and asphalt binders, researchers have used different storage stability (aluminum tube) testing procedures (Cong et al., 2016; Motamedi et al., 2017). Cong et al. (2011) used a combination of storage test and Soxhlet extraction to evaluate the compatibility

of EMA binders. In this adapted procedure, a measured quantity of EMA binder is placed in a sealed aluminum tube and then conditioned in a vertical position for eight hours at 120°C. After static heat conditioning, the binder is allowed to cure at room temperature. At the end of the conditioning period, the top and bottom portions of the aluminum tube are separated and subjected to further testing to determine the degree of separation. After this first step, the Soxhlet asphalt extraction test per ASTM C613M is conducted, where the binders are weighed and the asphaltic fraction is removed by means of Soxhlet extraction. The extracted residue is then dried and weighed. If epoxy resin is present in the residue, the two components are separated by filtering the residue. The relative difference (i.e., gravimetric difference) in percent residue between the top and bottom portions of the sample is then used as an indication of the chemical compatibility (phase separation) of EMA binders.

Morphology of EMA Binders

Fluorescence microscopy is capable of investigating heterogeneous surfaces where the components have different UV light excitation responses. It is the most used technique for assessing the status of dispersion of a polymer in a PMA binder. This technique has often been used to analyze the epoxy resin distribution in asphalt binder samples (Wei and Zhang, 2012; Cong et al., 2016; Xu et al., 2018; Cong et al., 2019). Figure 9 shows the morphology of two EMA binders (with an epoxy dosage rate of 8%) made with epoxies from two different sources prepared by NCAT under a UV microscope. As can be seen, the fluorescence micrographs showed that the epoxy resin from a foreign source [Figure 9(b)] was more uniformly dispersed in the asphalt binder than the epoxy resin from a domestic source [Figure 9(a)]. Nevertheless, there was no localized agglomeration of epoxy resin in either of the EMA binders, which indicates a good compatibility between the two epoxy resins and the base asphalt binder used.

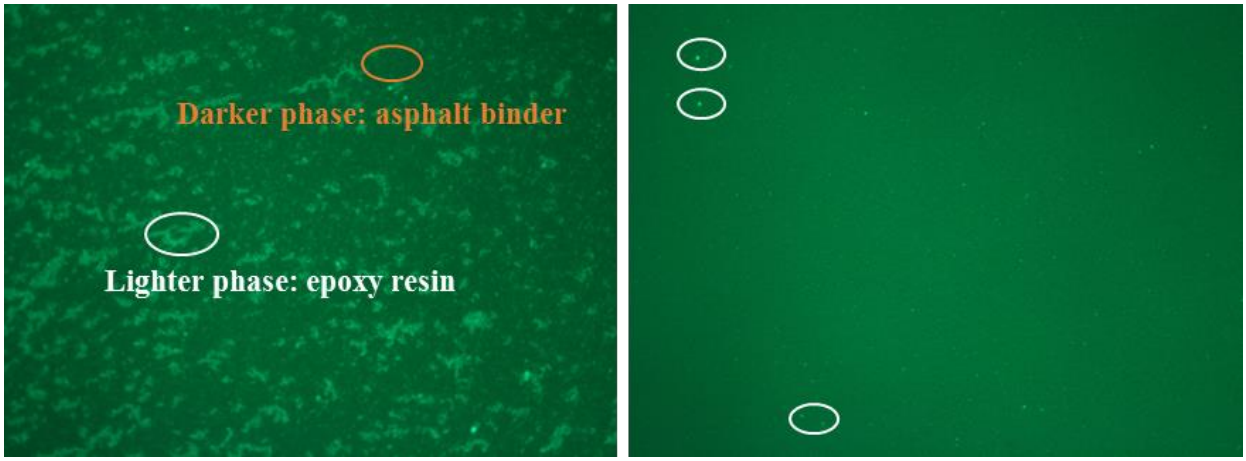

(a) (b)

Figure 9. Fluorescent Micrograph of Two EMA Binders: (a) Using Epoxy Resin and Curing Agent from a Domestic Source, (b) Using Epoxy Resin and Curing Agent from a Foreign Source

Cohesive and Adhesive Properties of EMA Binders

Epoxies are a popular material used in adhesives and bonding. Volatile-free curing and small shrinkage, combined with excellent shear strength, make epoxies a premier adhesive (Peng and Riedl, 1995). Thus, its incorporation in asphalt binders should result in asphalts with higher bond

strength. Regarding flexible pavements, cohesive failure happens due to the rupture of bonds between molecules in the asphalt film. On the other hand, adhesive failure happens due to rupture of bonds between molecules of different phases (i.e., asphalt film and aggregate surface). Youtcheff et al. (2005) used a pull-off tensile strength test [Figure 10(a)] to evaluate the development of the cohesive strength of EMA binders. As can be seen in Figure 10(b), the cohesive strength of EMA binders increases with curing time and temperature until it becomes constant, indicating that the material is fully cured.

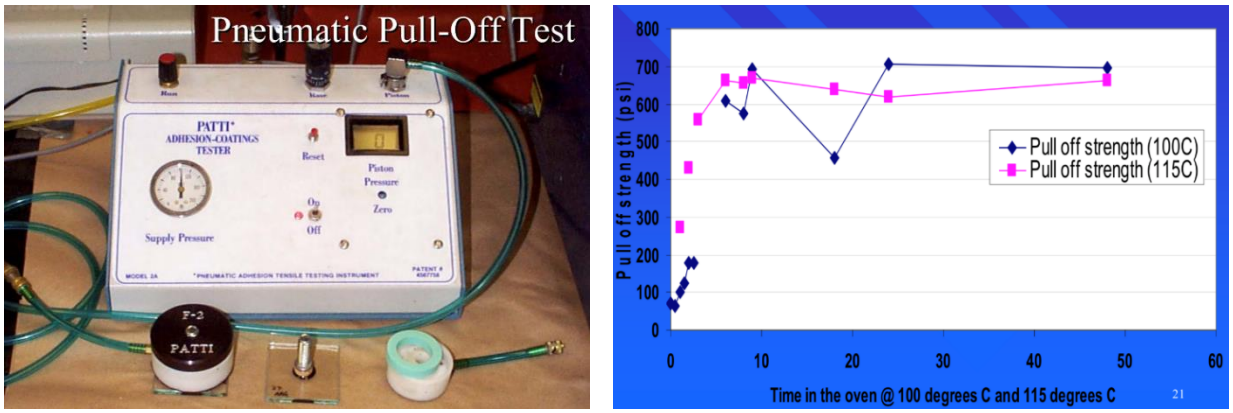

(a) (b)

Figure 10. Push-off Tensile Strength Test: (a) Test Device, (b) EMA Binder Curing Behavior (Youtcheff et al., 2005)

Chemical Characterization of EMA Binders

For chemical evaluation, two techniques are widely reported for investigation of the effect of epoxy resin on the thermal response and chemical composition of asphalt binders. An explanation of each technique is described below.

- Differential Scanning Calorimetry (DSC): In this technique, the difference in the amount of heat required to increase the temperature of a sample and a reference material are measured as a function of temperature. DSC has been used to measure the glass-transition temperature (T_g) of EMA binders (Xin et al., 2016; Motamedi et al., 2017). The T_g has been considered a characterization parameter that can determine the process and aging level of asphalts (Moraes and Bahia, 2015). The T_g depends on the asphalt source and the degree of aging, since complex arrangements of molecules are formed (Turner et al., 1997). The transition to glassy behavior is known to increase the brittleness of the binder extensively, reducing the potential for stress relaxation, increasing stiffness, and therefore result in higher cracking susceptibility. There are speculations in the asphalt community that the T_g of asphalt is responsible for low-temperature cracking of the mix (Marasteanu et al., 2007). Motamedi et al. (2017) reported that reduction in the T_g was observed when epoxy resin was incorporated to asphalt binders.
- Fourier Transform Infrared (FTIR) Spectroscopy: When infrared radiation is passed through a sample, some radiation is absorbed by the sample and some passes through (i.e., is transmitted). The resulting signal at the detector is a spectrum representing a molecular ‘fingerprint’ of the sample. The usefulness of infrared spectroscopy arises because different chemical structures (molecules) produce different spectral fingerprints. This technique has been applied to asphalt binder for characterization of chemical

composition and aging susceptibility, for detection of impurities, and for studying polymer modification (Jennings et al., 1980). Studies have shown that changes in peak intensity of the epoxy group obtained with FTIR can be used to investigate the curing process of EMA binders (Herrington and Alabaster, 2008; Cong et al., 2019). Furthermore, Wei and Zhang (2012) successfully used FTIR by attenuated total reflectance (ATR) to track the functional group changes of EMA binders at different curing times. Also using FTIR-ATR, Apostolidis et al. (2019) observed a decrease in the aging susceptibility of asphalt binder after modification with epoxy resin, especially at higher dosage rates.

Rheology of EMA Binders

Due to the thermosetting polymer nature of the epoxy resin, conventional Superpave rheological test methods may not be suitable to classify the properties of fully cured EMA binders with an epoxy dosage rate of 30% and above. Therefore, researchers have been implementing different approaches to investigate the rheological behavior of EMA binders.

With a DSR and a set of torsion bar fixtures, Youtcheff et al. (2006) applied very low levels of strain using a frequency sweep over the range of 0.1 to 100 rad/s and seven testing temperatures (i.e., 16, 22, 28, 34, 58, 64, and 70°C). The data were used to produce a master curve using the principle of time-temperature superposition at reference temperature of 28°C. The samples for the test were prefabricated using a BBR mold, then cut into two such that rectangular sample bars for the DSR torsion tests were obtained measuring 6.3 x 12 x 50 mm in dimension. Three research parameters were utilized for evaluation of the rheological behavior of EMA binders at different aging conditions: complex modulus ($|G^*|$), phase angle (δ), and $|G^*|/\sin(\delta)$. The authors reported that two recognizable rheological changes were observed for the EMA binder: the first was observed after one week, and the second after four weeks due to the initial and final cure of the resin, respectively. In the aging interval between four and sixteen weeks, the EMA binder showed no rheological change.

Using conventional geometry in the DSR, Holleran et al. (2017) evaluated the mechanical behavior of an EMA binder at a very low epoxy resin dosage rate (i.e., 7% to 8% epoxy resin in the final binder) by means of the Multiple Stress Creep Recovery (MSCR, AASHTO M 332) test, Linear Amplitude Sweep test (LAS, AASHTO TP 101), and Binder Yield Energy Test (BYET, AASHTO TP 123). The results were compared to those of PMA binders prepared with thermoplastic polymers. The MSCR %R results indicated the lack of elasticity of the diluted EMA binder. In both the BYET and LAS tests, the PMA binders exhibited rheological properties that indicate better resistance to cracking and raveling in comparison to the EMA binder with a low dosage rate of epoxy resin. An explanation of each test can be seen below.

- MSCR Test: Regarding the importance of the MSCR test for PMAs, it is well-established that the integrity of some polymer systems can be highly temperature dependent, meaning that although a certain polymer or polymer concentration may provide adequate performance within a certain climatic zone, it may be eliminated from usage consideration because it is tested at significantly higher temperature than that climatic temperature (Moraes et al., 2017). Therefore, a positive attribute of the AASHTO T 350 test method is that tests are conducted at the high pavement temperature for the climatic zone of the project and adjustments for traffic volume and speed are made by lowering

the maximum non-recoverable creep compliance (J_{nr}) limit. Furthermore, testing at higher temperatures can better differentiate between modified binders with respect to the interaction between the polymer and the base binder. Regarding field validation, it has been shown that the J_{nr} parameter has a better correlation to the rutting resistance of polymer-modified asphalts in comparison to the |G*|/sin(δ) parameter (Figure 11).

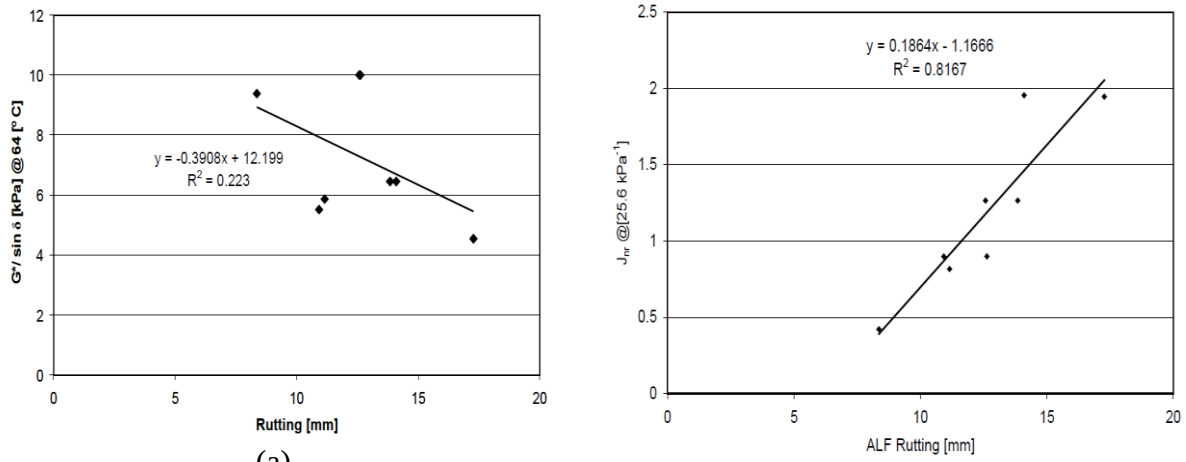

(a) (b)

Figure 11. Correlations of J_{nr} and |G*|/sin(δ) to Field Rutting Performance: (a) |G*|/sin(δ) *versus* ALF Rutting, (b) J_{nr} *versus* ALF Rutting (D'Angelo, 2009)

- LAS Test: Polymer modification has been shown to reduce the effect of age hardening (Ruan et al., 2003). By using the LAS test (AASHTO TP 101) to evaluate fatigue of asphalt binder, Hintz et al. (2011a) showed that some polymer modification decreases the effect of age on the fatigue damage resistance of asphalt binders. In this test, the use of viscoelastic continuum damage mechanics allows for prediction of fatigue life at any strain amplitude from a single 30-minute test, thus allowing for consideration of pavement structure (i.e., strain) and traffic (i.e., number of cycles to failure). As shown in Figure 12, the LAS fatigue test procedure was validated through comparison with performance of Long-Term Pavement Performance (LTPP) test sections showing good correlation with field measurements.

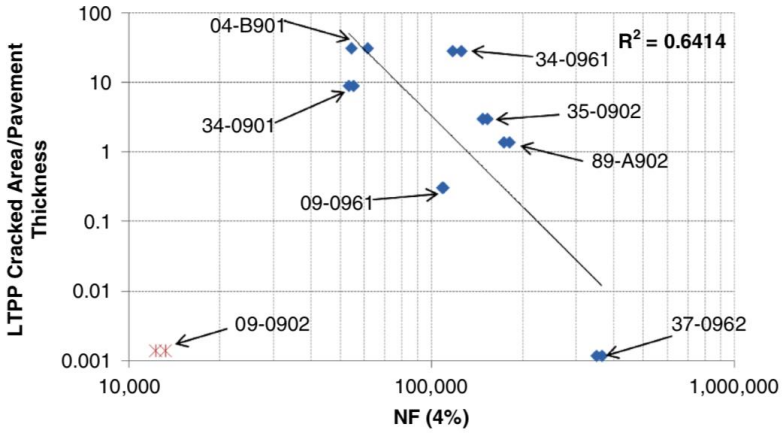

Figure 12. LTPP Measurements *versus* LAS Number of Cycles to Failure (Hintz et al., 2011b)

- BYET Test: Tabatabaee et al. (2013) showed that the conventional ductility test (AASHTO T 51) yields erratic and inconsistent results for two elastomeric (i.e., SBS and Elvaloy™) modifications of six asphalt base binders [Figure 13(a)]. When conducting the ductility test on the same materials in a controlled DSR geometry condition using BYET, the authors observed that all elastomeric modifiers significantly improved the ductility of the binders [Figure 13(b)]. The difference in results between the conventional ductility and the DSR-ductility is attributed to the sample cross sectional area and load geometry difference. Therefore, when evaluating modified binders, a test method that can maintain a stable geometry should be used, since the use of the conventional ductility test is misleading and could unscientifically disqualify modified binders with ductility that is superior to that of the conventional binders. Furthermore, DSR-ductility has the following advantages: smaller sample size, easier sample preparation, reduction in the testing time, better temperature control, and automated measurements. Regarding field validation, Gibson (2009) showed a very good correlation between the BYET results and full-scale ALF cracking.

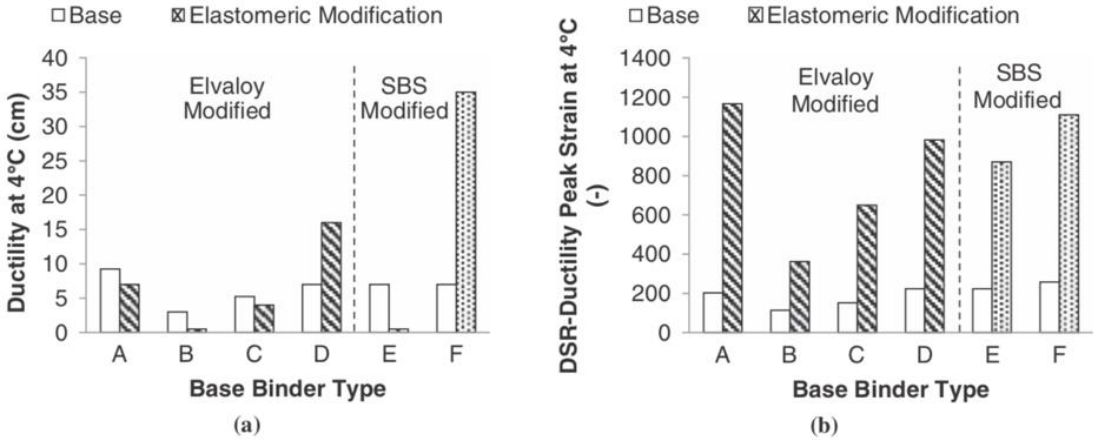

Figure 13. Ductility of Elastomeric Modifiers by means of: (a) AASHTO T 51, and (b) AASHTO TP 123-method b (Tabatabaee et al., 2013)

Aging of EMA Binders

Aging of asphalt binders occurs by chemical or physicochemical changes during production of asphalt mixtures and throughout the service life of the pavement. Variations in asphalt binder composition strongly affects an asphalt binder's mechanical properties, chemical reactivity, and number and type of products generated after oxidative aging. Therefore, the aging mechanisms of EMA binders are influenced by the characteristics of base asphalt binder and epoxy resin, as well as the molecular interaction between these components. Due to the thermosetting behavior of epoxy resins, the Superpave aging procedures [i.e., Rolling Thin Film Oven (RTFO) and Pressure Aging Vessel (PAV)] may not be applicable to undiluted EMA binders. Despite this challenge, a study performed in the Netherlands reported success on subjecting two diluted EMA binders (with an epoxy dosage rate of 20%) using two 70-100 penetration grade asphalt binders to both RTFO and PAV aging (Zegard et al., 2019).

Existing Studies in United States, New Zealand, the Netherlands

Since its introduction by Shell in 1960s, EMA has been used in a variety of projects around the world (Read and Whiteoak, 2003). Over the last decade, EMA has been widely used in deck surfacing asphalt mixtures for long-span orthotropic steel bridges in several Asian countries. In 2006, an FHWA study showed that rheological parameters for EMA binders are in a very different range than what is normally obtained for conventional unmodified or PMA binders (Youtcheff et al., 2006). For example, the high temperature Superpave parameter |G*|/sin(δ) of undiluted EMA binder indicates superior rutting resistance in comparison to an unmodified PG 70-22 control [Figure 14(a)]. Furthermore, the rutting resistance of the EMA binder appeared to increase with time until the material became fully cured [Figure 14(b)]. The study also highlighted encouraging results of the EMA binder in terms of resistance to moisture damage and aging.

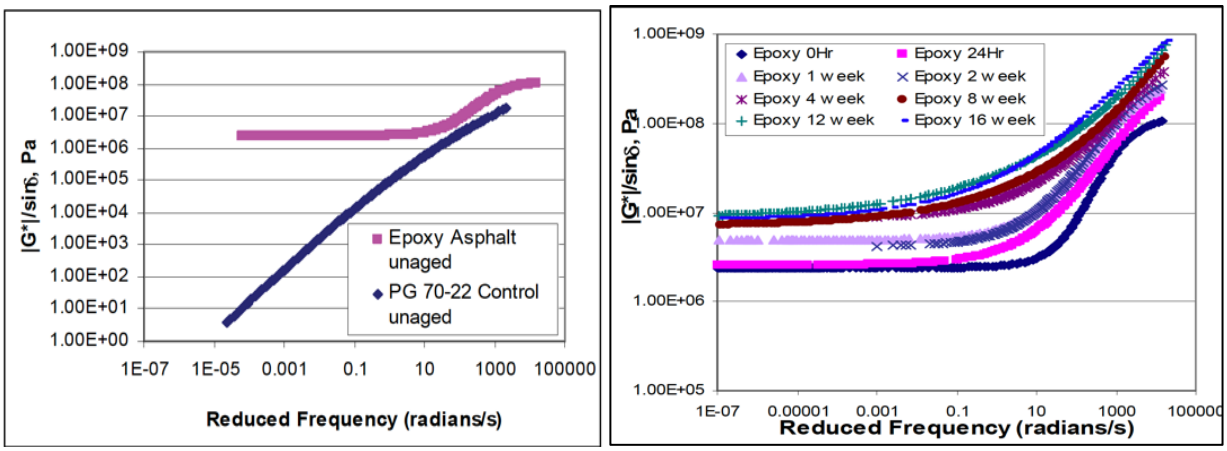

(a) (b)

Figure 14. |G*|/sin(δ) Results: (a) Undiluted EMA Binder *versus* Unmodified PG 70-22 at 28°C: (b) Undiluted EMA Binder over 16 Weeks at 28°C (Youtcheff et al., 2006)

A study performed in the Netherlands showed that two 70-100 penetration grade asphalt binders modified at a weight ratio of 25:75 of epoxy binder and local asphalt binder have better fatigue life in comparison to the unmodified binders (Zegard et al., 2019). Figure 15 presents the comparison of predicted fatigue life of two diluted EMA binders using the LAS test at 10 and 20°C. From the fatigue results, the authors concluded that different base binders will offer different rheological behavior for EMA binders. When comparing the two 70-100 penetration grade base asphalt binders, the EMA binder containing base binder A exhibits a higher fatigue life than that containing base binder B.

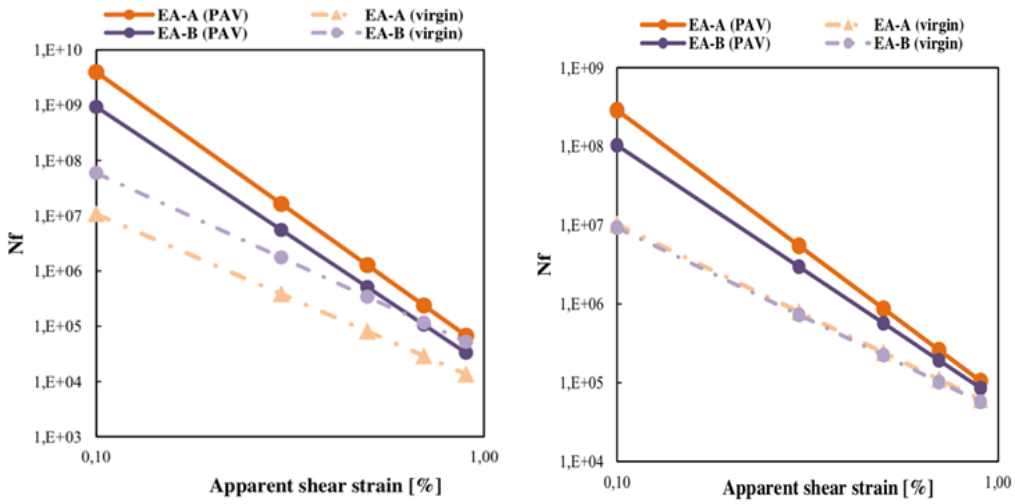

(a) (b)

Figure 15. Predicted LAS Fatigue Life *versus* Apparent Shear Strain: (a) 10°C, (b) 20°C (Zegard et al., 2019)

A study performed in New Zealand evaluated the rheological behavior of four types of asphalt binders (i.e., unmodified, low dosage rate EMA binder, and two thermoplastic modified binders) (Holleran et al., 2017). As shown in Figure 16, this study indicated that at a very low epoxy resin dosage rate (i.e., 7-8% epoxy resin in the final binder), no improvement in the fatigue life and ductility of the base asphalt binder was obtained. Therefore, an epoxy dosage rate above 8% is needed in order to produce EMA binders with comparable or better performance than the PMA binders.

(a) (b)

Figure 16. Comparison of Aged EMA and PMA Binders: (a) LAS Fatigue Life Results, (b) BYET Results (Holleran et al., 2017)

2.4 Epoxy-modified Asphalt (EMA) Mixtures

A dense-graded EMA mixture was first used on the steel deck of San Mateo-Hayward Bridge in 1967 by the California Bay Bridge Authority. The mixture is still in place and has been performing well over 50 years in service. Since then, EMA mixtures have been widely used as

durable deck surfaces on long-span orthotropic steel bridges in Canada, Australia, Brazil, and several Asian countries (ChemCo Systems, 2019). The first reported application of EMA OGFC mixture was on the upper deck of the San Francisco-Oakland Bay Bridge in 1969, which showed excellent skid and hydroplaning resistance, bond to the substrate, stability, and wearing resistance (Brewer, 1970). In 1992, the Japanese Asphalt Association (JAA) conducted a laboratory study confirming that the use of EMA OGFC mixture enhanced the durability and functionality of pavement surface course. Following the laboratory study, JAA placed several test sections in 1994 and constructed the first roadway project in 1996, which all achieved superior performance. In 1997, JAA published a manual of constructing EMA OGFC for roadways (Li, 1999). Over the last two decades, several research studies have been conducted to characterize the engineering properties of EMA mixtures through laboratory testing. These studies are discussed in the following sections.

Studies in New Zealand

The New Zealand Transport Agency (NZTA) has been evaluating EMA OGFC mixtures as part of the Organization for Economic Cooperation and Development (OECD) program. The OECD program was initiated by transportation agencies from over 20 countries to identify candidate materials for long life pavements with lifespans greater than 30 years (OECD, 2008). The objectives of the first NZTA study were to determine the effect of EMA on the raveling potential of OGFC mixtures and identify possible production and construction challenges (Herrington et al., 2007). The study found that EMA OGFC mixtures had superior resistance to oxidative aging and raveling, and thus were expected to last longer than conventional OGFC mixtures containing unmodified asphalt binders. As part of the study, a 6-meter long, 2-meter wide test section was constructed on the Canterbury Accelerated Pavement Testing Indoor Facility (CAPTIF), as shown in Figure 17. The study concluded that no significant modifications to plant setup, production, or construction procedures were needed to produce EMA OGFC mixtures.

Figure 17. EMA OGFC Test Section at CAPTIF (Herrington et al., 2007)

In early 2007, NZTA initiated a follow-up study to further investigate the durability of EMA OGFC mixtures and explore the use of diluted EMA binders with epoxy dosage rates of 10% and 20% (Herrington, 2010). The study found that undiluted EMA OGFC mixtures, when fully cured, had significantly better raveling resistance, fatigue life, and aging resistance than those with unmodified asphalt binders. As shown in Figure 18, the EMA OGFC mixture had

consistently lower Cantabro mass loss than the unmodified OGFC mixture over 80 days of oxidative aging at 85°C. The study also reported that OGFC mixtures containing diluted EMA binders with epoxy dosage rates of 10% and 20% still outperformed the unmodified OGFC mixture in terms of fatigue resistance (Table 7).

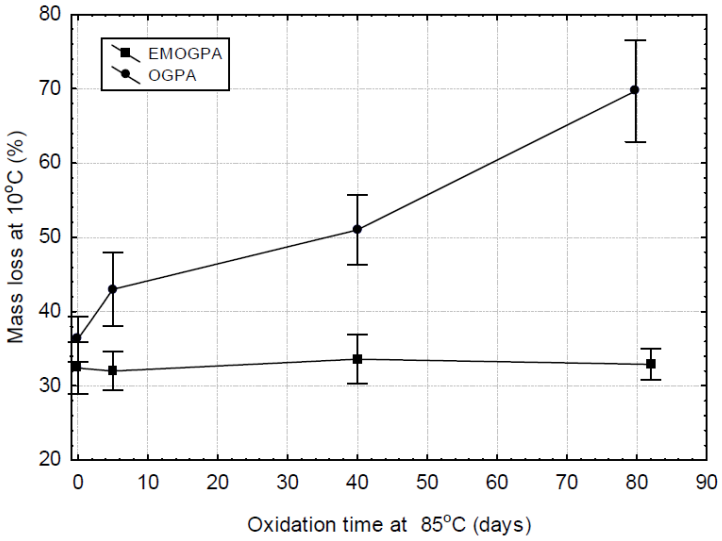

Figure 18. Cantabro Test Results of EMA OGFC *versus* Unmodified OGFC Mixtures (Herrington, 2010)

Table 7. Indirect Tensile Fatigue Test Results (Herrington, 2010)

Mix Type	Cycles to Failure at 100 Microstrain
Unmodified OGFC	8,700
10% EDR Diluted EMA OGFC	12,600
20% EDR Diluted EMA OGFC	10,300
Undiluted EMA OGFC	Over 223,000

Following the lab study, a field project was constructed in Christchurch in December 2007. The project consisted of three 60-meter long, 5-meter wide test sections. One section used New Zealand's standard unmodified OGFC mixture with 20% air voids and the other two sections used undiluted EMA OGFC mixtures with 20% and 30% air voids, respectively. Although all three mixtures had a design binder content of 5.0%, the EMA OGFC mixture with 30% air voids experienced significant asphalt draindown during production and had an as-constructed binder content of 4.0%. Field performance of the project was continuously monitored over three years after construction. In general, all three test sections performed well with minimal rutting and no cracking or raveling reported. Figure 19 shows the two EMA OGFC sections after three years of trafficking. Table 8 summarizes the field permeability test (per modified ASTM D4867) results of the three test sections. As shown, none of the sections showed a significant reduction in permeability over three years.

Figure 19. EMA OGFC Sections in Christchurch, New Zealand (Herrington, 2010)

Table 8. Permeability Test Results (Herrington, 2010)

Test Section	January 2008		January 2009		March 2010	
	Wheel Path	Outside wheel tracks	Wheel Path	Outside wheel tracks	Wheel Path	Outside wheel tracks
20% air voids unmodified OGFC	53 ± 2	51 ± 2	59 ± 2	63 ± 3	50 ± 2	55 ± 5
20% air voids EMA OGFC	50 ± 2	45 ± 5	52 ± 2	56 ± 3	48 ± 2	56 ± 6
30% air voids EMA OGFC	53 ± 2	49 ± 3	57 ± 2	61 ± 3	49 ± 2	57 ± 3

A more recent study by Wu et al. (2017) evaluated the long-term durability of EMA OGFC mixtures relative to mixtures containing an unmodified binder and an SBS-modified binder. Mixtures were compared based on Cantabro, IDT modulus, IDT fatigue, and surface abrasion test results. The study found that EMA OGFC mixtures had significantly better durability than the unmodified mixture and that the mixture durability improved as the centration of EMA binder increased. It was also found that EMA OGFC mixtures, especially those containing undiluted EMA binder and diluted EMA binder with an epoxy dosage rate of 30%, had significant better resistance to fatigue cracking and raveling than the SBS-modified OGFC mixture, as shown in Figure 20.

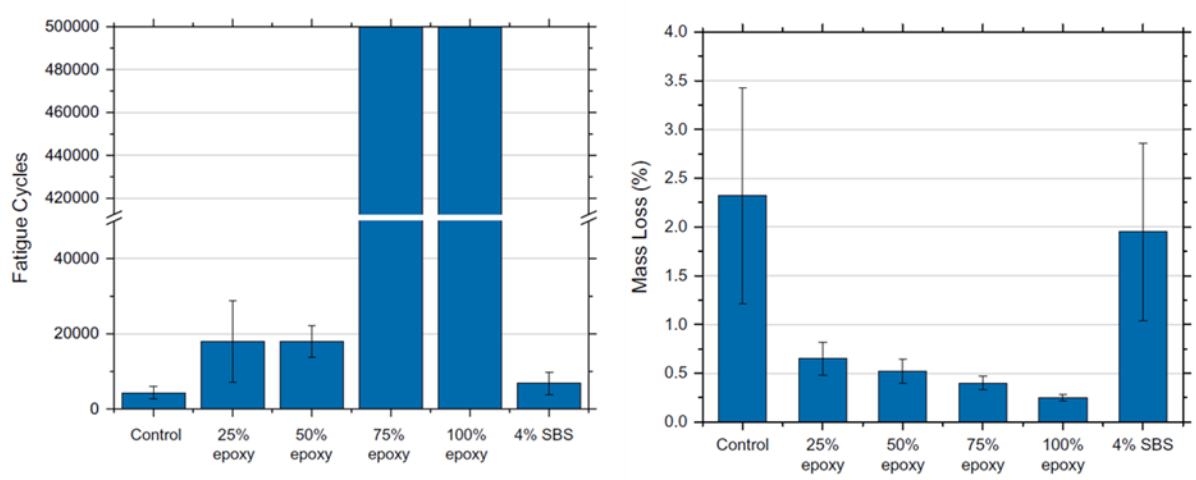

(a) (b)

Figure 20. Mixture Performance Test Results of Unmodified, Epoxy-modified, and SBS-modified OGFC Mixtures: (a) IDT Fatigue Test, (b) Cantabro Test (Wu et al., 2017)

Studies in the United States

As part of the OECD program, the FHWA Turner Fairbank Highway Research Center (TFHRC) conducted a laboratory study to characterize the performance properties of an undiluted EMA (epoxy dosage rate of 40%) dense-graded asphalt mixture (Youtcheff et al., 2006). The mixture tested was a 75-gyration Superpave mixture with a nominal maximum aggregate size (NMAS) of 12.5 mm. The design binder content of the EMA mixture was 5.3%. For performance comparison, the laboratory test results of the EMA mixture were compared against those of companion mixtures containing several different types of asphalt binders.

Figure 21 presents the flow number test results at 64°C. Among all the mixtures tested, the EMA mixture had the lowest accumulated permanent strain and showed no signs of tertiary flow, which indicated that the mixture had superior rutting resistance. A similar trend was also observed in the dynamic modulus test results. As shown in Figure 22, the EMA mixture had significantly higher stiffness at all frequencies and temperatures. For the evaluation of moisture susceptibility, HWTT and the Pine Wheel Tester (PWT) were conducted at 64°C and 60°C, respectively. For both tests, the EMA mixture had a maximum rut depth of less than 2 mm at 40,000 passes and showed no signs of stripping. These results indicated that the moisture susceptibility of the EMA mixture was negligible.

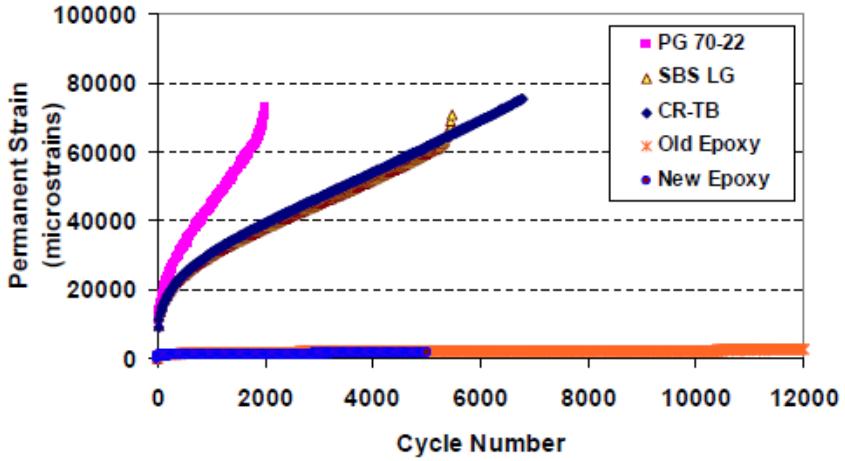

Figure 21. SPT Flow Number Test Results (Youtcheff et al., 2006)

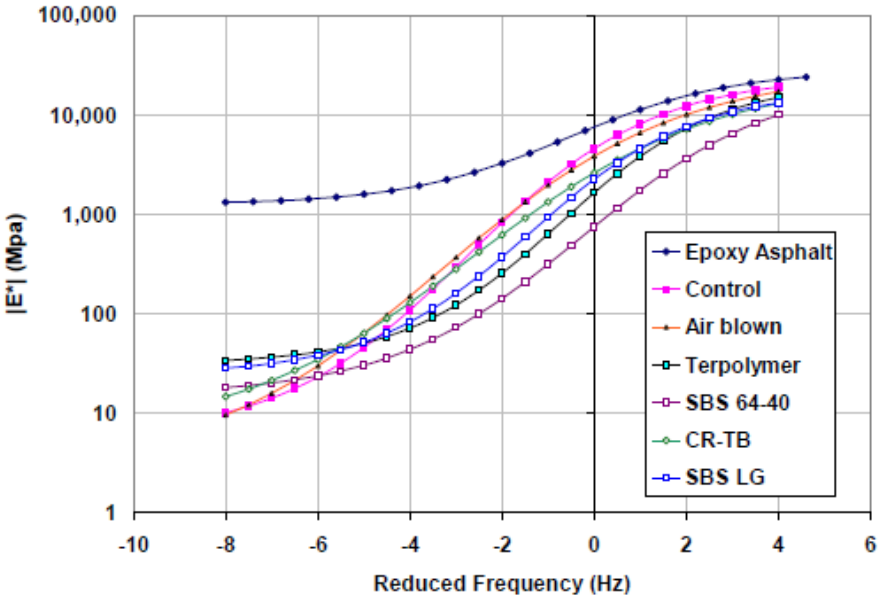

Figure 22. SPT Dynamic Modulus Test Results (Youtcheff et al., 2006)

The push-pull axial fatigue test, as shown in Figure 23(a), was conducted to evaluate the fatigue resistance of the EMA mixture. The selected test temperature was 19°C. At a platen-to-platen strain level of 1,300 microstrains, the EMA mixture showed no apparent fatigue deterioration over 100,000 loading cycles, while a companion mixture containing a rubber modified binder failed the test at 6,200 loading cycles [Figure 23(b)]. Similar findings were also observed in the IDT strength and resilient modulus test, where the EMA mixture showed significantly better fatigue life and fracture properties than conventional modified and unmodified mixtures. For the evaluation of thermal cracking resistance, three performance tests were conducted: thermal stress restrained specimen test (TSRST), disc-shaped compact tension (DCT) test, and semi-circular bending (SCB) test. The EMA mixture had a fracture temperature of -26°C in the TSRST test. For DCT and SCB tests, the EMA mixture had a critical fracture energy of 610 J/m2 and 690

J/m2, respectively, at -18°C. These results indicated that the EMA mixture was more resistant to thermal cracking than unmodified mixtures.

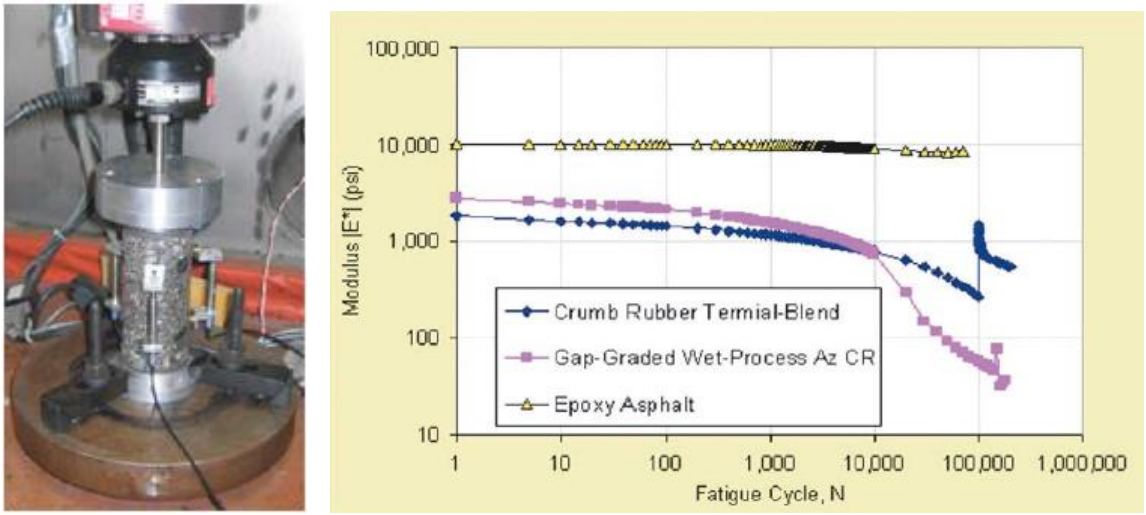

(a) (b)

Figure 23. Push-pull Axial Fatigue Test: (a) Test Setup, (b) Test Results (Youtcheff et al., 2006)

Studies in China

Luo et al. (2015) evaluated the performance properties of an undiluted EMA (epoxy dosage rate of 40%) OGFC mixture as compared to a conventional OGFC mixture containing a PG 64-16 unmodified binder. The optimum binder content of the two mixtures was 5.6% following the Marshall mix design method. Mixture tests included permeability, acoustic absorption, TSR, HWTT, Cantabro, British Pendulum Tester (BPT) in conjunction with Dynamic Friction Tester (DFT), Superpave Shear Tester (SST), and overlay test (OT). Test results are summarized in Table 9. As shown, the undiluted EMA OGFC mixture outperformed the unmodified OGFC mixture for all tests except permeability. Despite the performance benefits, the study identified two limitations for the use of EMA for roadway applications. Due to its thermosetting behavior, EMA binder requires a curing period before it gains full strength and can be opened to traffic. Further, epoxy asphalt can be five to ten times more expensive than conventional modified and unmodified asphalt binders. Whether or not the high material cost of epoxy asphalt can be justified by improved mixture performance remains unknown and needs further investigation.

Another study by Qian and Lu (2015) evaluated the use of small particle undiluted EMA OGFC mixtures for roadway pavements. A 4.75 mm NMAS aggregate gradation was used to improve the smoothness and durability of OGFC mixtures. The EMA mixture was designed with a balanced mix design approach, where the optimum binder content of 5.5% was selected by optimizing asphalt draindown and mix durability. As shown in Figure 24, as the binder content increased, the Cantabro mass loss decreased while asphalt draindown increased. After the mix design was established, mixture performance tests were conducted to assess the performance of the 4.75 mm EMA OGFC mixture as compared to conventional 9.5 mm and 12.5 mm polymer-modified OGFC mixtures. Test results indicated that the use of small particle aggregates and EMA binders reduced the permeability and rutting resistance of OGFC mixtures, but the

reduction was not significant. In addition, the 4.75 mm EMA OGFC mixture showed satisfactory moisture resistance and low temperature cracking resistance. Finally, the study concluded that small particle EMA OGFC mixtures can be designed to achieve adequate pavement performance and functionality.

Table 9. Summary of Mixture Performance Test Results (Luo et al., 2015)

Lab Test	Test Parameter	Unmodified OGFC	EMA OGFC
Permeability	Coefficient of permeability	0.30 cm/s	0.15 cm/s
Acoustic absorption	Sound absorption coefficient	0.36	0.40
TSR	TSR	62%	92%
HWTT	Number of passes to reach 12.5-mm rut depth	1,000	10,000
Cantabro	Mass loss on unaged samples	50%	18%
	Mass loss on aged samples	68%	16%
DFT	Friction coefficient at 20 km/h	0.55	0.58
	Friction coefficient at 50 km/h	0.33	0.52
	Friction coefficient at 80 km/h	0.28	0.46
SST	Cycles to 5% permanent shear strain, 70-kPa stress	100	Over 10,000
	Cycles to 5% permanent shear strain, 130-kPa stress	80	Over 10,000
OT	Cycles to failure	530	Over 1,000

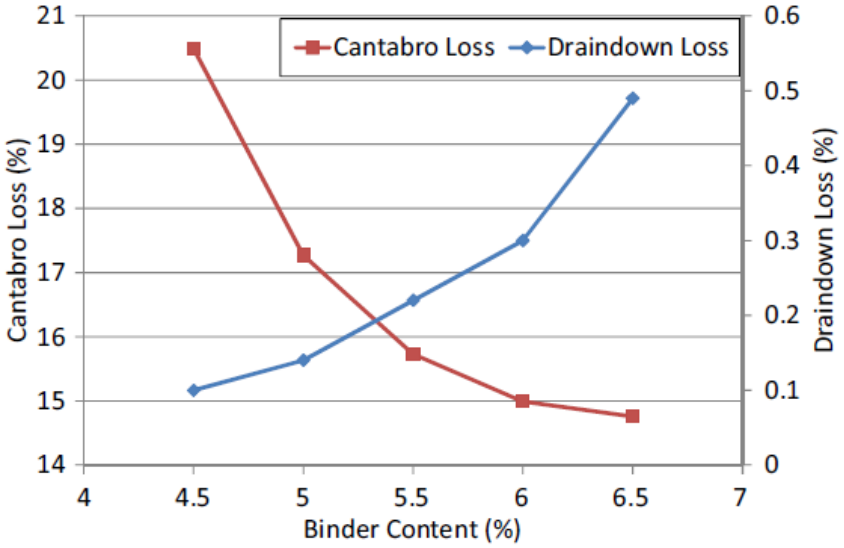

Figure 24. Selecting Optimum Binder Content by Balancing Cantabro Mass Loss and Asphalt Draindown (Qian and Lu, 2015)

2.5 Production and Construction of EMA Mixtures

One challenge reported for the production of EMA mixtures is the blending of EMA components at an asphalt plant. Because EMA binder is a thermosetting material, pre-blending the epoxy resin and curing agent prior to production is not feasible. Instead, the two components need to be blended at the plant during production.

Fulton Hogan, an asphalt contractor in New Zealand, has had good success producing EMA OGFC mixtures in continuous drum asphalt plants. An in-line blending system was used to blend the two epoxy asphalt components. As shown in Figure 25, component B (i.e., a blend of asphalt binder and epoxy curing agent) was stored in an asphalt tank at 120°C, which was connected to the asphalt feed line. Component A (i.e., epoxy resin) was stored in a separate heated drum at 85°C (Figure 25) and pumped into the asphalt feed line about 5 to 10 meters from the point of where the binder enters the drum. The flow rate of the pump was calibrated based on the proportion of the two components. At some plants, the asphalt feed line was customized to include several sharp bends or a mixing chamber (Figure 26) to achieve better mixing of the two components.

In New Zealand, undiluted EMA OGFC mixtures were typically produced at 120°C. When 25% diluted EMA binder was used, a higher production temperature of 135°C to 140°C was required to account for the increased viscosity of the diluted EMA binder. Use of a production temperature above 140°C was not recommended because it could increase the asphalt draindown potential and accelerate the cross-linking reaction between epoxy resin and curing agent, shortening the "pot life" of EMA binder with adequate workability and compactability. After production was completed, the in-line system used to introduce the EMA components was disconnected from the plant and flushed with straight asphalt binder and kerosene for clean-up.

Figure 25. Introduction of Epoxy Asphalt Components at a Drum Plant in New Zealand (Van de Linda, 2019)

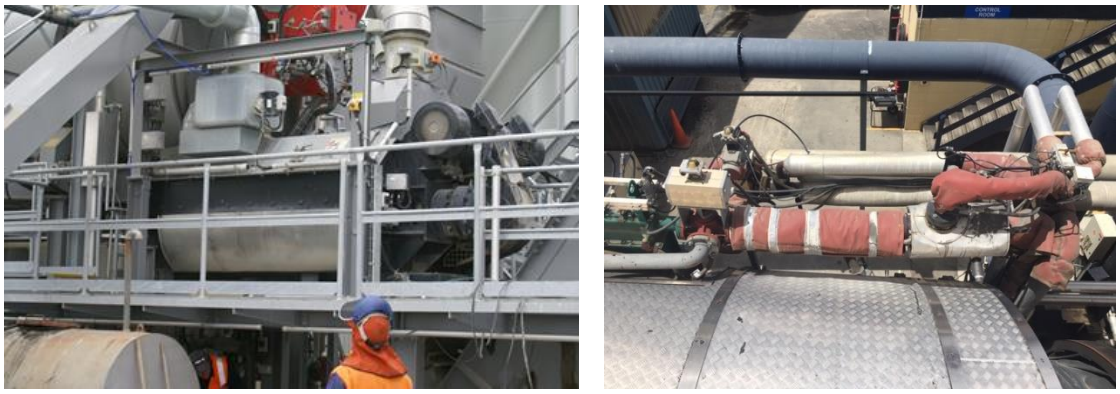

Figure 26. In-line Mixing Chamber at a Drum Plant in New Zealand (Waters et al., 2018; van de Linda, 2019)

In 2018, Dura Vermeer, a contractor in the Netherlands, successfully produced an EMA SMA mixture in a twin-axle batch asphalt plant. To accommodate the blending of epoxy asphalt components during production, an in-line temperature system and a mass flow-control automated distribution system was installed. As shown in Figure 27, component B was pre-heated in an asphalt distributor at 120°C and during production, it was directly pumped into the asphalt weigh vessel above the mixing pugmill. Component A was stored in a heated storage tank at 75°C, which was connected to the feed line for component B. The two components were thoroughly mixed in the asphalt weigh vessel and then discharged into the mixing pugmill to mix with aggregates. After mixing, the mixture was directly loaded into trucks and transported to the paving site without storage in the silo. The plant production temperature was set at 120°C.

Figure 27. Introduction of Epoxy Asphalt Components at a Batch Plant in the Netherlands (Zegard et al., 2019)

Asphalt contractors in China and Japan also reported success with producing undiluted EMA dense-graded and OGFC asphalt mixtures in batch asphalt plants. However, the approach used to blend epoxy asphalt components was different from that used by contractors in New Zealand and the Netherlands because of the different sources (i.e., types) of epoxy materials used. Figure 28 provides a graphical illustration of the mixture production process in Japan. As discussed

previously, foreign epoxy manufacturers provide epoxy resin, epoxy curing agent, and asphalt binder separately. During production, prewarmed epoxy resin and epoxy curing agent are either automatically blended in a distributing truck (Figure 29) or manually blended in an aluminum container using a portable mechanical blender. The blended epoxy resin and curing agent is then pumped into the asphalt weigh vessel where it is thoroughly mixed with base asphalt binder to produce EMA binder. Finally, EMA binder is discharged into the mixing pugmill to mix with aggregates. Typically, EMA mixtures in China and Japan are produced at an elevated temperature of 170 to 180°C. Note that the distinct difference in the production temperature of EMA mixtures in China and Japan versus New Zealand and the Netherlands is mainly due to the use of different types of epoxy materials. As discussed previously, contractors in China and Japan use a foreign source of epoxy materials, with Part A being epoxy resin and Part B being amine-based curing agent. Contractors in New Zealand and the Netherlands use a domestic source of epoxy materials, with Part A being epoxy resin but Part B being a blend of soft asphalt binder and acid-based curing agent. Because of the different compositions, these two types of epoxy materials have different temperature-dependent polymerization behavior when used for asphalt modification.

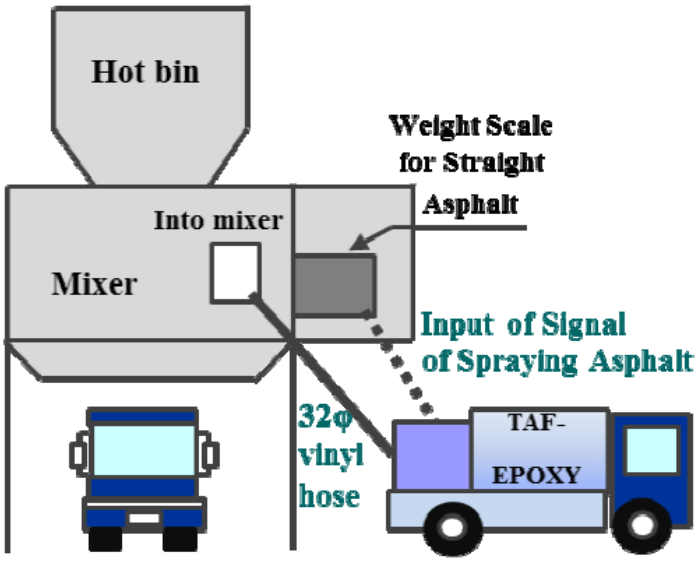

Figure 28. Illustration of the EMA Mixture Production Process (TAIYU Kensetsu Co., LTD.)

Figure 29. Epoxy Materials Distributing Truck in Japan

Experience in New Zealand and the Netherlands indicated that EMA mixtures can be placed in a similar manner as conventional asphalt mixtures. Figure 30 shows the compaction of two EMA OGFC pavements in New Zealand. The duration of the entire compaction process is typically less than 30 minutes. After compaction is completed, the asphalt mat temperature is usually between 65°C and 90°C. When undiluted EMA binder is used, the time between mixture production and construction is recommended to not exceed two hours. When diluted EMA binder is used, a longer time window of up to four hours can be acceptable depending on the epoxy dosage rate.

Figure 30. Compaction of EMA OGFC Pavements in New Zealand (Waters et al., 2018)

2.6 Summary of Findings

State of the Practice on Use of OGFC

- A survey of state highway agencies in 2015 identified over 20 states using OGFC mixtures. Currently, FDOT requires OGFC mixtures on all multi-lane roadways where the design speed is 50 mph or greater, except for curb and gutter areas.
- Compared to conventional dense-graded mixtures, OGFC mixtures provide significant safety and environmental benefits including reduced risk of hydroplaning, reduced splash and spray from vehicle tires, improved visibility, and in some cases, increased friction resistance and noise reduction for several years after construction. However, the

increased friction resistance and noise reduction benefits have not been encountered for OGFC in Florida.

- Three commonly reported shortcomings of OGFC are high material cost, more winter maintenance activities, and long-term durability issues.

OGFC Mix Design and Performance Testing

- OGFC mix design procedures consist of three main parts: selection of suitable materials, selection of a design gradation, and determination of the optimum binder content.
- Aggregate characteristics that are typically considered for OGFC mix design include durability, polish resistance, angularity, shape, cleanliness, abrasion resistance, and absorption.
- Use of polymer or rubber modified asphalt binders are effective in preventing asphalt draindown and improving the durability of OGFC mixtures.
- There are three approaches to determine the optimum binder content of OGFC mixtures: absorption calculation, visual determination, and compacted specimen evaluation.
- Commonly used performance tests of OGFC mixtures include permeability, Cantabro, TSR, HWTT, and I-FIT. The IDEAL-CT may be a suitable alternate to the I-FIT.

Epoxy Resin for Asphalt Modification

- Some manufacturers that produce epoxy resin for asphalt modification provide the epoxy resin and curing agent as separate components, while others provide the epoxy resin and a blend of asphalt binder with the epoxy curing agent.

Characterization of Asphalt Binders Containing Epoxy Resin

- From the literature review, the key testing methods used for evaluation of EMA binders are:
    - Viscosity for evaluation of curing behavior;
    - Storage stability for evaluation of compatibility;
    - Fluorescence microscopy for evaluation of polymer dispersion;
    - Bond strength for evaluation of cohesive and adhesive properties;
    - Glass-transition temperature for evaluation of ductile to brittle transition;
    - Infrared spectroscopy for functional groups characterization; and
    - DSR MSCR, LAS test, and master curve for rheological evaluation.
- If an epoxy resin dosage rate of 30% and above is used to modify asphalt binders, conventional Superpave binder test methods may not be suitable for rheological characterization due to the thermosetting behavior of the final EMA binders.

Epoxy Resin Dosage Rate for Asphalt Binder Modification

- An epoxy dosage rate above 8% is needed for epoxy asphalt binders to have comparable or better performance than asphalt binders modified with thermoplastic polymers at dosage rates higher than 3%.

Factors Influencing EMA Binder Behavior

- The curing rate of EMA binder is highly dependent on the epoxy resin dosage rate and temperature.
- Asphalt binder chemistry plays a role when considering modification with epoxy resin.

History and Reported Performance of EMA Mixture

- Dense-graded EMA mixtures have been widely used as durable deck surfaces on long-span orthotropic steel bridges in Canada, Australia, Brazil, and several Asian countries.
- The first reported application of EMA OGFC mixtures was on the San Francisco-Oakland Bay Bridge in 1969. Over the last two decades, several field projects using EMA OGFC mixtures were constructed in China, Japan, New Zealand, and the Netherlands.
- Existing studies showed that undiluted EMA (epoxy dosage rate of 40%) OGFC mixtures had significantly better resistance to oxidative aging, rutting, fatigue, raveling, and moisture damage than conventional OGFC mixtures containing unmodified asphalt binders.
- Several research studies highlighted that undiluted EMA OGFC mixtures outperformed PMA modified mixtures in terms of resistance to fatigue cracking and raveling.

Production and Construction of EMA Mixtures

- One major concern for the production of EMA mixtures is the blending of EMA components. Because EMA binder is a thermosetting material, pre-blending the epoxy resin and curing agent prior to production is not feasible.
- Contractors in New Zealand and the Netherlands had success with using an in-line blending system to blend asphalt binder, epoxy resin, and curing agent in continuous drum and batch asphalt plants.
- The recommended production temperature of EMA mixtures containing domestic and foreign EMA binder is 120 to 135°C and 170 to 180°C, respectively.
- When undiluted EMA binder is used, the time between mixture production and construction is recommended to not exceed two hours. When diluted EMA binder is used, a longer time window of up to four hours can be acceptable depending on the epoxy dosage rate.
- EMA mixtures can be placed in a similar manner as conventional asphalt mixtures.

CHAPTER 3. SELECTION OF CHEMICALLY COMPATIBLE EPOXY ASPHALT BINDERS

This chapter presents the experimental plan, test results, and findings of Experiment 1 of the study. The objective of this experiment was to investigate the chemical compatibility between two epoxy materials (i.e., one from a domestic source and the other from a foreign source) and four PG 67-22 base asphalt binders with different chemical compositions (i.e., crude oil source). This experiment consisted of three sub-experiments: investigation of the compatibility between the epoxy materials and the base asphalt binders by the storage stability test and Soxhlet asphalt extraction, evaluation of the morphology of EMA binders by fluorescence microscopy, and analysis of the SARA fractions [i.e., saturates (S), aromatics (A), resins (R), and asphaltenes (A)] of the base asphalt binders used for epoxy modification. The overall goal of this experiment was to select the most suitable (i.e., chemically compatible) base asphalt binder for each epoxy material.

3.1 Experimental Plan

Materials

In this study, two epoxy materials (i.e., one from a domestic source and the other from a foreign source) were used. The manufacturer of the domestic source (U) materials provided an epoxy resin (Part A) and a blend of acid-based epoxy curing agent and asphalt binder (Part B) [Figure 7(a)], while the manufacturer of the foreign (J) epoxy materials provided an epoxy resin (Part A) and an amine-based curing agent (Part B) by itself [Figure 7(b)]. The domestic epoxy materials after combining Part A and Part B had an EDR of approximately 40%, as defined in Equation 6 (page 38).

Four unmodified asphalt binders from the FDOT approved product list were selected for modification with the two epoxy materials. The four base binders were classified in terms of performance grade (PG) as 67-22, and are indicated in this report as binders A, C, G, and Z. Table 10 presents the testing matrix for Experiment 1. As shown, a total of 16 EMA binders, encompassing four unmodified asphalt binders from different crude sources (i.e., binders A, C, G and Z), two epoxy resins and curing agents from different sources [i.e., domestic source (U) and foreign source (J)], and two EDR (i.e., 15% and 25%), were screened for compatibility and morphology evaluations. The four base asphalt binders were evaluated in terms of SARA fractions. The nomenclature of "(epoxy source, U or J) (EDR, 15% and 25%) (base binder source, A, C, G and Z)" was followed to name EMA binders prepared with different sources of epoxy materials, EDRs, and base binders. For example, "U15C" denotes an EMA binder prepared with the domestic (U) epoxy materials, 15% EDR, and a PG 67-22 base binder C.

Table 10. Proposed Testing Matrix for Experiment 1

Factor Name	Factor No.	Description
Asphalt binder	4	Four unmodified asphalt binders (PG 67-22) from FDOT approved product list
Epoxy resin & curing agent	2	One domestic source (U), one foreign source (J)
Epoxy dosage rate	2	15%, 25%
Laboratory binder tests	3	Modified storage stability test Fluorescence microscopy SARA fractions of the base asphalt binders

Preparation of EMA Binders

The preparation of J-EMA binders started with preheating the PG 67-22 base binder Z for two hours at 130°C, and epoxy resin (Part A) and curing agent (Part B) for one hour at 60°C. The epoxy resin and curing agent were first blended for two minutes using a low shear mixer, which was placed on a hot plate to maintain a constant blending temperature of approximately 130°C. Then, the PG 67-22 base binder was added and blended for another 15 minutes. Table 11 presents the blending proportions of the component materials for J-EMA binders at the two selected EDRs (15% and 25%).

Table 11. Blending Proportions of Component Materials for J-EMA Binders

Binder ID	EDR	Proportions (% by weight)		
		PG 67-22 Base Binder	Part A: Epoxy Resin	Part B: Curing Agent
J15A	15%	85.00	8.80	6.20
J15C				
J15G				
J15Z				
J25A	25%	75.00	14.60	10.40
J25C				
J25G				
J25Z				

The preparation of EMA binders containing the epoxy material from a domestic source (i.e., U-EMA binders) started with preheating the base asphalt binders and Part B of the epoxy asphalt material (a blend of acid-based epoxy curing agent and soft asphalt binder) for two hours at 130°C, following by blending for 15 minutes using a low shear mixer. The epoxy resin (Part A) was preheated for 15 minutes at the same temperature (i.e., 130°C), and manually blended with the base asphalt binder, epoxy curing agent, and soft asphalt binder for approximately 30 to 40 seconds using a stirring rod. After the epoxy resin was added, it started to react with the acid-based curing agent, which significantly increased the viscosity of the U-EMA binders and sometimes triggered a thermosetting behavior when considering the EDR of 25%. Table 12 presents the blending proportions of the component materials for U-EMA binders at the two EDRs (15% and 25%).

Table 12. Blending Proportions of Component Materials for U-EMA Binders

Binder ID	EDR	Proportions (% by weight)		
		PG 67-22 Base Binder	Part A: Epoxy Resin	Part B: Blend of Curing Agent and Soft Asphalt Binder
U15A	15%	62.50	7.30	30.20
U15C				
U15G				
U15Z				
U25A	25%	37.50	12.10	50.40
U25C				
U25G				
U25Z				

Binder Testing Plan

SARA Fractions

The SARA analysis was performed to separate each of the four base asphalt binders into chemical fractions based on differences in solubility and polarity. These SARA fractions are commonly designated as saturates (S), aromatics (A), resins (R), and asphaltenes (A). This chemical separation was performed as follows: the asphaltenes were first extracted per Institute of Petroleum (IP) 143 Standard [Determination of Asphaltenes (Heptane Insolubles) in Crude Petroleum and Petroleum Products]; the maltenes (i.e., saturates, aromatics and resins) were then separated per IP 469 (Determination of Saturated, Aromatic and Polar Compounds in Petroleum Products by Thin Layer Chromatography and Flame Ionization Detection) with toluene:chloroform (85:15 v/v) solution using Iatroscan.

Evaluation of the Compatibility of EMA Binders

To investigate the compatibility between the epoxy materials and the base asphalt binders, a test procedure that combined the storage stability test (i.e., polymer separation) and Soxhlet asphalt extraction was used (Cong et al., 2011). The test for evaluation of polymer separation was adapted from ASTM D7173. In the adapted version of the procedure, 50 g of the EMA binder were placed in a sealed aluminum tube (25 mm in diameter and 140 mm in height) and then conditioned in a vertical position for eight hours at 120°C. After static heat conditioning, the binder was allowed to cure at room temperature. At the end of the conditioning period, the top and bottom portions of the aluminum tube were separated and subjected to Soxhlet extraction per ASTM C613M to determine the degree of separation between the base asphalt binder and the epoxy materials. In the Soxhlet extraction, 3 g of the EMA binder was first weighed in a filtering thimble, which was then placed into the Soxhlet extraction flask. The Soxhlet extraction flask was then filled with 45 mL of toluene, while another 45 mL of toluene were inserted in the reservoir flask (i.e., the boiling flask). The entire extraction apparatus was then placed over a hot plate operating above 110°C. The Soxhlet extraction operated as a closed-loop siphon with multiple cycles of reflux change, allowing the asphaltic fraction to be removed from each EMA binder blend after being "washed" with toluene (Figure 31). The "washing" process was terminated when the toluene became clear and transparent, which typically took up to four hours. The extracted residue was then dried and weighed. The relative difference (i.e., gravimetric

difference) in percent residue between the top and bottom portions of each sample was used as an indication of the chemical compatibility (i.e., phase separation) of the EMA binder. Two replicates were performed for each EMA binder.

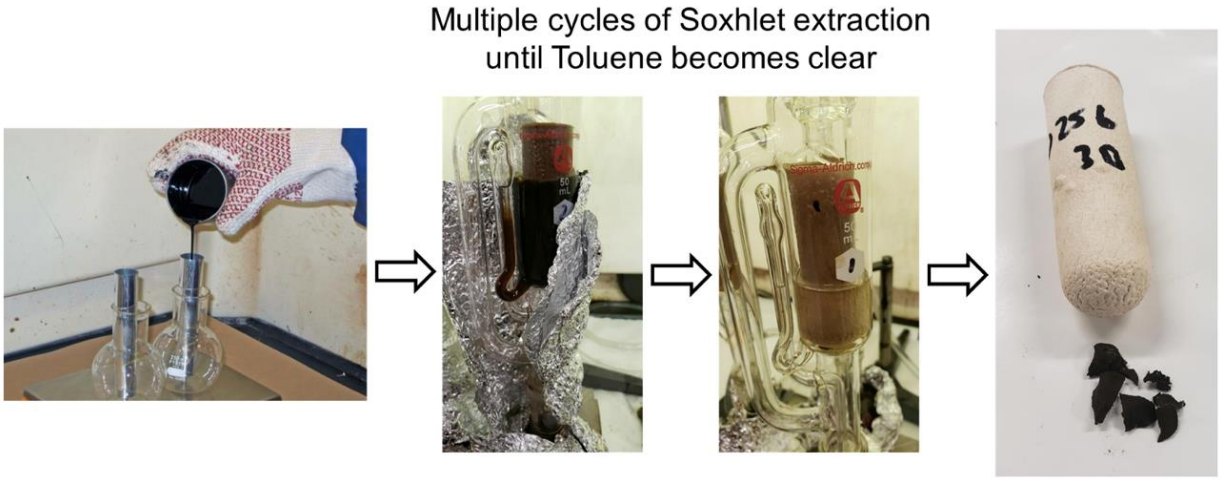

Figure 31. Storage Stability Test Followed by Soxhlet Extraction of EMA Binders

Evaluation of the Morphology of EMA Binders

Fluorescence microscopy is an imaging technique that allows the excitation of fluorophores and subsequent detection of the fluorescence signal, which has been widely used to investigate heterogeneous surfaces where components have different UV light excitation responses. Fluorescence is produced when light excites or moves an electron to a higher energy state, immediately generating light of a longer wavelength, lower energy, and different color to the original light absorbed (ONI). Fluorescence microscopy was employed in this experiment to evaluate the compatibility of the EMA binders by providing information about the distribution and network formation of the epoxy materials within the base asphalt binders. A Zeiss Axiovert 200 Inverted Fluorescence Microscope was used, as shown in Figure 32. For sample preparation, a small drop of heated EMA binder was placed on a microscopic glass slide, and a cover glass was then loaded on top of the asphalt sample and pressed firmly with caution to spread the EMA binder into a uniform thin film. The microscopic slides containing the EMA binder sample were then allowed to cool down to room temperature before testing. The microscope was supported by Nis-Elements BR 4.6 software, through which the images were visually assessed in 10x magnification and captured on a 100 µm scale. Three replicate images were obtained, and each image was analyzed for its particle size distributions using the ImageJ program.

ImageJ is an open-source image processing program designed for multidimensional scientific images. One of the many useful features of ImageJ is that it can calculate the area and pixel value statistics of user-defined selections and intensity-specified objects. This feature was used in this study to determine the area of each epoxy polymer particle in a fluorescence micrograph image and quantify its overall particle size distribution in the EMA binders. One difficulty encountered during the image analysis was deciding a suitable threshold value, as the outlines of the particles detected by the program were highly dependent on the threshold applied. The final threshold value for each EMA binder sample was selected such that visually all the particles were captured, and that the particles were spread enough for the program to avoid accidentally

combining or erasing multiple particles. Figure 33 presents the major steps of analyzing the fluorescence micrographs in ImageJ.

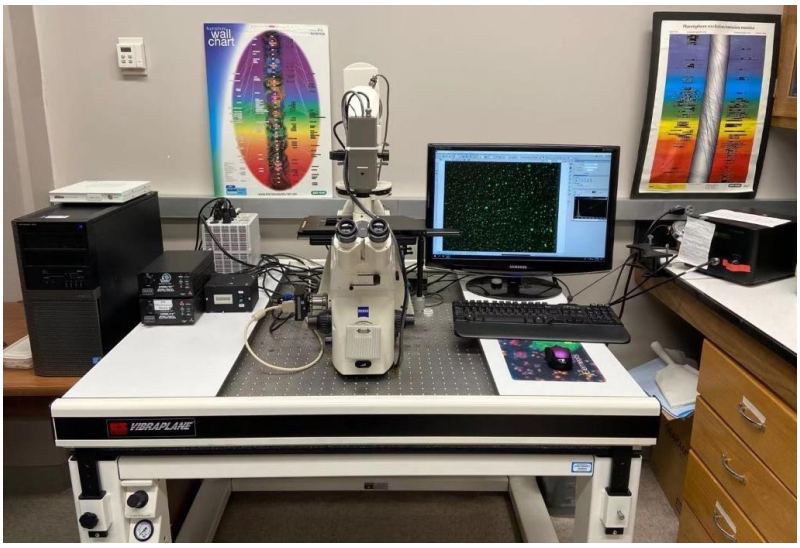

Figure 32. Zeiss Axiovert 200 Inverted Fluorescence Microscope

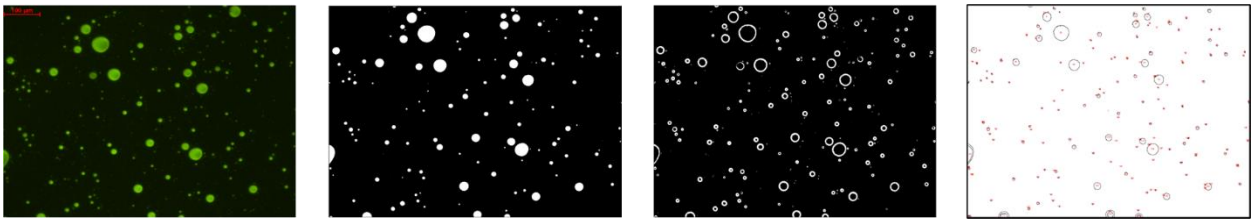

Figure 33. Major Steps of Analyzing Fluorescence Micrographs in ImageJ

3.2 Test Results and Discussion

SARA Fractions

Asphalt binder is often described as a colloidal model (Park and Mansoori, 1988). In this model, the asphaltenes occur in the form of resin-stabilized suspended particles dispersed in an oily matrix constituted by saturates, aromatics, and resins, where some of the resins are adsorbed on the surface of the asphaltenes while others are dissolved in the oily matrix. Figure 34 lists the SARA fractions of the four base asphalt binders selected for epoxy modification in this study. When ranking the asphalt binders from lower to higher content of saturates, the following order was observed: Binder Z < Binder G < Binder C < Binder A. In terms of aromatics, the following order was observed from lower to higher content: Binder C < Binder G = Binder Z < Binder A. When ranking the asphalt binders from lower to higher content of resins, the following order was observed: Binder A < Binder Z < Binder C < Binder G. Lastly, in terms of asphaltenes, the following order was observed from lower to higher content: Binder G < Binder A < Binder C < Binder Z.

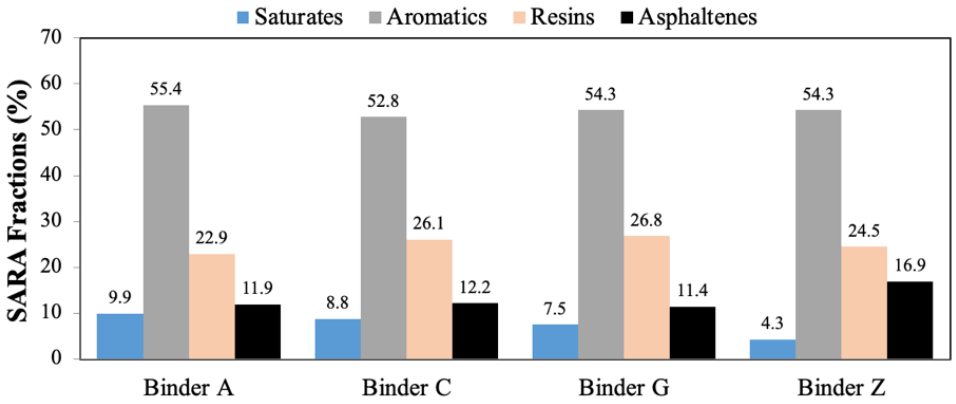

Figure 34. SARA Fractions of the Base Asphalt Binders

The colloidal stability of asphalts can be described by the Gaestel "Colloidal Instability Index" (known as CII or Ic), as shown in Equation 7 (Gaestel et al., 1971). CII is advantageous primarily when comparing the colloidal stabilities of different asphalt binders. As CII increases, the colloidal stability of the asphalt binder decreases. Figure 35 indicates the CII of the four base asphalt binders selected for evaluation in this study. As can be seen, when ranking the asphalt binders from less to more stable in terms of CII, the following order was observed: Binder A < Binder C ≈ Binder Z < Binder G. When assessing the colloidal stability of asphalt binders, which is related to the aggregation or agglomeration of the asphalt fractions, it is important to observe the content of asphaltenes. Asphaltenes from different crude oil sources and processing will differ in composition and chemical structure (Baginska and Gawel, 2004). Therefore, asphalt binders with the same asphaltenes content may differ in colloidal stability. Figure 2 indicates the CII of the six asphalt binders selected for evaluation in this study.

$$CII = \frac{Asphaltenes + Saturates}{Aromatics + Resins} \qquad \text{Equation 7}$$

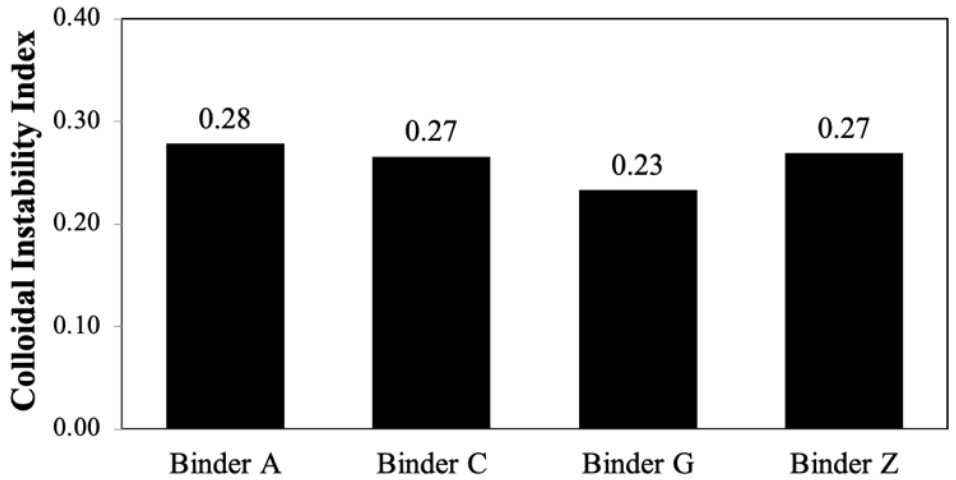

Figure 35. CII of the Base Asphalt Binders

Storage Stability Test and Soxhlet Asphalt Extraction Results

Figure 36(a) presents the gravimetric difference in the residue of the top and bottom portions of the J-EMA binders [i.e., EMA binders prepared with epoxy materials from a foreign source (J)], while Figure 36(b) indicates the aforementioned difference of the U-EMA binders [i.e., EMA binders prepared with epoxy materials from a domestic source (U)]. This difference was determined after the storage stability test followed by the Soxhlet asphalt extraction. As can be seen in Figure 36(a), for the J-EMA binders, the base asphalt binders A and Z showed the best compatibility (i.e., lowest epoxy residue) at 15% and 25% EDRs. When selecting among base Binder G and Z, it was observed that Binder Z allowed a lower epoxy residue (i.e., 0.5 g) at the highest utilized EDR (i.e., 25%) in comparison to Binder G (i.e., 0.8 g). Figure 36(b) shows that the base asphalt binders A and C showed the best compatibility (i.e., lowest epoxy residue) at the evaluated EDRs for the U-EMA binders. These findings were further investigated by fluoresce microscopy analysis.

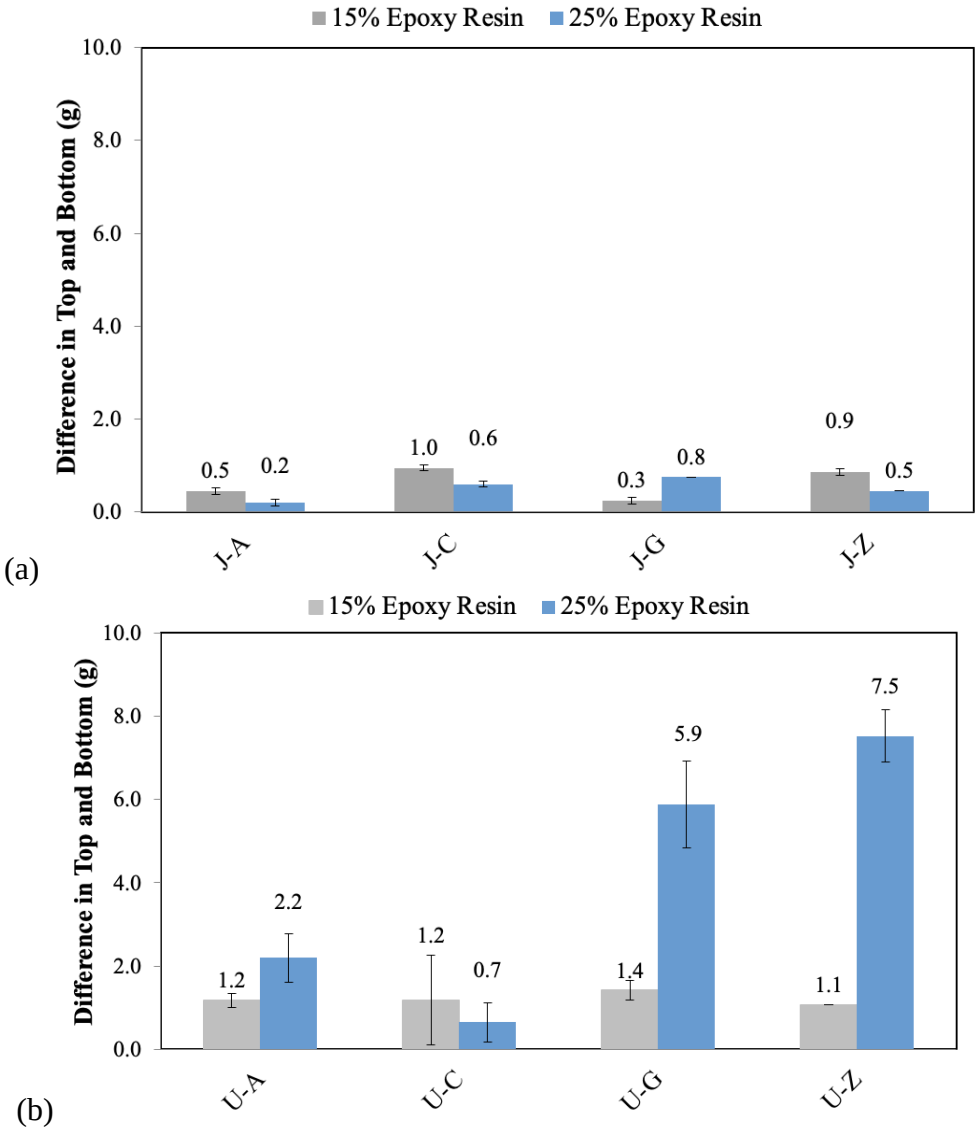

Figure 36. Difference in the Residue of the Top and Bottom Portions after Storage Stability Test Followed by Soxhlet Asphalt Extraction: (a) J-EMA Binders, (b) U-EMA Binders

When comparing the results in Figure 36 with the SARA fractions (Figure 34), it was found that the base asphalt binders with the lowest resin content (i.e., binders A and Z) correlated with the lowest difference in the residue of the top and bottom portions of the J-EMA binders [Figure 37(a)]. On the other hand, the base asphalt binders with highest saturates content (i.e., binders C and A) correlated with the lowest difference in the residue of the top and bottom portions of the U-EMA binders [Figure 37(b)]. Note that the evaluation of the correlation SARA fractions *versus* epoxy resin residue results was performed considering the EDR of 25%.

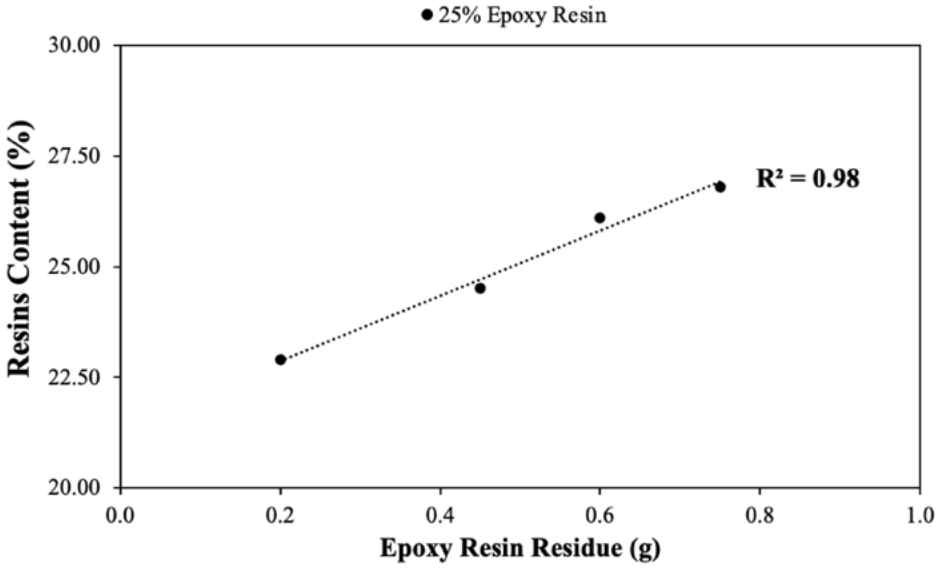

(a)

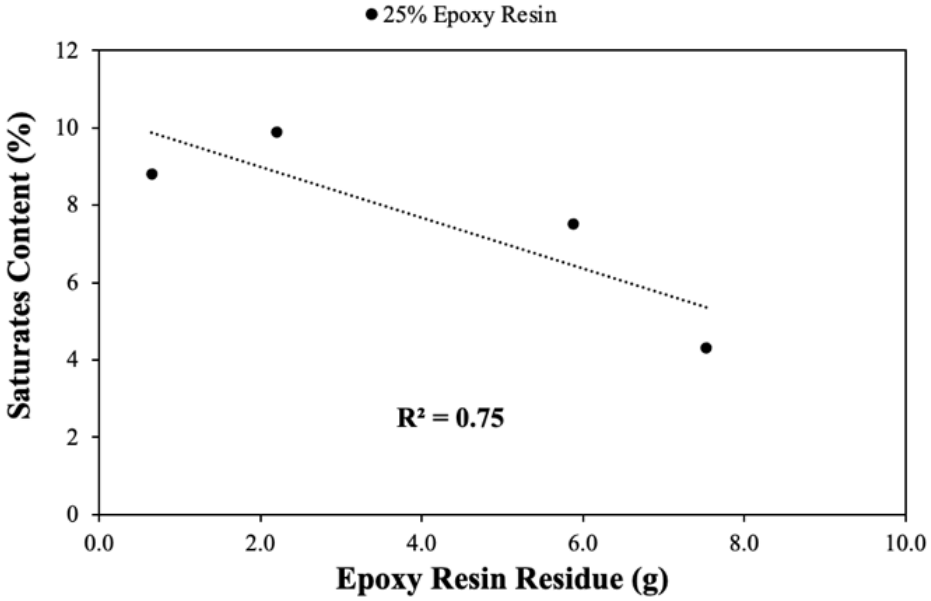

(b)

Figure 37. SARA Fractions *versus* Residue of the Top and Bottom Portions after Storage Stability Test Followed by Soxhlet Asphalt Extraction: (a) J-EMA Binders at 25% EDR, (b) U-EMA Binders at 25% EDR

Fluorescence Microscopy Results

To further screen the compatibility of the four base asphalt binders and the two epoxy materials, the morphology of EMA binders at 15% and 25% EDRs was characterized by means of fluorescence microscopy. In asphalt binders, only aromatics and resins produce strong fluorescence signals, while polymers do not fluoresce. Thus, the UV microscopy visualizes polymer-rich regions due to the presence of fluorescing aromatics and resins trapped in the polymer structure. Figure 38 presents the fluorescence micrographs of the J-EMA binders at 15% EDR, while Figure 39 presents those of the J-EMA binders at 25% EDR. In both figures, the fluorescent and dark phases correspond to the epoxy materials and the base asphalt binders, respectively. Overall, the compatibility between the base asphalt binders and the epoxy materials from a foreign source before curing was observed as fair since the distribution of the epoxy resin in the asphalt phase was not homogeneous. Moreover, as the EDR increased from 15% to 25%, a decrease in compatibility was observed as the distribution of the epoxy resin became less uniform. From the fluorescence micrographs indicated in Figure 38 and Figure 39, the base asphalt binder Z appeared to present the best compatibility with the epoxy materials from a foreign source (J) at both evaluated EDRs.

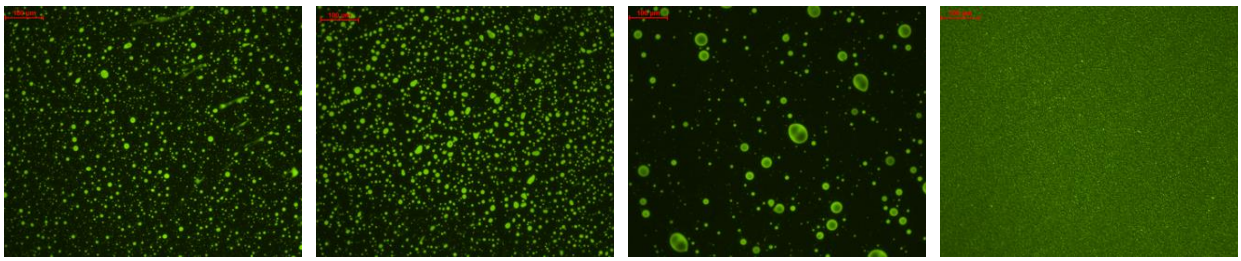

(a) (b) (c) (d)

Figure 38. Fluorescence Micrographs of J-EMA Binders at 15% EDR: (a) Base Binder A, (b) Base Binder C, (c) Base Binder G, (d) Base Binder Z

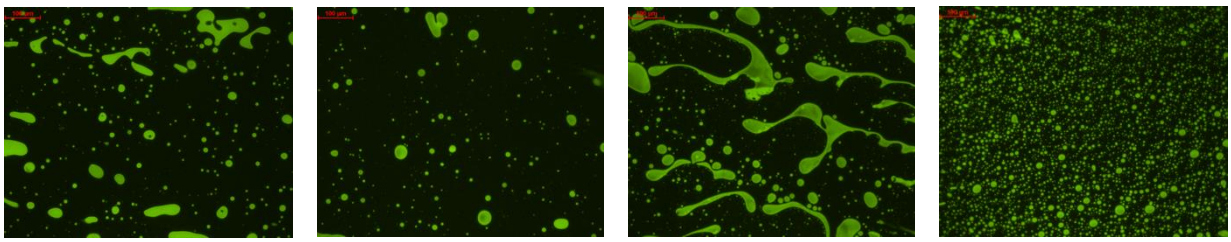

(a) (b) (c) (d)

Figure 39. Fluorescence Micrographs of J-EMA Binders at 25% EDR: (a) Base Binder A, (b) Base Binder C, (c) Base Binder G, (d) Base Binder Z

Figure 40 presents the fluorescence micrographs of the U-EMA binders at 15% EDR, while Figure 41 presents those of the U-EMA binders at 25% EDR. As observed for the J-EMA binders, the compatibility between the base asphalt binders and epoxy materials from a domestic source before curing was also observed as fair, which decreased as the EDR increased from 15% to 25%. From the fluorescence micrographs indicated in Figure 40 and Figure 41, the base asphalt binder C appeared to present the best compatibility with the epoxy materials from a domestic source (U) at both evaluated EDRs.

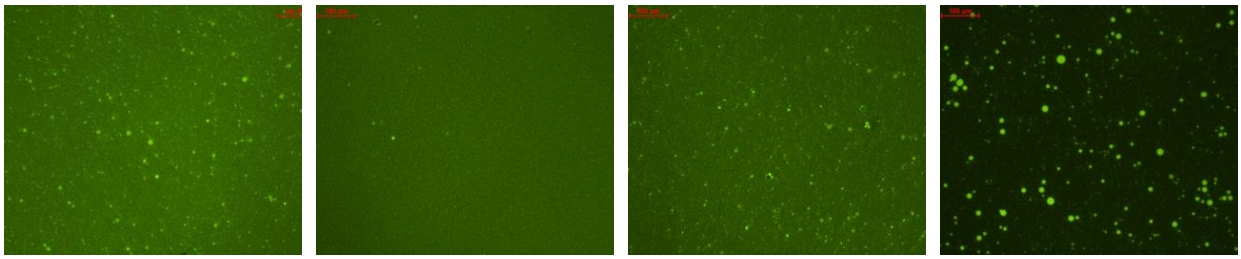

(a) (b) (c) (d)

Figure 40. Fluorescence Micrographs of U-EMA Binders at 15% EDR: (a) Base Binder A, (b) Base Binder C, (c) Base Binder G, (d) Base Binder Z

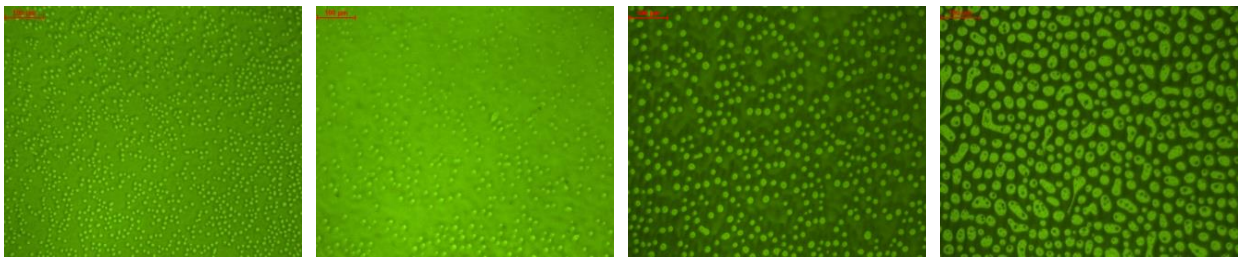

(a) (b) (c) (d)

Figure 41. Fluorescence Micrographs of U-EMA Binders at 25% EDR: (a) Base Binder A, (b) Base Binder C, (c) Base Binder G, (d) Base Binder Z

Table 13 presents a summary of the epoxy particle sizes for each EMA binder obtained from the image analysis using ImageJ. The cumulative distribution curves of the epoxy particle sizes are graphically illustrated in Figure 42 through Figure 45 for J-EMA binders at 15% EDR, J-EMA binders at 25% EDR, U-EMA binders at 15%, and U-EMA binders at 25%, respectively. Using the lowest average and median particle sizes as well as the lowest standard deviation as criteria, the J15Z, J25Z, U15G, and U25A binders seemed to have the best compatibility in their corresponding categories (i.e., combinations of the source of epoxy materials and EDR). Nevertheless, the U15C and U15G binders as well as the U25A and U25C binders had very similar particle size distribution curves as shown in Figure 44 and Figure 45, respectively. Overall, EMA binders at 15% EDR were more compatible than those at 25% EDR because they did not exhibit large-size agglomerated epoxy resin particles, while the agglomeration was prominent in EMA binders at 25% EDR. Furthermore, epoxy materials from a domestic source (U) were more uniformly dispersed within the base binders than those from a foreign source (J). Finally, based on the storage stability test, Soxhlet asphalt extraction, and fluorescent microscopy results, base binders Z and C were selected as the best suitable for modification with epoxy materials from a foreign source and domestic source, respectively.

Table 13. Summary of Epoxy Particle Sizes of EMA Binders at 15% and 25% EDRs

Binder ID	Source of Epoxy Materials	EDR	Average Particle Size (μm^2)	Median Particle Size (μm^2)	Standard Deviation (μm^2)
J15A	Foreign Source (J)	15%	22.08	17.70	19.98
J15C			20.92	15.00	21.51
J15G			46.12	31.00	50.69
J15Z			12.01	7.09	15.52
J25A		25%	45.86	35.40	79.06
J25C			42.10	28.30	61.30
J25G			34.64	22.60	239.20
J25Z			31.55	23.00	34.10
U15A	Domestic Source (U)	15%	17.99	8.80	34.43
U15C			12.14	7.09	18.30
U15G			11.71	6.64	17.22
U15Z			26.22	12.80	35.23
U25A		25%	15.73	6.20	22.62
U25C			17.07	3.54	33.86
U25G			42.05	7.09	44.21
U25Z			24.37	7.97	80.87

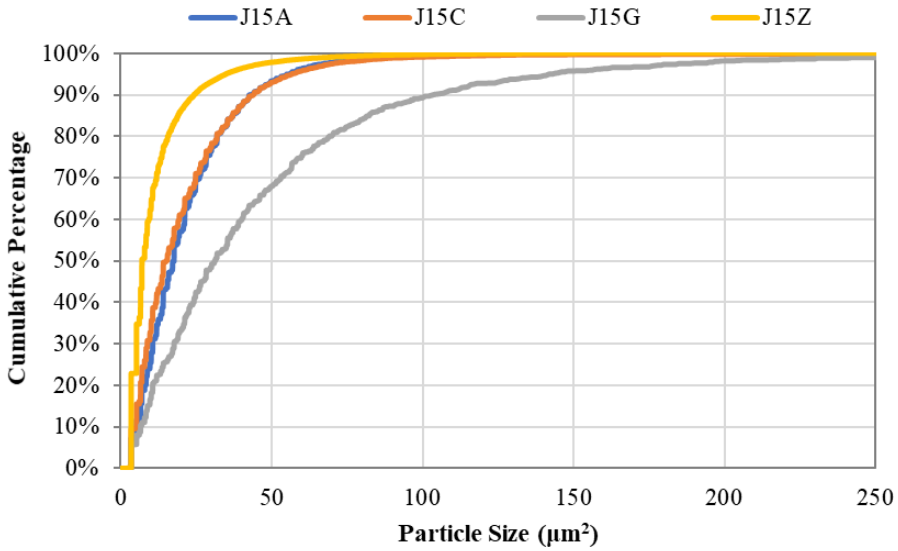

Figure 42. Cumulative Distribution Curves of Epoxy Particle Sizes for J-EMA Binders at 15% EDR

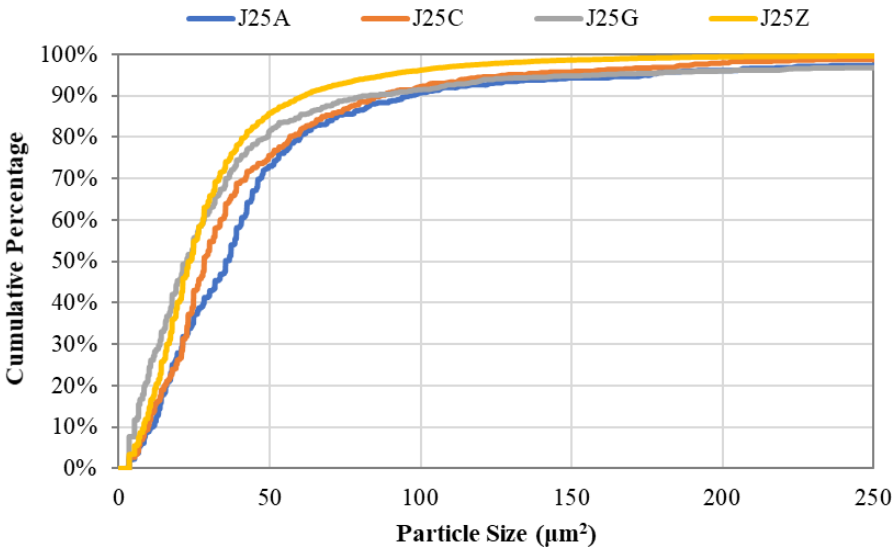

Figure 43. Cumulative Distribution Curves of Epoxy Particle Sizes for J-EMA Binders at 25% EDR

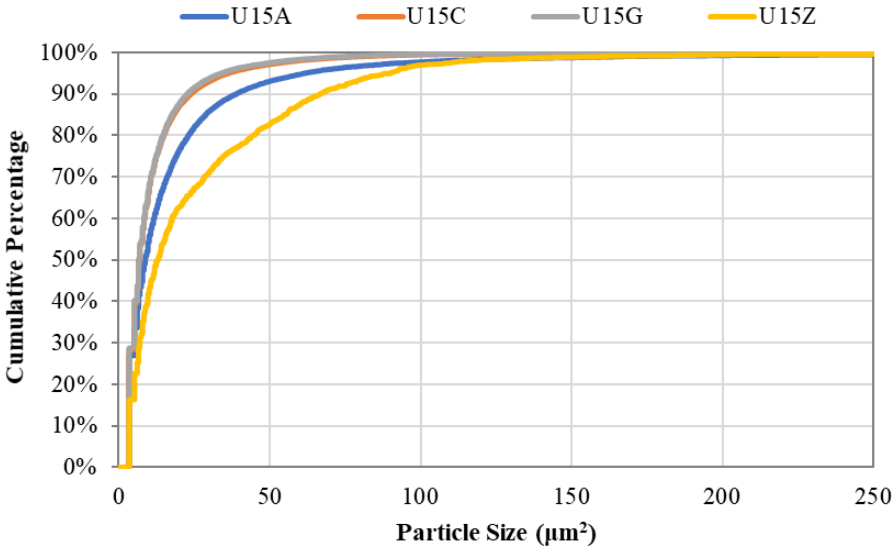

Figure 44. Cumulative Distribution Curves of Epoxy Particle Sizes for U-EMA Binders at 15% EDR

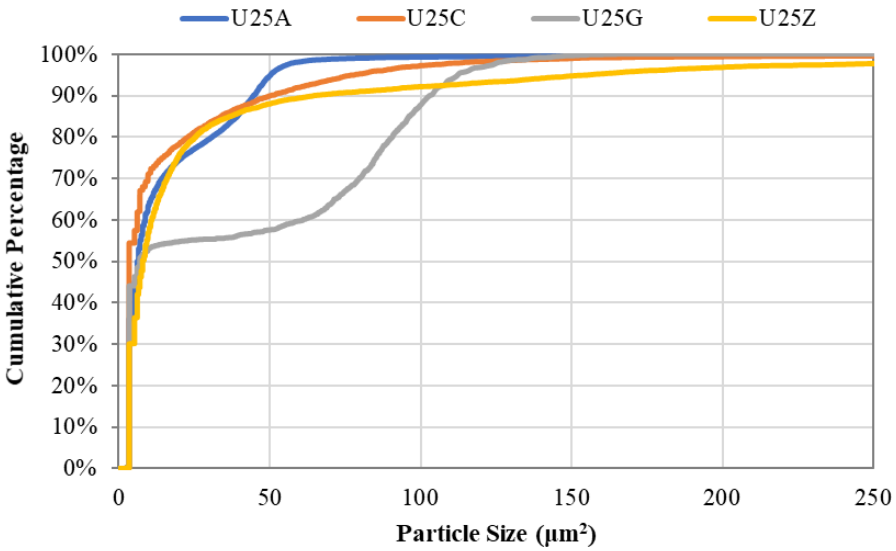

Figure 45. Cumulative Distribution Curves of Epoxy Particle Sizes for U-EMA Binders at 25% EDR

3.3 Summary of Findings

From the SARA analysis, it was observed that the four base asphalt binders were chemically different in terms of content of saturates, aromatics, resins, and asphaltenes. Moreover, when ranking the four base asphalt binders from least stable to most stable in terms of CII, the following order was observed: Binder A < Binder C ≈ Binder Z < Binder G. When analyzing the epoxy residue (i.e., gravimetric difference in the residue of the top and bottom samples) of the EMA binders at 15% and 25% EDRs, which was determined after the storage stability test followed by the Soxhlet asphalt extraction, it was observed that the base asphalt binders A and Z showed the best compatibility with the epoxy materials from a foreign source (J). On the other hand, results indicated that the base asphalt binders A and C were most compatible with the epoxy materials from a domestic source (U). Furthermore, base asphalt binders with the lowest resin content (i.e., binders A and Z) allowed lower precipitation of the epoxy resin from foreign source; while the base asphalt binders with the highest saturates content (i.e., binders C and A) allowed lower precipitation of the epoxy resin from domestic source.

Moreover, fluorescence microscopy showed that the compatibility between the four base asphalt binders and the two epoxy materials was fair (i.e., not homogeneous). As the EDR increased from 15% to 25%, a decrease in compatibility of the EMA binders was observed as the distribution of the epoxy resin became less uniform. Based on visual observation and image analysis of the fluorescence micrographs, J-EMA binders prepared with base asphalt binder Z and U-EMA binders prepared with base asphalt binder C, at both 15% and 25% EDRs, exhibited the best morphology and were considered to be most compatible. Therefore, binders Z and C were selected as the most suitable (i.e., chemically compatible) base binders for modification with the epoxy materials from a foreign and domestic source, respectively.

CHAPTER 4. DETERMINATION OF OPTIMUM EPOXY DOSAGE RATE

This chapter presents the experimental plan, test results, and findings of Experiment 2 of the study. The objective of this experiment was to determine the optimum (i.e., most cost-effective) EDR with respect to material cost and mixture performance properties. This experiment consisted of two sub-experiments: binder testing experiment and mixture testing experiment. The binder testing experiment focused on evaluating the curing behavior, aging characteristics, rheological properties, cohesive and adhesive properties, and moisture susceptibility of EMA binders at 15% and 25% EDRs *versus* a PG 76-22 PMA binder and a HP binder. The mixture testing experiment was to evaluate the raveling resistance, tensile strength, and fracture resistance of OGFC mixtures prepared with EMA binders at different EDRs ranging from 15% to 40% *versus* a control PG 76-22 PMA binder. All the EMA mixtures were prepared with a "drop-in" approach following two existing mix designs provided by FDOT and had the same aggregate gradations and asphalt binder contents as the control PMA mixtures. Three mix aging conditions were included to account for the impact of asphalt aging on the performance properties of OGFC mixtures. Results of this experiment were analyzed to select a cost-effective EDR that could consistently provide EMA OGFC mixtures with better performance properties than the control PMA mixtures so that they would have the potential of increasing the life span of OGFC in Florida.

4.1 Experimental Plan

Materials and Mix Designs

As with Experiment 1, two different sources of epoxy materials were used. The domestic (U) epoxy materials consist of epoxy resin (Part A) and a blend of acid-based curing agent and soft asphalt binder (Part B), while the foreign (J) epoxy materials consist of epoxy resin (Part A) and amine-based curing agent (Part B). Based on the findings of Experiment 1, as discussed in Chapter 3, a PG 67-22 base binder from source C was used for modification with the epoxy materials from a domestic source, while a PG 67-22 base binder from source Z was used to prepare EMA binders with the epoxy materials from a foreign source. The same nomenclature of "(epoxy source, U or J) (EDR, 15% to 40%) (base binder source, C or Z)" as explained in Chapter 3 is followed to name EMA binders prepared with different sources of epoxy materials, EDRs, and base binders. For example, "U15C" denotes an EMA binder prepared with the domestic epoxy materials, 15% EDR, and a PG 67-22 base binder from source C.

Due to the thermosetting behavior of epoxy materials, conventional Superpave asphalt binder tests may not be applicable to EMA binders at a EDR of 30% and above. Therefore, Superpave asphalt binder tests were conducted on EMA binders at 15% and 25% EDRs only to avoid the risk of damaging the test devices. These two dosages were selected based on the findings of a preliminary proof-of-concept experiment at NCAT, which indicated that an EMA binder at 8% EDR did not perform as well as a PG 76-22 PMA binder in terms of creep compliance, fatigue resistance, and aging resistance (Moraes and Yin, 2020). Table 14 presents the proposed binder testing matrix for Experiment 2. Four EMA (i.e., U15C, U25C, J15Z, and J25Z) binders were tested in comparison against a PG 76-22 PMA binder and a HP binder as control.

Table 14. Proposed Binder Testing Matrix for Experiment 2

Factor Name	Factor No.	Description
Epoxy materials and base binder	2	Domestic source epoxy materials + base binder C Foreign source epoxy materials + base binder Z
Epoxy dosage rate	2	15%, 25%
EMA binders	4	U15C, U25C, J15Z, J25Z
PMA control binder	1	Selected from FDOT's approved product list
HP control binder	1	Selected from FDOT's approved product list

Table 15 presents the proposed mixture testing matrix for Experiment 2. Eight EMA binders were prepared by blending two base binders (i.e., C and Z) with their respective epoxy materials at four EDRs ranging from 15% to 40%. These eight EMA binders and a PG 76-22 PMA binder (as control) were used to prepare OGFC mixtures based on two FDOT approved FC-5 mix designs. Table 16 presents the job mix formula (JMF) of these two mixes: one with granite aggregates (GRN1) and the other with limestone aggregates (LMS).

Table 15. Proposed Mixture Testing Matrix for Experiment 2

Factor Name	Factor No.	Description
Epoxy materials and base binder	2	Domestic source epoxy materials + base binder C Foreign source epoxy materials + base binder Z
Epoxy dosage rate	4	15%, 25%, 30%, 40%
EMA binders	8	U15C, U25C, U30C, U40C J15Z, J25Z, J30Z, J40Z
PMA control binder	1	Selected from FDOT's approved product list
Mix design (aggregate source)	2	Granite (GRN1), limestone (LMS)

Table 16. Job Mix Formula Summary of GRN1 and LMS Mixes

Mix Design ID		GRN1	LMS
Aggregate Gradation (% Passing)	3/4"	100	100
	1/2"	99	94
	3/8"	71	74
	No. 4	24	23
	No. 8	9	10
	No. 16	5	8
	No. 30	4	6
	No. 50	3	5
	No. 100	3	4
	No. 200	2.5	3.3
Combined G_{sb}		2.769	2.417
JMF OBC (%)		6.8	6.9
Additives		0.3% Cellulose Fiber, 1.0% Hydrated Lime	Cellulose Fiber 0.3%

Preparation of EMA Binders and Mixtures

J-EMA Binders and Mixtures

The preparation of J-EMA binders started with preheating the PG 67-22 base binder Z for two hours at 130°C, and epoxy resin (Part A) and curing agent (Part B) for one hour at 60°C. The epoxy resin and curing agent were first blended for two minutes using a low shear mixer, which was placed on a hot plate to maintain a constant blending temperature of approximately 130°C. Then, the PG 67-22 base binder was added and blended for another 15 minutes. It is important to follow the above order of mixing different component materials for preparing J-EMA binders. A different blending procedure was previously followed in which the PG 67-22 base binder was first blended with epoxy resin before adding the curing agent. Because the curing agent was added later in the process, it did not fully react with the epoxy resin and as a result, created a significant amount of fumes when the J-EMA binder was mixed with hot aggregates. Table 17 presents the blending proportions of the component materials for J-EMA binders at various EDRs.

Table 17. Blending Proportions of Component Materials for J-EMA Binders

Binder ID	EDR	Proportions (% by weight)		
		PG 67-22 Base Binder Z	Part A: Epoxy Resin	Part B: Curing Agent
J15Z	15%	85.00	8.80	6.20
J25Z	25%	75.00	14.60	10.40
J30Z	30%	70.00	17.55	12.45
J40Z	40%	60.00	23.40	16.60

For the preparation of J-EMA mixtures, the aggregates were preheated at 188°C overnight. Immediately after the J-EMA binder was prepared, the aggregates, lime, and fiber (if used) were added into the mixing bucket and mixed for 30 seconds. Then the J-EMA binder was added into the mixer and mixed for one minute. The final mixing temperature of the mixture was around 157 to 160°C. After mixing, the loose mixture was conditioned in an oven for two hours at 157°C and then compacted for 50 gyrations using a SGC. The compacted specimen was allowed to cool in the SGC mold for five minutes and then extruded for further cooling in front of a fan.

U-EMA Binders and Mixtures

For the preparation of U-EMA binders, the PG 67-22 base binder C and Part B of the epoxy materials (a blend of acid-based epoxy curing agent and soft asphalt binder) were preheated for two hours at 130°C and blended for 15 minutes using a low shear mixer. The epoxy resin (Part A) was preheated for 15 minutes at 130°C and manually blended with the mixture of the PG 67-22 base binder, epoxy curing agent, and soft asphalt binder for approximately 30 to 40 seconds using a stirring rod. After the epoxy resin was added, it started to react with the acid-based curing agent, which significantly increased the viscosity of the U-EMA binder and sometimes triggered thermosetting behavior for those at a EDR of 25% or higher. Therefore, high EDR U-EMA binders had a limited time window to remain workable before they could be mixed with the aggregates for mixture production. The duration of this time window varied greatly depending on the base binder used for epoxy modification, EDR, temperature, and other factors. Beyond the workable time window, the U-EMA binders reached the final stage of

polymerization wherein the cross-linking reaction took place and as a result, could not be reheated for additional testing or mixing with the aggregates. Table 18 presents the blending proportions of the component materials for U-EMA binders at various EDRs.

Table 18. Blending Proportions of Component Materials for U-EMA Binders

Binder ID	EDR	Proportions (% by weight)		
		PG 67-22 Base Binder	Part A: Epoxy Resin	Part B: Blend of Curing Agent and Soft Asphalt Binder
U15C	15%	62.50	7.30	30.20
U25C	25%	37.50	12.10	50.40
U30C	30%	25.00	14.50	60.50
U40C	40%	0.00	19.40	80.60

The U-EMA mixtures were prepared in a similar manner as the J-EMA mixtures with three exceptions. The first exception was that the aggregates were preheated at a lower temperature of 143°C instead of 188°C to ensure a final mixing temperature of approximately 121°C per recommendations of the epoxy asphalt manufacturer. The second one was that hydrated lime was not used in U-EMA mixtures per recommendations of the epoxy asphalt supplier because of the concern that hydrated lime may have an undesired reaction with the acid-based epoxy curing agent. The last exception was that after mixing, the loose mixture was conditioned for 30 to 50 minutes at 121°C instead of two hours at 157°C prior to compaction. This reduced conditioning time and temperature was selected based on the viscosity curing data of the U-EMA binders provided by the epoxy asphalt manufacturer.

Binder Testing Plan

Table 19 summarizes the selected laboratory tests for performance evaluation of EMA, PMA, and HP binders in the binder testing experiment. Test procedures are provided as follows.

- Curing Behavior: When the two components of the epoxy materials (i.e., Part A and Part B) are blended, the resulting EMA binder becomes more viscous during curing, and is chemically cross-linked (i.e., irreversibly) when fully cured, which means that it cannot be melted or dissolved in solution. Thus, it is important to determine the amount of time available for EMA binders to remain workable, where this time period depends on the curing rate of the epoxy resin, EDR, and temperature. In this study, the rotational viscosity test (AASHTO T 316) was conducted to characterize the curing time of EMA binders at various temperatures (i.e., 120, 145, 165, and 190°C).
- Aging Characteristics: Aging of asphalt binders is induced by chemical or physicochemical changes that occur during mixture production (i.e., short-term aging) and later throughout the service life of a pavement (i.e., long-term aging). To understand its aging mechanism, each EMA binder was subjected to short-term aging in an oven at 120°C for a specific duration as follows: J15C – five hours, J25C – eight hours, U15C – six hours, and U25C – five hours. The duration of the short-term aging of the EMA binders reflects the time required for each binder to be fully cured at 120°C, which was obtained from the rotational viscosity results. The EMA binders were then subjected to long-term aging in PAV for 20 hours at 100°C, per AASHTO R 28.

- Rheological Characterization: The performance grades of the base asphalt binders and EMA binders was determined per AASHTO M 320. Moreover, three DSR tests were performed to evaluate their rheological properties: MSCR at 67°C (AASHTO M 332), LAS test at 28°C (AASHTO TP 101), and temperature-frequency sweep test with master-curve generation over the range of 0.1 to 10 rad/s and seven test temperatures (i.e., 10, 20, 30, 40, 50, 60 and 70°C). The MSCR test was used to assess the impact of EMA binders on the rutting resistance of asphalt mixtures. The LAS test was used to evaluate the fatigue resistance of EMA binders at an intermediate temperature. The master-curve data was used to evaluate the Glover Rowe (*G-R*) parameter criteria of 180 kPa and 600 kPa in a Black Space diagram with $\delta_{15°C,\ 0.005\ rad/s}$ *versus* $|G^*|_{15°C,\ 0.005\ rad/s}$ as an indication of the effect of epoxy materials on the cracking potential of EMA binders at intermediate temperature. In addition, the BBR ΔT_c parameter was also determined for evaluating the non-load related cracking potential of EMA binders.
- Cohesive and Adhesive Properties: Volatile-free curing, low shrinkage, and excellent shear strength make epoxy resin a premier adhesive (Peng and Riedl, 1995). Thus, the incorporation of epoxy resin in asphalt binders is expected to result in higher bond strength and reduced risk of adhesive and cohesive failures in asphalt mixtures. In this study, the adhesive and cohesive properties of EMA binders, as well as the impacts of aggregate chemistry (i.e., mineralogy) and the presence of moisture on the adhesive properties of EMA binders, were evaluated using the BBS Test (AASHTO T 361). As shown in Figure 46, the BBS device is comprised of a portable pneumatic adhesion tester, pressure hose, piston, reaction plate, and a metal pull-out stub. The BBS testing procedure is briefly summarized as follows: (1) before testing, the air supply and pressure hose connection should be checked. Set the rate of loading to 100 psi/sec; (2) place circular spacer under the piston to make sure that the pull-off system is straight, and that eccentricity of the stub is minimized; (3) carefully place the piston around the stubs and resting on the spacers not to disturb the stub or to induce unnecessary strain in the sample. Screw the reaction plate into the stub until the pressure plate just touches the piston; (4) apply pressure at specified rate. After testing, the maximum pull-off tension is recorded, the failure type at the asphalt-aggregate interface is observed, and the surface area exposed is manually interpreted to differentiate the mode of failure (cohesive, adhesive, or combined failure mode) (Moraes et al., 2011), as shown in Figure 47. The pull-off tensile strength (POTS), also referred to as the bond strength, is calculated in accordance with Equation 8 before and after the immersion of each asphalt-aggregate system in water for 24 hours at 40°C (Figure 48). The average pull-off strength was calculated from three replicates. In this study, the aggregate substrates used were two types of granite selected by FDOT.

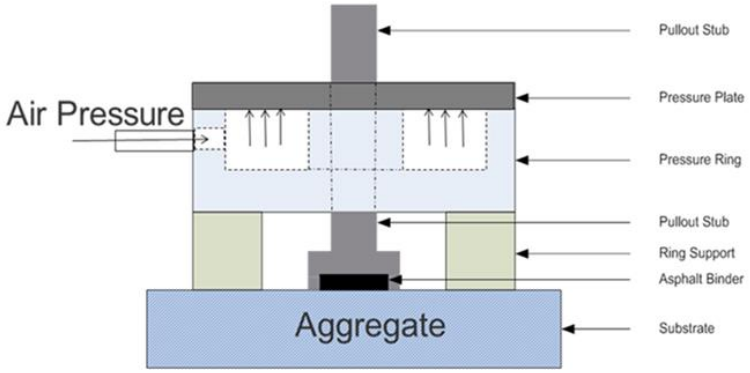

Figure 46. Binder Bond Strength Test Schematic (Moraes et al., 2011)

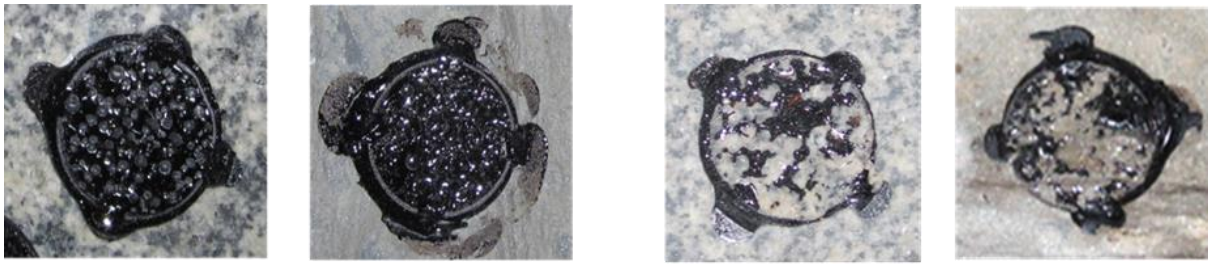

Granite **Limestone** **Granite** **Limestone**

(a) (b)

Figure 47. BBS Test Failure Type: (a) Mainly Cohesive Failure, (b) Mainly Adhesive Failure (Moraes et al., 2011)

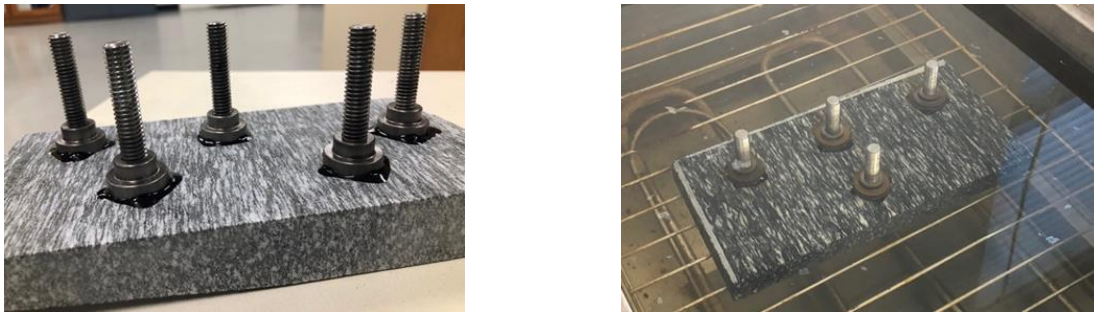

(a) (b)

Figure 48. Binder Bond Strength Test: (a) Asphalt-Aggregate System, (c) Moisture Conditioning @ 40°C

$$POTS = \frac{(BP \times Ag) - C}{A_{ps}}$$ Equation 8

Where,

A_g = Contact Area of Gasket with Reaction Plate (mm^2);
BP = Burst pressure (kPa);
A_{ps} = Area of Pull-off Stub (mm^2); and
C = Piston Constant.

Table 19. Laboratory Tests for Performance Evaluation of EMA, PMA, and HP Binders

Property	Test Type	Research Parameter
Curing Behavior	Rotational Viscometer	Viscosity Curve
Oxidative Aging	Short-term Aging in an Oven at 120°C, PAV	Rheological Properties
Rheological Characterization	DSR & BBR	Performance Grade High Temperature: MSCR Intermediate Temperature: LAS, G-R parameter Low Temperature: ΔT_c
Cohesive & Adhesive Properties and Moisture Susceptibility	Binder Bond Strength	Pull-off Tensile Strength

Mixture Testing Plan

The mixture testing plan of Experiment 2 focused on evaluating the raveling resistance, tensile strength, and fracture resistance of OGFC mixtures containing EMA binders at different EDRs *versus* a control PMA binder using the Cantabro and IDT tests. Both tests were conducted under three mix aging conditions to account for the impact of asphalt oxidative aging. The first aging condition corresponded to a short-term aging (STA) (or the unaged) condition per AASHTO R 30. The second aging condition was a long-term aging (LTA1) condition where the mixture specimens were aged in an environmental chamber for 10 days at 85°C prior to being tested (Figure 49). The last aging condition was an extended long-term aging (LTA2) where the mixture specimens were aged in an environmental chamber for 20 days at 85°C prior to testing. These two LTA protocols were selected for this study instead of those recently developed for aging loose mixtures prior to compaction, because the loose mixtures could be very difficult to be compacted after the EMA binders (especially those at high EDRs) become completely polymerized. However, it remains unknown how these two LTA protocols correlate to the field aging of OGFC in Florida, which is a limitation of this study and warrants further investigation.

Figure 49. Aging of Compacted OGFC Mixture Specimens in the Environmental Chamber

The Cantabro test was performed in accordance with AASHTO TP 108-14. During the test, an OGFC specimen was placed inside the Los Angeles abrasion machine without the steel charges and allowed to freely rotate within the drum at a rate of 30 to 33 revolutions per minute for 300 revolutions. The specimen was then removed from the abrasion machine and weighed after discarding the loose mixture particles (Figure 50). Three replicate specimens were tested for each mixture. The Cantabro mass loss was calculated as the relative change between the final weight and the initial weight of the specimen. The Cantabro mass loss is indicative of the overall durability of OGFC mixtures, where a lower value is desired for better durability and raveling resistance.

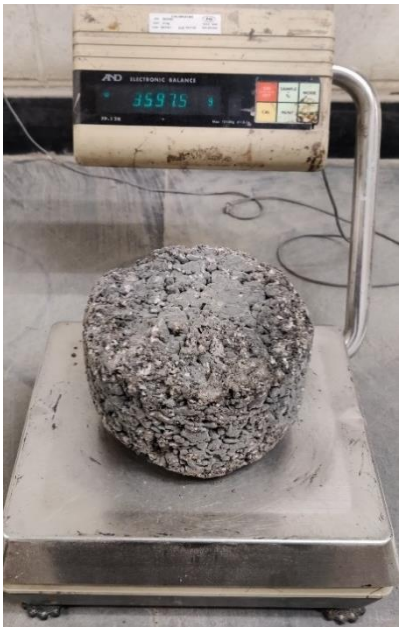

Figure 50. Weighing an OGFC Mixture Specimen after the Cantabro Test

The IDT test was conducted in the same manner as the IDEAL-CT per ASTM D8225-19. The OGFC specimens were compacted to 50 gyrations and then cut into two halves with a height of appropriately 56 mm. During the test, a monotonic load was applied along the specimen at a constant displacement rate of 50 mm/min. Figure 51 presents an example of the load-displacement curve from the test. Six replicate specimens were tested for each mixture.

In this study, the IDT test results were analyzed based on the tensile strength and fracture energy parameters instead of the cracking tolerance index (CT_{Index}) as described in ASTM D8225-19. Although CT_{Index} has proved to be an effective index parameter for evaluating the cracking resistance of dense-graded and gap-graded asphalt mixtures, its calculation requires the determination of the post-peak slope of the load-displacement curve to indicate the relative brittleness of the mixture, which, however, is not applicable to OGFC mixtures because of the significantly high air voids associated with the open-graded aggregate structure. Furthermore, the CT_{Index} results of OGFC mixtures was found to have extremely high variability among the replicates. The coefficient of variation (COV) (out of six replicates) of different mixtures tested in this experiment varied greatly from 6% to 107%.

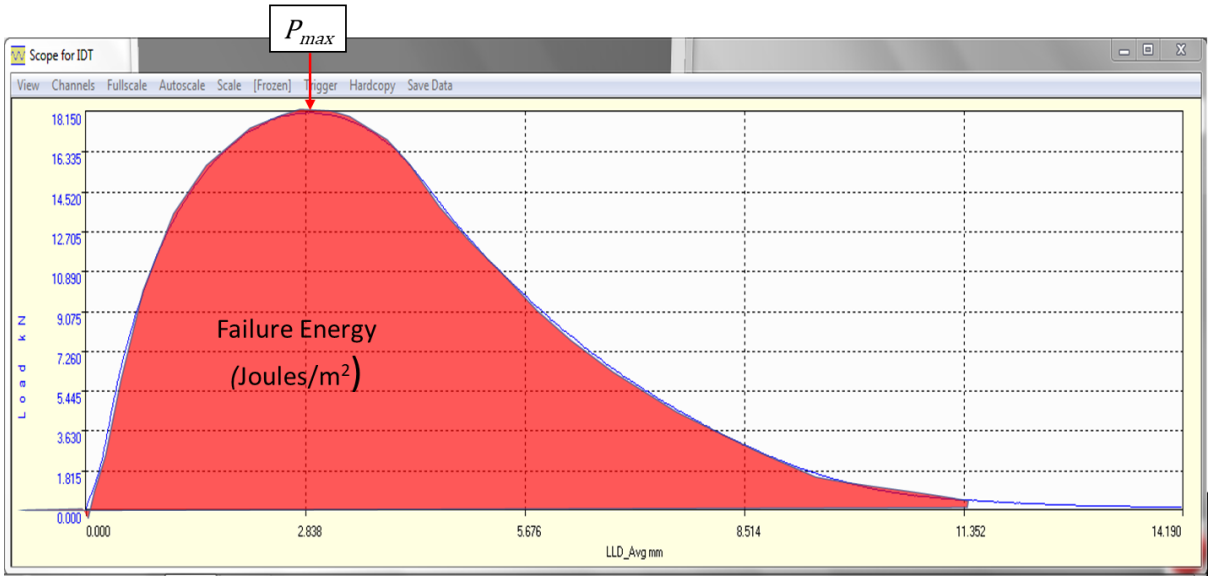

Figure 51. Example of Load-Displacement Curve from the IDT Test

Tensile strength (σ) was calculated based on the peak load and dimensions of the specimen, as shown in Equation 9. Fracture energy (G_f) was calculated as the area under the entire load-displacement curve (Figure 51) divided by the area of the cracking face using Equation 10. G_f indicates the amount of energy required to create a unit surface area of a crack within the mixture. Higher σ and G_f values are desired for OGFC mixtures with better strength and fracture resistance characteristics.

$$\sigma = \frac{2 * P_{max}}{\pi * T * D} \qquad \text{Equation 9}$$

Where,

σ = tensile strength, psi;
P_{max} = peak load, lbf;
T = sample thickness, inch; and
D = sample diameter, inch.

$$G_f = \frac{W}{A} \qquad \text{Equation 10}$$

Where,

G_f = fracture energy, J/m2;
W = work of failure, J; and
A = area of cracking face, m^2.

4.2 Test Results and Discussion

Binder Testing Experiment Results

Investigation of Curing Behavior of EMA Binders by Means of Rotational Viscosity Results

Figure 52 presents the rotational viscosity results of the J-EMA binders collected at different curing intervals (i.e., time) and three temperatures (i.e., 120, 145, and 165ºC). As can be

observed for both 15% [Figure 52(a)] and 25% [Figure 52(b)] EDRs, as the temperature increased, the viscosity of the J-EMA binders decreased, and the time required to achieve a fully cured stage (i.e., a quasi-plateau in viscosity) became shorter. Moreover, as the EDR increased from 15% to 25%, the time to reach the cured stage slightly decreased for each temperature. Note that the stage of a constant viscosity in this study was selected as the indication of a complete epoxy reaction within the EMA binder. Table 20 presents the rotational viscosity results and indicates the time required by the J-EMA binders to be fully cured (i.e., presenting constant viscosity) at a specific temperature.

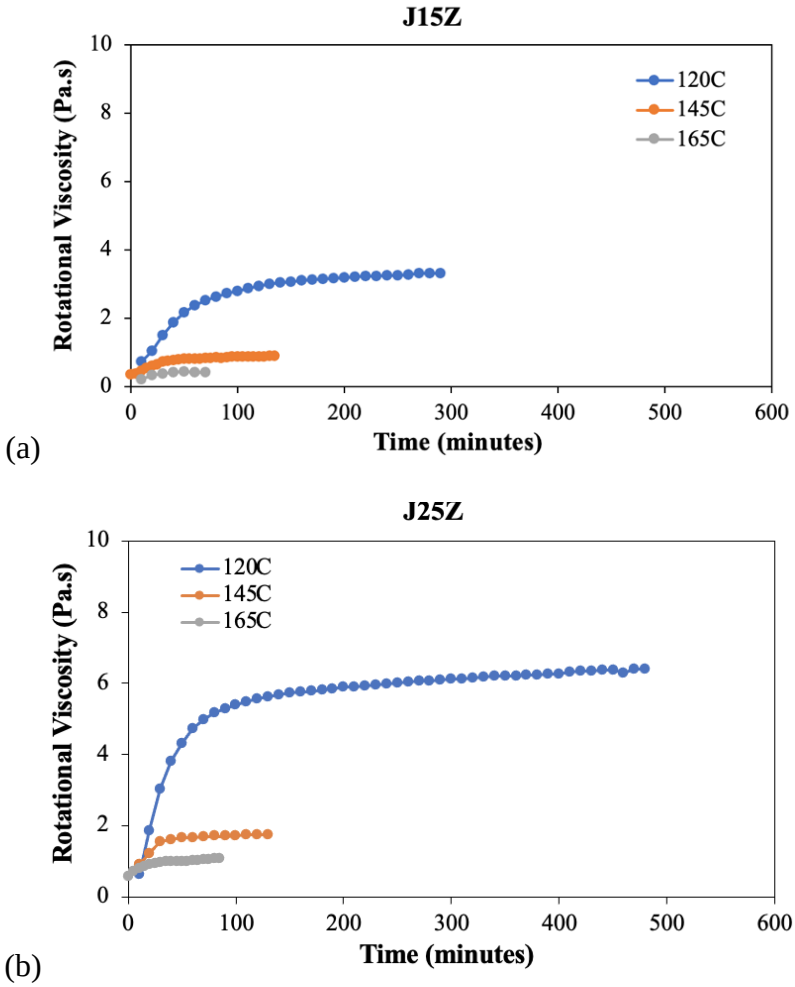

Figure 52. Rotational Viscosity Results *versus* Time at 120, 145, and 165°C: (a) J15C EMA Binder, (b) J25C EMA Binder

Figure 53 presents the rotational viscosity results of the U-EMA binders collected at different curing intervals and temperatures (i.e., 120 and 165ºC). The findings were similar to those of the J-EMA binders. Regardless of the EDRs, as the temperature increased, the viscosity of the U-EMA binders decreased and the time to achieve a fully cured stage shortened. Furthermore, as the EDR increased from 15% [Figure 53(a)] to 25% [Figure 53(b)], the duration of the curing process decreased for each temperature. Furthermore, different than what was observed when comparing the curing time of the J-EMA binders at 15% and 25% EDR, the curing rate of the U25C was much faster than the U15C at both 120 and 160°C. Table 21 presents the summary of

the rotational viscosity results and indicates the time required for each U-EMA binder to be fully cured at a specific temperature.

Table 20. Curing Behavior of J-EMA Binders by Means of Rotational Viscosity at 20 RPM

Binder ID	Temperature (°C)	Initial Viscosity* (Pa·s)	Fully Cured EMA Binder	
			Viscosity at Fully Cured Stage (Pa·s)	Time to Reach the Fully Cured Stage (Minutes)
J15Z	120	1.033	3.212	220
	145	0.588	0.863	100
	165	0.315	0.400	60
J25Z	120	1.875	5.887	200
	145	1.212	1.762	120
	165	0.913	1.000	45

*Measured after sample was conditioned at the testing temperature for 20 minutes.

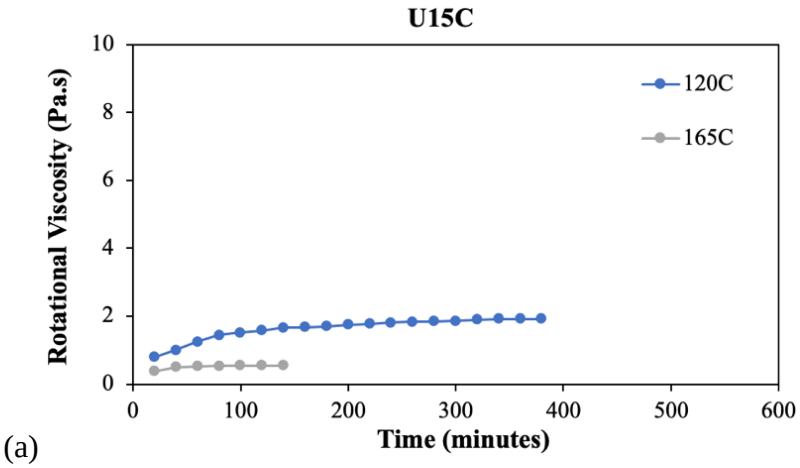

(a)

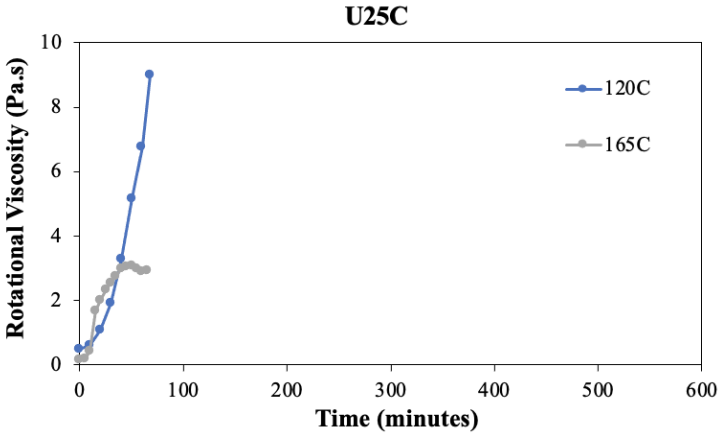

(b)

Figure 53. Rotational Viscosity Results *versus* Time at 120, 145, and 165°C: (a) U15C EMA Binder, (b) U25C EMA Binder

Table 21. Curing Behavior of U-EMA Binders by Means of Rotational Viscosity at 20 RPM

Binder ID	Temperature (°C)	Initial Viscosity* (Pa·s)	Fully Cured EMA Binder	
			Viscosity at Fully Cured Stage (Pa·s)	Time Period to Reach the Fully Cured Stage (Minutes)
U15C	120	0.788	1.925	360
	165	0.500	0.550	140
U25C	120	1.087	8.996	68
	165	2.000	3.062	50

*Measured after sample was conditioned at the testing temperature for 20 minutes.

Table 22 summarizes the rotational viscosity results at different temperatures (i.e., 120, 145, 165, and 190°C) of the base asphalt binders C and Z, as well as the PMA and HP binders. As expected, the SBS-modified binders showed higher viscosity values than the base binders at the four testing temperatures. Due to the higher dosage of SBS polymer, the HP binder showed higher viscosity than the PMA binder at all testing temperatures.

Table 22. Rotational Viscosity at 20 RPM and Different Temperatures

Binder ID	Temperature (°C)	Viscosity (Pa·s)
Base Binder C	120	1.051
	145	0.290
	165	0.127
	190	0.055
Base Binder Z	120	1.380
	145	0.370
	165	0.165
	190	0.074
PMA	120	3.575
	145	0.988
	165	0.450
	190	0.200
HP	120	8.771
	145	1.262
	165	0.563
	190	0.275

Figure 54 presents the rotational viscosity results of the cured J-EMA binders in comparison to those of the base asphalt binder Z, as well as the PMA and HP binders. When comparing among the modified binders, the J-EMA binder at 15% EDR showed lower viscosity values than both the PMA and HP binders at 120, 145, and 165°C. As the temperature increased to 190°C, the J15Z binder showed lower viscosity than the HP binder but slightly higher viscosity than the PMA binder. At 120°C, the J25Z binder showed lower viscosity than the HP binder but higher viscosity than the PMA binder. As the temperature increased to 145, 165, and 190°C, the J25Z binder showed higher viscosity than both the PMA and HP binders.

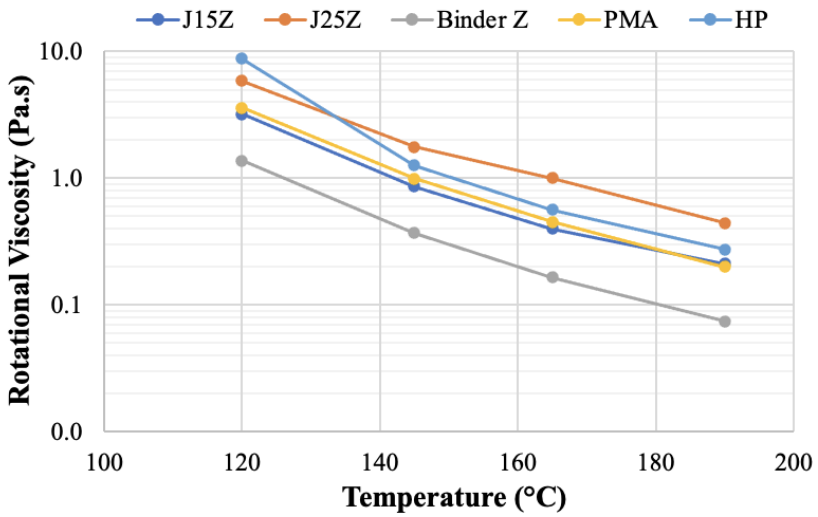

Figure 54. Rotational Viscosity Results *versus* Temperature: J15C, J25C, Base Asphalt Binder Z, PMA, and HP Binders

Figure 55 presents the rotational viscosity results of the cured U-EMA binders in comparison to the base asphalt binder C and the PMA and HP binders. When comparing among the modified binders, the U-EMA binder at 15% EDR showed lower viscosity value than both the PMA and HP binders at temperatures of 120 and 145°C. As the temperature increased to 165 and 190°C, the U15C binder showed lower viscosity than the HP binder, but higher viscosity than the PMA binder. The U25C and HP binders had similar viscosity at 120°C, which was higher than that of the PMA binder. As the temperature increased to 165 and 190°C, the U25C binder showed higher viscosity than both the PMA and HP binders.

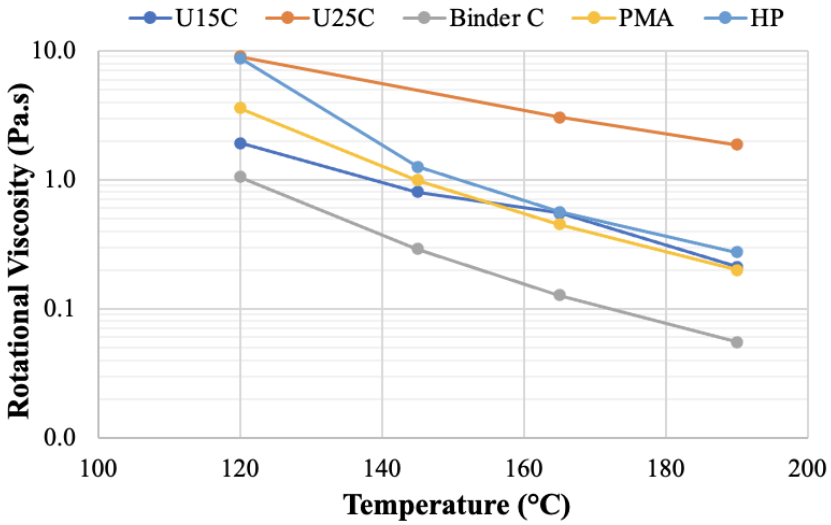

Figure 55. Rotational Viscosity Results *versus* Temperature: U15C, U25C, Base Asphalt Binder C, PMA and HP Binders

Superpave Performance Grade Classification

The final PG classifications of all asphalt binders evaluated in this study are presented in Table 23. The base asphalt binders C and Z, as well as the PMA and HP binders, were tested unaged

(i.e., original) and after RTFO and PAV aging in accordance with AASHTO M320. The EMA binders were not subjected to RTFO because the curing of these samples in an oven at 120°C was considered a short-term aging condition (see Table 20 and Table 21 for the results of J-EMA and U-EMA binders, respectively). After this short-term aging, the EMA binders were aged at 100°C for 20 hours in PAV. The U-EMA binder at 25% EDR was not graded due to difficulties in the sample preparation mainly because it became thermoset after the PAV aging.

Table 23. Performance Grade Classification of Asphalt Binders at High and Low Temperatures

Binder ID	T_{cont}, High, Unaged, °C	T_{cont}, High, RTFO, °C	T_{cont}, Intermediate, °C	T_{cont}, Low S, °C	T_{cont}, Low m-value, °C	ΔT_c	PG HT	PG LT
Base Binder C	68.8	70.4	24.6	-24.8	-24.8	0.0	64 (67)	-22
Base Binder Z	69.1	72.4	21.0	-27.9	-27.6	-0.3	64 (67)	-22
PMA	79.6	80.1	21.2	-28.9	-26.0	-2.9	76	-22
HP	97.4	85.4	13.4	-32.6	-33.7	1.1	82	-28
J15Z (cured)	79.9	N/A	17.4	-28.1	-26.2	-1.9	76	-22
J25Z (cured)	88.2		20.4	-24.2	-21.3	-2.9	88	-16
U15C (cured)	72.6		18.0	-26.6	-27.2	0.5	70	-22

When considering the high-temperature performance grade of the EMA binders, a one-grade "bump" (i.e., from PG 64 to PG 70) was observed for the U15C binder compared to the base binder C. On the other hand, for the base binder Z, a two-grade "bump" was observed for the J15Z binder (i.e., from PG 64 to PG 76), while a four-grade "bump" was observed for the J25Z binder (i.e., from PG 64 to PG 88). "Bumping" or increasing the binder high temperature grade is indicative of improved asphalt stiffness to support slow-moving or standing traffic or very high traffic volumes, which also contributes to the structural capability of asphalt mixtures. Moreover, the J15Z binder presented the same high-temperature PG as the PMA binder but lower than that of the HP binder. On the other hand, the J25Z binder presented higher high-temperature PG than both the HP and PMA binders. Finally, the U15C binder showed a lower high-temperature PG than both the HP and PMA binders.

With respect to the intermediate-temperature performance grade, an improvement in the asphalt binder fatigue resistance is indicated by a decrease in the temperature at which the limiting DSR fatigue parameter [$|G^*|\sin(\delta)$] is satisfied. As can be seen in Table 23, the addition of epoxy materials at both 15% and 25% EDR improved the intermediate temperature true grade results of the two base binders (i.e., binder Z for the foreign epoxy materials and binder C for the domestic epoxy materials). When comparing the EMA binders with the HP binder, the HP binder showed much lower intermediate pass/fail temperature (i.e., 13.4°C) than the J-EMA and U-EMA binders. On the other hand, at 15% and 25% EDR, the J-EMA and U-EMA binders presented lower intermediate pass/fail temperature than the PMA binder (i.e., 21.2°C). Therefore, in terms

of the asphalt binder contribution, the HP is expected to have the best fatigue resistance, followed by the EMA binders and the PMA binder.

When considering the low-temperature performance grade of the EMA binders, the epoxy materials from a domestic source at 15% EDR did not affect the low-temperature PG of the base binder C, which remained at PG-22. However, a lower low pass/fail temperature was achieved by the U15C binder (i.e., from -24.8 to -26.6°C), indicating potentially improved low-temperature cracking resistance. The epoxy materials from a foreign source at 15% EDR did not affect the low-temperature PG of the base binder Z (i.e., -22°C). On the other hand, a drop of one grade interval (i.e., from PG-22 to PG-16) was observed for the J-EMA binder at 25% EDR. Thus, at both 15% and 25% EDRs, the foreign epoxy materials did not improve the low-temperature PG of the base binder Z. The low-temperature true grade results showed a trend similar to that observed for the high-temperature results, where the introduction of both epoxy materials stiffened the base asphalt binders. When evaluating the EMA binders against the HP binder, the HP binder showed much lower low-temperature PG (i.e., PG -28) than the EMA binders. On the other hand, at 15% EDR, the J-EMA and U-EMA binders presented equal low-temperature PG as the PMA binder (i.e., PG -22). At 25% EDR, the J-EMA binder showed higher low-temperature PG (i.e., PG -16) than the PMA binder.

Lastly, the effect of the addition of epoxy materials was evaluated in terms of the ΔT_c parameter, which concerns the low-temperature relaxation properties of asphalt binders. ΔT_c is intended to provide an indication of loss of ductility, indicating when the asphalt binder cannot relax the stresses fast enough to prevent cracking. It has been suggested that asphalt binders with lower (i.e., more negative) ΔT_c have less ductility and reduced relaxation properties than asphalt binders with higher (less negative or positive) ΔT_c and thus, are more prone to block cracking and raveling issues. Results presented in Table 23 indicated that the addition of the epoxy materials from a foreign source to the base binder Z had a negative impact on the ΔT_c parameter; a decrease of 1.6°C was observed at 15% EDR, while at 25% EDR the decrease was 2.6°C. On the other hand, a slight improvement (i.e., increase of 0.5°C) was observed for the ΔT_c of the base binder C after the addition of the epoxy materials from a domestic source at 15% EDR. Moreover, when evaluating all the modified binders, the ranking from lower (more negative) to higher (less negative or positive) ΔT_c was: J25Z = PMA < J15Z < U15C < HP.

Multiple Stress Creep and Recovery (MSCR) Test Results

MSCR testing was performed on all binder samples at 67°C. This temperature is in accordance with the FDOT specification for the base asphalt binders and the PMA binder; however, the specification indicates that the HP binder should be tested at 76°C. Considering that this study was to evaluate the performance properties of the EMA binders in comparison to the unmodified and SBS-modified binders, a uniform testing temperature among all samples was selected (i.e., 67°C). As previously described, the base asphalt binders C and Z, as well as the PMA and the HP binders, were tested after being subjected to RTFO aging. The EMA binders were not subjected to RTFO prior to MSCR testing since the curing of these samples in an oven at 120°C was considered a short-term aging condition.

The desirable MSCR results are a function of low J_{nr} and high %Recovery. In certain cases where the asphalt binder is meant for pavements that do not experience large deformation, only

low J_{nr} may be of interest. However, most asphalt pavements experience some deformation in the asphalt binder component of the mix. Therefore, a balance of low J_{nr} and high %Recovery is advantageous.

Figure 56 presents the MSCR J_{nr} at 3.2 kPa results for all the asphalt binders evaluated in this study, while Figure 57 presents the results for the %Recovery parameter at 3.2 kPa. Based on the creep compliance data of the base asphalt binder C *versus* the U15C and U25C EMA binders, it appeared that the epoxy modification worked successfully for the 25% EDR (i.e., U25C binder). The U25C binder had a reduced J_{nr} value as compared to the unmodified base asphalt C. The reduction in creep compliance was also associated with an increase in the %Recovery, which is another desired rheological property. With respect to the 15% EDR (i.e., U15C binder), it appeared that the base binder C softened rather than stiffened after epoxy modification, which may stem from incomplete curing reaction of the epoxy materials. With respect to comparisons of the base asphalt binder Z *versus* the J15C and J25C EMA binders, it appeared that the epoxy modification worked successfully at both 15% and 25% EDR. However, as compared to U-EMA binders, the effect of the epoxy modification in terms of J_{nr} reduction and %Recovery improvement was less pronounced. This may be a result of different base binder chemistry and/or different chemical composition of the epoxy materials. Furthermore, the MSCR data indicates that the PMA and HP binders provided the best balance of the J_{nr} and %Recovery parameters due to the polybutadiene contribution within the SBS copolymer. In the case of permanent deformation to which MSCR pertains, the referenced deformation in the asphalt phase relates to the deformation that happens during pavement rutting. It is not meant to be confused with the strain deformation that the asphalt binder typically experiences in the bottom of the pavement when fatigue cracking is considered.

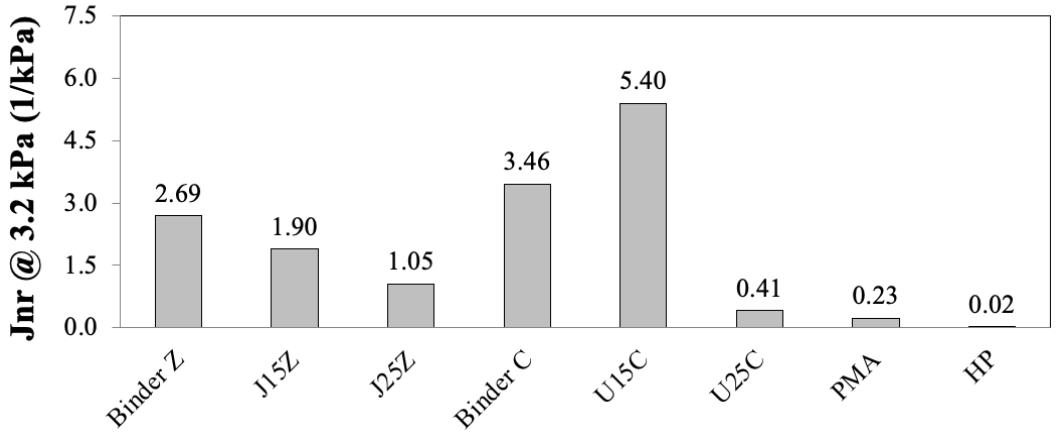

Figure 56. J_{nr} at 3.2 kPa and 67°C

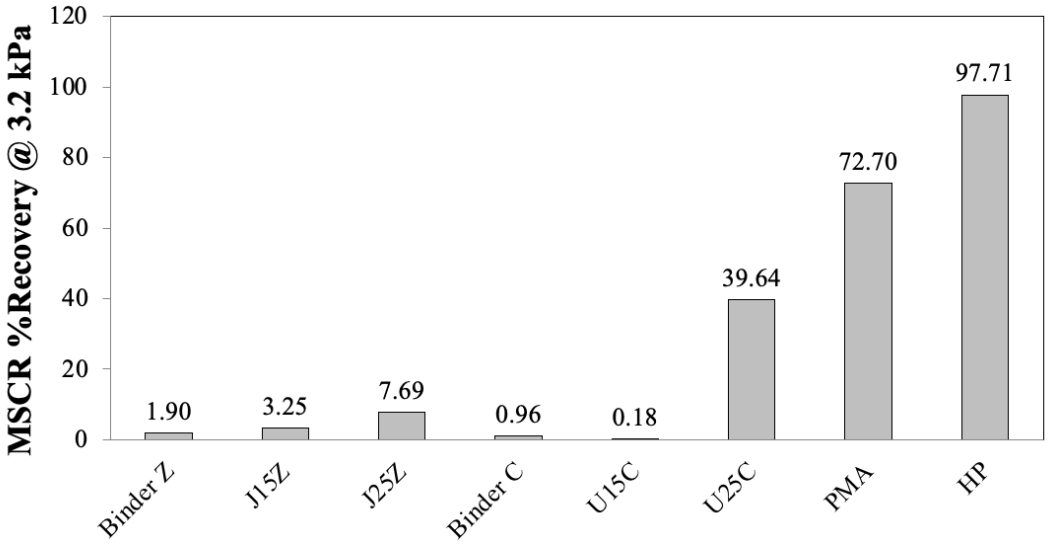

Figure 57. %Recovery at 3.2 kPa and 67°C

Linear Amplitude Sweep (LAS) Test Results

LAS testing was performed at 28°C after the binders were subjected to long-term PAV aging (20 hours at 100°C). As indicated in the performance grade discussion, the U25C binder became unworkable after PAV aging and could not be evaluated by means of the LAS test. In the LAS test, the asphalt binders were evaluated using the simplified viscoelastic continuum damage (S-VECD) model with two different strain levels (i.e., 2.5% and 5.0%). These strain levels are representative of the asphalt binder deflection in thick and thin asphalt pavements, respectively. Therefore, the number of cycles to failure (N_f) is always lower at 5.0% relative to the 2.5% strain level. During the LAS test, a sample is subjected to a frequency sweep and an amplitude sweep. The frequency sweep is used to determine the material stiffness, while the amplitude sweep corresponds to measuring the material damage. In the amplitude sweep evaluation, the material is subjected to a gradual deformation ranging from a very small strain (0.01%) up to a high strain (i.e., 30%); therefore, the test is strain controlled rather than stress controlled, as is the case in the MSCR test. If the asphalt binder adheres to the sample geometry of the DSR, a micro-crack will start to develop in the middle of the sample at the outer edge and subsequently, propagate towards the middle of the sample. If the material is damage resistant, the crack may be very small or do not propagate to the middle of the sample. Typically, the smaller the crack, the better the result in terms of the number of cycles to failure.

Figure 58 presents the LAS test results of N_f at 2.5% and 5.0% strains. Based on the N_f data of the base asphalt binder Z *versus* the J15Z and J25Z EMA binders, the epoxy modification at 15% EDR using epoxy materials from a foreign source did not improve the fatigue life at either 2.5% or 5.0% strain level. However, the epoxy modification at 25% EDR did improve the fatigue resistance relative to the base binder Z at both strain levels, as indicated by higher N_f values. This improvement can also be visualized in Figure 59(a), which shows that the |G*| curve for the J25Z binder stayed above those of the base binder Z and the J15Z binder, specially towards the end of the test. This indicates that even at very high strain levels, the J25Z binder retained a higher level of material integrity with less fatigue damage.

With respect to comparisons of the base binder C *versus* the U15C EMA binder, the epoxy modification at 15% EDR using epoxy materials from a domestic source did not improve the fatigue life of the base binder. According to the MSCR data, the possible cause for such behavior was the reduced material stiffness stemming from the incomplete curing reaction [Figure 59(b)]. When considering all the evaluated binders, the materials modified with styrenic block copolymers (i.e., HP and PMA binders) had higher N_f values and are expected to have better fatigue resistance in comparison to the EMA and base binders. This superior performance of HP and PMA binders is likely attributed to the positive effect of the elastomeric polymer network in resisting the material damage. As the SBS dosage increases from the PMA binder to the HP binder, the continuity of the polymer network increases, which eventually reaches a continuous network within the HP binder and provides high strength to the material. Another advantage of the HP binder is the relative material softness at intermediate temperature, allowing it to absorb more deformation without cracking.

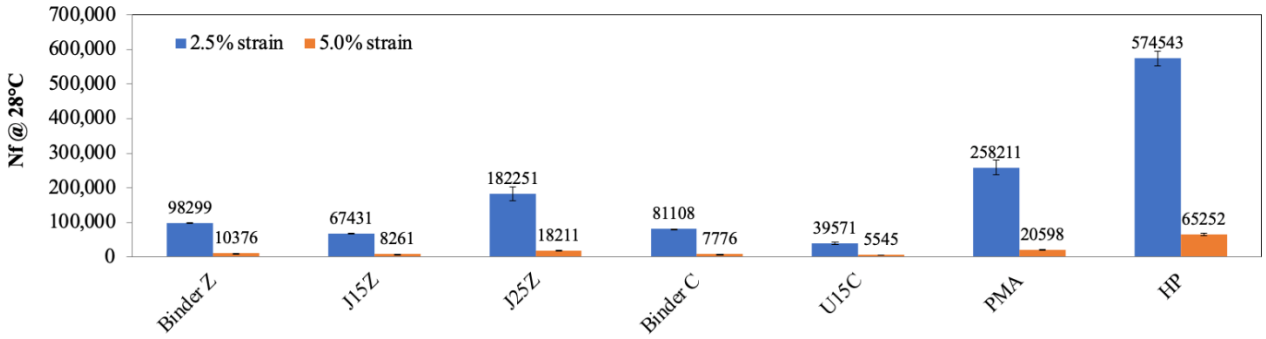

Figure 58. LAS Number of Cycles to Failure at 2.5% and 5.0% Strain and 28°C

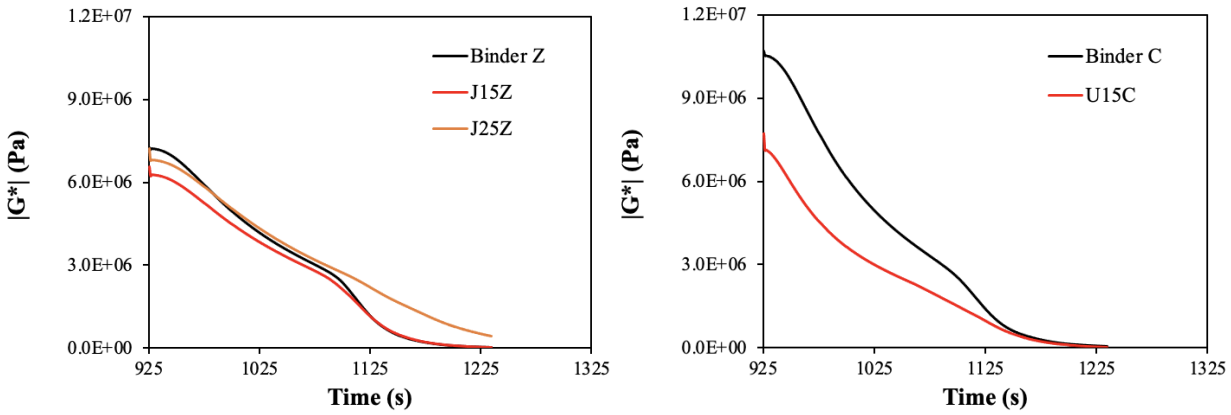

(a) (b)

Figure 59. |G*| *versus* Time at 28°C: (a) Base Binder Z *versus* J-EMA Binders, (b) Base Binder C *versus* U-EMA Binder

Glover-Rowe Parameter, Black Space Diagram, and Master Curve Analysis Results

The *G-R* parameter considers both binder stiffness (i.e., $|G^*|$) and embrittlement (i.e., δ). It is indicative of the cracking potential at intermediate temperatures (Rowe, 2011). Table 24 summarizes the $|G^*|$ and δ at 15°C and 0.005 rad/s as well as the *G-R* parameter. The results were determined for unaged and PAV-aged samples of base binders C and Z, PMA binder, HP

binder, and four EMA binders. Results were not reported for the two EMA binders modified at 25% EDR. The U25C binder was thermoset after PAV aging, so it could not be tested. For the J25Z binder, the frequency sweep data did not fit in the rheological models in the RHEA software for *G-R* calculation, which will be discussed further in this section.

Overall, the modified binders showed higher *G-R* parameter than the base binders before PAV aging. These results highlighted the potential binder stiffening effect due to the use of the modifiers. After long-term aging, the HP and EMA binders showed lower *G-R* parameter than the base binders C and Z, while the PMA presented higher *G-R* parameter. Furthermore, only the PMA binder exceeded the preliminary *G-R* parameter criterion of 180 kPa for the onset of block cracking; and thus, the possibility of this binder having premature block cracking in the field should be considered. However, the validity of using the *G-R* parameter and its thresholds for evaluating polymer-modified binders is a topic of debate in the asphalt community.

Table 24. |*G| and δ at 15°C and 0.005 rad/s and *G-R* Parameter Results Before and After PAV Aging**

Sample	15°C, 0.005 rad/s (unaged)			15°C, 0.005 rad/s (PAV aging)		
	|G*| (kPa)	δ (°)	G-R (kPa)	|G*| (kPa)	δ (°)	G-R (kPa)
Base Binder C	12.0	77.3	0.6	390.8	59.3	118.1
Base Binder Z	13.1	77.2	0.7	366.0	60.0	105.7
PMA	29.8	65.0	5.8	403.7	52.3	190.7
HP	20.6	55.0	8.3	116.5	51.6	57.4
J15Z	46.7	64.3	9.7	231.7	57.0	81.9
J25Z	96.1	56.3	35.6	Model could not be fitted		
U15C	48.4	71.5	5.1	192.3	64.4	39.8
U25C	46.3	65.7	8.6	Could not be tested after PAV		

Figure 60 presents the *G-R* parameter results on a Black Space diagram for all the asphalt samples, where the binder |G*| at 15°C and 0.005 rad/s was plotted on the y-axis *versus* δ at the same condition on the x-axis at both unaged [Figure 60(a)] and aged [Figure 60(b)] conditions. The bold and dashed curves in the figure represent the two preliminary *G-R* parameter criteria of 180 kPa and 600 kPa for the onset of block cracking and significant cracking, respectively. As can be seen, as aging occurred for each binder, the |G*| and δ data migrated from the lower right corner [i.e., low stiffness (|G*|) and high ductility (δ)] to the upper left corner [i.e., increased stiffness (|G*|) and increased brittleness (δ)] of the Black Space diagram. However, even after the long-term aging, with exception of the PMA binder, the evaluated binders were located below the *G-R* 180 kPa limit and are not likely to experience premature block cracking in the field. Care should be taken when considering the PMA binder as having failed, since as mentioned previously the *G-R* parameter and its thresholds are actively contested among the asphalt industry. Moreover, the PMA binder presented a *G-R* of 190.7 kPa, which is only slightly higher than the 180 kPa limit. Regarding the epoxy materials, it was observed that the modification of the base binders C and Z with the foreign and domestic epoxy at 15% and 25% EDR increased the stiffness of the base binders before PAV aging. Additionally, this increase in stiffness was followed by a decrease in the phase angle (δ). After long-term aging, the base binders C and Z showed higher stiffness than the EMA binders at 15% EDR, with J15Z

presenting a slighter higher stiffness and slighter lower phase angle (|G*| = 231.7 kPa, δ = 57°) than the U15C (|G*| = 192.3 kPa, δ = 64.4°). When evaluating the SBS-modified binders, these binders presented smaller phase angle than the base binders and the EMA binders before and after aging.

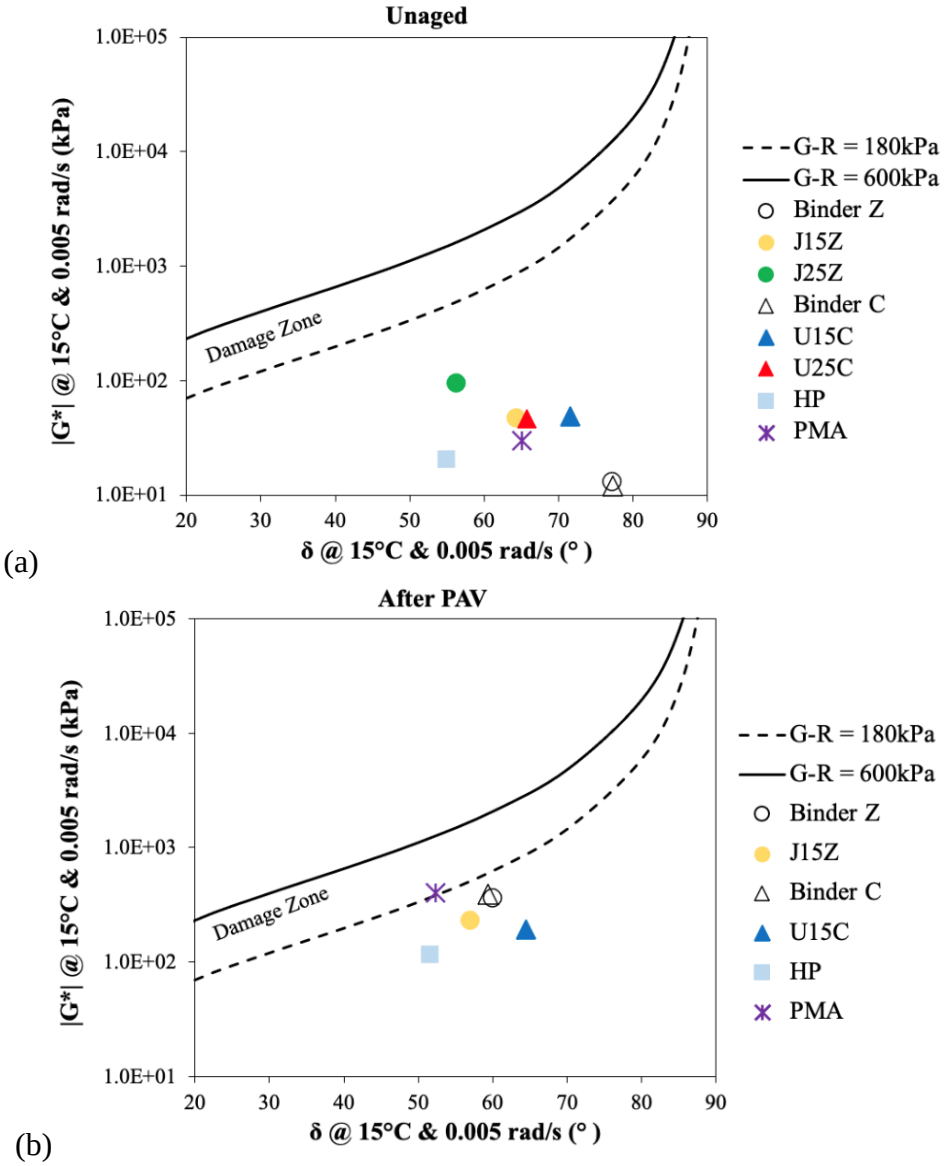

Figure 60. |*G| and *δ* Results on a Black Space Diagram: (a) Unaged Asphalt Binders, (b) Long-Term Aged Asphalt Binders**

To evaluate the susceptibility to oxidative aging in terms of binder stiffness and embrittlement, an aging index in terms of *G-R* was calculated for each binder by dividing its PAV aged *G-R* parameter by its unaged *G-R* parameter. The resulting aging indexes are shown in Figure 61 and the ranking for the modified binders from lower to higher aging susceptibility in terms of G-R aging index was HP < U15C < J15Z < PMA. This ranking can be divided into three groups. The first group includes higher aging indexes for base binders C and Z. The second group includes

the intermediate aging index for the PMA binder. The third group consists of lower aging indexes for J15Z, U15C, and HP.

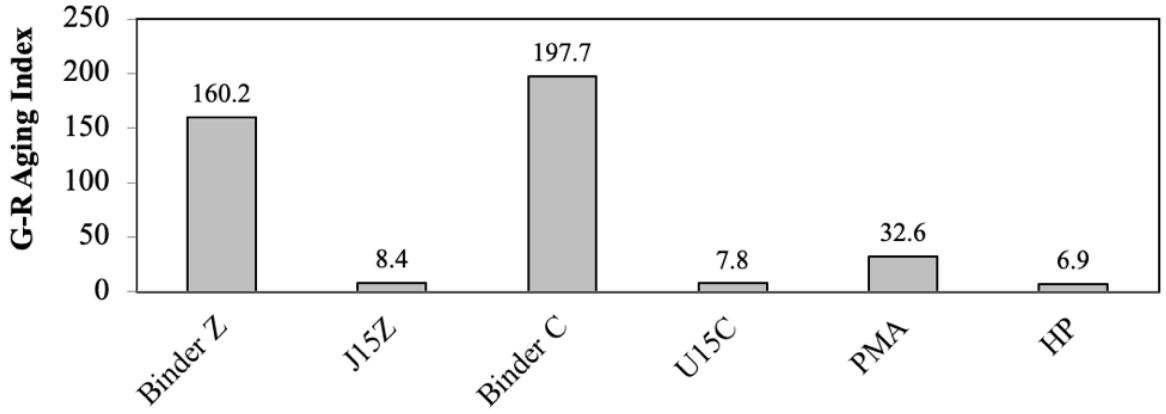

Figure 61. *G-R* Aging Index Results

Figure 62(a) shows that modification can significantly affect the shape of the master curve, decreasing its slope and altering the time-dependency of the material response in a specific frequency range. Moreover, the effect of modifiers on the materials is visible through the phase angle behavior [Figure 62(b)]. For conventional unmodified binder, as the temperature increases or the frequency decreases, the phase angle tends towards 90° (i.e., fully viscous material). With the incorporation of modifiers, this behavior changes to different phase angle degrees and different frequency or temperature ranges depending on both the type and dosage of the modifier. Hence, certain materials such as the J25Z and U25C EMA binders exhibited a short plateau of the phase angle, followed by further increase towards 90° as the frequency of the test was reduced. Other materials such as the PMA binder maintained the phase angle plateau until the lowest test frequency, indicating a continuous elastic response. The HP binder showed a further decrease in phase angle, which indicates a highly elastic response even at low frequency or high temperature. The phase angle curve of the HP binder also indicated that this material showed two locations of δ equal to 45°, one at higher temperature/lower frequency and another at lower temperature/higher frequency conditions. Thus, it seems unlikely that traditional parameters for performance characterization of unmodified binders are suitable to adequately characterize specially modified binders such as HP and EMA.

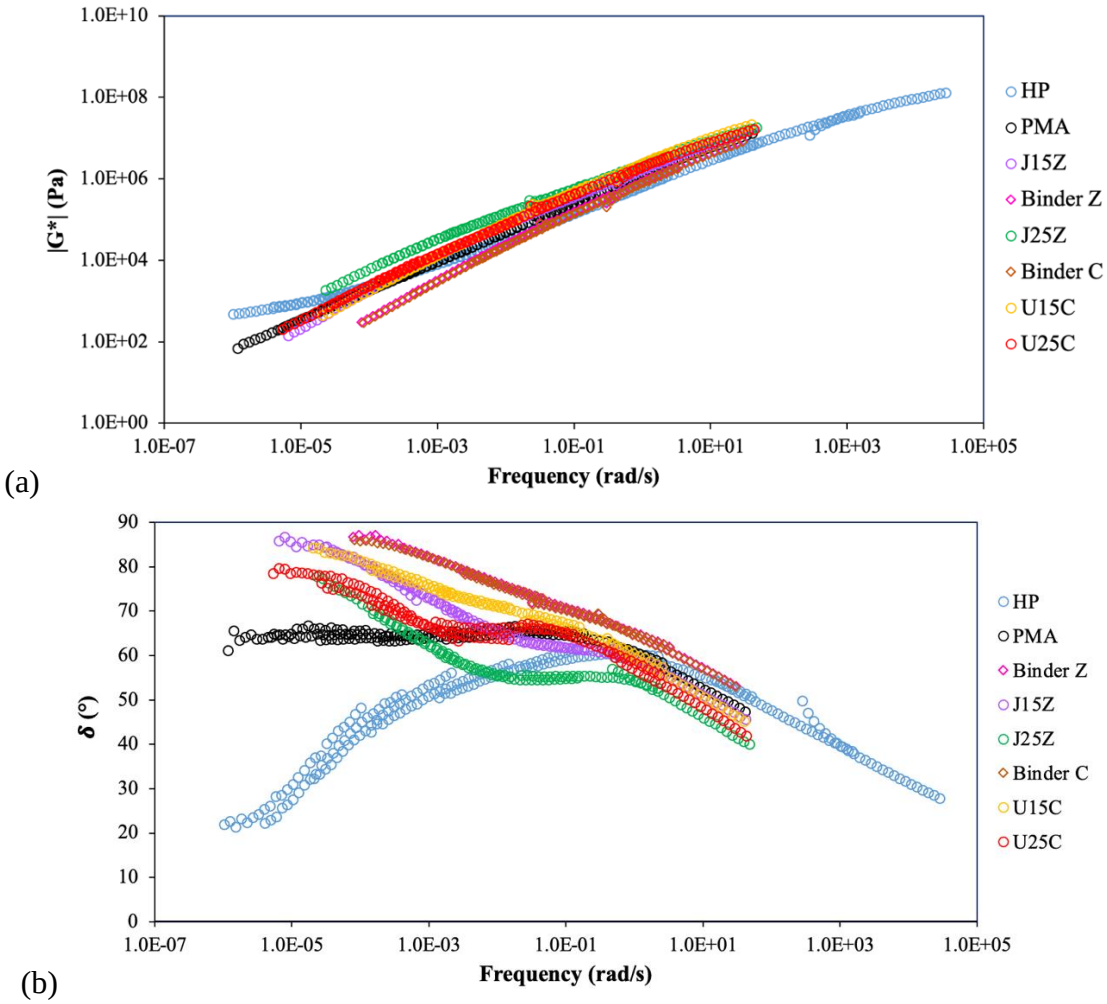

Figure 62. Master Curves: (a) |G*|, (b) Phase Angle (δ)

Binder Bond Strength (BBS) Test Results

The BBS test was conducted to evaluate the effects of moisture conditioning time and modification on the bond strength of asphalt-aggregate systems. Prior to testing, the EMA binders at 15% and 25% EDRs were cured in an oven at 120°C; the required curing time is shown in Table 20 and Table 21 for J-EMA and U-EMA binders, respectively. In addition, both the PMA and HP binders were also conditioned in an oven at 120°C for six hours to minimize the differences originated from different aging protocols.

Figure 63 presents the dry bond strength results for the asphalt-aggregate systems with GRN1 and GRN2. For the J-EMA binders at 15% EDR, the GRN1 conferred a higher dry bond strength than the GRN2. However, at 25% EDR was the GRN2 that imparted a higher dry bond strength. For the U-EMA binders, at 15% EDR the GRN2 granite conveyed higher dry bond strength, while at 25% EDR the GRN1 was more effective. For both the PMA and HP binders, a higher dry bond strength was observed for the asphalt-aggregate systems containing the GRN1.The highest dry bond strength with the GRN1 aggregate was observed for the PMA binder, while for the GRN2 the highest dry bond strength was obtained with the J25Z binder.

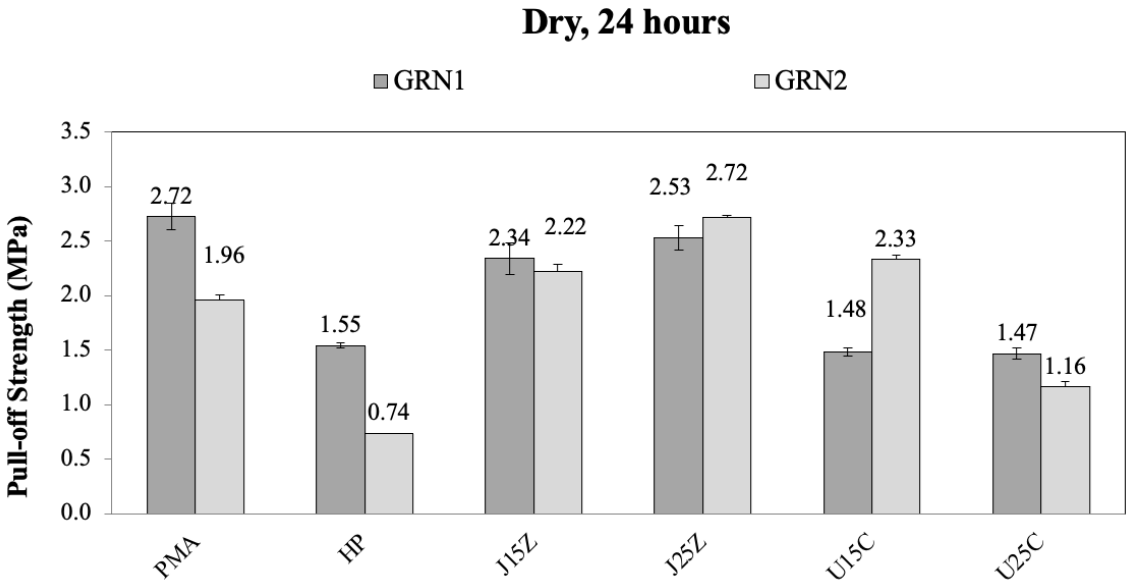

Figure 63. Dry Bond Strength of PMA, HP, and EMA Binders

Figure 64 presents the wet bond strength results for the granite aggregates. Note that moisture damage is a time-dependent phenomenon. An indirect way to investigate this time-dependency behavior is to measure the variation in the bond strength with time in the presence of water. As can be seen for all binders tested, a decrease in the bond strength was observed after 24 hours of moisture conditioning. When evaluating among the EMA binders and the PMA and HP binders, the highest wet bond strength with the GRN1 was observed for the PMA binder, while for the GRN2, the highest wet bond strength was obtained with the J25Z binder. The best performing asphalt-aggregate systems in terms of wet bond strength agreed with the best performing asphalt-aggregate systems in terms of dry bond strength (i.e., PMA + GRN1 and J25Z + GRN2). It can be observed from Figure 63 and Figure 64 that the trends were similar for the PMA and HP binders, where the asphalt-aggregate systems with GRN1 exhibited higher bond strength than with GRN2. At 15% and 25% EDRs and for GRN1 and GRN2, the asphalt-aggregate systems with the J-EMA binders appeared to have higher bond strength than the asphalt-aggregate systems with the J-EMA binders. Exceptions occurred for the systems considering J15Z and U15C with GRN2 aggregate.

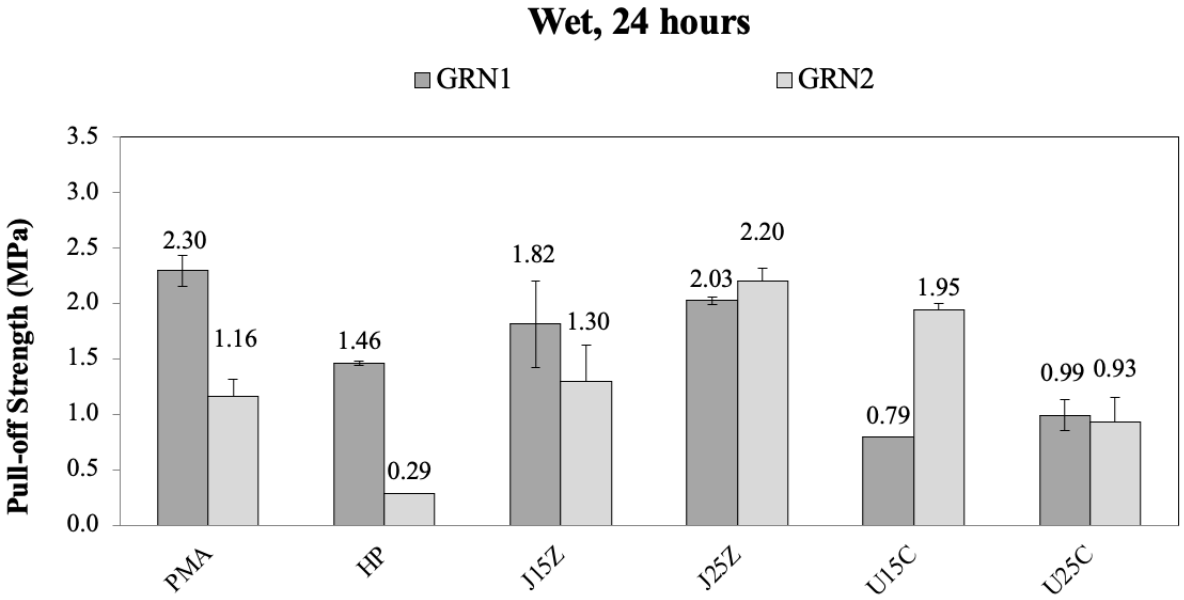

Figure 64. Wet Bond Strength of PMA, HP, and EMA Binders

The bond strengths presented in Figure 63 and Figure 64 were used to calculate the loss of bond strength due to moisture conditioning based on Equation 8 (page 79). The results are shown in Figure 65. In the case of the EMA binders, the lowest loss of bond strength after moisture conditioning occurred at 25% EDR for the J25Z + GRN1 system, while at 15% EDR for the U15C + GRN2 system. In comparison to the PMA and HP binders, the J25Z + GRN2 outperformed both the PMA + GRN2 and HP + GRN2 systems. On the other hand, the J25Z + GRN1 outperformed the PMA + GRN1 system but underperformed when compared to the HP + GRN1 system. The asphalt-aggregate systems less susceptible to moisture were HP + GRN1 and U15C + GRN2. In was observed for the EMA binders that the type and chemical characteristics of the GRN1 and GRN2 aggregates, the different chemistry of the epoxy materials from domestic and foreign sources, and the EDR played a role in the affinity for each type of granite aggregate, resulting in different degrees of adhesion captured in this study by bonds of different strength.

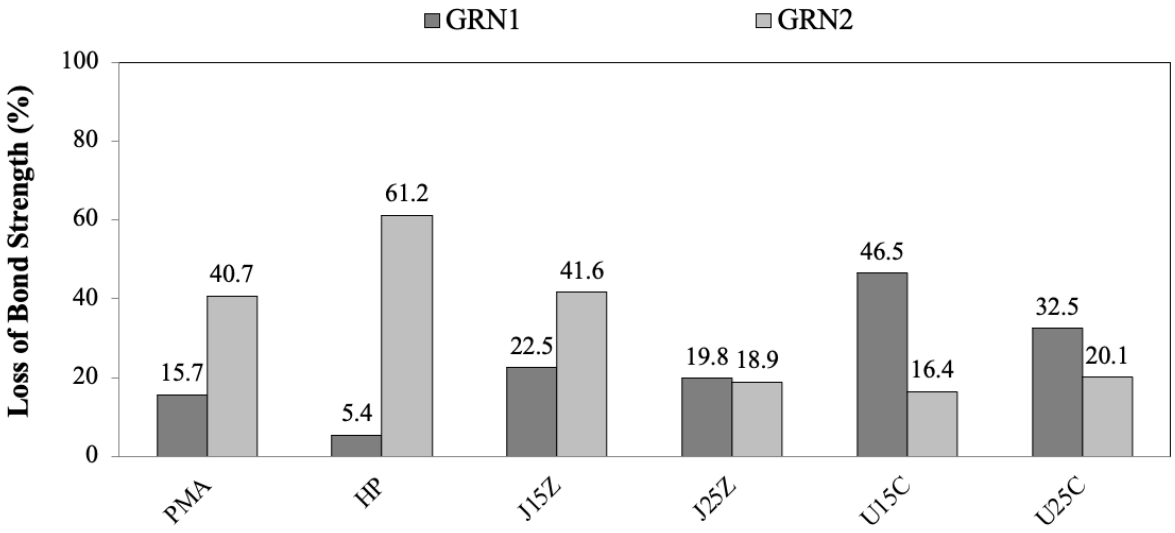

Figure 65. Loss of Bond Strength of HP, PMA, and EMA Binders

Mixture Testing Experiment Results

Cantabro Loss Results

The Cantabro test was performed on OGFC mixtures prepared with two FDOT approved FC-5 mix designs (i.e., GRN1 and LMS) and three mix aging conditions (i.e., STA, LTA1, and LTA2). For each mix design, eight EMA mixtures and a control PMA mixture were tested. The eight EMA mixtures corresponded to two combinations of epoxy materials and base binder as well as four EDRs ranging from 15% to 40%. Table 25 and Table 26 summarize the Cantabro test results of the GRN1 and LMS mixtures, respectively. More detailed discussions of these results are presented in the following sections.

Table 25. Summary of Cantabro Loss Results for GRN1 Mixtures

Binder ID	STA			LTA1			LTA2		
	Avg. (%)	Std Dev. (%)	COV	Avg. (%)	Std Dev. (%)	COV	Avg. (%)	Std Dev. (%)	COV
PMA	7.7	0.5	6.8%	17.9	2.7	14.8%	31.4	9.9	31.4%
J15Z	16.9	4.6	27.1%	22.3	1.2	5.6%	27.6	4.7	16.9%
J25Z	11.4	1.1	10.0%	14.6	2.7	18.2%	20.4	5.3	26.0%
J30Z	13.7	2.8	20.1%	10.7	1.0	9.1%	12.3	4.0	32.4%
J40Z	7.2	1.2	16.6%	7.5	2.0	27.0%	8.9	1.8	19.7%
U15C	13.9	1.9	14.1%	29.3	4.2	14.3%	26.7	1.3	4.9%
U25C	16.0	3.3	20.4%	22.4	5.7	25.3%	18.4	5.1	27.9%
U30C	17.3	3.4	19.8%	12.0	1.6	13.7%	13.1	2.7	20.9%
U40C	11.2	2.4	21.5%	9.0	0.6	7.2%	9.6	1.3	13.6%

Table 26. Summary of Cantabro Loss (%) Results for LMS Mixtures

Binder ID	STA			LTA1			LTA2		
	Avg. (%)	Std Dev. (%)	COV	Avg. (%)	Std Dev. (%)	COV	Avg. (%)	Std Dev. (%)	COV
PMA	10.8	1.5	14.0%	14.2	3.2	22.6%	19.9	3.9	19.6%
J15Z	11.1	0.6	5.5%	14.7	2.8	19.3%	19.9	2.7	13.4%
J25Z	9.9	1.5	14.9%	8.9	1.4	15.8%	16.7	1.8	10.6%
J30Z	7.0	1.3	18.2%	8.4	1.0	11.5%	12.0	0.7	6.0%
J40Z	7.9	0.3	4.1%	7.4	1.2	16.2%	9.2	0.5	5.6%
U15C	10.5	2.1	20.1%	13.5	3.2	23.9%	18.7	3.0	16.1%
U25C	10.5	0.5	5.0%	11.9	1.3	11.2%	12.0	0.8	7.0%
U30C	11.3	1.5	13.2%	9.5	0.3	3.5%	10.5	0.2	1.7%
U40C	7.9	0.5	6.5%	7.4	1.0	13.2%	8.2	0.4	4.8%

GRN1 Mix Design

Figure 66 presents the Cantabro loss results of GRN1 mixtures containing the PMA and J-EMA binders at various EDRs. In all cases except one, the Cantabro loss of the J-EMA mixtures decreased as the EDR increased, which indicated improved raveling resistance. The exception was the J30Z mixture, which had a slightly higher average Cantabro loss value than the J25Z mixture under the STA condition. However, this difference may not be significant if considering the variability of the test results as indicated by the error bars. The comparison between the PMA and J-EMA mixtures was highly dependent on the EDR and mix aging condition (i.e., aging time). Under the STA condition, the PMA mixture had a similar or lower average Cantabro loss value than the J-EMA mixtures at all EDRs. Under the LTA1 and LTA2 conditions, most EMA mixtures, especially those at higher EDRs, outperformed the PMA mixture in the Cantabro test and are expected to have better raveling resistance after long-term aging.

To consider the variability of the Cantabro test results, statistical analysis was conducted to better discriminate the raveling resistance of PMA *versus* J-EMA mixtures at each mix aging condition. Specifically, the ANOVA and Tukey's HSD tests were used to determine whether the PMA and J-EMA mixtures have significantly different Cantabro loss results at a 95% confidence level. According to the Tukey's rankings in Table 27 through Table 29, the statistical comparisons for the Cantabro loss results of PMA *versus* J-EMA mixtures are summarized as follows:

- STA: PMA < J15Z and J30Z; PMA = J25Z and J40Z.
- LTA1: PMA = J15Z and J25Z; PMA > J30Z and J40Z.
- LTA2: PMA = J15Z and J25Z; PMA > J30Z and J40Z.

  Notes: "=" indicates that the PMA and J-EMA mixtures have statistically equivalent Cantabro loss results; "<" indicates that the PMA mixture has statistically lower Cantabro loss results and is expected to have better raveling resistance than the J-EMA mixtures; ">" indicates that the PMA mixture has statistically higher Cantabro loss results and is expected to be more susceptible to raveling than the J-EMA mixtures.

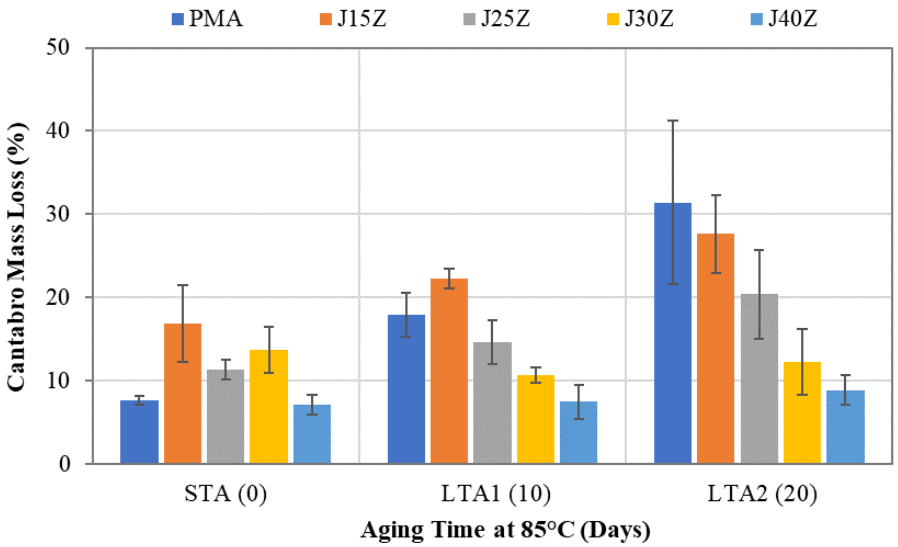

Figure 66. Cantabro Mass Loss Results of GRN1 Mixtures with PMA and J-EMA Binders under Different Mix Aging Conditions

Table 27. Tukey's Groupings for Cantabro Loss Results of GRN1 Mixtures with PMA and J-EMA Binders under the STA Condition

Mix ID	N	Mean (%)	Grouping	
J15Z	3	16.9	A	
J30Z	6	13.7	A	
J25Z	3	11.4	A	B
PMA	3	7.7		B
J40Z	3	7.2		B

Table 28. Tukey's Groupings for Cantabro Loss Results of GRN1 Mixtures with PMA and J-EMA Binders under the LTA1 Condition

Mix ID	N	Mean (%)	Grouping			
J15Z	2	22.3	A			
PMA	3	17.9	A	B		
J25Z	3	14.6		B	C	
J30Z	6	10.7			C	D
J40Z	3	7.5				D

Table 29. Tukey's Groupings for Cantabro Loss Results of GRN1 Mixtures with PMA and J-EMA Binders under the LTA2 Condition

Mix ID	N	Mean (%)	Grouping	
PMA	3	31.4	A	
J15Z	3	27.6	A	
J25Z	3	20.4	A	B
J30Z	6	12.3		B
J40Z	3	8.9		B

Figure 67 presents the Cantabro test results of GRN1 mixtures containing the PMA and U-EMA binders at various EDRs. An unexpected trend was observed for the results under the STA condition where the Cantabro loss of U-EMA mixtures increased with an increase in EDR up to 30%. Furthermore, the PMA mixture had a lower average Cantabro loss value than all the U-EMA mixtures. Different trends were observed for the comparison of PMA and U-EMA mixtures after long-term aging. At both the LTA1 and LTA2 conditions, the Cantabro loss of the U-EMA mixtures consistently increased with an increase in EDR, which indicated that U-EMA mixtures at a higher EDR are expected to have better raveling resistance than those at a lower EDR. Under the LTA1 condition, the PMA mixture had an average Cantabro loss of 17.9%, which was lower than those of the U15C and U25C mixtures but higher than the U30C and U40C mixtures. Under the LTA2 condition, the average Cantabro loss of the PMA mixture was higher than those of the U-EMA mixtures at all EDRs. These results indicated that the U-EMA mixtures are expected to have better raveling resistance than the PMA mixture after long-term aging. According to the Tukey's groupings for the Cantabro loss results in Table 30 through Table 32, the statistical comparisons for the Cantabro loss results of PMA *versus* U-EMA mixtures are summarized as follows:

- STA: PMA < U25C and U30C; PMA = U15C and U40C.
- LTA1: PMA < U15C; PMA = U25C, U30C, and U40C.
- LTA2: PMA = U15C and U25C; PMA > U30C and U40C.

  (see explanations of the ranking symbols in notes above Figure 66)

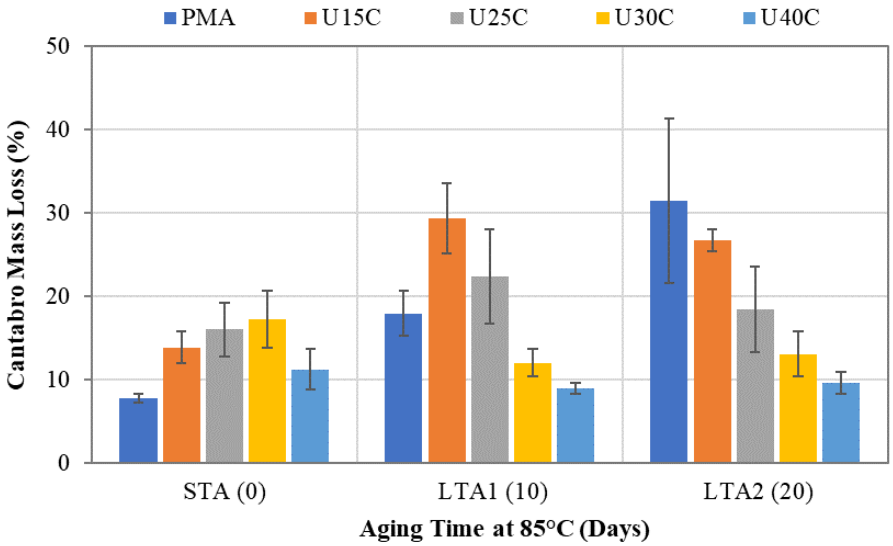

Figure 67. Cantabro Mass Loss Results of GRN1 Mixtures with PMA and U-EMA Binders under Different Mix Aging Conditions

Table 30. Tukey's Groupings for Cantabro Loss Results of GRN1 Mixtures with PMA and U-EMA Binders under the STA Condition

Mix ID	N	Mean (%)	Grouping	
U30C	3	17.3	A	
U25C	3	16.0	A	
U15C	3	13.9	A	B
U40C	3	11.2	A	B
PMA	3	7.7		B

Table 31. Tukey's Groupings for Cantabro Loss Results of GRN1 Mixtures with PMA and U-EMA Binders under the LTA1 Condition

Mix ID	N	Mean (%)	Grouping		
U15C	3	29.3	A		
U25C	3	22.4	A	B	
PMA	3	17.9		B	C
U30C	3	12.0			C
U40C	3	9.0			C

Table 32. Tukey's Groupings for Cantabro Loss Results of GRN1 Mixtures with PMA and U-EMA Binders under the LTA2 Condition

Mix ID	N	Mean (%)	Grouping		
PMA	3	31.4	A		
U15C	3	26.7	A	B	
U25C	3	18.4	A	B	C
U30C	3	13.1		B	C
U40C	3	9.6			C

LMS Mix Design

Figure 68 shows the Cantabro loss results of LMS mixtures containing the PMA and J-EMA binders at different EDRs. For all the aging conditions, there was a general trend that the Cantabro loss values decreased with an increase in EDR for the J-EMA mixtures. Under the STA condition, the PMA and J-EMA mixtures at various EDRs had similar Cantabro loss results, indicating equivalent raveling resistance before long-term aging. Under the LTA1 and LTA2 conditions, most of the J-EMA mixtures, especially those at high EDRs, performed better in the Cantabro test and are expected to have better raveling resistance than the PMA mixture. These results were affirmed with the statistical analysis results. According to Tukey's groupings in Table 33 through Table 35, the statistical comparisons for the Cantabro loss results of PMA *versus* J-EMA mixtures are summarized as follows:

- STA: PMA > J30Z; PMA = J15Z, J25Z, and J40Z.
- LTA1: PMA = J15Z and J25Z; PMA > J30Z and J40Z.
- LTA2: PMA = J15Z and J25Z; PMA > J30Z and J40Z.

(see explanations of the ranking symbols in notes above Figure 66)

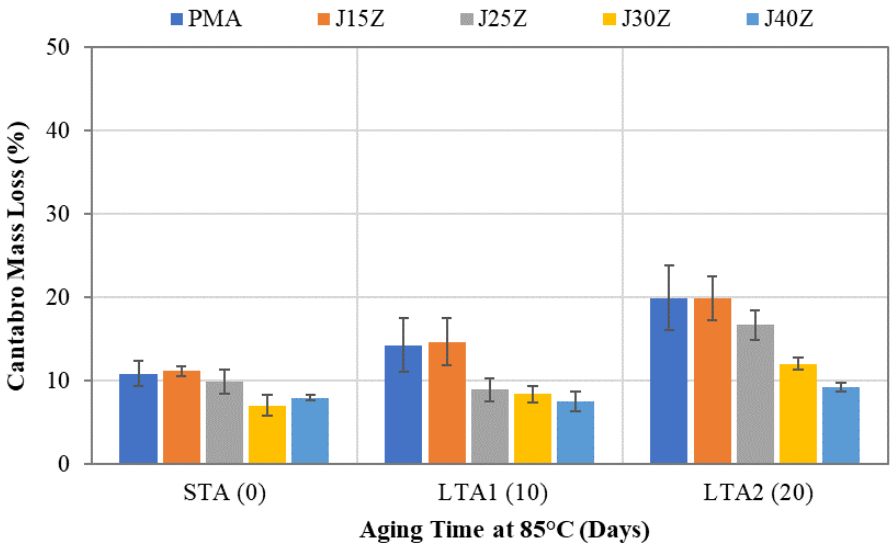

Figure 68. Cantabro Mass Loss Results of LMS Mixtures with PMA and J-EMA Binders under Different Mix Aging Conditions

Table 33. Tukey's Groupings for Cantabro Loss Results of LMS Mixtures with PMA and J-EMA Binders under the STA Condition

Mix ID	N	Mean (%)	Grouping		
J15Z	3	11.1	A		
PMA	3	10.8	A	B	
J25Z	3	9.9	A	B	C
J40Z	3	7.9		B	C
J30Z	3	7.0			C

Table 34. Tukey's Groupings for Cantabro Loss Results of LMS Mixtures with PMA and J-EMA Binders under the LTA1 Condition

Mix ID	N	Mean (%)	Grouping		
J15Z	3	14.7	A		
PMA	3	14.2	A	B	
J25Z	3	8.9		B	C
J30Z	3	8.4			C
J40Z	3	7.4			C

Table 35. Tukey's Groupings for Cantabro Loss Results of LMS Mixtures with PMA and J-EMA Binders under the LTA2 Condition

Mix ID	N	Mean (%)	Grouping		
PMA	3	14.7	A		
J15Z	3	14.2	A		
J25Z	3	8.9	A	B	
J30Z	3	8.4		B	C
J40Z	3	7.4			C

The Cantabro loss results of LMS mixtures containing the PMA and U-EMA binders at different EDRs are shown in Figure 69. Under the STA condition, the average Cantabro loss of the PMA mixture was nearly identical to those of the U-EMA mixtures except for the U40C mixture, which had a slightly lower average Cantabro loss than the other mixtures. Under the LTA1 and LTA2 conditions, the average Cantabro loss of U-EMA mixtures decreased with an increase in the EDR, which indicated improved raveling resistance due to epoxy modification of the asphalt binder. Furthermore, most of the U-EMA mixtures, particularly those with high EDRs, outperformed the PMA mixture in the Cantabro test; thus, they are expected to have better raveling resistance than the PMA mixture after long-term aging. Based on the Tukey's rankings in Table 36 through Table 38, the statistical comparisons for the Cantabro loss results of PMA *versus* U-EMA mixtures are summarized as follows:

- STA: PMA = U15C, U25C, U30C, and U40C.
- LTA1: PMA = U15C, U25C, and U30C; PMA > U40C.
- LTA2: PMA = U15C; PMA > U25C, U30C, and U40C.

  (see explanations of the ranking symbols in notes above Figure 66)

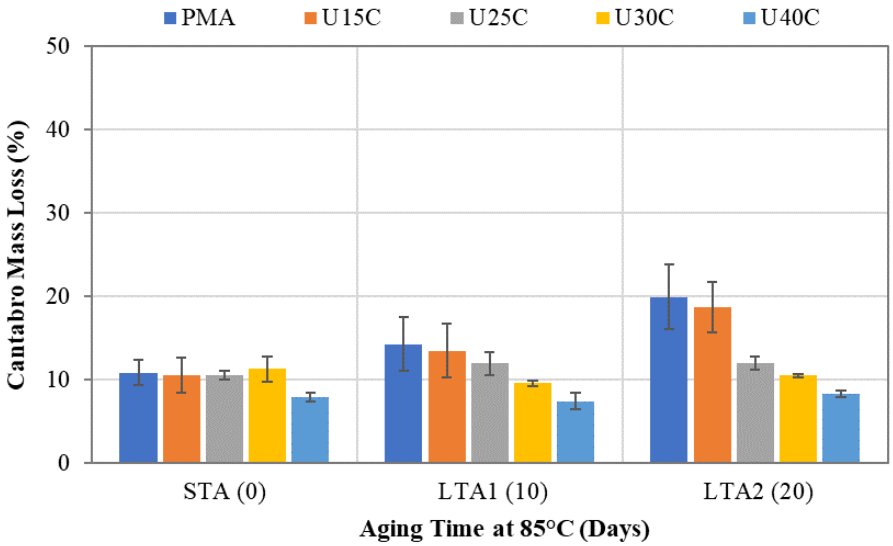

Figure 69. Cantabro Mass Loss Results of LMS Mixtures with PMA and U-EMA Binders under Different Mix Aging Conditions

Table 36. Tukey's Groupings for Cantabro Loss Results of LMS Mixtures with PMA and U-EMA Binders under the STA Condition

Mix ID	N	Mean (%)	Grouping
U30C	3	10.8	A
PMA	3	10.5	A
U25C	3	10.5	A
U15C	3	7.9	A
U40C	3	10.8	A

Table 37. Tukey's Groupings for Cantabro Loss Results of LMS Mixtures with PMA and U-EMA Binders under the LTA1 Condition

Mix ID	N	Mean (%)	Grouping	
PMA	3	14.2	A	
U15C	3	13.5	A	
U25C	3	11.9	A	B
U30C	3	9.5	A	B
U40C	3	7.4		B

Table 38. Tukey's Groupings for Cantabro Loss Results of LMS Mixtures with PMA and U-EMA Binders under the LTA2 Condition

Mix ID	N	Mean (%)	Grouping	
PMA	3	19.9	A	
U15C	3	18.7	A	
U25C	3	12.0		B
U30C	3	10.5		B
U40C	3	8.2		B

Aging Resistance Evaluation

To quantitatively evaluate the aging resistance of OGFC mixtures containing EMA and PMA binders, an aging index parameter, Cantabro Aging Index (CAI), was proposed based on the Cantabro test results under different mix aging conditions. CAI is defined as the percentage change in the Cantabro loss of the mixture under the STA condition to the LTA condition (Equation 11). A lower (i.e., less positive, or higher negative) CAI value indicates that the mixture is more resistant to aging in terms of raveling resistance.

$$CAI = \frac{CL_{LTA} - CL_{STA}}{CL_{STA}} * 100 \qquad \text{Equation 11}$$

Where,

CL_{STA} = Cantabro loss under the STA condition; and
CL_{LTA} = Cantabro loss under the LTA condition.

Figure 70 and Figure 71 present the CAI results of GRN1 and LMS mixtures containing the PMA, J-EMA, and U-EMA binders for the LTA1 and LTA2 conditions. For both mix designs, the PMA mixture has the highest CAI value, which indicates that it is most susceptible to aging in terms of raveling resistance. There is a general trend among the EMA mixtures with a few exceptions that the CAI values decrease as the EDR increases. These results indicate that EMA mixtures at higher EDRs are expected to have better aging resistance than those at lower EDRs. In some cases, the EMA mixture has a negative CAI value because it had lower Cantabro loss results after aging than before aging. This improvement is mainly attributed to the post-compaction curing of the EMA binder during aging, which is expected to significantly increase the cohesive strength of the mixture. Therefore, the negative CAI values of certain EMA mixtures are caused by the combined effects of asphalt aging and curing on the Cantabro test results. For both the GRN1 and LMS mix designs, the two lowest CAI values correspond to the U30C and U40C mixtures at both long-term aging conditions. Overall, the CAI results in Figure

70 and Figure 71 indicate that the U-EMA mixtures have the greatest aging resistance, followed by the J-EMA mixtures and the PMA mixtures, respectively.

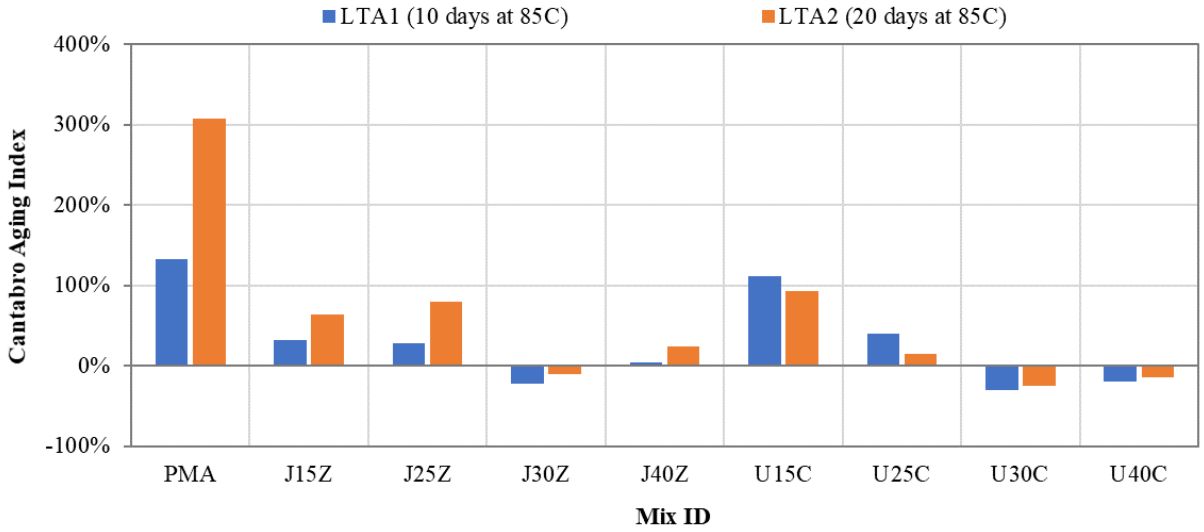

Figure 70. Cantabro Aging Index Results of GRN1 Mixtures

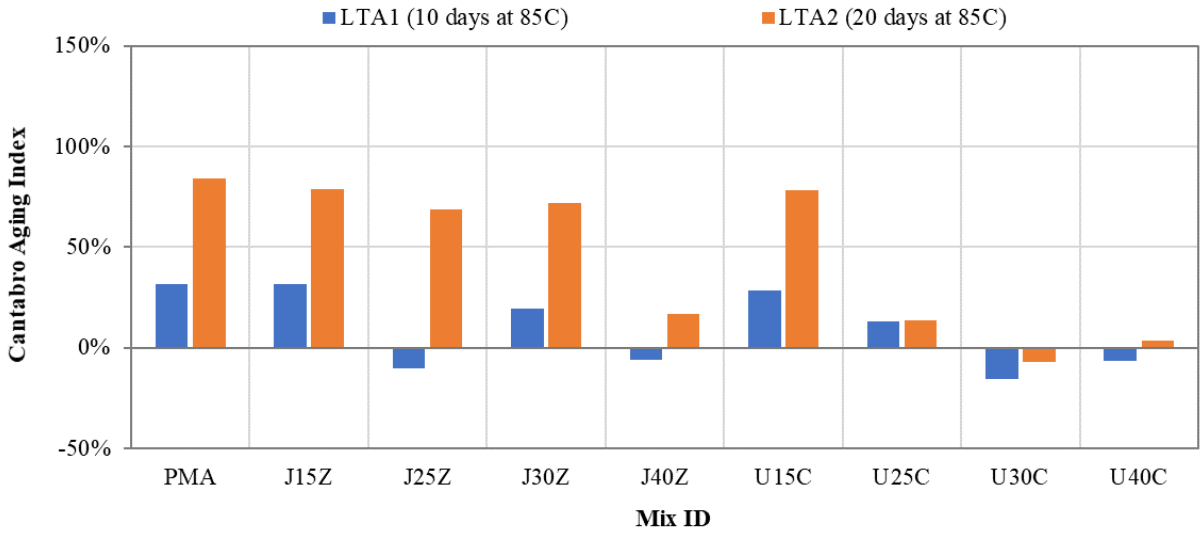

Figure 71. Cantabro Aging Index Results of LMS Mixtures

IDT Strength Results

Table 39 and Table 40 summarize the IDT strength results of the GRN1 and LMS mixtures, respectively. These results are discussed further in the following sections. Statistical analysis using the ANOVA and Tukey's HSD tests were conducted at a 95% confidence interval to better discriminate the IDT strength results of PMA *versus* EMA mixtures at each mix aging condition while taking into consideration the variability of the test results.

Table 39. Summary of IDT Strength Results for GRN1 Mixtures

Binder ID	STA			LTA1			LTA2		
	Avg. (psi)	Std Dev. (psi)	COV	Avg. (psi)	Std Dev. (psi)	COV	Avg. (psi)	Std Dev. (psi)	COV
PMA	48.3	7.2	15.0%	64.1	4.6	7.1%	71.7	4.2	5.8%
J15Z	54.5	5.1	9.4%	83.1	9.6	11.5%	78.8	2.8	3.5%
J25Z	70.6	7.4	10.5%	91.4	4.2	4.6%	104.9	5.0	4.7%
J30Z	63.0	33.0	52.4%	121.4	7.6	6.3%	105.5	9.3	8.8%
J40Z	163.8	19.9	12.2%	146.7	1.9	1.3%	139.1	9.0	6.5%
U15C	25.8	5.8	22.4%	38.4	1.9	4.8%	53.3	11.0	20.7%
U25C	45.0	4.6	10.2%	65.2	9.7	14.9%	88.5	15.2	17.2%
U30C	69.9	3.9	5.6%	146.2	10.7	7.3%	166.2	13.4	8.1%
U40C	166.0	17.2	10.4%	208.0	15.6	7.5%	225.8	19.4	8.6%

Table 40. Summary of IDT Strength Results for LMS Mixtures

Binder ID	STA			LTA1			LTA2		
	Avg. (psi)	Std Dev. (psi)	COV	Avg. (psi)	Std Dev. (psi)	COV	Avg. (psi)	Std Dev. (psi)	COV
PMA	81.7	2.7	3.3%	91.5	4.5	4.9%	106.9	7.2	6.7%
J15Z	93.4	7.0	7.5%	96.5	9.4	9.7%	103.5	15.3	14.8%
J25Z	117.1	3.6	3.0%	137.3	5.7	4.1%	121.5	14.9	12.3%
J30Z	154.4	9.2	6.0%	149.1	26.3	17.7%	146.1	13.7	9.4%
J40Z	193.3	11.0	5.7%	163.8	5.8	3.5%	180.2	12.2	6.8%
U15C	46.5	18.6	10.1%	80.1	8.7	10.9%	99.0	12.7	12.8%
U25C	97.3	3.1	3.2%	160.8	17.2	10.7%	168.9	20.9	12.4%
U30C	107.3	18.7	17.4%	226.2	11.5	5.1%	212.7	16.5	7.8%
U40C	221.2	11.7	5.3%	279.7	23.5	8.4%	311.1	24.3	7.8%

GRN1 Mix Design

Figure 72 presents the IDT strength results of GRN1 mixtures containing the PMA and J-EMA binders at various EDRs. In all cases except two, the IDT strength of the J-EMA mixtures increased as the EDR increased. The two exceptions were the J30Z mixture under the STA and LTA2 conditions. Although the J30Z mixture had a slightly lower average IDT strength than the J25Z mixture under the STA condition, it had considerably higher variability than the other mixtures, which made the comparison inconclusive. Under the LTA2 condition, the J25Z and J30Z mixtures had almost identical average IDT strength results. For all the mix aging conditions, the PMA mixture had consistently lower average IDT strength results than the EMA mixtures regardless of the EDR, and the differences were more pronounced in comparison with the EMA mixtures at higher EDRs. Based on the Tukey's rankings in Table 41 through Table 43, the statistical comparisons for the IDT strength results of GRN1 mixtures containing the PMA *versus* J-EMA binders are summarized as follows:

- STA: PMA = J15Z, J25Z, and J30Z; PMA < J40Z.
- LTA1: PMA < J15Z, J25Z, J30Z, and J40Z.

- LTA2: PMA = J15Z; PMA < J25Z, J30Z, and J40Z.

  Notes: "=" indicates that the PMA and J-EMA mixtures have statistically equivalent IDT strength results; "<" indicates that the PMA mixture has statistically lower IDT strength results than the J-EMA mixtures; ">" indicates that the PMA mixture has statistically higher IDT strength results than the J-EMA mixtures.

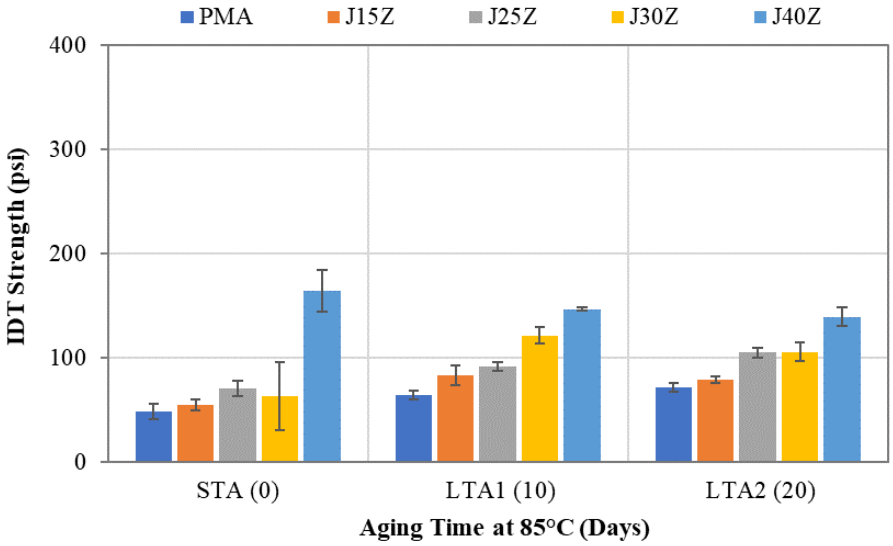

Figure 72. IDT Strength Results of GRN1 Mixtures with PMA and J-EMA Binders under Different Mix Aging Conditions

Table 41. Tukey's Groupings for IDT Strength Results of GRN1 Mixtures with PMA and J-EMA Binders under the STA Condition

Binder ID	N	Mean (psi)	Grouping	
J40Z	8	163.8	A	
J25Z	6	70.6		B
J30Z	4	63.0		B
J15Z	6	54.5		B
PMA	6	48.3		B

Table 42. Tukey's Groupings for IDT Strength Results of GRN1 Mixtures with PMA and J-EMA Binders under the LTA1 Condition

Binder ID	N	Mean (psi)	Grouping			
J40Z	4	146.7	A			
J30Z	6	121.4		B		
J25Z	6	91.4			C	
J15Z	4	83.1			C	
PMA	6	64.1				D

Table 43. Tukey's Groupings for IDT Strength Results of GRN1 Mixtures with PMA and J-EMA Binders under the LTA2 Condition

Binder ID	N	Mean (psi)	Grouping		
J40Z	4	139.1	A		
J30Z	6	105.5		B	
J25Z	6	104.9		B	
J15Z	5	78.8			C
PMA	6	71.7			C

Figure 73 presents the IDT strength results of GRN1 mixtures containing the PMA and U-EMA binders at various EDRs. In all cases, the IDT strength of the U-EMA mixtures increased with an increase in EDR, which indicated that epoxy modification of the asphalt binder has a positive impact on the strength properties of OGFC mixtures. The comparison between the PMA and U-EMA mixtures was dependent on the EDR. Under all the mix aging conditions, the PMA and U25C mixtures had similar IDT strength results, which were consistently higher than those of the U15C mixture. On the other hand, the U30C and U40C mixtures had considerably higher IDT strength results than the PMA mixture. Based on the Tukey's rankings in Table 44 through Table 46, the statistical comparisons for the IDT strength results of GRN1 mixtures containing the PMA *versus* U-EMA binders are summarized as follows:

- STA: PMA > U15C; PMA = U25C; PMA < U30C and U40C.
- LTA1: PMA > U15C; PMA = U25C; PMA < U30C and U40C.
- LTA2: PMA = U15C and U25C; PMA < U30C and U40C.

  (see explanations of the ranking symbols in notes above Figure 72)

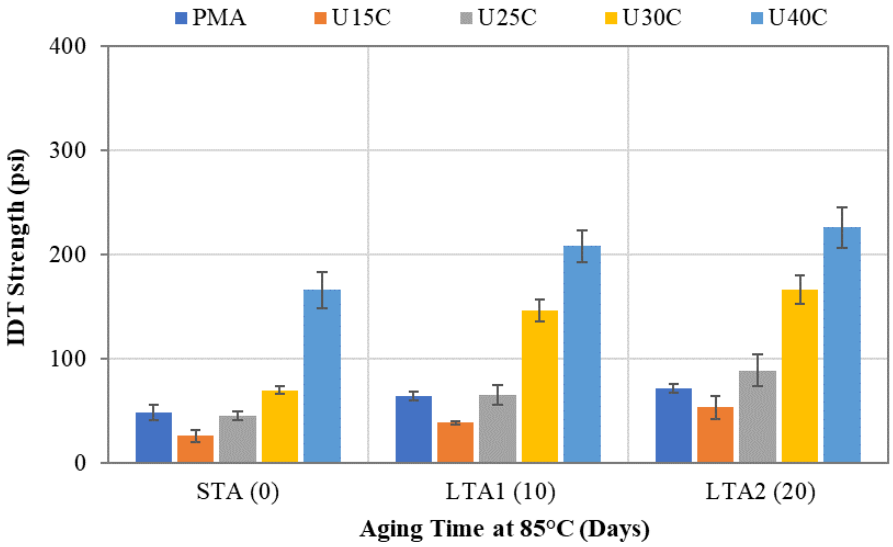

Figure 73. IDT Strength Results of GRN1 Mixtures with PMA and U-EMA Binders under Different Mix Aging Conditions

Table 44. Tukey's Groupings for IDT Strength Results of GRN1 Mixtures with PMA and U-EMA Binders under the STA Condition

Binder ID	N	Mean (psi)	Grouping			
U40C	6	166.0	A			
U30C	6	69.9		B		
PMA	6	48.3			C	
U25C	6	45.0			C	
U15C	6	25.8				D

Table 45. Tukey's Groupings for IDT Strength Results of GRN1 Mixtures with PMA and U-EMA Binders under the LTA1 Condition

Binder ID	N	Mean (psi)	Grouping			
U40C	6	208.0	A			
U30C	6	146.2		B		
U25C	6	65.2			C	
PMA	6	64.1			C	
U15C	6	38.4				D

Table 46. Tukey's Groupings for IDT Strength Results of GRN1 Mixtures with PMA and U-EMA Binders under the LTA2 Condition

Binder ID	N	Mean (psi)	Grouping			
U40C	6	225.8	A			
U30C	5	166.2		B		
U25C	6	88.5			C	
PMA	6	71.7			C	D
U15C	6	53.3				D

LMS Mix Design

The IDT strength results of LMS mixtures containing the PMA and J-EMA binders at various EDRs are presented in Figure 74. As can be seen, the IDT strength of the J-EMA mixtures increased with an increase in EDR for all the three mix aging conditions. Under the STA and LTA1 conditions, the PMA mixture had lower average IDT strength results compared to the J-EMA mixtures. Under the LTA2 condition, the PMA mixtures had the second-lowest average IDT strength after the J15Z mixture, but the difference was not practically significant. Overall, the J-EMA mixtures had similar or higher IDT strength than the PMA mixture. Based on the Tukey's rankings in Table 47 through Table 49, the statistical comparisons for the IDT strength results of LMS mixtures with PMA *versus* J-EMA binders are summarized as follows:

- STA: PMA = J15Z; PMA < J25Z, J30Z, and J40Z.
- LTA1: PMA = J15Z; PMA < J25Z, J30Z, and J40Z.
- LTA2: PMA = J15Z and J25Z; PMA < J30Z and J40Z.

(see explanations of the ranking symbols in notes above Figure 72)

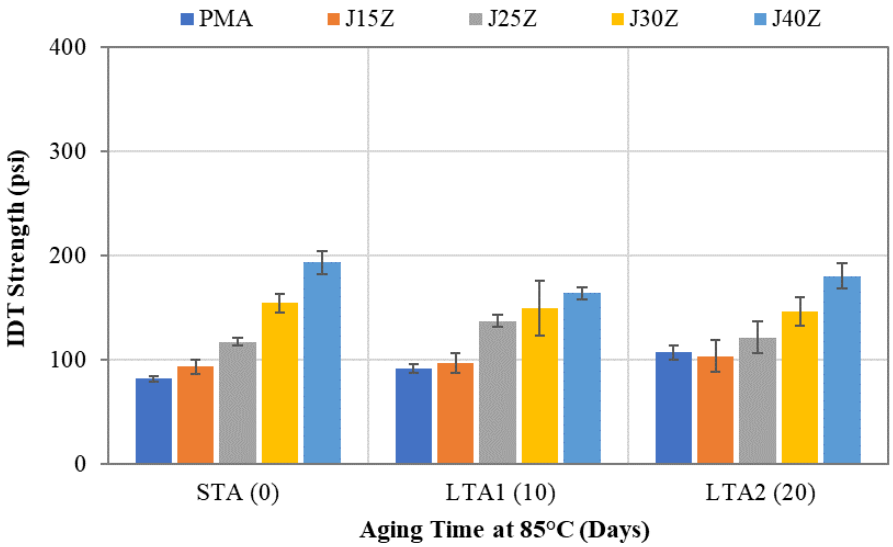

Figure 74. IDT Strength Results of LMS Mixtures with PMA and J-EMA Binders under Different Mix Aging Conditions

Table 47. Tukey's Groupings for IDT Strength Results of LMS Mixtures with PMA and J-EMA Binders under the STA Condition

Binder ID	N	Mean (psi)	Grouping			
J40Z	6	193.3	A			
J30Z	6	154.4		B		
J25Z	6	117.1			C	
J15Z	6	93.4				D
PMA	6	81.7				D

Table 48. Tukey's Groupings for IDT Strength Results of LMS Mixtures with PMA and J-EMA Binders under the LTA1 Condition

Binder ID	N	Mean (psi)	Grouping		
J40Z	6	163.8	A		
J30Z	6	149.1	A	B	
J25Z	6	137.3		B	
J15Z	6	96.5			C
PMA	6	91.5			C

Table 49. Tukey's Groupings for IDT Strength Results of LMS Mixtures with PMA and J-EMA Binders under the LTA2 Condition

Binder ID	N	Mean (psi)	Grouping		
J40Z	6	180.2	A		
J30Z	6	146.1		B	
J25Z	6	121.5			C
PMA	6	106.9			C
J15Z	6	103.5			C

Figure 75 shows the IDT strength results of LMS mixtures containing the PMA and U-EMA binders at various EDRs. The IDT strength of the U-EMA mixtures increased with an increase in EDR for the three mix aging conditions. All the EMA mixtures except U15C had similar or higher IDT strength results than the PMA mixture, regardless of the mix aging condition. These results were further confirmed by the statistical analysis results presented in Table 50 through Table 52. The statistical comparisons for the IDT strength results of LMS mixtures with PMA *versus* U-EMA binders are summarized as follows:

- STA: PMA > J15Z; PMA = J25Z; PMA < J30Z and J40Z.
- LTA1: PMA = J15Z; PMA < J25Z, J30Z, and J40Z.
- LTA2: PMA = J15Z; PMA < J25Z, J30Z, and J40Z.

  (see explanations of the ranking symbols in notes above Figure 72)

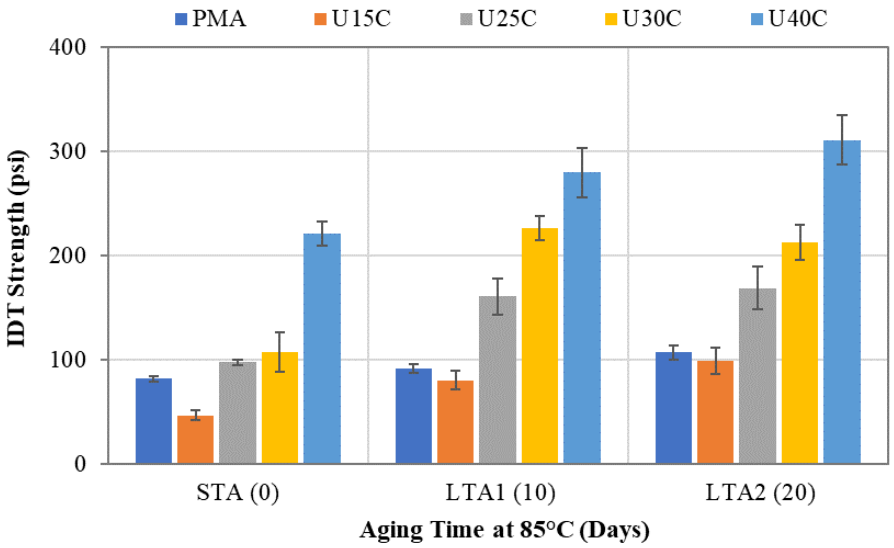

Figure 75. IDT Strength Results of LMS Mixtures with PMA and U-EMA Binders under Different Mix Aging Conditions

Table 50. Tukey's Groupings for IDT Strength Results of LMS Mixtures with PMA and U-EMA Binders under the STA Condition

Binder ID	N	Mean (psi)	Grouping			
U40C	6	221.2	A			
U30C	6	107.3		B		
U25C	6	97.3		B	C	
PMA	6	81.7			C	
U15C	6	46.5				D

Table 51. Tukey's Groupings for IDT Strength Results of LMS Mixtures with PMA and U-EMA Binders under the LTA1 Condition

Binder ID	N	Mean (psi)	Grouping			
U40C	6	279.7	A			
U30C	6	226.2		B		
U25C	6	160.8			C	
PMA	6	91.5				D
U15C	6	80.1				D

Table 52. Tukey's Groupings for IDT Strength Results of LMS Mixtures with PMA and U-EMA Binders under the LTA2 Condition

Binder ID	N	Mean (psi)	Grouping			
U40C	6	311.1	A			
U30C	6	212.7		B		
U25C	6	168.9			C	
PMA	6	106.9				D
U15C	6	99.0				D

IDT Fracture Energy (G_f) Results

Table 53 and Table 54 summarize the IDT G_f results of the GRN1 and LMS mixtures, respectively. More detailed discussions of these results along with the statistical analysis results are presented in the following section.

Table 53. Summary of IDT G_f Results for GRN1 Mixtures

Binder ID	STA			LTA1			LTA2		
	Avg. (J/m^2)	Std Dev. (J/m^2)	COV	Avg. (J/m^2)	Std Dev. (J/m^2)	COV	Avg. (J/m^2)	Std Dev. (J/m^2)	COV
PMA	6,535	591	9.0%	8,235	733	8.9%	7,995	1,293	16.2%
J15Z	5,897	502	8.5%	7,546	1,180	15.6%	6,881	488	7.1%
J25Z	8,112	1,614	19.9%	7,577	899	11.9%	9,012	819	9.1%
J30Z	4,670	3,466	74.2%	10,561	859	8.1%	10,116	1,498	14.8%
J40Z	16,084	2,202	13.7%	15,710	994	6.3%	13,503	1,428	10.6%
U15C	2,549	349	13.7%	4,339	546	12.6%	4,701	965	20.5%
U25C	4,438	631	14.2%	5,831	428	7.3%	8,614	1,523	17.7%
U30C	8,643	1,355	15.7%	17,069	4,338	25.4%	19,065	3,944	20.7%
U40C	27,142	2,084	7.7%	30,143	5,108	16.9%	30,550	5,197	17.0%

Table 54. Summary of IDT G_f Results for LMS Mixtures

Binder ID	STA			LTA1			LTA2		
	Avg. (J/m^2)	Std Dev. (J/m^2)	COV	Avg. (J/m^2)	Std Dev. (J/m^2)	COV	Avg. (J/m^2)	Std Dev. (J/m^2)	COV
PMA	8,669	360	4.2%	8,641	571	6.6%	7,664	543	7.1%
J15Z	6,980	1,108	15.9%	7,201	349	4.8%	6,390	299	4.7%
J25Z	9,707	848	8.7%	10,513	1,410	13.4%	8,899	981	11.0%
J30Z	14,791	1,523	10.3%	13,601	2,673	19.7%	10,744	1,280	11.9%
J40Z	13,998	1,150	8.2%	15,015	954	6.4%	13,874	1,265	9.1%
U15C	2,744	393	14.3%	4,048	258	6.4%	4,803	414	8.6%
U25C	6,231	596	9.6%	8,585	415	4.8%	9,003	1,010	11.2%
U30C	8,972	969	10.8%	14,199	1,495	10.5%	14,461	2,371	16.4%
U40C	21,606	1,765	8.2%	21,631	2,492	11.5%	21,268	1,931	9.1%

GRN1 Mix Design

The IDT G_f results of GRN1 mixtures containing the PMA and J-EMA binders at different EDRs are plotted in Figure 76. In all cases except two, the IDT G_f of J-EMA mixtures increased with an increase in EDR, which indicated improved fracture resistance. The two exceptions were the J30Z mixture under the STA condition and the J25Z mixture under the LTA1 condition. The comparison between the PMA and J-EMA mixtures was dependent on the EDR and mixing aging condition. Under the STA condition, the PMA mixture had a similar or slightly higher average IDT G_f value than the J15Z and J30Z mixtures, while the opposite trend was observed for the comparison with the J25Z and J40Z mixtures. The J30Z mixture had considerably higher variability than the other mixtures, which made the comparison inconclusive. Under the LTA1 condition, the J30Z and J40Z mixtures outperformed the PMA mixture in terms of mixture resistance, but the PMA mixture had slightly higher average G_f results than the J15Z and J25Z mixtures. Under the LTA2 condition, the J-EMA mixtures at 25%, 30%, and 40% EDRs showed higher average G_f results than the PMA mixture while the J15Z mixture had a marginally lower G_f value. Overall, the EMA mixtures at high EDRs had higher IDT G_f results and thus, better fracture resistance than the PMA mixture under all the mix aging conditions. According to the Tukey's rankings in Table 55 through Table 57, the statistical comparisons for the IDT G_f results of GRN1 mixtures with PMA *versus* J-EMA binders are summarized as follows:

- STA: PMA = J15Z, J25Z, and J30Z; PMA < J40Z.
- LTA1: PMA = J15Z and J25Z; PMA < J30Z and J40Z.
- LTA2: PMA = J15Z and J25Z; PMA < J30Z and J40Z.

  Notes: "=" indicates that the PMA and J-EMA mixtures have statistically equivalent IDT G_f results; "<" indicates that the PMA mixture has statistically lower IDT G_f results and are expected to have reduced fracture resistance compared to the J-EMA mixtures; ">" indicates that the PMA mixture has statistically higher G_f strength results and are expected to have better fracture resistance than the J-EMA mixtures.

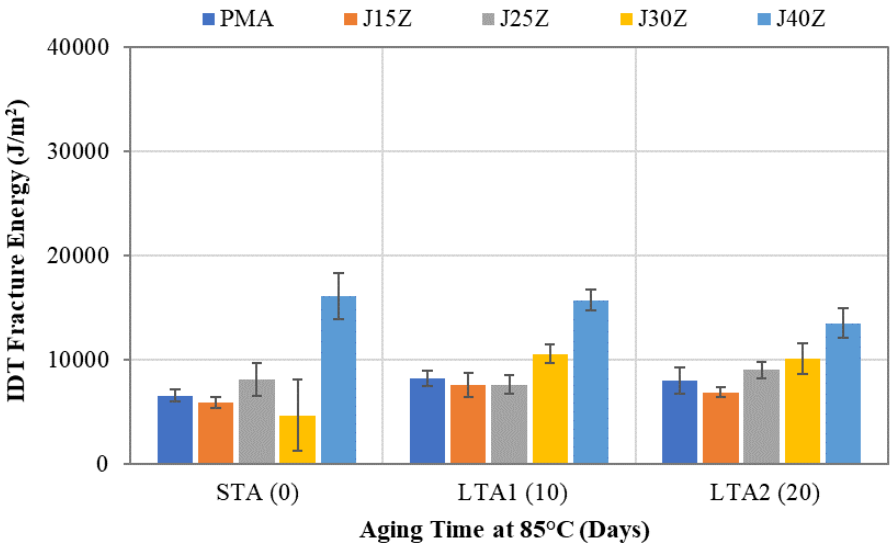

Figure 76. IDT G_f Results of GRN1 Mixtures with PMA and J-EMA Binders under Different Mix Aging Conditions

Table 55. Tukey's Groupings for IDT G_f Results of GRN1 Mixtures with PMA and J-EMA Binders under the STA Condition

Binder ID	N	Mean (J/m^2)	Grouping	
J40Z	8	16,084	A	
J25Z	6	8,112		B
PMA	5	6,535		B
J15Z	6	5,897		B
J30Z	6	4,670		B

Table 56. Tukey's Groupings for IDT G_f Results of GRN1 Mixtures with PMA and J-EMA Binders under the LTA1 Condition

Binder ID	N	Mean (J/m^2)	Grouping		
J40Z	4	15,710	A		
J30Z	6	10,561		B	
PMA	6	8,235			C
J25Z	6	7,577			C
J15Z	4	7,546			C

Table 57. Tukey's Groupings for IDT G_f Results of GRN1 Mixtures with PMA and J-EMA Binders under the LTA2 Condition

Binder ID	N	Mean (J/m^2)	Grouping			
J40Z	4	13,503	A			
J30Z	6	10,116		B		
J25Z	6	9,012		B	C	
PMA	6	7,995			C	D
J15Z	5	6,881				D

The IDT G_f results of GRN1 mixtures containing the PMA and U-EMA binders are presented in Figure 77. The results show that the IDT G_f of the U-EMA mixtures increased with an increase in EDR under all three mix aging conditions. The comparison between the PMA and U-EMA mixtures was highly dependent on the EDR. Under all three mix aging conditions, the U30C and U40C mixtures had consistently higher IDT G_f results and are expected to have better fracture resistance than the PMA mixture, while the U15C and U20C mixtures had similar or lower IDT G_f results than the PMA mixture. According to the Tukey's rankings in Table 58 through Table 60, the statistical comparisons for the IDT G_f results of GRN1 mixtures with PMA *versus* U-EMA binders are summarized as follows:

- STA: PMA > U15C; PMA = U25C and U30C; PMA < U40C.
- LTA1: PMA = U15C and U25C; PMA < U30C and U40C.
- LTA2: PMA = U15C and U25C; PMA < U30C and U40C.

  (see explanations of the ranking symbols in notes above Figure 76)

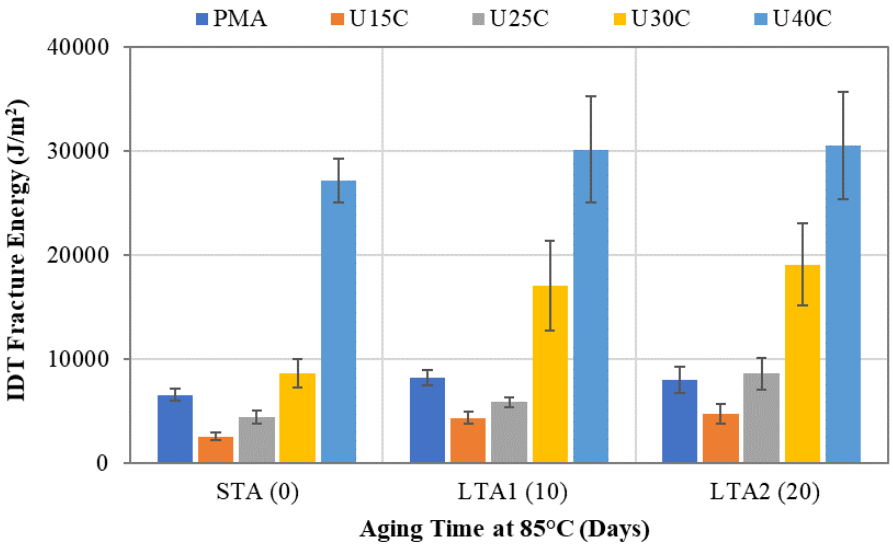

Figure 77. IDT G_f Results of GRN1 Mixtures with PMA and U-EMA Binders under Different Mix Aging Conditions

Table 58. Tukey's Groupings for IDT G_f Results of GRN1 Mixtures with PMA and U-EMA Binders under the STA Condition

Binder ID	N	Mean (J/m²)	Grouping			
U40C	6	27,142	A			
U30C	6	8,643		B		
PMA	5	6,535		B	C	
U25C	6	4,438			C	D
U15C	6	2,549				D

Table 59. Tukey's Groupings for IDT G_f Results of GRN1 Mixtures with PMA and U-EMA Binders under the LTA1 Condition

Binder ID	N	Mean (J/m^2)	Grouping		
U40C	6	30,143	A		
U30C	6	17,069		B	
PMA	6	8,235			C
U25C	5	5,831			C
U15C	6	4,339			C

Table 60. Tukey's Groupings for IDT G_f Results of GRN1 Mixtures with PMA and U-EMA Binders under the LTA2 Condition

Binder ID	N	Mean (J/m^2)	Grouping		
U40C	6	30,550	A		
U30C	5	19,065		B	
U25C	6	8,614			C
PMA	6	7,995			C
U15C	6	4,701			C

LMS Mix Design

Figure 78 present the IDT G_f results of LMS mixtures containing the PMA and J-EMA binders under three mix aging conditions. For all the J-EMA mixtures except one, the IDT G_f increased as the EDR increased. The only exception was the J40Z mixture, which had a slightly lower average IDT G_f value than the J30Z mixture under the STA condition. However, this difference may not be practically significant if considering the variability of the results (as indicated by the error bars). Under all three mix aging conditions, the J25Z, J30Z, and J40Z mixtures had higher average IDT G_f results and are expected to have better fracture resistance than the PMA mixture. The opposite trend was observed for the comparison between the J15Z and PMA mixtures. According to the Tukey's rankings provided in Table 61 through Table 63, the statistical comparisons for the IDT G_f results of LMS mixtures with PMA *versus* J-EMA binders are summarized as follows:

- STA: PMA = J15Z and J25Z; PMA < J30Z and J40Z.
- LTA1: PMA = J15Z and J25Z; PMA < J30Z and J40Z.
- LTA2: PMA = J15Z and J25Z; PMA < J30Z and J40Z.

(see explanations of the ranking symbols in notes above Figure 76)

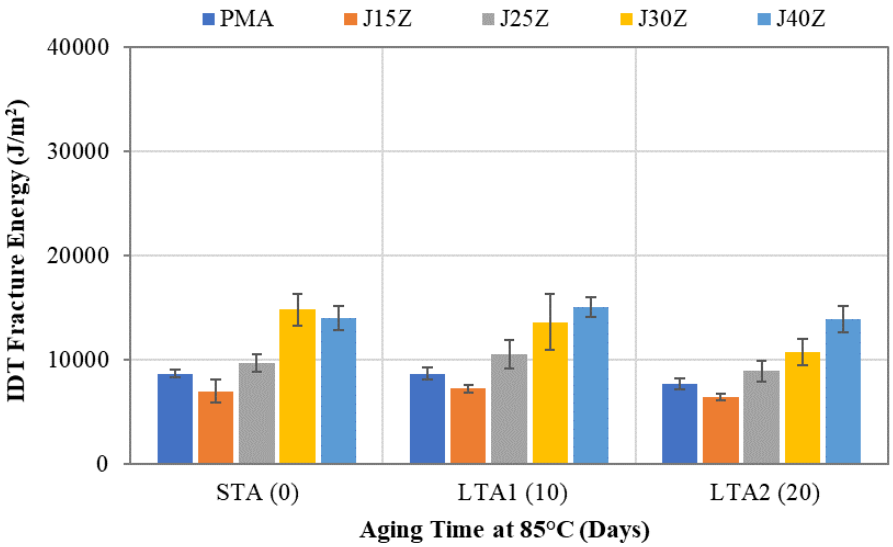

Figure 78. IDT G_f Results of LMS Mixtures with PMA and J-EMA Binders under Different Mix Aging Conditions

Table 61. Tukey's Groupings for IDT G_f Results of LMS Mixtures with PMA and J-EMA Binders under the STA Condition

Binder ID	N	Mean (J/m^2)	Grouping		
J30Z	6	14,791	A		
J40Z	6	13,998	A		
J25Z	6	9,707		B	
PMA	6	8,669		B	C
J15Z	6	6,980			C

Table 62. Tukey's Groupings for IDT G_f Results of LMS Mixtures with PMA and J-EMA Binders under the LTA1 Condition

Binder ID	N	Mean (J/m^2)	Grouping		
J40Z	6	15,015	A		
J30Z	6	13,601	A		
J25Z	6	10,513		B	
PMA	6	8,641		B	C
J15Z	6	7,201			C

Table 63. Tukey's Groupings for IDT G_f Results of LMS Mixtures with PMA and J-EMA Binders under the LTA2 Condition

Binder ID	N	Mean (J/m^2)	Grouping			
J40Z	6	13,874	A			
J30Z	6	10,744		B		
J25Z	6	8,899			C	
PMA	6	7,664			C	D
J15Z	6	6,390				D

The IDT G_f results of LMS mixtures containing the PMA and U-EMA binders at different EDRs are shown in Figure 79. For all three mix aging conditions, the IDT G_f of the U-EMA mixtures increased with an increase in EDR. The comparison between the PMA and U-EMA mixtures was dependent on the EDR and mix aging condition. Only the U40C mixture had consistently higher IDT G_f results than the PMA mixture under the three mix aging conditions. The opposite trend was observed for the comparison between the U15C and PMA mixtures. The U30C and PMA mixtures had similar IDT G_f results under the STA condition, but after long-term aging, the U30C mixture showed significantly higher IDT G_f results. According to the Tukey's rankings in Table 64 through Table 66, the statistical comparisons for the IDT G_f results of LMS mixtures with PMA *versus* U-EMA binders are summarized as follows:

- STA: PMA > U15C and U25C; PMA = U30C; PMA < U40C.
- LTA1: PMA > U15C; PMA = U25C; PMA < U30C and U40C.
- LTA2: PMA > U15C; PMA = U25C; PMA < U30C and U40C.

  (see explanations of the ranking symbols in notes above Figure 76)

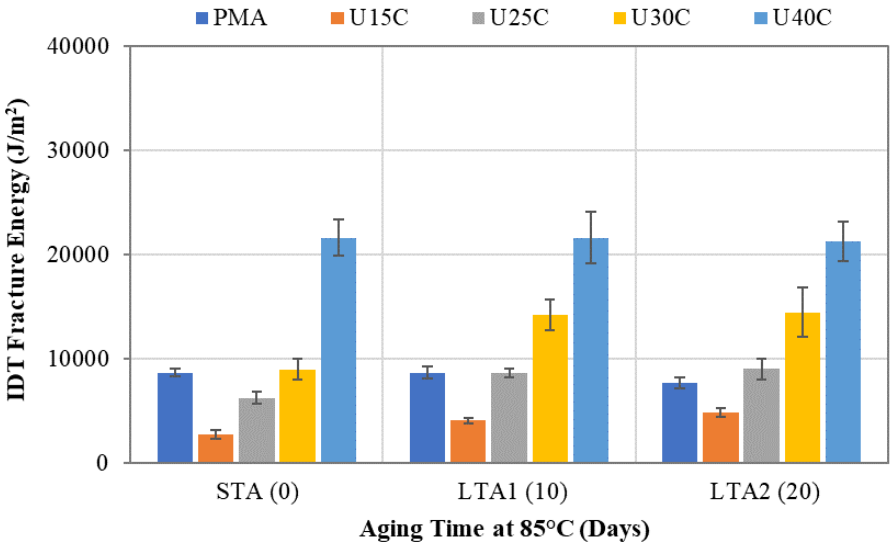

Figure 79. IDT G_f Results of LMS Mixtures with PMA and U-EMA Binders under Different Mix Aging Conditions

Table 64. Tukey's Groupings for IDT G_f Results of LMS Mixtures with PMA and U-EMA Binders under the STA Condition

Binder ID	N	Mean (J/m^2)	Grouping			
U40C	6	21,606	A			
U30C	6	8,972		B		
PMA	6	8,669		B		
U25C	6	6,231			C	
U15C	6	2,744				D

Table 65. Tukey's Groupings for IDT G_f Results of LMS Mixtures with PMA and U-EMA Binders under the LTA1 Condition

Binder ID	N	Mean (J/m^2)	Grouping			
U40C	6	21,631	A			
U30C	6	14,199		B		
PMA	6	8,641			C	
U25C	5	8,585			C	
U15C	6	4,048				D

Table 66. Tukey's Groupings for IDT G_f Results of LMS Mixtures with PMA and U-EMA Binders under the LTA2 Condition

Binder ID	N	Mean (J/m^2)	Grouping			
U40C	6	21,268	A			
U30C	6	14,461		B		
U25C	6	9,003			C	
PMA	6	7,664			C	
U15C	6	4,803				D

Selection of Optimum EDR

The optimum EDR of EMA binders was selected based on the following three criteria applicable to the Cantabro and IDT test results determined under three mix aging conditions:

1) Under the STA condition, the EMA mixture at the optimum EDR should have an average Cantabro loss of less than 20%. This criterion is selected based on recommendations from NCHRP project 1-55, which also matches FDOT's current Cantabro test criterion for mix design approval of FC-5 mixtures with a PMA or HP binder. Criterion 1 is mainly to ensure that the EMA mixture has adequate raveling resistance before long-term aging.
2) Under the LTA1 condition, the EMA mixture at the optimum EDR should have statistically lower Cantabro loss results, but statistically higher IDT strength and G_f results than the corresponding PMA mixture. This evaluation requires statistical comparisons (i.e., ANOVA and Tukey's HSD tests) to account for the variability of the test results and is considered a more conservative approach than using the numerical comparisons of the average test results. Criterion 2 is to ensure that the EMA mixture has significantly better raveling resistance, tensile strength, and fracture resistance than the PMA mixture after long-term aging.
3) Under the LTA2 condition, the EMA mixture at the optimum EDR should have statistically lower Cantabro loss, but statistically higher IDT strength and G_f results than the corresponding PMA mixture. This criterion is essentially the same as Criterion 2 but requires statistical comparisons of the Cantabro and IDT test results after extended long-term aging. Criterion 3 is to ensure that the EMA mixture continues to have better performance properties compared to the PMA mixture after extended long-term aging and provides the potential of extending the life span of OGFC in Florida.

Table 67 summarizes statistical comparisons of the Cantabro and IDT test results *versus* the proposed criteria for the selection of optimum EDR for J-EMA mixtures. The comparison results are denoted as "Pass" or "Fail", where "Pass" indicates that the test results meet the proposed

criterion and "Fail" indicates that the results fail the criterion. As shown, all the J-EMA mixtures had acceptable Cantabro loss results under the STA condition and thus, pass Criterion 1 regardless of the EDR. Under the LTA1 and LTA2 conditions, most of the J-EMA mixtures at 15% and 25% EDRs did not statistically outperform the PMA mixtures in the Cantabro and IDT tests and thus, fail Criterion 2 and Criterion 3. The J-EMA mixtures at 30% and 40% EDR, on the other hand, pass both criteria corresponding to the Cantabro and IDT test results after long-term aging for both mix designs.

Table 67. Selection of Optimum EDR for J-EMA Binders

EDR	FC-5 Mix Design	Criterion 1	Criterion 2			Criterion 3		
		Cantabro Loss	Cantabro Loss	IDT Strength	IDT G_f	Cantabro Loss	IDT Strength	IDT G_f
15%	GRN1	Pass	Fail	Pass	Fail	Fail	Fail	Fail
	LMS	Pass	Fail	Fail	Fail	Fail	Fail	Fail
25%	GRN1	Pass	Fail	Pass	Fail	Fail	Pass	Fail
	LMS	Pass	Fail	Pass	Fail	Fail	Fail	Fail
30%	GRN1	Pass	Pass	Pass	Pass	Pass	Pass	Pass
	LMS	Pass	Pass	Pass	Pass	Pass	Pass	Pass
40%	GRN1	Pass	Pass	Pass	Pass	Pass	Pass	Pass
	LMS	Pass	Pass	Pass	Pass	Pass	Pass	Pass

Similar trends can be observed for the comparison results of U-EMA mixtures in Table 68. For both mix designs, the U-EMA mixtures at 15% to 40% EDRs pass Criterion 1 with an average Cantabro loss of less than 20% under the STA condition. Most of the U-EMA mixtures at 15% and 25% EDRs fail Criterion 2 and Criterion 3 based on comparisons of the long-term aged Cantabro and IDT test results against the PMA mixtures. The U-EMA mixtures at 30% EDR pass both criteria for most of the test result comparisons. The only two exceptions are a mixture with the GRN1 mix design and a mixture with the LMS mix design. In both cases, the U-EMA mixtures at 30% EDR had lower average Cantabro loss results than the corresponding PMA mixtures under the LTA condition, but the differences are not statistically significant according to the Tukey's groupings. Finally, the U-EMA mixtures at 40% EDR pass both Criterion 2 and Criterion 3 for all the test result comparisons except one. The exception is a mixture with the GRN1 mix design, which had a lower average Cantabro loss than the corresponding PMA mixture under the LTA1 condition, but the results are considered statistically equivalent based on the Tukey's HSD test.

Table 68. Selection of Optimum EDR for U-EMA Binders

EDR	FC-5 Mix Design	Criterion 1	Criterion 2			Criterion 3		
		Cantabro Loss	Cantabro Loss	IDT Strength	IDT G_f	Cantabro Loss	IDT Strength	IDT G_f
15%	GRN1	Pass	Fail	Fail	Fail	Fail	Fail	Fail
	LMS	Pass	Fail	Fail	Fail	Fail	Fail	Fail
25%	GRN1	Pass	Fail	Fail	Fail	Fail	Fail	Fail
	LMS	Pass	Fail	Pass	Fail	Pass	Pass	Fail
30%	GRN1	Pass	Fail	Pass	Pass	Pass	Pass	Pass
	LMS	Pass	Fail	Pass	Pass	Pass	Pass	Pass
40%	GRN1	Pass	Fail	Pass	Pass	Pass	Pass	Pass
	LMS	Pass	Pass	Pass	Pass	Pass	Pass	Pass

Based on the comparison results in Table 67 and Table 68, both 30% and 40% EDR pass all the proposed criteria for J-EMA mixtures and most of the criteria for U-EMA mixtures; therefore, either of the two could be selected as the optimum EDR from a mixture performance evaluation perspective. However, OGFC mixtures at these two EDRs would have considerably different material cost. Based on the limited cost information of epoxy materials that is available, it is estimated that U-EMA binders at 30% and 40% EDR will cost approximately $5,000/ton and $6,500/ton, respectively, and that J-EMA binders at 30% and 40% EDR will cost approximately $3,300/ton and $4,200/ton, respectively. Using these estimated binder costs, OGFC mixtures with U-EMA binders at 30% and 40% EDR are estimated to cost approximately $380/ton and $480/ton, respectively, while those containing J-EMA binders at 30% and 40% EDR will cost approximately $260/ton and $330/ton, respectively. Because of the significantly high costs of epoxy materials, the lower EDR of 30% was selected as the final optimum (i.e., most cost-effective) EDR for both U-EMA and J-EMA binders for further evaluation in the study. At this EDR, the overall material cost of OGFC mixtures with an EMA binder are approximately 3.5 to 5 times higher than that of the traditional PMA mixtures with an estimated material cost of $75/ton.

4.3 Summary of Findings

For the binder testing experiment, rotational viscosity results have indicated that as temperature increased, the viscosity of EMA binders at 15% and 25% EDRs decreased and the time required to achieve a plateau in viscosity became shorter, which in this study was selected as an indication of the completion of the curing process of the EMA binders. When considering performance grading, both the high-temperature and low-temperature true grade results showed that the epoxy materials stiffened the base asphalt binders. At 15% and 25% EDR, the epoxy materials improved the intermediate-temperature true grade of the base binders used for the modification. When comparing the modified binders, the HP binder had the lowest intermediate pass/fail temperature, followed by the EMA binders and then the PMA binder. The ranking of these modified binders from lower (i.e., more negative) to higher (i.e., less negative, or more positive) ΔT_c was: J25Z = PMA < J15Z < U15C < HP. However, this ranking should be interpreted with caution because the EMA binders were formulated with different base binders than the PMA and HP binders.

MSCR test results indicated that epoxy modification in the U25C binder led to a reduction in the J_{nr} and an increase in the %Recovery as compared to the unmodified base binder C, while the U15C binder softened rather than stiffened after epoxy modification. On the other hand, the epoxy modification at both 15% and 25% EDRs was effective for J-EMA binders. Furthermore, compared to the base and EMA binders, the PMA and HP binders provided better balance of both the J_{nr} and %Recovery parameters. LAS test results indicated that both the domestic and foreign epoxy materials at 15% EDR did not improve the fatigue life of the EMA binders relative to the unmodified binders. The PMA and HP binders presented a higher number of cycles to failure (N_f) in comparison to the unmodified and EMA binders. The *G*-*R* parameter results in Black Space indicated that, with exception of the PMA binder, the evaluated binders are not likely to experience premature block cracking in the field. |G*| and phase angle master curves suggested that traditional parameters for performance characterization of unmodified binders are not suitable to adequately characterize the rheological properties of HP and EMA binders. Lastly, BBS test results demonstrated that the asphalt-aggregate systems that were least susceptible to moisture damage were the "HP + GRN1" and "U15C + GRN2" combinations.

For the mixture testing experiment, as EDR increased in the range between 15% and 40%, the Cantabro loss gradually decreased while the IDT strength and G_f results increased, which indicated that epoxy modification of the asphalt binder has a positive impact on improving the raveling resistance, tensile strength, and fracture resistance of OGFC mixtures. The comparison in the Cantabro and IDT test results between the PMA and EMA mixtures was highly dependent on the EDR and mix aging condition. In general, the EMA mixtures at high EDRs (i.e., 30% and 40%) outperformed the PMA mixtures in the Cantabro and IDT tests, and the differences were more pronounced after long-term aging. On the other hand, the EMA mixtures at low EDRs of 15% and 25% had similar or reduced Cantabro and IDT test results than the PMA mixtures. Based on the CAI results, the U-EMA mixtures are expected to have the best aging resistance, followed by the J-EMA mixtures and PMA mixtures, respectively. Finally, three criteria based on statistical comparisons of the Cantabro and IDT test results under various mix aging conditions were proposed for the selection of optimum EDR of EMA binders. The comparison results showed that EMA mixtures at 30% and 40% EDR had consistently better performance properties than the PMA mixtures and have the potential of extending the life span of OGFC in Florida. Because of the high costs of epoxy materials, the lower EDR of 30% was selected as the final optimum (i.e., most cost-effective) EDR of EMA binders prepared with both the domestic source and foreign source epoxy materials. At this EDR, OGFC mixtures with an EMA binder are estimated to be approximately 3.5 to 5 times more expensive than those containing a PMA binder from the material cost perspective.

CHAPTER 5. MIX DESIGN OF EMA OGFC MIXTURES

This chapter presents the experimental plan, test results, and findings of Experiment 3 of the study. The objective of this experiment was to determine an effective method to design OGFC mixtures containing EMA binders. Currently, FDOT uses the pie plate method for selecting the OBC of FC-5 mixtures per FM 5-588. In this method, pie plate samples of OGFC mixtures containing a PG 67-22 binder at different binder contents are prepared and examined to visually assess the degree of bonding between the mixture and the bottom of the pie plate as well as asphalt draindown on the pie plate. Based on visual observation of the pie plates, the OBC is selected as the binder content of which the corresponding pie plate exhibits sufficient bonding without excessive asphalt draindown. In 2018/2019, FDOT added an additional step in the FC-5 mix design approval process, which requires the Cantabro testing (per AASHTO TP 108-14) of the OGFC mixture prepared with a PMA or HP binder at the OBC to evaluate its raveling resistance. The mix design will only be accepted if the PMA or HP mixture has a Cantabro loss of less than 20% when tested at the unaged condition (i.e., without additional long-term aging after compaction). Therefore, this experiment sought to develop a similar mix design procedure for OGFC mixtures containing EMA binders.

5.1 Experimental Plan

Materials and Mix Design

Table 69 presents the proposed testing matrix of Experiment 3. Four FDOT approved FC-5 mix designs were evaluated, which corresponded to three granite (i.e., GRN1, GRN2, and GRN3) mixes and one limestone (i.e., LMS) mix. Table 70 summarizes the job mix formula of these mix designs. Two EMA binders prepared with two sources of epoxy materials at 30% EDR were included. Based on a partial factorial design, four combinations of mix design and EMA binder were evaluated with the proposed procedure of designing OGFC mixtures containing EMA binders, which will be discussed later in this chapter. These combinations are GRN1 mix design with U30C EMA binder, GRN2 mix design with J30Z EMA binder, GRN3 mix design with J30Z EMA binder, and LMS mix design with U30C EMA binder.

Table 69. Testing Matrix of Experiment 3

Factor Name	Factor No.	Description
Binder source & epoxy resin source	2	Two combinations selected in Experiment 1
Epoxy dosage rate	1	Optimum epoxy dosage rate selected in Experiment 2
Mix Design	4	GRN1, GRN2, GRN3, LMS
Combination	4	GRN1 + U30C EMA binder GRN2 + J30Z EMA binder GRN3 + J30Z EMA binder LMS + U30C EMA binder

Table 70. Job Mix Formula Summary of GRN1, GRN2, GRN3, and LMS Mixes

Mix Design ID		GRN1	GRN2	GRN3	LMS
Aggregate Gradation (% Passing)	3/4"	100	100	100	100
	1/2"	99	95	95	94
	3/8”	71	75	69	74
	No. 4	24	23	24	23
	No. 8	9	10	10	10
	No. 16	5	6	4	8
	No. 30	4	4	3	6
	No. 50	3	3	3	5
	No. 100	3	3	3	4
	No. 200	2.5	2.1	3.0	3.3
Combined G_{sb}		2.769	2.625	2.633	2.417
JMF OBC (%)		6.8	6.6	6.5	6.9
Additives		0.3% Cellulose Fiber, 1.0% Hydrated Lime	0.4% Mineral Fiber, 1.0% Hydrated Lime	0.3% Cellulose Fiber, 1.0% Hydrated Lime	0.3% Cellulose Fiber

Proposed Mix Design Procedure for EMA OGFC Mixtures

Figure 80 presents the graphical illustration of the proposed mix design procedure for OGFC mixtures containing EMA binders. The procedure is similar to the current FDOT mix design procedure for OGFC mixtures with PMA or HP binders but requires additional pie plate testing of mixtures containing an EMA binder.

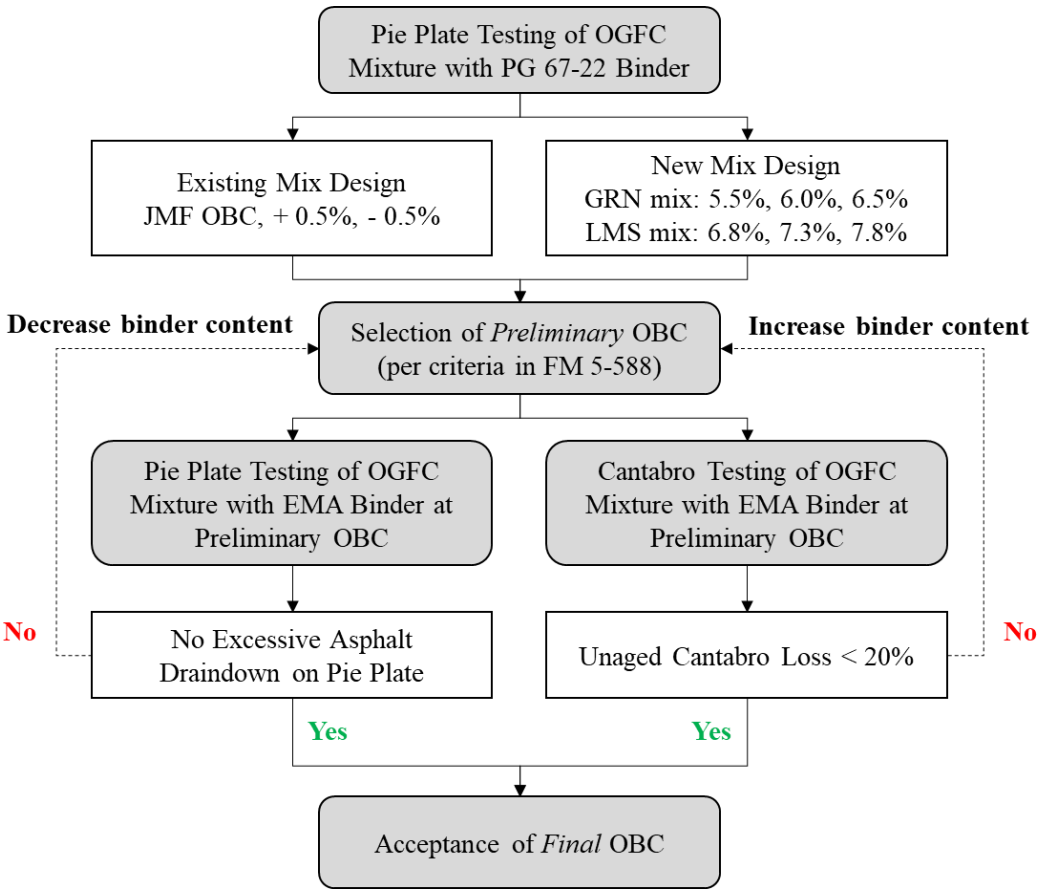

Figure 80. Proposed Mix Design Procedure for EMA OGFC Mixtures

As shown in Figure 81, the proposed procedure starts with the pie plate testing of OGFC mixtures prepared with a PG 67-22 unmodified binder at three binder contents. For existing mix designs, the three binder contents recommended for pie plate testing are the OBC in the JMF, JMF OBC plus 0.5%, and JMF OBC minus 0.5%. For new mix designs, it is suggested to follow recommendations in FM 5-588 of using 5.5%, 6.0%, and 6.5% for mixtures with granite aggregate, and 6.8%, 7.3%, and 7.8% for mixtures with limestone aggregate. For all the pie plates prepared, the asphalt draindown is visually assessed in comparison with the reference pie plate pictures in FM 5-588 (Figure 81). The preliminary OBC is selected as the binder content of which the corresponding pie plate displays sufficient bonding between the mixture and the bottom of the pie plate without evidence of excessive asphalt draindown, as shown in Figure 81(b). After the preliminary OBC is selected, another pie plate is prepared for the OGFC mixture with an EMA binder (instead of a PG 67-22 unmodified binder) at the preliminary OBC using a modified pie plate test procedure, which will be discussed later in the chapter. The pie plate is then visually examined to assess the degree of bonding between the mixture and the pie plate as well as asphalt draindown. Furthermore, a set of unaged EMA OGFC mixture specimens is prepared and tested with the Cantabro test to evaluate the raveling resistance. The preliminary OBC will be accepted as the final OBC if the mixture does not exhibit excessive asphalt draindown and has a Cantabro loss of less than 20%. Otherwise, the preliminary OBC needs to be adjusted and the mixture retested until acceptable results are obtained in both the pie plate and Cantabro tests.

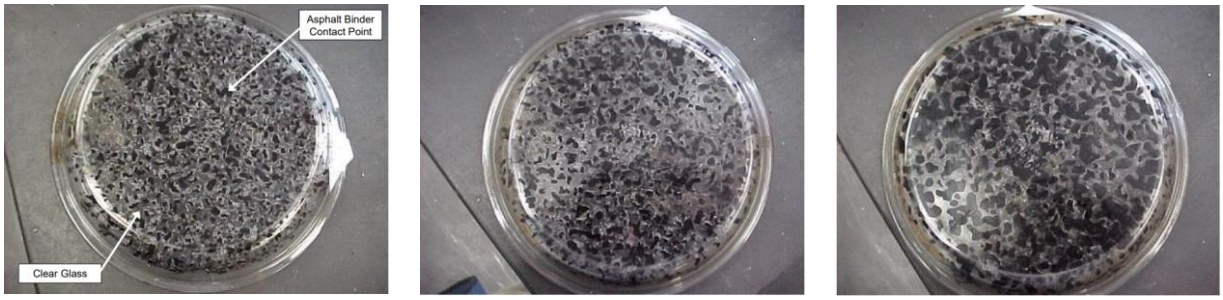

(a) (b) (c)

Figure 81. Reference Pie Plates of OGFC Mixtures with PG 67-22 Unmodified Binder at Different Binder Contents: (a) 5.5% Asphalt Binder (Insufficient Bonding/Drainage – Asphalt Binder Content Too Low), (b) 6.0% Asphalt Binder (Insufficient Bonding/Drainage – Asphalt Binder Content Slightly Low), (c) 6.5% Asphalt Binder (Excessive Bonding/Drainage – Asphalt Binder Content Slightly High) (FDOT, 2020)

Modified Pie Plate Test Procedure for OGFC Mixtures with EMA Binders

Trial-and-error attempts were first made to prepare pie plate samples for OGFC mixtures containing U30C and J30Z EMA binders following the test procedure in FM 5-588. In general, the existing test procedure worked well for the J30Z EMA binder. Therefore, no major modifications to the pie plate test procedure are needed for the J30Z EMA binder except for revising Sections 5.5 and 5.6 to as follows:

- Revise Section 5.5 to "*Heat aggregate batches ~~and the asphalt binder~~ for a minimum of two hours in an oven at ~~320 ± 5°F (160 ± 3°C)~~370 ± 5°F (188 ± 3°C). Heat the PG 67-22 base binder for two hours at 266 ± 5°F (130 ± 3°C). Heat the epoxy resin (Part A) and epoxy curing agent (Part B) for 1 hour at 140 ± 5°F (60 ± 3°C).*"
- Revise Section 5.6 to "*Mix the epoxy resin (Part A) and epoxy curing agent (Part B) and blend for 2 minutes using a low shear mixer. Then add the PG 67-22 base binder and continue to blend with a low shear mixer for 15 minutes at 266 ± 5°F (130 ± 3°C). Add the preheated aggregate and J-EMA binder into the mixing bowl. Using the spatula, gently mix the aggregate batch and ~~asphalt~~ J-EMA binder in the mixing bowl at the following three prescribed asphalt binder contents (by weight of total mix): 5.5%, 6.0%, and 6.5% for mixtures containing granite aggregate or 6.8%, 7.3%, and 7.8% for mixtures containing limestone aggregate. Continue mixing until all of the aggregate particles are thoroughly coated, ensuring that there are no large conglomerates of fine particles*." The final mixing temperature of the J30Z EMA mixture was around 160 ± 3°C.

Initial attempts using the existing pie plate test procedure were not successful for the U30C EMA binder because of its fast rate of curing behavior after mixing the epoxy resin (Part A) with the curing agent in Part B of the epoxy materials provided by the manufacturer. Using the recommended mixing temperature (i.e., 160°C) and post-mixing conditioning condition (i.e., one hour at 160°C) in FM 5-588, the U30C EMA mixture became thermoset in the pie plate, which made it difficult to visually assess the asphalt draindown and degree of bonding between the mixture and the pie plate. Therefore, to accommodate the thermosetting behavior of the U30C EMA binder, several modifications to the pie plate test procedure in FM 5-588 are proposed, which are described as follows:

- Revise Section 5.5 to "*Heat aggregate batches ~~and the asphalt binder~~ for a minimum of two hours in an oven at ~~320 ± 5°F (160 ± 3°C)~~290 ± 5°F (143 ± 3°C). Heat the PG 67-22 base binder and Part B of the epoxy materials for two hours at 266 ± 5°F (130 ± 3°C). Heat the epoxy resin (Part A) for 15 minutes at 266 ± 5°F (130 ± 3°C).*"
- Revise Section 5.6 to "*Mix the PG 67-22 base binder and Part B of the epoxy materials and blend for 15 minutes using a low shear mixer. Then add the epoxy resin (Part A) and manually blend for 30 to 40 seconds using a stirring rod. Add the preheated aggregate and U-EMA binder into the mixing bowl. Using the spatula, gently mix the aggregate batch and ~~asphalt~~ U-EMA binder in the mixing bowl at the following three prescribed asphalt binder contents (by weight of total mix): 5.5%, 6.0%, and 6.5% for mixtures containing granite aggregate or 6.8%, 7.3%, and 7.8% for mixtures containing limestone aggregate. Continue mixing until all of the aggregate particles are thoroughly coated, ensuring that there are no large conglomerates of fine particles*." The final mixing temperature of the U30C EMA mixture was around 121 ± 3°C).
- Revise Section 5.7 to "*Immediately after mixing, carefully transfer the mixture from the mixing bowl into a pie plate using a method that will evenly distribute the mixture over the entire bottom surface of the pie plate without causing segregation. Care should be taken to ensure that the mixture is not disturbed once it has contacted the pie plate. After placing the mixture in the pie plate, place the pie plate on a level surface in an oven and heat for ~~one hour at 320 ± 5°F (160 ± 3°C)~~ 40 minutes at 250 ± 5°F (121 ± 3°C). Repeat this step for each of the remaining samples*." This modified post-mixing conditioning procedure was selected based on the viscosity curing data of the U30C binder provided by the epoxy asphalt manufacturer.

5.2 Test Results and Discussion

Following the proposed mix design procedure in Figure 80, for each FC-5 mix design included in the study, pie plate samples were prepared for OGFC mixtures with a PG 67-22 unmodified binder at three binder contents (i.e., JMF OBC, JMF OBC+0.5%, and JMF OBC-0.5%). In this report, the pie plate images are presented in two ways. Initially, photos were taken with the loose mixture inside the pie plate per FM 5-588. Though this process allowed for visual assessment of the pie plate samples with different binder contents, the glare of the glass combined with the concentration of black-colored asphalt mixture made it challenging to differentiate the pie plate samples in the photos. Hence, another set of pictures were taken after carefully removing the loose mixture from the pie plate to allow for better discrimination of the pie plate samples based on visual observation, but these pictures are used for documentation purposes only. The procedure followed to remove the loose mixture from the pie plate is briefly described as follows. After conditioning, the pie plate was rested on an insulating surface to allow the loose mixture to cool. Once the system reached room temperature, the pie plate was overturned. At this point, the loose mixture was not fully set but was hard enough to fall off the plate at once upon overturning without sliding and creating smudge. After that, large-size aggregate particles that had stuck to the plate, if any, were removed carefully with caution by hand. Finally, the empty pie plate was placed over a white oilpaper for pictures.

GRN1 Mix Design

Figure 82 and Figure 83 present the pie plates with and without the loose mixture, respectively, of GRN1 mixtures containing a PG 67-22 binder. As shown, the pie plate at the JMF OBC-0.5% (6.3%) had the least asphalt draindown and bonding between the mixture and the bottom of the pie plate, while that of the JMF OBC+0.5% (7.3%) had the most asphalt draindown. In comparison with the reference pictures in FM 5-588 (Figure 81), the pie plate at the JMF OBC (6.8%) seemed to have more asphalt draindown than it should at the OBC; in this case, the preliminary OBC would have been selected between the JMF OBC-0.5% (6.3%) and JMF OBC (6.8%) based on visual observation of the pie plates. However, given this is an existing FDOT mix design, the research team and project panel decided to proceed with 6.8% as the preliminary OBC for further evaluation of the EMA mixture using the pie plate and Cantabro tests.

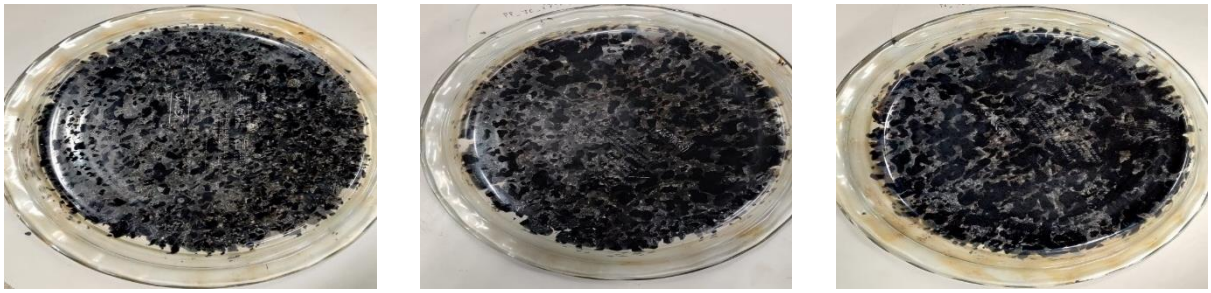

(a) (b) (c)

Figure 82. Pie Plates (With Loose Mixture) of GRN1 Mixtures with PG 67-22 Binder at (a) JMF OBC-0.5% (6.3%), (b) JMF OBC (6.8%), (c) JMF OBC+0.5% (7.3%)

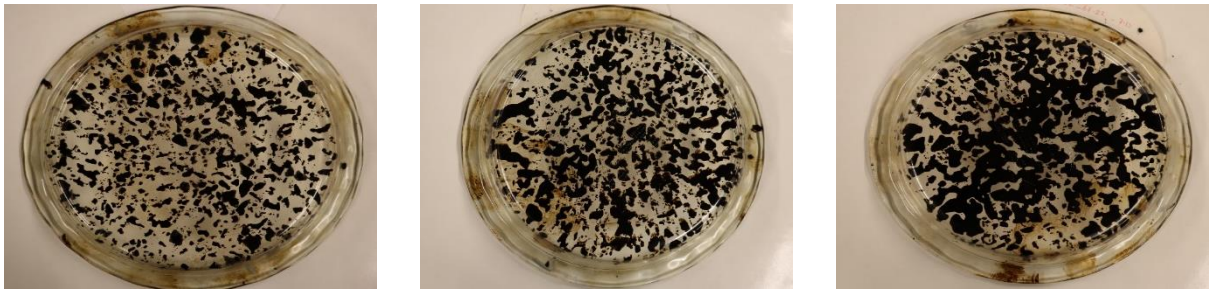

(a) (b) (c)

Figure 83. Pie Plates (Without Loose Mixture) of GRN1 Mixtures with PG 67-22 Binder at (a) JMF OBC-0.5% (6.3%), (b) JMF OBC (6.8%), (c) JMF OBC+0.5% (7.3%)

Figure 84 presents the pie plates of the GRN1 mixture prepared with the U30C EMA binder at the preliminary OBC of 6.8%. As compared to the PG 67-22 binder at the same binder content [Figure 82(b)], the U30C EMA binder significantly reduced the amount of asphalt draindown in the pie plate. When tested at the unaged condition, the U30C EMA mixture had an average Cantabro loss of 17%, which met the proposed maximum 20% criterion. Therefore, the JMF OBC of 6.8% was accepted as the final OBC for the U30C EMA mixture.

(a) (b)

Figure 84. Pie Plates of GRN1 Mixture with U30C EMA Binder at JMF OBC (6.8%): (a) With Loose Mixture, (b) Without Loose Mixture

GRN2 Mix Design

Figure 85 and Figure 86 present the pie plates with and without the loose mixture, respectively, of GRN2 mixtures containing a PG 67-22 binder at different binder contents. The degree of bonding between the mixture and the pie plate as well as the asphalt draindown consistently increased as the binder content increased from 6.1% to 6.6% and then to 7.1%. As compared to the reference picture at the OBC in FM 5-588 [Figure 81(b)], the pie plate at the JMF OBC-0.5% (6.1%) seemed to have insufficient bonding and asphalt draindown while those at the JMF OBC (6.6%) and JMF OBC+0.5% (7.1%) exhibited excessive draindown. Therefore, based on the pie plates in Figure 85, the preliminary OBC would have been selected between 6.1% and 6.6% instead of 6.6% as provided in the JMF.

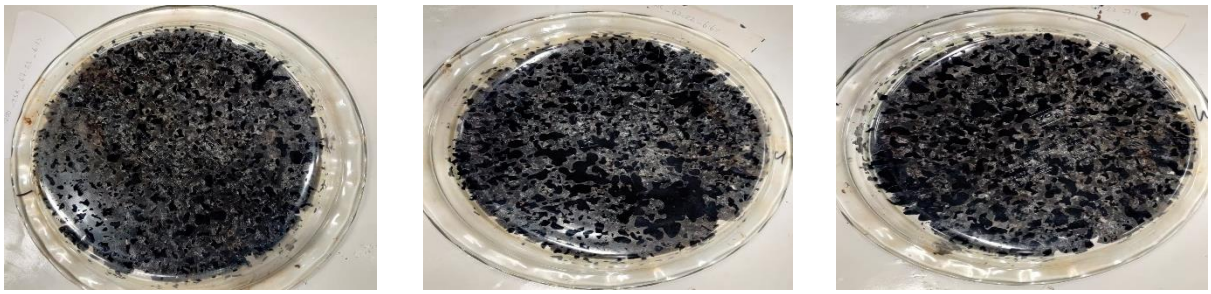

(a) (b) (c)

Figure 85. Pie Plates (With Loose Mixture) of GRN2 Mixtures with PG 67-22 Binder at (a) JMF OBC-0.5% (6.1%), (b) JMF OBC (6.6%), (c) JMF OBC+0.5% (7.1%)

(a) (b) (c)

Figure 86. Pie Plates of GRN2 Mixtures with PG 67-22 Binder at (a) JMF OBC-0.5% (6.1%), (b) JMF OBC (6.6%), (c) JMF OBC+0.5% (7.1%)

Figure 87 presents the pie plates of the GRN2 mixture prepared with the J30Z EMA binder at the JMF OBC of 6.6%. As compared to the PG 67-22 binder at the same binder content [Figure 85(b)], the J30Z EMA binder significantly reduced the amount of asphalt draindown in the pie plate. The J30Z EMA mixture had an average Cantabro loss of 17% at the unaged condition, which met the proposed criterion of maximum 20%. Therefore, the JMF OBC of 6.6% was accepted as the final OBC for the J30Z EMA mixture.

(a) (b)

Figure 87. Pie Plates of GRN2 Mixture with J30Z EMA Binder at JMF OBC (6.6%): (a) With Loose Mixture, (b) Without Loose Mixture

GRN3 Mix Design

Figure 88 and Figure 89 present the pie plates with and without the loose mixture, respectively, of GRN3 mixtures containing a PG 67-22 binder at different binder contents. The pie plates at the JMF OBC-0.5% (6.0%) and JMF OBC (6.5%) exhibited sufficient bonding and asphalt draindown, while that at the JMF OBC+0.5% (7.0%) showed excessive bonding and asphalt draindown. Based on visual observation of the pie plates in Figure 88, the preliminary OBC would have been selected as 6.5%, which matches the JMF OBC.

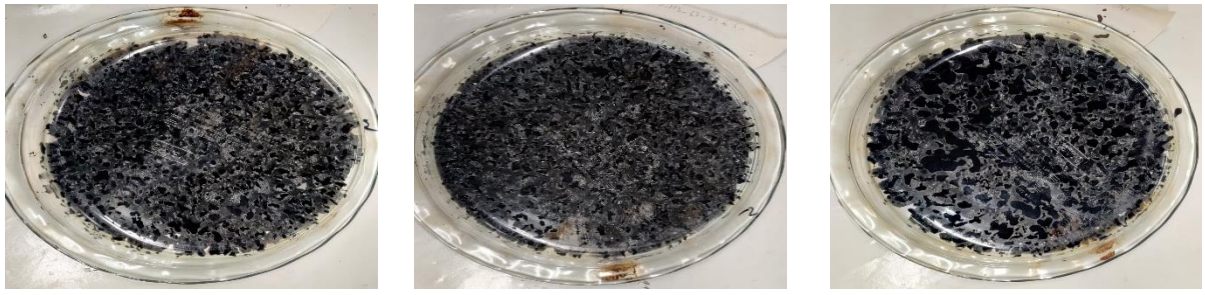

(a) (b) (c)

Figure 88. Pie Plates (With Loose Mixture) of GRN3 Mixtures with PG 67-22 Binder at (a) JMF OBC-0.5% (6.0%), (b) JMF OBC (6.5%), (c) JMF OBC+0.5% (7.0%)

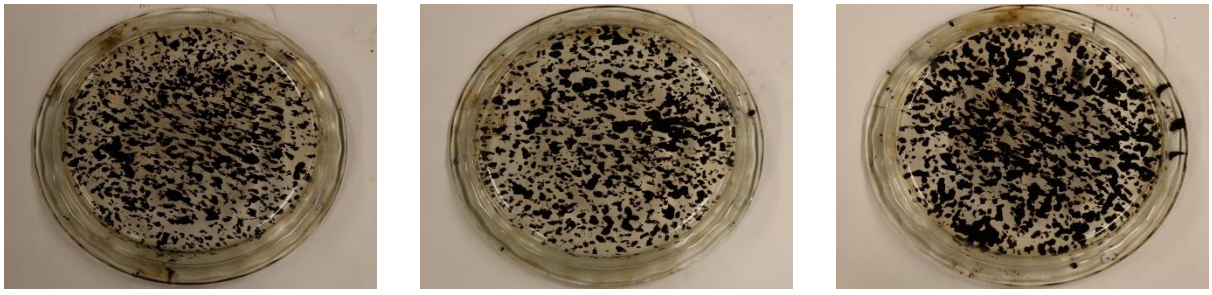

(a) (b) (c)

Figure 89. Pie Plates (Without Loose Mixture) of GRN3 Mixtures with PG 67-22 Binder at (a) JMF OBC-0.5% (6.0%), (b) JMF OBC (6.5%), (c) JMF OBC+0.5% (7.0%)

Figure 90 presents the pie plates of the GRN3 mixture prepared with the J30Z EMA binder at the JMF OBC of 6.5%. As compared to the PG 67-22 binder at the same binder content [Figure 88(b)], the J30Z EMA binder significantly reduced the degree of asphalt draindown in the pie plate. When tested at the unaged condition, the J30Z EMA mixture had an average Cantabro loss of 11%, which met the proposed criterion maximum of 20%. Therefore, the JMF OBC of 6.5% was accepted as the final OBC for the J30Z EMA mixture.

(a) (b)

Figure 90. Pie Plates of GRN3 Mixture with J30Z EMA Binder at JMF OBC (6.5%): (a) With Loose Mixture, (b) Without Loose Mixture

LMS Mix Design

Figure 91 and Figure 92 present the pie plates with and without the loose mixture, respectively, of LMS mixtures containing a PG 67-22 binder. Based on visual observation, the pie plate at the JMF OBC-0.5% (6.4%) had insufficient bonding, and that at the JMF OBC+0.5% (7.4%) showed excessive asphalt draindown. No considerable difference was observed between the pie plates at the JMF OBC-0.5% (6.4%) and JMF OBC (6.9%). The mixture prepared at the JMF OBC (6.9%) exhibited slightly insufficient bonding and asphalt draindown. Therefore, based on the pie plates in Figure 91, the preliminary OBC would have been selected between the JMF OBC (6.9%) and JMF OBC+0.5% (7.4%). However, for the same reasons mentioned previously, the JMF OBC of 6.9% was used for further evaluation of the EMA mixture using the pie plate and Cantabro tests.

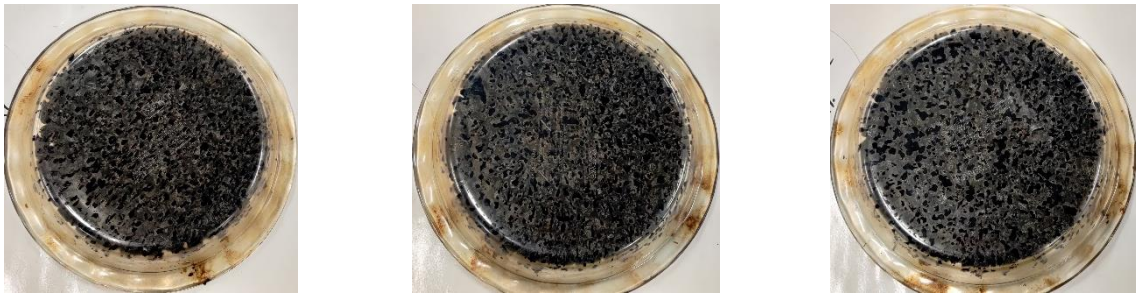

(a) (b) (c)

Figure 91. Pie Plates (With Loose Mixture) of LMS Mixtures with PG 67-22 Binder at (a) JMF OBC-0.5% (6.4%), (b) JMF OBC (6.9%), (c) JMF OBC+0.5% (7.4%)

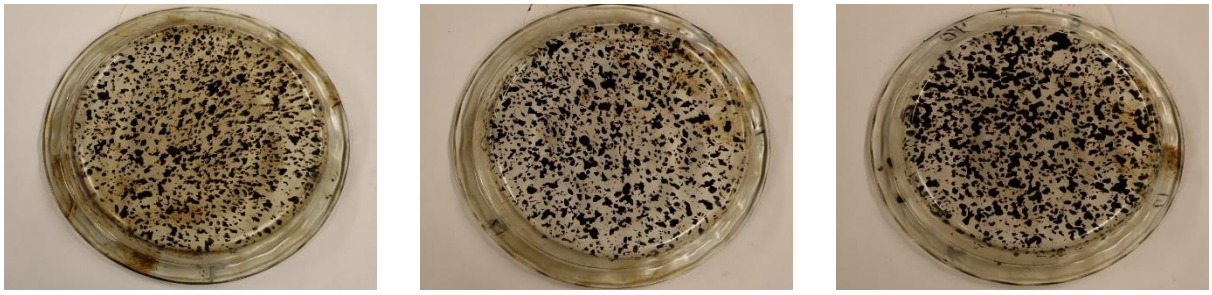

(a) (b) (c)

Figure 92. Pie Plates (Without Loose Mixture) of LMS Mixtures with PG 67-22 Binder at (a) JMF OBC-0.5% (6.4%), (b) JMF OBC (6.9%), (c) JMF OBC+0.5% (7.4%)

Figure 93 presents the pie plates of the LMS mixture prepared with the U30C EMA binder at the JMF OBC of 6.9%. As compared to the PG 67-22 binder at the same binder content [Figure 91(b)], the U30C EMA binder yielded a significantly reduced amount of asphalt draindown in the pie plate. The U30C EMA mixture had an average Cantabro loss of 11% when tested at the unaged condition, which met the proposed criterion maximum of 20%. Therefore, the JMF OBC of 6.9% was accepted as the final OBC for the U30C EMA mixture.

(a) (b)

Figure 93. Pie Plate Pictures of LMS Mixture with U30C EMA Binder at JMF OBC (6.9%): (a) with Loose Mixture, (b) without Loose Mixture

5.3 Summary of Findings

For the four FC-5 mix designs evaluated in this experiment, OGFC mixtures prepared with U30C and J30Z EMA binders at the JMF OBC had less asphalt draindown in the pie plate test than those containing the PG 67-22 unmodified binder. This trend is consistent with FDOT's experience with pie plate testing of OGFC mixtures with PMA and HP binders. All the EMA mixtures at their corresponding JMF OBC had an average Cantabro loss of less than 20% at the unaged condition, which indicated adequate raveling resistance before long-term aging. In summary, the proposed mix design procedure for OGFC mixtures containing EMA binders was successfully validated with four FDOT approved mix designs. The modified pie plate and Cantabro test results in this experiment indicate that the proposed procedure has the potential of designing EMA OGFC mixtures with minimal potential for asphalt draindown during production and adequate raveling resistance before aging.

CHAPTER 6. PERFORMANCE CHARACTERIZATION OF EMA OGFC MIXTURES

This chapter presents the experimental plan, test results, and findings of Experiment 4 of the study. The objective of this experiment was to characterize the performance properties of OGFC mixtures with EMA, PMA, and HP binders. Four FDOT approved FC-5 mix designs were included, which corresponded to three sources of granite aggregates and one source of limestone aggregate. For each mix design, four sets of OGFC mixtures were prepared with two EMA binders, one PMA binder, and one HP binder. Cantabro, IDT, TSR, and HWTT tests were conducted to characterize the raveling resistance, tensile strength, fracture resistance, moisture susceptibility, and rutting resistance of OGFC mixtures containing different types of asphalt binders. Specifically, this experiment sought to determine if the use of EMA binders at the optimum EDR (determined in Experiment 3) would yield OGFC mixtures with better performance properties than those containing a PMA or HP binder and have the potential of increasing the current life span of OGFC mixtures in Florida.

6.1 Experimental Plan

Materials and Mix Design

This experiment used the same four FC-5 mix designs (i.e., GRN1, GRN2, GRN3, and LMS) in Experiment 3. For each mix design, four sets of OGFC mixtures were prepared, which corresponded to two EMA binders at the 30% EDR (i.e., J30Z and U30C binders), one PMA binder, and one HP binder. The same procedure used to prepare EMA binders and mixtures in Experiment 2 was followed (see discussions in Chapter 4).

Laboratory Testing

Cantabro Test

The Cantabro test was performed following AASHTO TP 108-14 on OGFC mixtures subjected to two mix aging conditions: STA and LTA2 (i.e., aging compacted specimens for 20 days at 85°C prior to testing). The Cantabro loss was used to evaluate the raveling resistance of OGFC mixtures before and after extended long-term aging.

Indirect Tensile (IDT) Test

The IDEAL-CT procedure per ASTM D8225-19 was used for the IDT test in this experiment. Data analysis of the IDT test results was based on the tensile strength and G_f parameters. As with the Cantabro test, the IDT test was conducted after two mix aging conditions (i.e., STA and LTA2) to consider the impact of asphalt aging on the tensile strength and fracture resistance of OGFC mixtures prepared with different asphalt binders.

Tensile Strength Ratio (TSR) Test

The TSR test was performed in accordance with AASHTO T 283 with a few modifications made to accommodate OGFC mixtures. These modifications included: (1) specimens were compacted to N_{design}, (2) moisture conditioned specimens were saturated at 26 inches Hg below atmospheric pressure for 10 minutes regardless of the level of saturation, and (3) moisture conditioned specimens were kept submerged in water during the freeze conditioning cycle. Both the unconditioned and moisture conditioned specimens were tested to determine their IDT strengths

using a Marshall Stability press with a loading rate of 2 inches per minute. TSR was calculated as the ratio of the average wet (i.e., moisture conditioned) strength over the average dry (i.e., unconditioned) strength. A higher TSR value is desired for OGFC mixtures with better moisture resistance.

Hamburg Wheel Tracking Test (HWTT)

The HWTT test was used to evaluate the moisture susceptibility and rutting resistance of OGFC mixtures containing different types of asphalt binders and aggregates. The test was performed in accordance with AASHTO T 324. Test temperature was 50°C. During the test, four cylindrical specimens were placed in a water bath at 50°C and subjected to running steel wheel load at a speed of 52 passes per minute. Rut depths were recorded at various positions along the specimens with each wheel pass. Typical HWTT test parameters include SIP and rut depth at a critical number of wheel passes (e.g., 10,000 and 20,000 passes). In this study, HWTT specimens were prepared by compacting a large SGC sample at N_{design} with a final height of approximately 115 mm, which was then cut into two halves of approximately 50mm height each. A 12mm thick plastic plate was placed at the bottom of the HWTT mold to align the surface of the specimen with the surface of the mold for testing.

6.2 Test Results and Discussion

Cantabro Loss Results

Table 71 summarizes the Cantabro loss results of 16 OGFC mixtures corresponding to a combination of four FDOT approved FC-5 mix designs and four types of asphalt binders. In addition, the CAI results for the extended long-term aging (LTA2) protocol of compacted specimen aging for 20 days at 85°C were included. As discussed in Chapter 4, CAI is defined as the percentage change in the Cantabro loss of the mixture after long-term aging. Overall, the HP mixtures had lower Cantabro loss results and thus, are expected to have better raveling resistance than the PMA and EMA mixtures at both the STA and LTA2 conditions. The PMA mixture performed similarly or better than the EMA mixtures in the Cantabro test under the STA condition. However, upon extended long-term aging, the PMA mixtures showed significantly higher Cantabro loss results than the EMA mixtures, indicating increased susceptibility to raveling. In most cases, the two EMA mixtures had similar Cantabro loss results as the HP mixtures under the LTA2 condition, which indicated comparable raveling resistance after extended long-term aging. It should be noted that the Cantabro test results obtained after long-term aging are believed to provide more meaningful evaluation for the long-term raveling resistance and durability of OGFC mixtures than those at the short-term aging (or unaged) condition, since the impact of asphalt aging on mix embrittlement is considered. According to the CAI results, the U30C mixtures seemed to have the best aging resistance, followed by the J30Z mixtures, and then the HP and PMA mixtures. Detailed discussions of the Cantabro loss results for each mix design are provided as follows.

Table 71. Summary of Cantabro Loss and Cantabro Aging Index (CAI) Results

Mix Design ID	Binder Type	Cantabro Loss (%)						CAI
		STA			LTA2			
		Avg.	Std Dev.	COV	Avg.	Std Dev.	COV	
GRN1	PMA	7.7	0.5	6.8%	31.4	9.9	31.4%	307%
	HP	3.3	1.2	36.7%	11.2	4.0	35.6%	238%
	J30Z	14.7	2.5	17.3%	13.6	3.0	21.9%	-7%
	U30C	17.3	3.4	19.8%	13.1	2.7	20.9%	-24%
GRN2	PMA	21.7	5.0	23.1%	43.1	1.5	3.4%	84%
	HP	2.6	0.9	36.4%	12.3	2.1	16.8%	85%
	J30Z	16.6	3.0	18.4%	21.6	0.6	2.7%	72%
	U30C	26.1	1.6	6.2%	29.9	0.8	2.7%	-7%
GRN3	PMA	12.9	0.7	5.6%	26.8	1.9	7.2%	98%
	HP	6.2	1.7	27.6%	11.5	2.2	19.4%	376%
	J30Z	11.0	1.6	14.9%	13.9	0.6	4.6%	30%
	U30C	12.5	3.3	26.0%	10.8	1.4	12.5%	15%
LMS	PMA	10.8	1.5	14.0%	19.9	3.9	19.6%	108%
	HP	3.6	0.3	7.7%	6.8	0.2	3.3%	84%
	J30Z	7.0	1.3	18.2%	12.0	0.7	6.0%	26%
	U30C	11.3	1.5	13.2%	10.5	0.2	1.7%	-14%

Figure 94 presents the average Cantabro loss of OGFC mixtures prepared with the GRN1 mix design. Table 72 and Table 73 provide the Tukey's rankings of these mixtures at each mix aging condition. Under the STA condition, all the mixtures met FDOT's current mix design requirement with an average Cantabro loss of less than 20%. Comparatively, the HP mixture had the lowest average Cantabro loss and thus, is expected to have the best raveling resistance, followed by the PMA mixture and the two EMA mixtures. However, the difference between the HP and PMA mixtures was not statistically significant according to the Tukey's rankings indicated in Table 72. Under the LTA2 condition, the HP and EMA mixtures had similar Cantabro loss results, which were significantly lower than that of the PMA mixture. This indicated that the PMA mixture was more susceptible to raveling after extended long-term aging than both the HP and EMA mixtures. Furthermore, the Cantabro loss of the PMA and HP mixtures increased significantly after the extended long-term aging for 20 days at 85°C, which indicated that the two mixtures became more susceptible to raveling because of asphalt aging and probably mix embrittlement. On the other hand, the two EMA mixtures had similar or slightly reduced Cantabro loss results under the LTA2 condition compared to the STA condition, which highlighted the superior aging resistance of the EMA binders. As discussed previously in Chapter 4, the changes in the Cantabro test results of EMA mixtures before and after aging were due to the combined effects of aging and curing of the EMA binder. A remaining question that warrants further investigation is how the LTA2 condition correlates to the field aging of OGFC mixtures in Florida. If it is representative of medium-term field aging (e.g., four to six years of aging), then the EMA mixtures have the potential of providing better raveling resistance after longer-term aging because of their superior resistance to oxidative aging, which could possibly extend the current life span of OGFC mixtures in Florida. However, if the LTA2 condition simulates long-term field aging (e.g., over 10 to 12 years of aging), then the EMA and HP mixtures are likely to have similar raveling resistance throughout their service lives.

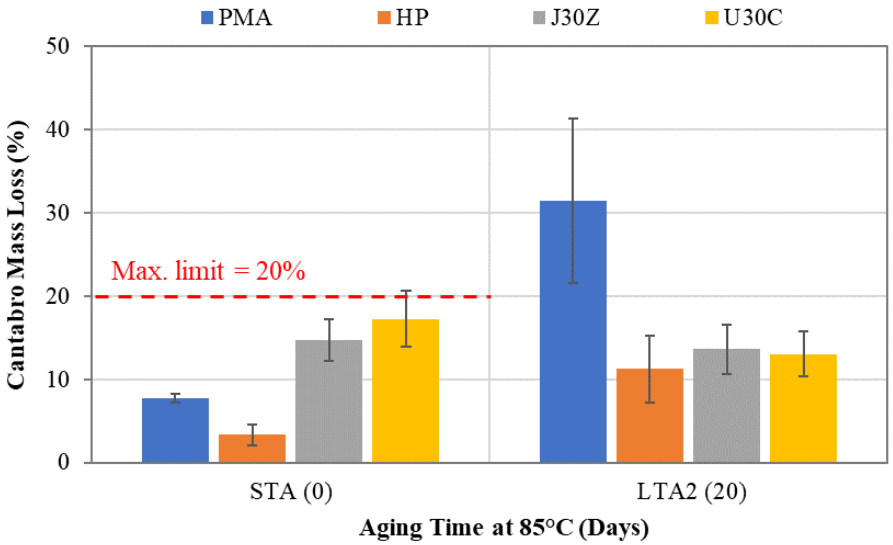

Figure 94. Cantabro Mass Loss of GRN1 Mixtures with Different Asphalt Binders under Two Mix Aging Conditions

Table 72. Tukey's Groupings for Cantabro Loss Results of GRN1 Mixtures with Different Asphalt Binders under the STA Condition

Binder ID	N	Mean (%)	Grouping	
U30C	3	17.3	A	
J30Z	6	14.7	A	
PMA	3	7.7		B
HP	3	3.3		B

Table 73. Tukey's Groupings for Cantabro Loss Results of GRN1 Mixtures with Different Asphalt Binders under the LTA2 Condition

Binder ID	N	Mean (%)	Grouping	
PMA	3	31.4	A	
J30Z	6	13.6		B
U30C	3	13.1		B
HP	3	11.3		B

Figure 95 shows the Cantabro loss results of the GRN2 mixtures containing different asphalt binders. Table 74 and Table 75 provide the Tukey's rankings of these mixtures at each mix aging condition. At both conditions, the HP mixture had significantly lower average Cantabro loss results than the other three mixtures and is expected to have better raveling resistance before and after extended long-term aging. Under the STA condition, the PMA and U30C mixtures had an average Cantabro loss of over 20%, which failed FDOT's current mix design requirement for FC-5 mixtures. Upon extended long-term aging for 20 days at 85°C, the PMA mixture had a significantly higher Cantabro loss than the two EMA mixtures and is expected to be more susceptible to raveling. At both aging conditions, the J30Z mixture outperformed the U30C mixture with lower Cantabro loss results.

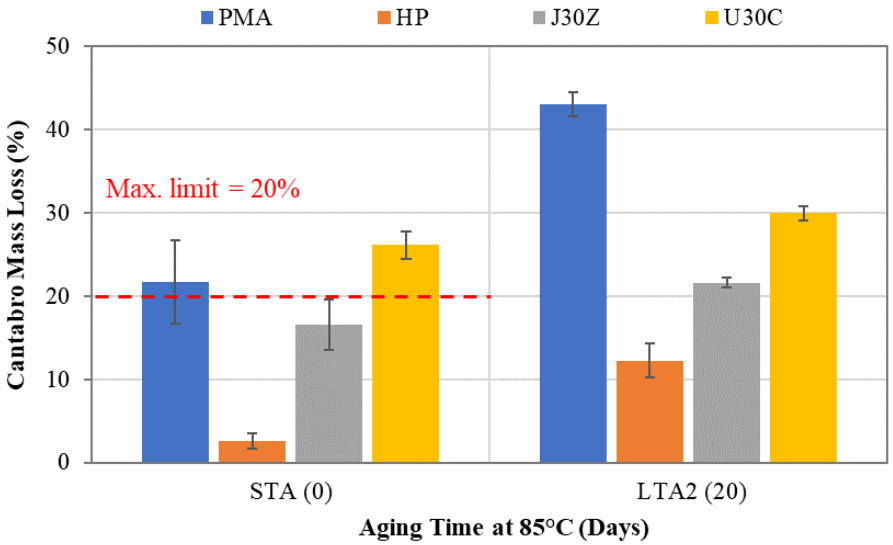

Figure 95. Cantabro Mass Loss of GRN2 Mixtures with Different Asphalt Binders under Two Mix Aging Conditions

Table 74. Tukey's Groupings for Cantabro Loss Results of GRN2 Mixtures with Different Asphalt Binders under the STA Condition

Binder ID	N	Mean (%)	Grouping		
U30C	3	26.1%	A		
PMA	6	21.7%	A	B	
J30Z	3	16.6%		B	
HP	3	2.6%			C

Table 75. Tukey's Groupings for Cantabro Loss Results of GRN2 Mixtures with Different Asphalt Binders under the LTA2 Condition

Binder ID	N	Mean (%)	Grouping			
PMA	3	43.1%	A			
U30C	2	29.9%		B		
J30Z	3	21.6%			C	
HP	3	12.3%				D

Figure 96 shows the Cantabro loss results of OGFC mixtures prepared with the GRN3 mix design. Table 76 and Table 77 provide the Tukey's rankings of these mixtures under two mix aging conditions. Under the STA condition, all the mixtures passed FDOT's current mix design requirement for FC-5 mixtures with an average Cantabro loss of less than 20%. The HP mixture had a significantly lower Cantabro loss and is expected to have better raveling resistance than the other three mixtures. However, the difference between the HP and J30Z mixtures was not statistically significant according to the Tukey's rankings in Table 76. After the LTA2 conditioning, the PMA mixture had an average Cantabro loss of 26.8%, which was significantly higher than those of the other three mixtures. These results indicated that the PMA mixture was significantly more susceptible to raveling than the HP and PMA mixtures after extended long-

term aging for 20 days at 85°C. Different from the PMA and HP mixtures, the two EMA mixtures had similar Cantabro loss results under the STA and LTA2 conditions, which could indicate a potential superior aging resistance.

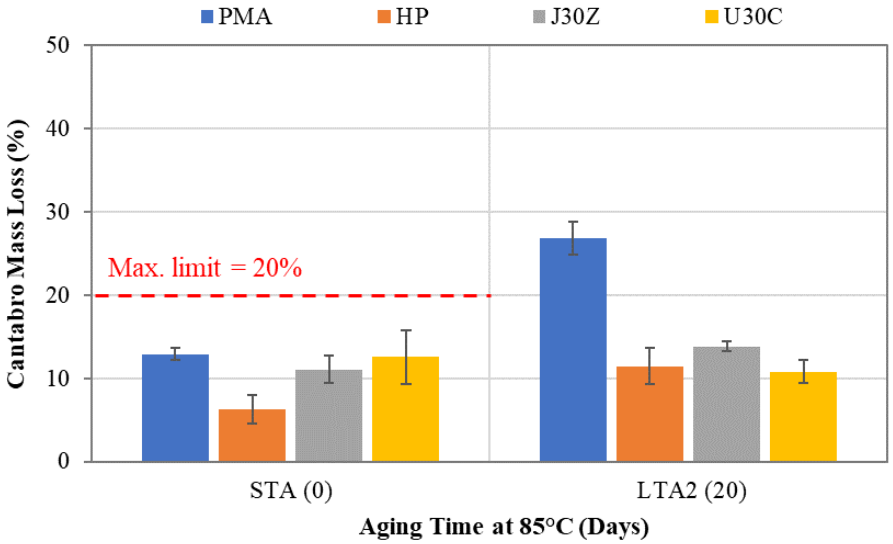

Figure 96. Cantabro Mass Loss of GRN3 Mixtures with Different Asphalt Binders under Two Mix Aging Conditions

Table 76. Tukey's Groupings for Cantabro Loss Results of GRN3 Mixtures with Different Asphalt Binders under the STA Condition

Binder ID	N	Mean (%)	Grouping	
PMA	3	12.9%	A	
U30C	3	12.5%	A	
J30Z	3	11.0%	A	B
HP	3	6.2%		B

Table 77. Tukey's Groupings for Cantabro Loss Results of GRN3 Mixtures with Different Asphalt Binders under the LTA2 Condition

Binder ID	N	Mean (%)	Grouping	
PMA	3	26.8%	A	
J30Z	3	13.9%		B
HP	3	11.5%		B
U30C	3	10.8%		B

Figure 97 presents the Cantabro loss results of the LMS mixtures containing different types of asphalt binders. Table 78 and Table 79 provide the Tukey's rankings of these mixtures under two mix aging conditions. Under the STA condition, all the mixtures had an average Cantabro loss of less than 20%, passing FDOT's current mix design requirement for FC-5 mixtures. Comparatively, the HP mixture had the lowest average Cantabro loss, followed by the J30Z mixture, and then the PMA and U30C mixtures. Upon extended long-term aging for 20 days at 85°C, the PMA mixture had a more substantial increase in the Cantabro loss than the other three

mixtures. As a result, the PMA mixture had a significantly higher Cantabro loss and is expected to be more susceptible to raveling than the two EMA mixtures, while the HP mixture remained to the best performer with the lowest Cantabro loss under the LTA2 condition.

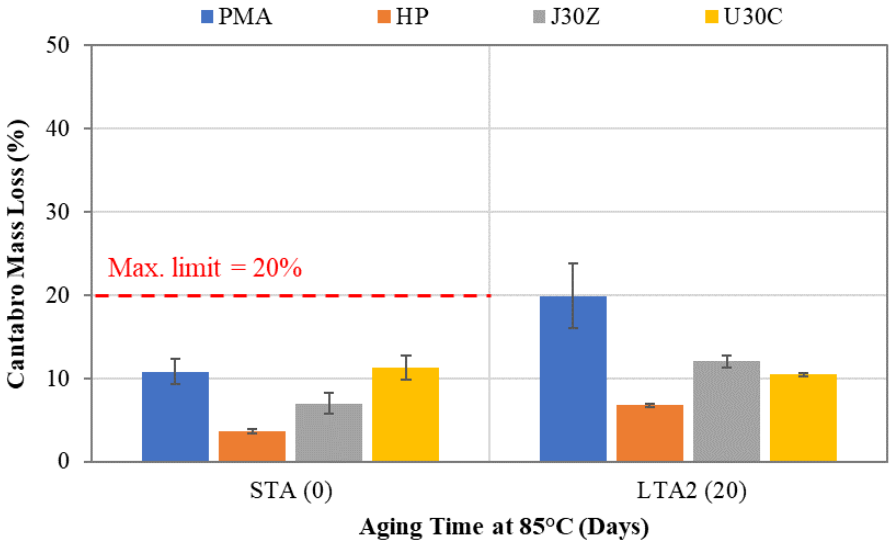

Figure 97. Cantabro Mass Loss of LMS Mixtures with Different Asphalt Binders under Two Mix Aging Conditions

Table 78. Tukey's Groupings for Cantabro Loss Results of LMS Mixtures with Different Asphalt Binders under the STA Condition

Binder ID	N	Mean (%)	Grouping		
U30C	3	11.3%	A		
PMA	3	10.8%	A		
J30Z	3	7.0%		B	
HP	3	3.6%			C

Table 79. Tukey's Groupings for Cantabro Loss Results of LMS Mixtures with Different Asphalt Binders under the LTA2 Condition

Binder ID	N	Mean (%)	Grouping		
PMA	3	19.9%	A		
J30Z	3	12.0%		B	
U30C	3	10.5%		B	C
HP	3	6.8%			C

IDT Strength Results

Table 80 summarizes the IDT strength results of the 16 OGFC mixtures under two mix aging conditions. Overall, most of the EMA mixtures had higher IDT strength than the PMA and HP mixtures before and after extended long-term aging. There were two exceptions where the U30C mixtures had lower IDT strength than the other three mixtures under the STA condition when the EMA binder was still at the early stage of its curing process to gain strength. Detailed discussions of the IDT strength results for each mix design are provided as follows.

Table 80. Summary of IDT Strength Results

Mix Design ID	Binder Type	IDT Strength (psi)					
		STA			LTA2		
		Avg.	Std Dev.	COV	Avg.	Std Dev.	COV
GRN1	PMA	48.3	7.2	15.0%	71.7	4.2	5.8%
	HP	39.0	1.2	3.0%	57.9	2.7	4.7%
	J30Z	63.0	33.0	52.4%	105.5	9.3	8.8%
	U30C	69.9	3.9	5.6%	166.2	13.4	8.1%
GRN2	PMA	51.0	1.3	2.5%	55.8	7.4	13.3%
	HP	31.8	2.6	8.0%	47.9	3.8	8.0%
	J30Z	81.6	9.0	11.1%	90.6	6.7	7.4%
	U30C	22.4	2.9	12.8%	121.9	14.8	12.1%
GRN3	PMA	56.1	2.9	5.1%	77.0	1.7	2.2%
	HP	49.1	3.4	7.0%	64.8	3.6	5.5%
	J30Z	84.7	3.7	4.4%	117.3	5.8	5.0%
	U30C	33.7	3.4	10.0%	187.8	20.5	10.9%
LMS	PMA	81.7	2.7	3.3%	106.9	7.2	6.7%
	HP	54.1	2.8	5.3%	83.5	4.1	4.9%
	J30Z	154.4	9.2	6.0%	146.1	13.7	9.4%
	U30C	107.3	18.7	17.4%	212.7	16.5	7.8%

Figure 98 presents the IDT strength results of the GRN1 mixtures containing four types of asphalt binders. Under both mix aging conditions, the U30C mixture had the highest average IDT strength, followed by the J30Z, PMA, and HP mixtures, respectively. The difference among these mixtures was more pronounced under the LTA2 condition than under the STA condition. According to the Tukey's rankings in Table 81, only the HP and U30C mixtures had statistically different IDT strength under the STA condition if considering the variability of the test results. Under the LTA2 condition, all the differences in the IDT strength results among the four mixtures were statistically significant (Table 82). The increase in the IDT strength of the PMA and HP mixtures from the STA to LTA2 condition was because of asphalt aging; however, for the J30Z and U30C mixtures, this increase was due to the combined effects of curing and aging of the EMA binders. Comparatively, the U30C mixture experienced a greater extent of post-compaction curing than the J30Z mixture.

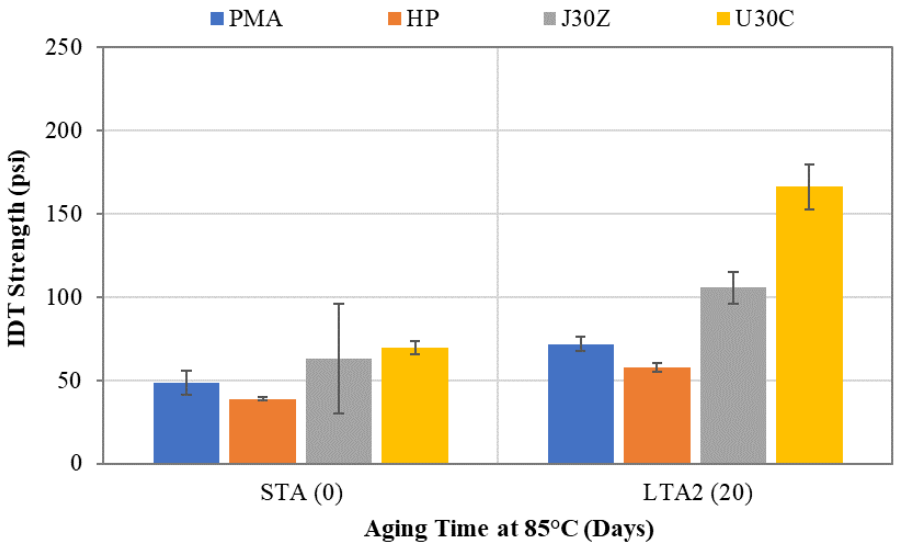

Figure 98. IDT Strength of GRN1 Mixtures with Different Asphalt Binders under Two Mix Aging Conditions

Table 81. Tukey's Groupings for IDT Strength Results of GRN1 Mixtures with Different Asphalt Binders under the STA Condition

Binder ID	N	Mean (psi)	Grouping	
U30C	6	69.9	A	
J30Z	4	63.0	A	B
PMA	6	48.3	A	B
HP	6	39.0		B

Table 82. Tukey's Groupings for IDT Strength Results of GRN1 Mixtures with Different Asphalt Binders under the LTA2 Condition

Binder ID	N	Mean (psi)	Grouping			
U30C	5	166.2	A			
J30Z	6	105.5		B		
PMA	6	71.7			C	
HP	6	57.9				D

Figure 99 shows the IDT strength results of OGFC mixtures prepared with the GRN2 mix design. Table 83 and Table 84 provide the Tukey's rankings of these mixtures under two mix aging conditions. Under the STA condition, the J30Z mixture had the highest IDT strength, followed by the PMA, HP, and U30C mixtures, respectively. All the differences in the IDT strength results among these mixtures were statistically significant. Upon extended long-term aging for 20 days at 85°C, the IDT strength of the U30C mixture increased by approximately five times (i.e., from 22 psi to 122 psi), while those of the other three mixtures increased by only 10% to 50%. This substantial increase in the IDT strength of the U30C mixture was due to the combined effects of aging and continued curing of the EMA binder. Under the LTA2 condition, the U30C mixture had the highest IDT strength, followed by the J30Z mixture and then the PMA and HP mixtures.

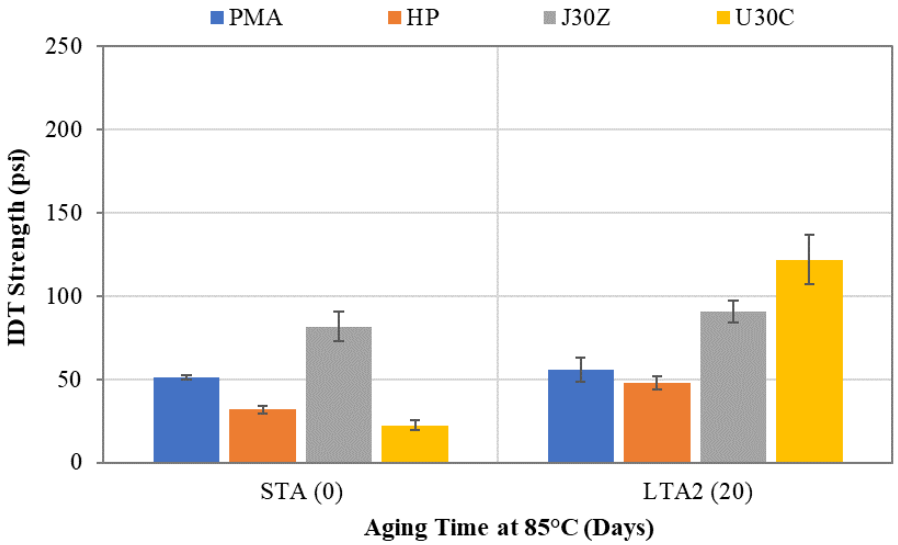

Figure 99. IDT Strength of GRN2 Mixtures with Different Asphalt Binders under Two Mix Aging Conditions

Table 83. Tukey's Groupings for IDT Strength Results of GRN2 Mixtures with Different Asphalt Binders under the LTA2 Condition

Binder ID	N	Mean (psi)	Grouping			
J30Z	6	81.6	A			
PMA	6	51.0		B		
HP	6	31.8			C	
U30C	6	22.4				D

Table 84. Grouping Information of Mixtures with GRN2 Aggregates using the Tukey Method and 95% Confidence at LTA2 Condition based on IDT Strength

Binder ID	N	Mean (psi)	Grouping		
U30C	6	121.9	A		
J30Z	6	90.6		B	
PMA	6	55.8			C
HP	6	47.9			C

Figure 100 presents the IDT strength results of OGFC mixtures prepared with the GRN3 mix design. Table 85 and Table 86 provide the Tukey's rankings of these mixtures under two mix aging conditions. The results in Figure 100 showed a consistent trend as those of the GRN2 mixtures in Figure 99. Under the STA condition, the J30Z mixture had the highest IDT strength, followed by the PMA, HP, and U30C mixtures, respectively. Because of the continued curing of the EMA binder, the U30C mixture exhibited the highest IDT strength, followed by the J30Z mixture, and then the PMA and HP mixtures under the LTA2 condition.

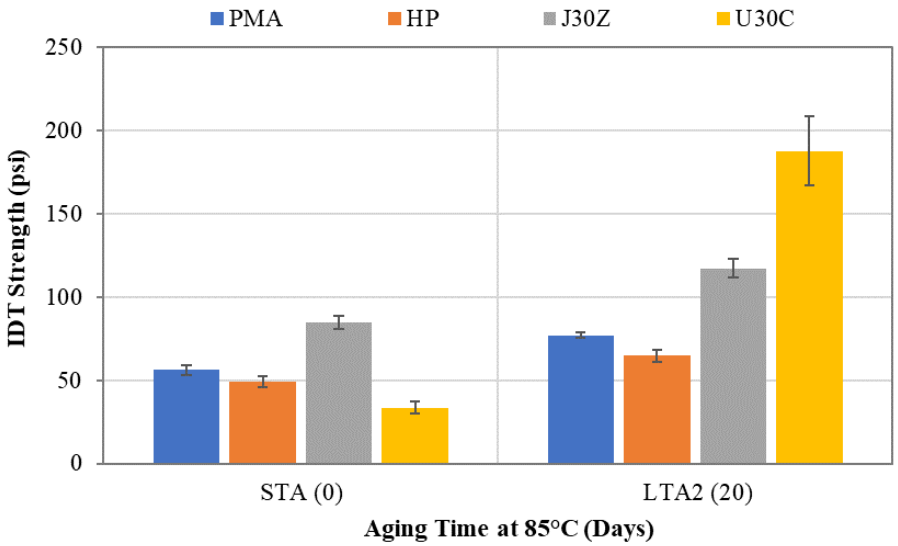

Figure 100. IDT Strength of GRN3 Mixtures with Different Asphalt Binders under Two Mix Aging Conditions

Table 85. Tukey's Groupings for IDT Strength Results of GRN3 Mixtures with Different Asphalt Binders under the STA Condition

Binder ID	N	Mean (psi)	Grouping			
J30Z	5	84.7	A			
PMA	6	56.1		B		
HP	6	49.1			C	
U30C	6	33.7				D

Table 86. Tukey's Groupings for IDT Strength Results of GRN3 Mixtures with Different Asphalt Binders under the LTA2 Condition

Binder ID	N	Mean (psi)	Grouping		
U30C	6	187.8	A		
J30Z	6	117.3		B	
PMA	6	77.0			C
HP	6	64.8			C

Figure 101 presents the IDT strength results of the LMS mixtures containing different types of asphalt binders. Table 87 and Table 88 provide the Tukey's rankings of these mixtures at each mix aging condition. At both aging conditions, the two EMA mixtures had statistically higher IDT strength than the PMA and HP mixtures. Under the STA condition, the IDT strength of the J30Z mixture was higher than that of the U30C mixture, but the opposite trend was observed under the LTA2 condition. These results indicated that the U30C mixture was significantly more susceptible to post-compaction curing for gaining strength than the J30Z mixture, which was consistent with the results of OGFC mixtures prepared with the other three FC-5 mix designs.

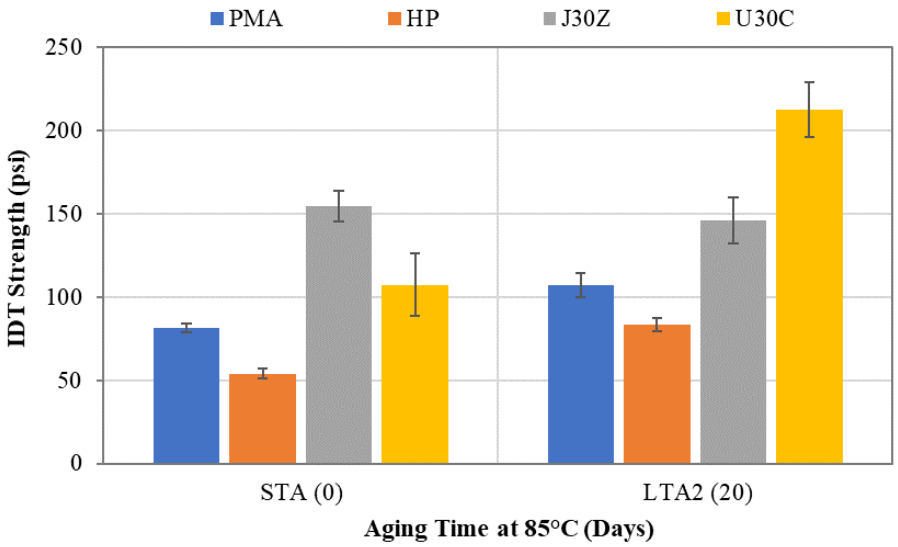

Figure 101. IDT Strength of LMS Mixtures with Different Asphalt Binders under Two Mix Aging Conditions

Table 87. Tukey's Groupings for IDT Strength Results of LMS Mixtures with Different Asphalt Binders under the STA Condition

Binder ID	N	Mean (psi)	Grouping			
J30Z	6	154.4	A			
U30C	6	107.3		B		
PMA	6	81.7			C	
HP	6	54.1				D

Table 88. Tukey's Groupings for IDT Strength Results of LMS Mixtures with Different Asphalt Binders under the LTA2 Condition

Binder ID	N	Mean (psi)	Grouping			
U30C	6	212.7	A			
J30Z	6	146.1		B		
PMA	6	106.9			C	
HP	6	83.5				D

IDT Fracture Energy (G_f) Results

Table 89 summarizes the IDT G_f results of 16 OGFC mixtures corresponding to a combination of four FC-5 mix designs and four asphalt binders. Overall, the J30Z mixture had higher G_f than the other three mixtures under the STA condition. However, after extended long-term aging for 20 days at 85°C (i.e., LTA2), the U30C mixture consistently showed the highest G_f and is expected to have the best fracture resistance, followed by the J30Z mixture and then the PMA and HP mixtures for all the mix designs. Detailed discussions of the IDT G_f results for each mix design are provided in the following sections.

Table 89. Summary of IDT G_f Results

Mix Design ID	Binder Type	IDT G_f (J/m^2)					
		STA			LTA2		
		Avg.	Std Dev.	COV	Avg.	Std Dev.	COV
GRN1	PMA	6,535	591	9.0%	7,995	1,293	16.2%
	HP	6,792	644	9.5%	7,739	969	12.5%
	J30Z	4,670	3,466	74.2%	10,116	1,498	14.8%
	U30C	8,643	1,355	15.7%	19,065	3,944	20.7%
GRN2	PMA	6,819	256	3.7%	7,324	1,224	16.7%
	HP	5,660	424	7.5%	6,973	404	5.8%
	J30Z	7,511	1,185	15.8%	7,715	747	9.7%
	U30C	3,388	214	6.3%	12,861	2,302	17.9%
GRN3	PMA	6,795	473	7.0%	6,962	367	5.3%
	HP	6,764	422	6.2%	7,344	547	7.4%
	J30Z	8,387	531	6.3%	9,459	2,385	25.2%
	U30C	3,890	615	15.8%	12,318	1,995	16.2%
LMS	PMA	8,669	360	4.2%	7,664	543	7.1%
	HP	7,093	720	10.1%	8,979	1,498	16.7%
	J30Z	14,791	1,523	10.3%	10,744	1,280	11.9%
	U30C	8,972	969	10.8%	14,461	2,371	16.4%

Figure 102 presents the IDT G_f results of OGFC mixtures prepared with the GRN1 mix design. Tukey's rankings of these mixtures at each mix aging condition are summarized in Table 90 and Table 91. Comparable G_f results were observed for the four mixtures under the STA condition. According to the Tukey's rankings in Table 90, only the difference between the two EMA mixtures was statistically significant, while the rest was not. However, the J30Z mixture had a considerably higher variability (as indicated by the error bars) in the IDT G_f results compared to the other three mixtures, which made the statistical comparisons inconclusive. Upon extended long-term aging for 20 days at 85°C, the U30C mixture had significantly higher IDT G_f results and thus better fracture resistance than the other three mixtures. The considerable improvement in IDT G_f results of the U30C mixture was due to the combined effects of aging and continued curing of the EMA binder.

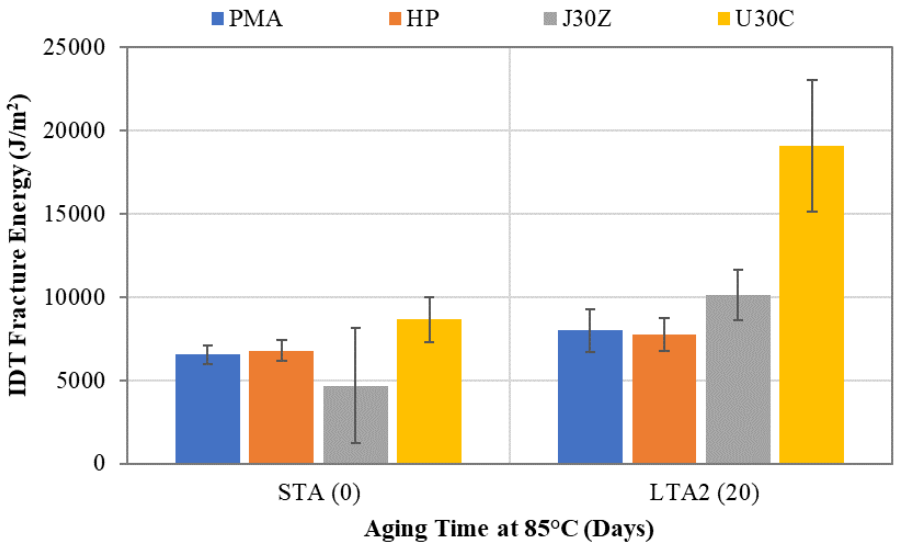

Figure 102. IDT G_f Results of GRN1 Mixtures with Different Asphalt Binders under Two Mix Aging Conditions

Table 90. Tukey's Groupings for IDT G_f Results of GRN1 Mixtures with Different Asphalt Binders under the STA Condition

Binder ID	N	Mean (J/m^2)	Grouping	
U30C	6	8,643	A	
HP	6	6,792	A	B
PMA	5	6,535	A	B
J30Z	6	4,670		B

Table 91. Tukey's Groupings for IDT G_f Results of GRN1 Mixtures with Different Asphalt Binders under the LTA2 Condition

Binder ID	N	Mean (J/m^2)	Grouping	
U30C	5	19,065	A	
J30Z	6	10,116		B
PMA	6	7,995		B
HP	6	7,739		B

Figure 103 shows the IDT G_f results of the GRN2 mixtures containing different types of asphalt binders. Table 92 and Table 93 present the Tukey's rankings of these mixtures at each mix aging condition. Under the STA condition, the J30Z and PMA mixtures had similar G_f results, which were statistically higher than those of the HP and U30C mixtures. Under the LTA2 condition, the U30C mixture had significantly higher G_f and thus, better fracture resistance than the other three mixtures. Consistent with the results of the GRN1 mixtures in Figure 102, the G_f value of the U30C mixture increased substantially upon extended long-term aging for 20 days at 85°C largely due to the continued curing of the EMA binder, while the PMA, HP, and J30Z mixtures exhibited similar G_f results under the STA and LTA2 conditions.

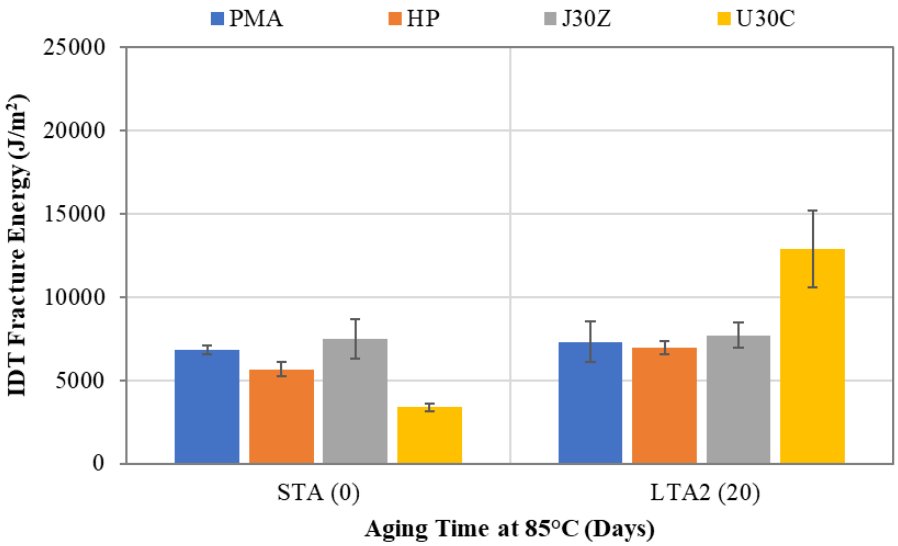

Figure 103. IDT G_f Results of GRN2 Mixtures with Different Asphalt Binders under Two Mix Aging Conditions

Table 92. Tukey's Groupings for IDT G_f Results of GRN2 Mixtures with Different Asphalt Binders under the STA Condition

Binder ID	N	Mean (J/m^2)	Grouping		
J30Z	6	7,511	A		
PMA	6	6,819	A		
HP	6	5,660		B	
U30C	6	3,388			C

Table 93. Tukey's Groupings for IDT G_f Results of GRN2 Mixtures with Different Asphalt Binders under the LTA2 Condition

Binder ID	N	Mean (J/m^2)	Grouping	
U30C	6	12,861	A	
J30Z	6	8,362		B
PMA	6	7,324		B
HP	6	6,973		B

Figure 104 presents the IDT G_f results of OGFC mixtures prepared with the GRN3 mix design. Table 94 and Table 95 present the Tukey's rankings of these mixtures at each mix aging condition. Similar trends were observed in the comparison of the mixtures containing different asphalt binders for the GRN2 and GRN3 mix designs. Under the STA condition, the PMA and HP mixtures had similar G_f results, which were statically lower than that of the J30Z mixture but statistically higher than that of the U30C mixture. Under the LTA2 condition, the U30C mixture had the highest G_f and thus, is expected to have the best fracture resistance, followed by the J30Z mixture and then the PMA and HP mixtures. The differences between the J30Z *versus* the PMA and HP mixtures, however, were not statistically significant according to the Tukey's rankings in Table 95. Same with the GRN1 and GRN2 mix designs, the U30C mixture prepared with the GRN3 mix design showed significant improvement in fracture resistance, as indicated by higher

IDT G_f results, due to the continued curing of the EMA binder during the extended long-term aging process.

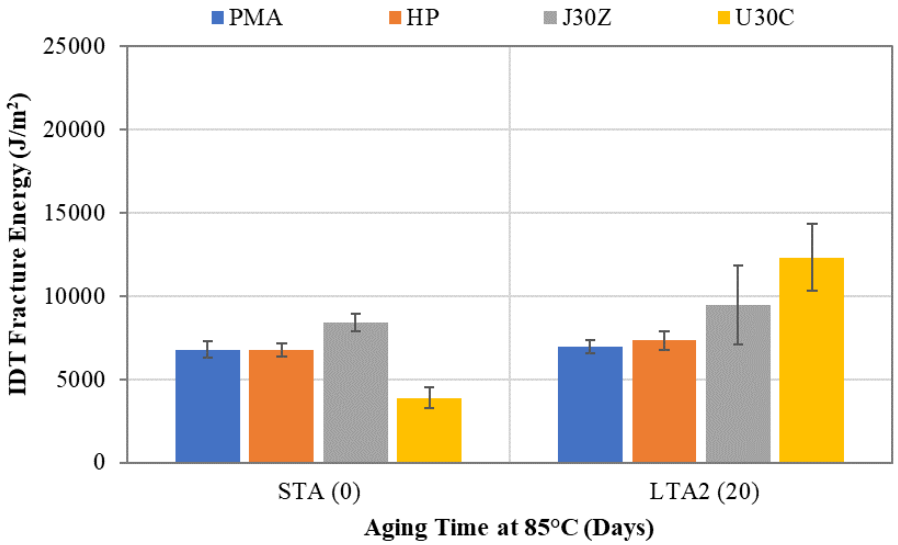

Figure 104. IDT G_f Results of GRN3 Mixtures with Different Asphalt Binders under Two Mix Aging Conditions

Table 94. Tukey's Groupings for IDT G_f Results of GRN3 Mixtures with Different Asphalt Binders under the STA Condition

Binder ID	N	Mean (J/m^2)	Grouping		
J30Z	5	8,387	A		
PMA	6	6,795		B	
HP	6	6,764		B	
U30C	6	3,890			C

Table 95. Tukey's Groupings for IDT G_f Results of GRN3 Mixtures with Different Asphalt Binders under the LTA2 Condition

Binder ID	N	Mean (J/m^2)	Grouping	
J30Z	6	12,318	A	
PMA	6	9,459		B
HP	6	7,344		B
U30C	6	6,962		B

Figure 105 presents the IDT G_f results of the OGFC mixtures prepared with the LMS mix design. Table 96 and Table 97 present the Tukey's rankings of these mixtures at each mix aging condition. Under the STA condition, the J30Z mixture had the highest G_f results, followed by the U30C and PMA mixtures and then the HP mixture. After extended long-term aging for 20 days at 85°C, the U30C mixture had a highest average G_f value and is expected to have the best fracture resistance, followed by the J30Z mixture, HP mixture, and PMA mixture, respectively. The difference between the HP *versus* the J30Z and PMA mixtures, however, was not statistically significant according to the Tukey's rankings in Table 97.

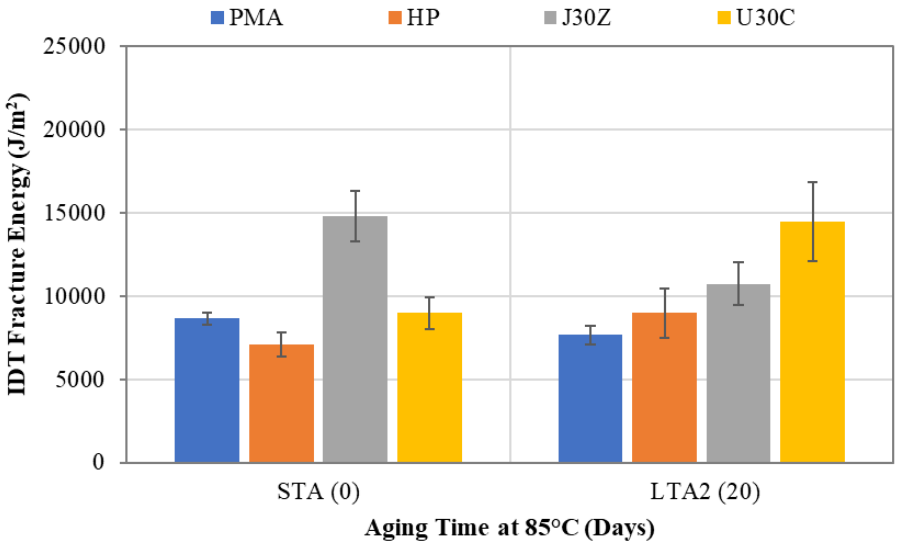

Figure 105. IDT G_f Results of LMS Mixtures with Different Asphalt Binders under Two Mix Aging Conditions

Table 96. Tukey's Groupings for IDT G_f Results of LMS Mixtures with Different Asphalt Binders under the STA Condition

Binder ID	N	Mean (J/m^2)	Grouping		
J30Z	6	14,791	A		
U30C	6	8,972		B	
PMA	6	8,669		B	C
HP	6	7,093			C

Table 97. Tukey's Groupings for IDT G_f Results of LMS Mixtures with Different Asphalt Binders under the LTA2 Condition

Binder ID	N	Mean (J/m^2)	Grouping		
U30C	6	14,461	A		
J30Z	6	10,744		B	
HP	6	8,979		B	C
PMA	6	7,664			C

TSR Results

Table 98 summarizes the dry (i.e., unconditioned) strength, wet (i.e., moisture conditioned) strength, and TSR results of 16 OGFC mixtures prepared with a combination of four FC-5 mix designs and four types of asphalt binders. First, all mixtures except one had a TSR of over 80% and thus, are expected to have acceptable moisture resistance. The J30Z mixture had consistently higher dry strength than the other three mixtures. After moisture conditioning, the two EMA mixtures had higher wet strength results than the PMA and HP mixtures. For all U30C mixtures, a considerable increase in the tensile strength was observed after moisture conditioning. It is speculated that this increase can be attributed to the accelerated curing of the EMA binder when the mixture was conditioned in a water bath at 60°C as part of the moisture conditioning process

for the TSR test. Because of the higher strength obtained after moisture conditioning, all the U30C mixtures had TSR values that were considerably higher than 100%. Detailed discussion of the TSR test results for each mix design is provided below.

Table 98. Summary of TSR Test Results

Mix Design ID	Binder Type	Dry Strength (psi)			Wet Strength (psi)			TSR
		Avg.	Std Dev.	COV	Avg.	Std Dev.	COV	
GRN1	PMA	63.5	1.5	2.4%	53.6	3.3	6.1%	85%
	HP	51.7	12.7	24.6%	46.9	2.7	5.7%	91%
	J30Z	104.7	4.8	4.6%	82.3	4.2	5.1%	79%
	U30C	61.8	4.9	7.9%	85.0	10.6	12.5%	138%
GRN2	PMA	50.9	5.4	10.6%	50.2	3.0	6.1%	99%
	HP	40.4	4.6	11.4%	40.7	1.8	4.4%	101%
	J30Z	81.6	7.5	9.2%	72.8	3.4	4.6%	89%
	U30C	30.2	6.0	19.9%	71.6	9.5	13.2%	237%
GRN3	PMA	70.6	8.6	12.2%	72.4	6.4	8.8%	103%
	HP	55.2	4.8	8.8%	49.8	6.5	13.1%	90%
	J30Z	96.7	14.8	15.3%	102.4	3.6	3.5%	106%
	U30C	47.2	10.7	22.6%	66.7	6.1	9.1%	141%
LMS	PMA	99.2	15.7	15.8%	85.8	4.6	5.4%	86%
	HP	67.2	4.0	6.0%	64.7	1.1	1.7%	96%
	J30Z	124.1	8.2	6.6%	113.4	7.5	6.6%	91%
	U30C	97.4	4.8	4.9%	133.1	14.0	10.5%	137%

Figure 106 presents the TSR results of the GRN1 mixtures containing different asphalt binders. The J30Z mixture had the highest dry strength compared to the other three mixtures. After moisture conditioning, the J30Z and U30C mixtures had similar wet strength results, which were higher than those of the PMA and HP mixtures. Different from the PMA, J30Z, and HP mixtures, the U30C mixture had a higher tensile strength after moisture conditioning than before, which is likely attributable to accelerated curing of the EMA binder when the mixture was conditioned in a 60°C water bath for moisture conditioning. The U30C mixture had the highest TSR value of 138%, followed by the HP, PMA, and J30Z mixtures, respectively. However, the differences between the HP *versus* PMA mixtures and PMA *versus* J30Z mixtures are not considered significant because they are less than the allowable difference between two test results (i.e., d2s value) of 9.3% as recommended in NCHRP project 9-26 (Azari, 2010). Finally, all mixtures except one met the recommended test criteria in NCHRP project 1-55 (Watson et al., 2018) with a TSR of over 70% and an average wet strength of over 50 psi. The only exception was the HP mixture, which had an average wet strength of 46.9 psi, marginally failing the wet strength threshold. These results indicated that the four OGFC mixtures prepared with the GRN1 mix design were not expected to be moisture susceptible.

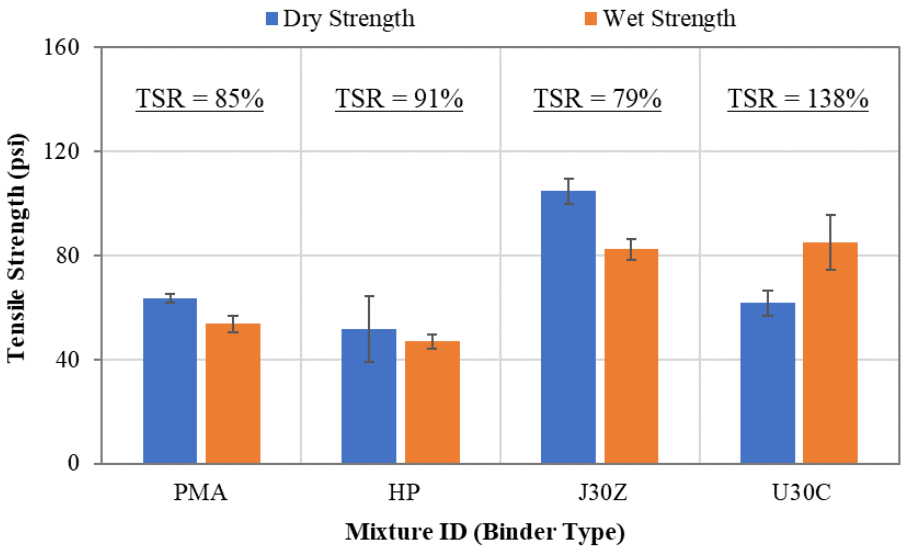

Figure 106. TSR Test Results of GRN1 Mixtures with Different Asphalt Binders

Figure 107 presents the TSR results of the GRN2 mixtures containing different asphalt binders. The J30Z mixture had the highest dry strength followed by the PMA, HP, and U30C mixtures, respectively. After moisture conditioning, the two EMA mixtures had similar wet strength results, which were higher than those of the PMA and HP mixtures. As with the results in Figure 106, the U30C mixture had a significantly higher wet strength than the dry strength because of the continued curing of the EMA binder during the moisture conditioning process. As a result, the U30C mixture had an extraordinarily high TSR of 237%. The comparison of the TSR results indicated that the PMA and HP mixtures are expected to be more resistant to moisture damage than the J30Z mixture as their differences in TSR results are over the d2s value of 9.3%. Nevertheless, all the GRN2 mixtures are expected to have satisfactory moisture resistance with TSR values of over 85%. In comparison against the test criteria recommended in NCHRP project 1-55, the HP mixture failed the minimum wet strength threshold of 50 psi (Watson et al., 2018). However, this mixture did not show any deterioration in the tensile strength after moisture conditioning and is not likely to be susceptible to moisture damage.

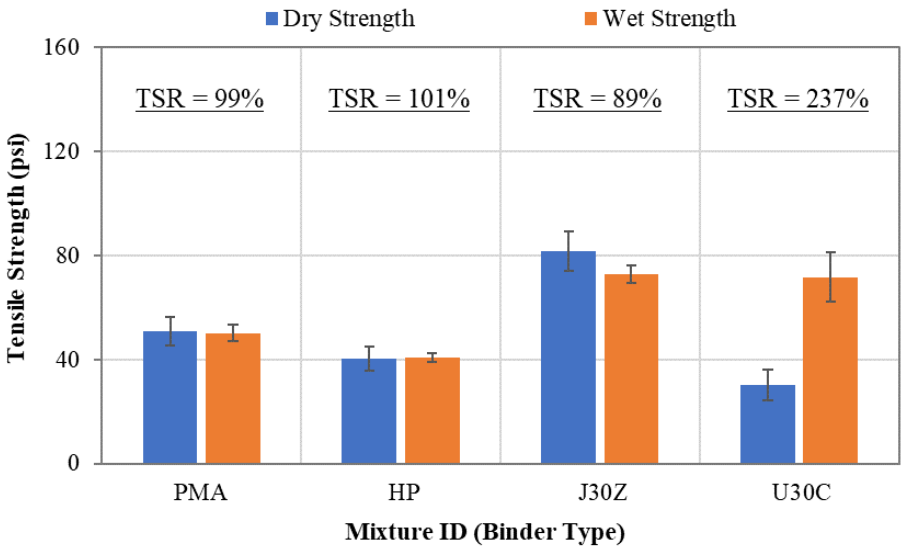

Figure 107. TSR Test Results of GRN2 Mixtures with Different Asphalt Binders

Figure 108 presents the TSR results of OGFC mixtures prepared with the GRN3 mix design. The J30Z mixture had the highest dry and wet strength results followed by the PMA mixture. In comparing the remaining HP and U-EMA mixtures, the HP mixture had slightly higher dry strength while the U-EMA mixture had higher wet strength. As discussed previously, the considerable increase in the tensile strength of the U30C mixture was due to the continued curing of the EMA binder during the moisture conditioning process. Finally, the U-EMA mixture had the highest TSR, followed by the J-EMA and PMA mixtures and then the HP mixture. Nevertheless, all the mixtures met the recommended TSR test criteria in NCHRP project 1-55 (i.e., a minimum TSR of 70% and a minimum wet strength of 50 psi) (Watson et al., 2018) and thus, are not expected to be prone to moisture damage.

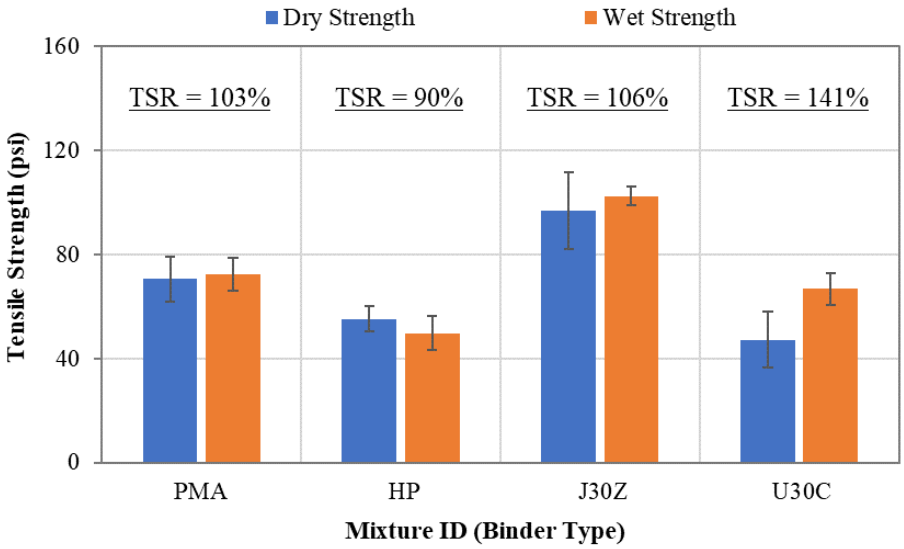

Figure 108. TSR Test Results of GRN3 Mixtures with Different Asphalt Binders

Figure 109 presents the TSR results of LMS mixtures containing different asphalt binders. The J30Z mixture had the highest dry strength, followed by the PMA and U30C mixtures and then the HP mixture. Consistent with the results of the other mix designs discussed previously, the tensile strength of the U30C mixture increased significantly after moisture conditioning. As a result, it had a higher wet strength than the other three mixtures. The ranking of the wet strength results for the PMA, HP, and J30Z mixtures was the same as that of the dry strength results. Finally, all the mixtures met the recommended TSR test criteria in NCHRP project 1-55 (Watson et al., 2018) with a TSR of over 70% and a wet strength of over 50 psi and thus, are expected to have good moisture resistance.

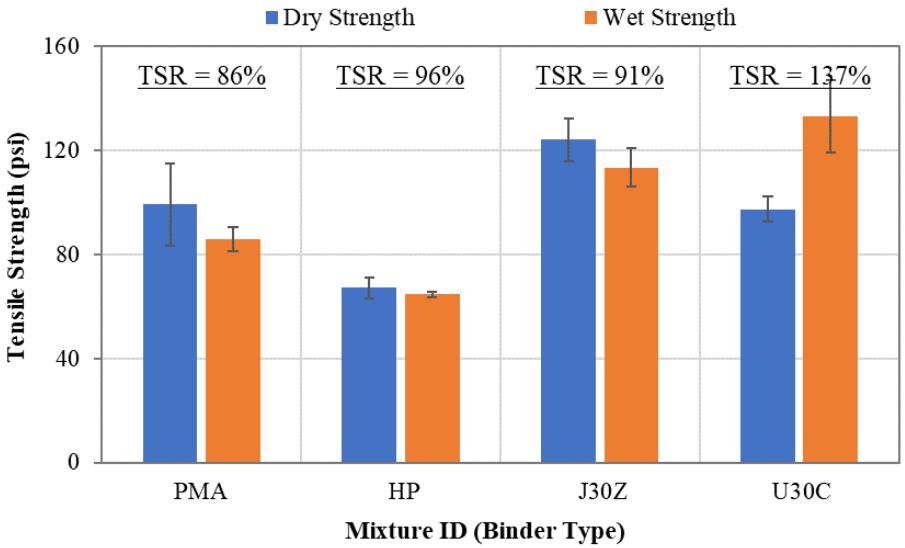

Figure 109. TSR Test Results of LMS Mixtures with Different Asphalt Binders

HWTT Results

Table 99 summarizes the HWTT results of 16 OGFC mixtures prepared with a combination of four FC-5 mix designs and four types of asphalt binders. All the mixtures were tested under the STA condition without additional long-term aging to evaluate their rutting resistance at their most vulnerable conditions. Overall, the HWTT results for mixtures prepared with the GRN1 and LMS mix designs were significantly better than those prepared with the GRN2 and GRN3 mix designs. All the GRN1 and LMS mixtures rutted less than 12.5 mm and had no signs of stripping. For the GRN2 and GRN3 mix designs, the J30Z mixture showed better rutting and moisture resistance performance than the HP and PMA mixtures. The U30C mixtures exhibited high severity stripping failures in HWTT and did not last more than 7,000 passes before reaching 12.5 mm rut depth. Detailed discussions of the HWTT results for each mix design are provided in the following sections.

Table 99. Summary of HWTT Results

Mix Design ID	Binder Type	Average Rut Depth at 20,000 Passes (mm)	Average Passes to 12.5 mm Rut Depth
GRN1	PMA	9.4	> 20,000
	HP	4.9	> 20,000
	J30Z	6.3	> 20,000
	U30C	6.8	> 20,000
GRN2	PMA	> 12.5	10,000
	HP	> 12.5	17,000
	J30Z	6.3	> 20,000
	U30C	> 12.5	5,000
GRN3	PMA	11.6	> 20,000
	HP	7.0	> 20,000
	J30Z	3.7	> 20,000
	U30C	> 12.5	6,800
LMS	PMA	6.1	> 20,000
	HP	7.4	> 20,000
	J30Z	4.8	> 20,000
	U30C	4.9	> 20,000

Figure 110 presents the HWTT rutting curves of the OGFC mixtures prepared with the GRN1 mix design. As shown, all the mixtures lasted over 20,000 passes before reaching 12.5 mm rut depth and had no signs of stripping; therefore, they are expected to have good rutting resistance and moisture resistance. The rut depth results at 20,000 passes indicate that the HP mixture has the best rutting resistance, followed by the J30Z and U30C mixtures and then the PMA mixtures. However, the difference between the HP and J30Z mixtures was only 1.4 mm, which is not considered practically significant for HWTT. On the other hand, the difference between the HP and U30Z mixtures was largely limited to the post-compaction phase of the HWTT curve, while the two mixtures exhibited similar behavior in the creep phase.

Figure 111 presents the HWTT rutting curves of OGFC mixtures prepared with the GRN2 mix design. All mixtures except one had significantly more rutting in HWTT than those prepared with the GRN1 mix design as shown in Figure 110. Overall, the J30Z mixture had the best HWTT results and is expected to have the best rutting resistance and moisture resistance, followed by the HP, PMA, and U30C mixtures, respectively. As shown in Figure 112(a) and Figure 112(b), both the PMA and HP mixtures showed low to medium severity stripping failures during the test, which was also confirmed by the shape of the HWTT curves in Figure 111. High severity stripping was observed in the U30C mixture [Figure 112(c)], which only lasted approximately 5,000 passes before reaching 12.5 mm rut depth. It was also observed during testing that some mixture particles got “picked out” and stuck to the HWTT wheels upon deterioration of the mixture, as shown in Figure 115. It is speculated that the U30C mixture exhibited an early failure in HWTT when tested under the STA condition because the EMA binder was still at the early stage of its curing process and had not gained sufficient cohesive strength to resist the severe conditions of the HWTT. This result was supported by the low IDT strength and G_f results of the mixture under the STA condition (Figure 99 and Figure 103), which raises a concern that the U30C mixture prepared with the GRN2 mix design may

experience premature rutting and possibly shoving failures immediately after construction due to lack of strength. To address this concern, heavy vehicle simulator (HVS) testing of this mixture is recommended to evaluate the post-compaction curing behavior and more importantly, determine the amount of time after construction required for the mixture to gain sufficient strength before it can be allowed to open to traffic on the roadway.

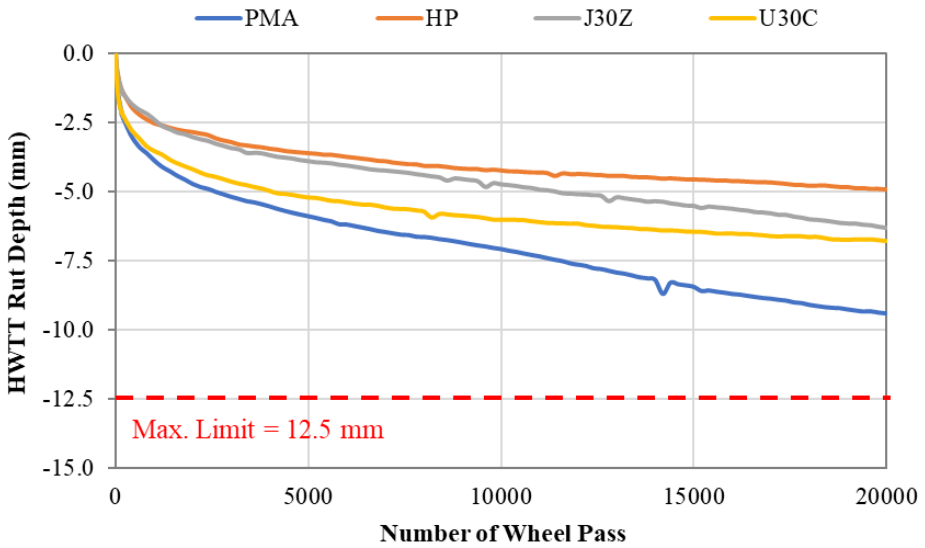

Figure 110. HWTT Rutting Curves of GRN1 Mixtures with Different Asphalt Binders

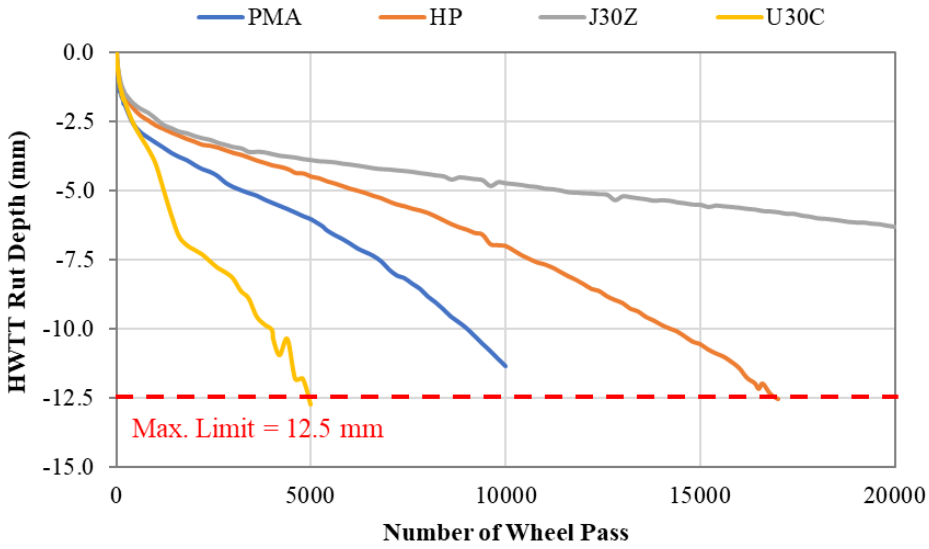

Figure 111. HWTT Rutting Curves of GRN2 Mixtures with Different Asphalt Binders

(a) (b) (c)

Figure 112. Pictures of GRN2 Mixture Specimens prepared with (a) PMA Binder, (b) HP Binder, (c) U30C Binder after Testing in HWTT

Figure 113 presents the HWTT rutting curves of OGFC mixtures prepared with the GRN3 mix design. In general, these mixtures showed similar trends, but overall better HWTT results compared to those prepared with the GRN2 mix design in Figure 112. The J30Z remained the best performer, followed by the HP mixture and then the PMA mixture. These three mixtures lasted over 20,000 passes before reaching 12.5 mm rut depth and had no signs of stripping, which indicated adequate rutting resistance and moisture resistance. The U30C mixture failed HWTT at approximately 6,800 passes mainly because of stripping. Figure 114 presents the U30C mixture specimens after testing, where a considerable amount of uncoated fine aggregate particles is visible. This mixture also exhibited the mixture particle "picking up" issue shown in Figure 115. As discussed previously, the early failure of this mixture in HWTT is also likely attributed to its low cohesive strength because of the lack of curing of the EMA binder when tested under the STA condition. Therefore, HVS testing of the U30C mixture prepared with the GRN3 mix design is recommended to determine when the OGFC pavement constructed with this mixture can be allowed for trafficking after construction.

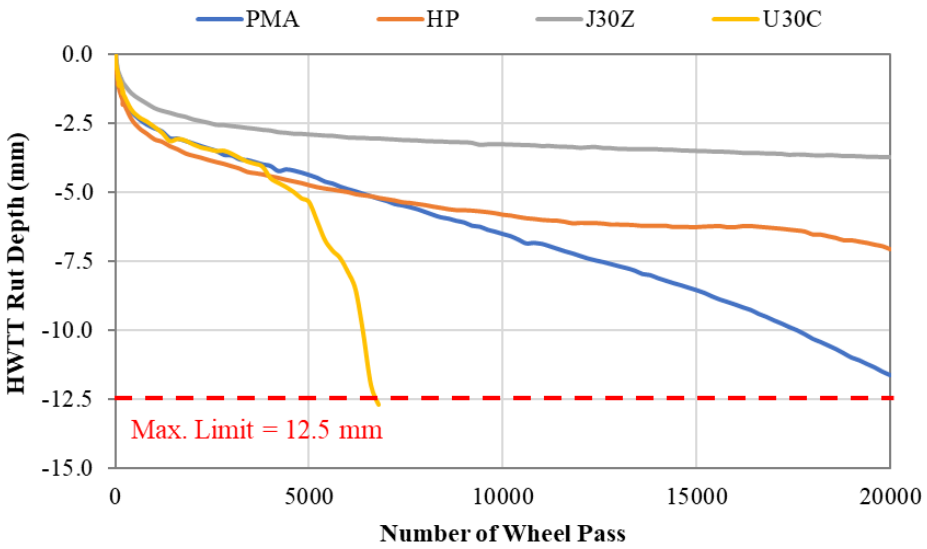

Figure 113. HWTT Rutting Curves of GRN3 Mixtures with Different Asphalt Binders

Figure 114. U30C GRN3 Mixture Specimens after Testing in HWTT

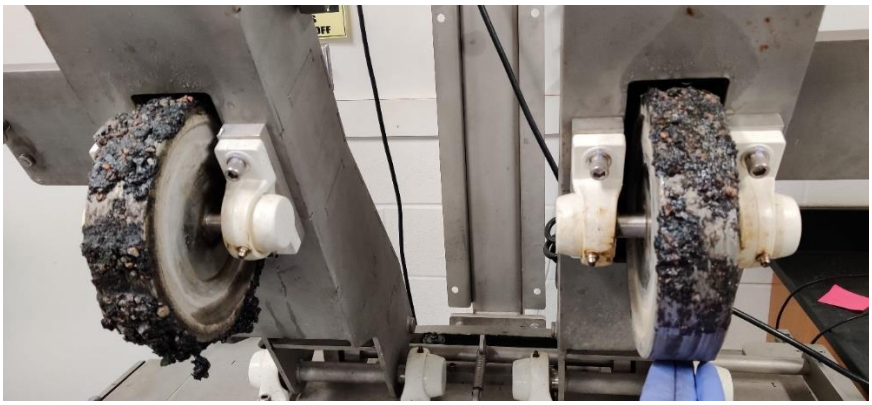

Figure 115. HWTT Wheels Stuck with U30C GRN3 Mixture Particles

Figure 116 presents the HWTT rutting curves of OGFC mixtures prepared with the LMS mix design. All of the LMS mixtures containing different asphalt binders had good results in the HWTT, with less than 12.5 mm of rutting at 20,000 passes and no signs of stripping. Therefore,

these mixtures are expected to have good rutting resistance and moisture resistance. Comparatively, the two EMA mixtures had the best rutting resistance with the lowest rut depths at 20,000 passes, followed by the PMA mixture and then the HP mixture. However, the differences among all the mixtures were less than 2.5 mm and are not considered practically significant given the variability of the test results and the high air voids of OGFC mixtures.

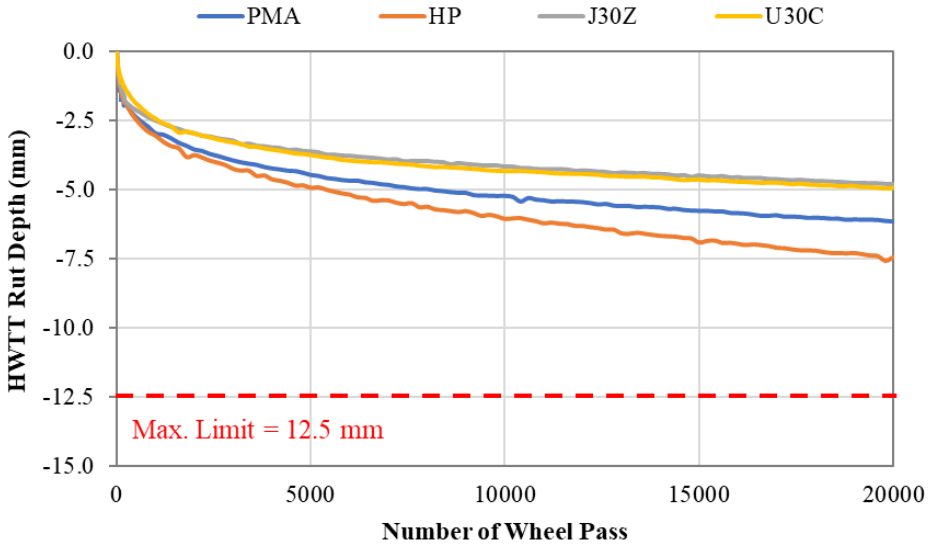

Figure 116. HWTT Rutting Curves of LMS Mixtures with Different Asphalt Binders

6.3 Summary of Findings

Overall, OGFC mixtures prepared with the HP binder had the lowest Cantabro loss results under the STA and LTA2 conditions and thus, are expected to have the best raveling resistance before and after extended long-term aging for 20 days at 85°C. The two EMA mixtures had much better Cantabro results than the mixtures containing a PMA binder under the LTA2 condition. Furthermore, in most cases, the EMA mixtures showed similar Cantabro loss results as the HP mixture, which indicated comparable raveling resistance after extended long-term aging.

Although the J30C mixtures had consistently higher IDT strength and G_f results than the other mixtures under the STA condition, the U30C mixtures became the best performer with the best tensile strength and fracture resistance after extended long-term aging for 20 days at 85°C. All the OGFC mixtures prepared with different FC-5 mix designs and asphalt binders except one had a TSR of over 80% when tested under the STA condition and are expected to have acceptable resistance to moisture damage. Different from the PMA, HP, and J30Z mixtures, the U30C mixtures exhibited considerably higher wet strength than the dry strength, which yielded unusual TSR values that are significantly higher than 100%. The substantial increase in the tensile strength of the U30C mixtures is likely attributed to the accelerated curing of the EMA binder when the mixture was conditioned in a 60°C water bath for moisture conditioning of the TSR test.

The HWTT results for the OGFC mixtures were highly dependent on the mix design used. All mixtures prepared with the GRN1 and LMS mix designs had less than 12.5 mm of rutting at 20,000 passes and showed no signs of stripping. Comparatively, the J30Z and U30C mixtures

had similar or slightly better results than the HP and PMA mixtures in HWTT. For the GRN2 and GRN3 mix designs, the J30Z mixtures significantly outperformed the other three mixtures in terms of rutting resistance and moisture resistance. The PMA and HP mixtures prepared with the GRN2 mix design reached 12.5 mm rut depth before 20,000 passes and had low to medium severity stripping failures. The U30C mixtures prepared with the same mix designs showed high severity stripping failures and lasted less than 7,000 passes before reaching 12.5 mm rut depth. It is believed that this early failure of U30C mixtures was because the EMA binder, when tested under the STA condition, was in the early stage of its curing process and had not gained sufficient cohesive strength to resist the severe conditions of the HWTT. These results raise a concern that the U30C mixtures prepared with the GRN2 and GRN3 mix designs may not be allowed to open to traffic immediately after construction due to lack of strength. HVS testing of these mixtures is needed to determine the amount of time required for the mixtures to gain sufficient strength before they should be allowed for trafficking on the roadway.

CHAPTER 7. RECYCLABILITY EVALUATION OF EMA OGFC MIXTURES

This chapter presents the experimental plan, test results, and findings of Experiment 5 of the study. The objective of this experiment was to determine the feasibility of using OGFC mixtures containing EMA binders as RAP in dense-graded asphalt mixtures. To that end, four types of laboratory-produced artificial RAP materials were prepared by aging the compacted specimens of OGFC mixtures containing PMA, HP, J30Z, and U30C binders for 20 days at 85°C and then crushing them into loose mixture particles using a jaw crusher. Trial attempts were made to extract, recover, and grade the asphalt binders in the EMA RAP. Furthermore, dense-graded asphalt mixtures were prepared using the different RAP materials and tested in the HWTT and IDEAL-CT. Performance diagram analysis was conducted to determine the effect of RAP type on the rutting resistance and intermediate-temperature cracking resistance of dense-graded asphalt mixtures as an indirect approach of assessing the recyclability of OGFC mixtures containing EMA binders.

7.1 Experimental Plan

Two randomly selected FC-5 mix designs (i.e., GRN2 and GRN3) were used to prepare OGFC mixtures with four different types of asphalt binders: PMA, HP, J30Z, and U30C. The OGFC specimens (i.e., compacted to 50 gyrations with a final height of approximately 110 to 120 mm) were aged in an environmental chamber for 20 days at 85°C to simulate the accelerated asphalt aging. This aging procedure was the same as the LTA2 conditioning used in Experiments 2 and 4 of the study. After aging, the OGFC specimens were crushed into loose mixture particles using a jaw crusher to mimic the milling of OGFC mixtures as RAP. Figure 117 shows pictures of the jaw crusher and loose mixture particles after crushing. The loose mixture particles were then treated as artificial RAP materials for further evaluation in this experiment.

Figure 117. Jaw Crusher (left) and Loose Mixture Particles after Crushing (right)

The experimental plan consisted of two parts. The first part was to determine if the asphalt binders in the EMA RAP could be extracted and recovered. Trial attempts were made to perform the asphalt extraction and recovery in accordance with AASHTO T 164 [using trichloroethylene (TCE) as the extraction solvent] and ASTM D5404, respectively. The recovered asphalt binders were then tested to determine their PG grades. Asphalt extraction, recovery, and PG grading were also conducted on the PMA RAP for comparison purposes.

The second part of the experimental plan focused on mix design and performance testing of dense-graded asphalt mixtures prepared with the artificial RAP materials. A total of eight dense-graded mixtures were evaluated, which corresponded to a combination of two mix designs and four artificial RAP materials. The two mix designs were a FC-12.5 friction course mix and a SP-12.5 structural course mix. Both mixes were designed with 15% artificial RAP and a PG 76-22 PMA binder. The FC-12.5 mix design used the same granite aggregates as the GRN3 FC-5 mix design used in Experiment 4 of the study, while the SP-12.5 mix design used the same granite aggregates as the GRN1 FC-5 mix design. Although attempts were made to design the two mixes with a fine gradation to remain consistent with FDOT's practice, they were not successful because the artificial RAP and sands used were much coarser than those in the reference mix designs provided by FDOT. Therefore, both the FC-12.5 and SP-12.5 mixes were designed with a coarse gradation. After the two mix designs were established, mixture specimens were prepared with different artificial RAP materials for performance testing. HWTT was conducted in accordance with AASHTO T 324 at 50°C to evaluate the rutting resistance of these mixtures. Furthermore, IDEAL-CT was conducted per ASTM D8225-19 for the evaluation of intermediate-temperature cracking resistance. Both tests were performed on short-term aged specimens that had been aged for four hours at 135°C prior to compaction per AASHTO R 30.

7.2 Test Results and Discussion

Characterization of Artificial RAP Materials

Table 100 presents the dry sieve analysis results of the artificial RAP materials obtained after crushing the OGFC specimens using a jaw crusher. Four replicates were tested to check the variability of the results. Table 100 also includes the dry sieve analysis results of the RAP aggregates after burning off the asphalt binder in an ignition furnace. As can be seen, the as-crushed RAP has a much coarser gradation than the actual RAP aggregates.

Table 100. Gradations of Crushed RAP and RAP Aggregates after Ignition Furnace

Sieve Size	Crushed RAP (% Passing)					RAP Aggregate (% Passing)
	Rep. #1	Rep. #2	Rep. #3	Rep. #4	Average	
1"	100	100	100	100	100	100
3/4"	95	94	90	92	92	100
1/2"	62	60	42	56	56	95
3/8"	38	39	29	37	37	76
#4	9	11	7	11	11	29
#8	3	4	2	5	5	13
#16	1	2	1	2	2	9
#30	0	0	0	0	0	7
#50	0	0	0	0	0	5
#100	0	0	0	0	0	4
#200	0	0	0	0	0	3.1

Trial attempts were made to extract and recover asphalt binders from the EMA RAP using TCE as the solvent, but they were not very successful. The J30Z and U30C RAP had an extractable asphalt binder content of 5.5% and 2.8%, respectively, which were lower than the asphalt binder contents used to prepare the OGFC mixtures (i.e., 6.6% for GRN2 and 6.5% for GRN3). For

comparison purpose, the PMA RAP had an asphalt binder content of 5.8% from solvent extraction. Figure 118 presents the post-extraction aggregate residues of different RAP. As shown, the aggregate residues of the two EMA RAP, especially the U30C RAP, were still coated with asphalt binder. Therefore, solvent extraction using TCE is not a feasible approach to determine the asphalt binder content of RAP materials containing EMA binders at 30% EDR.

(a) (b) (c)

Figure 118. Post-extraction RAP Aggregate Residues: (a) PMA RAP, (b) J30Z RAP, (c) U30C RAP

Finally, the extracted asphalt binders from the J30Z and U30C RAP were tested to determine their PG grades. The DSR and BBR tests were conducted on the as-extracted binder samples without additional RTFO or PAV aging. As shown in Table 101, the extracted asphalt binder from the J30Z RAP was graded as PG 94-16 with a true grade of PG 96.8-21.2 and delta T_c (ΔT_c) of -5.9°C. The extracted U30C RAP binder was remarkably soft, which was graded as PG 46-34 and had a true grade of PG 47.8-34.8 and ΔT_c of 3.9°C. However, these PG grade results should be interpreted with caution because the extracted asphalt binder from EMA RAP, especially the U30C RAP, is not representative of the asphalt binder in the RAP because of the solvent extraction issues discussed above. For comparison purposes, the extracted binder from the PMA RAP (without additional RTFO or PAV aging) was graded as PG 82-22 with a true grade of PG 87.7-22.4 and ΔT_c of -4.6°C. Note that the PMA RAP was prepared with a PG 76-22 base binder.

Table 101. PG Grades of As-Extracted Asphalt Binders from PMA, J30Z, and U30C RAP

RAP Type	High-temp. True Grade (°C)	Low-temp. True Grade, Stiffness (°C)	Low-temp. True Grade, m-value (°C)	PG Grade	True Grade	ΔT_c (°C)
PMA	87.7	-27.1	-22.4	82-22	87.7-22.4	-4.6
J30Z	96.8	-27.2	-21.2	94-16	96.8-21.2	-5.9
U30C	47.8	-34.8	-38.7	46-34	47.8-34.8	3.9

FC-12.5 and SP-12.5 Mix Designs

Table 102 summarizes the FC-12.5 and SP-12.5 mix designs. Both mixes were designed with a coarse gradation, 15% artificial RAP, and a PG 76-22 PMA binder. Although these two mix designs seem to have higher asphalt binder contents and voids in mineral aggregate (VMA) than most of FDOT's approved FC-12.5 and SP-12.5 mixes, they are sufficient in determining, on a relative basis, the impacts of different artificial RAP materials on the rutting and cracking resistance of dense-graded asphalt mixtures in this experiment.

Table 102. Summary of FC-12.5 and SP-12.5 Mix Designs

Mix Design Parameters		FC-12.5	SP-12.5
Aggregate Gradation (% Passing)	1"	100	100
	3/4"	100	100
	1/2"	96	98
	3/8"	84	84
	#4	52	51
	#8	34	35
	#16	24	24
	#30	17	16
	#50	10	10
	#00	6	6
	#200	3.2	3.5
N_{design}, gyrations		100	75
NMAS, mm		12.5	12.5
Asphalt Binder Content, %		5.7	5.7
Air Voids, %		4.2	4.4
VMA, %		15.6	16.2
VFA, %		72.9	72.8
D/B Ratio		0.64	0.69

HWTT and IDEAL-CT Testing

Figure 119 presents the HWTT rutting curves of FC-12.5 mixtures prepared with different artificial RAP materials. All of the mixtures performed well with less than 3.0 mm of rutting at 20,000 passes and no signs of stripping. The largest difference in the final rut depth among the four mixtures was 0.7 mm, which is not considered practically significant. These results indicate that the FC-12.5 mixtures have good rutting resistance regardless of the type of artificial RAP materials used.

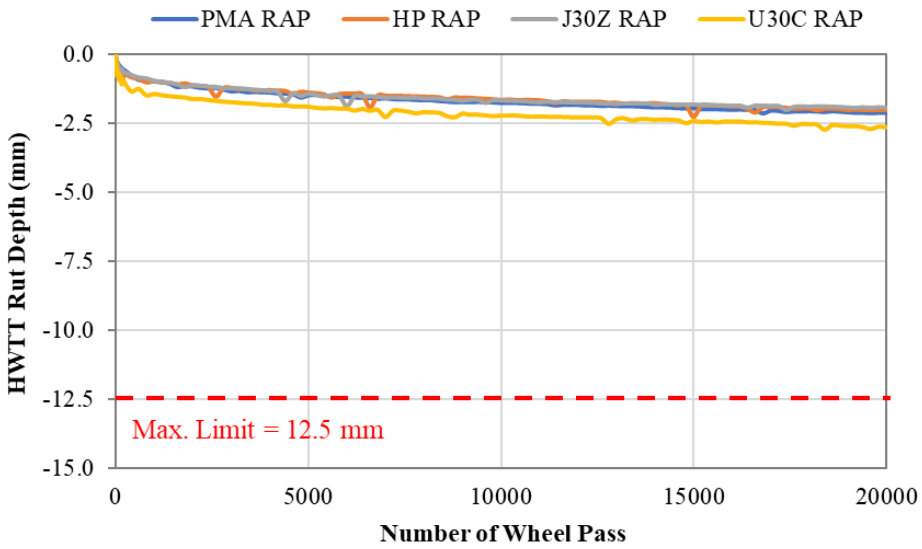

Figure 119. HWTT Rutting Curves of FC-12.5 Mixtures with Different Artificial RAP

Figure 120 presents the IDEAL CT_{Index} results of the four FC-12.5 mixtures. Comparatively, the HP RAP mixture had the highest average CT_{Index}, followed by the U30C RAP and PMA RAP mixtures and then the J30Z RAP mixture. However, Tukey's HSD test results showed that only the difference in the CT_{Index} between the HP RAP and J30Z RAP mixtures was statistically significant, while the rest were not. Overall, these results indicate that the different types of artificial RAP materials are not likely to significantly affect the intermediate temperature cracking resistance of FC-12.5 mixtures.

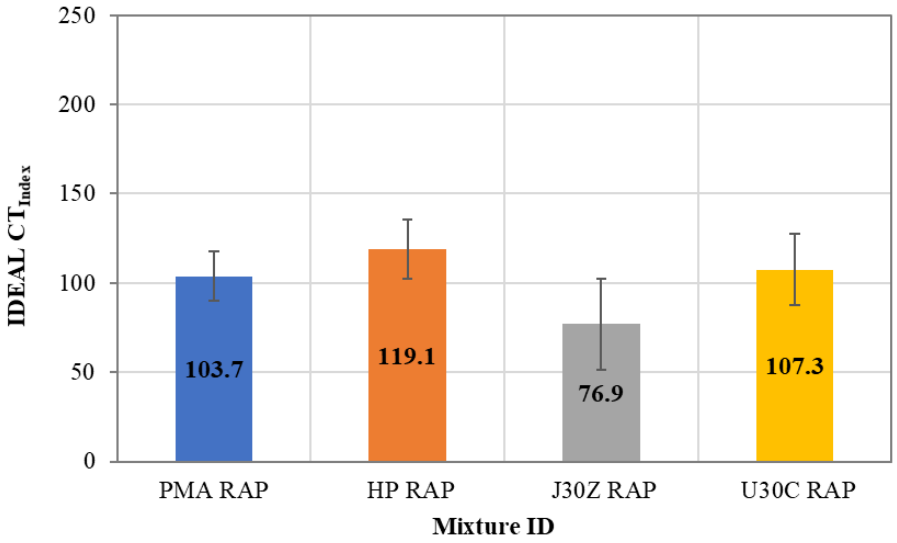

Figure 120. IDEAL CT_{Index} Results of FC-12.5 Mixtures with Different Artificial RAP

Figure 121 and Figure 122 present the HWTT rutting curves and IDEAL CT_{Index} results of the four SP-12.5 mixtures, respectively. Overall, these results are consistent with those of the FC-12.5 mixtures discussed previously. All the SP-12.5 mixtures, regardless of the type of artificial

RAP materials used, had very good HWTT results with less than 3.0 mm of rutting at 20,000 passes and no signs of stripping. The differences in the final HWTT rut depth among the mixtures were less than 1.0 mm, which is not considered practically significant. Regarding the IDEAL-CT results, mixtures containing the PMA, HP, and U30C RAP had similar average CT_{Index} values, which were higher than that of the J30Z RAP mixture. However, according to the Tukey's rankings of these results, only the difference between the PMA RAP and J30Z RAP mixtures was statistically significant. Therefore, the different types of artificial RAP materials are not expected to have a significant impact on the rutting resistance and intermediate-temperature cracking resistance of SP-12.5 mixtures, which are consistent with the results of the FC-12.5 mixtures.

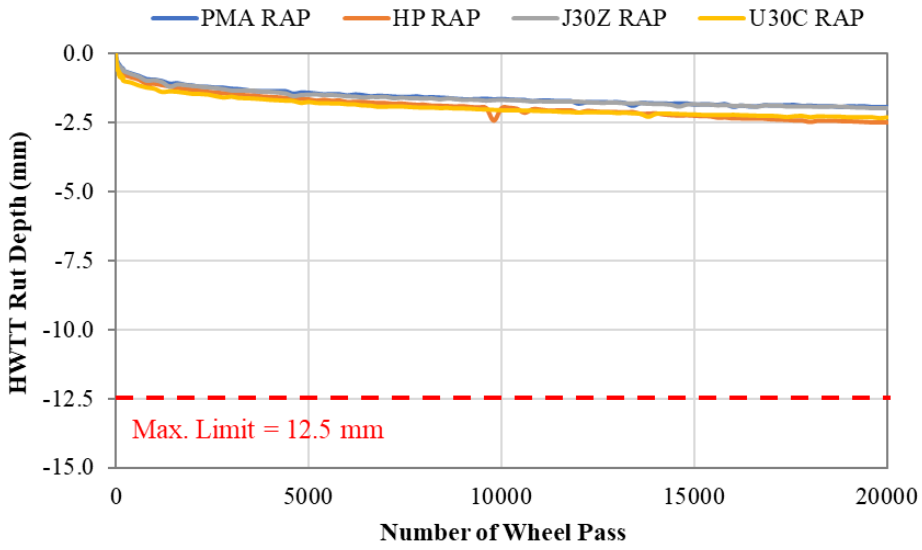

Figure 121. HWTT Rutting Curves of SP-12.5 Mixtures with Different Artificial RAP

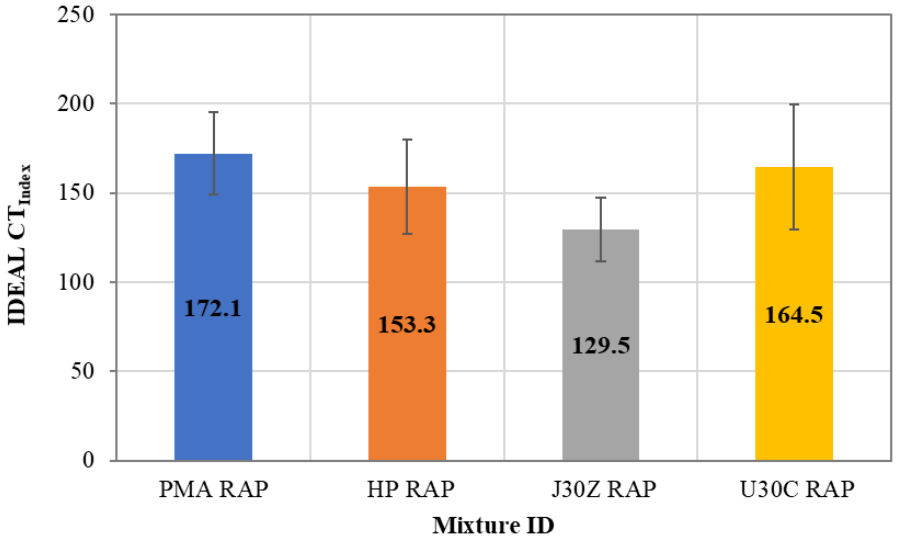

Figure 122. IDEAL CT_{Index} Results of SP-12.5 Mixtures with Different Artificial RAP

Finally, Figure 123 presents the performance diagrams of the FC-12.5 and SP-12.5 mixtures, where the HWTT rut depth at 20,000 passes are plotted on the x-axis *versus* the IDEAL CT_{Index} results on the y-axis. As shown, for both mix designs, mixtures prepared with different artificial RAP materials are located adjacently on the performance diagram, which indicates that they have similar rutting resistance and intermediate temperature cracking resistance. Given that the recyclability of asphalt mixtures containing PMA and HP binders has been proven in practice and that the FC-12.5 and SP-12.5 mixtures containing different artificial RAP materials had similar HWTT and IDEAL-CT results in this experiment, it is reasonable to conclude that use of EMA binders will not jeopardize the recyclability of OGFC mixtures. In other words, if the EMA mixtures can only be recycled as "black rock" instead of RAP, the FC-12.5 and SP-12.5 mixtures prepared with the artificial J30Z and U30C RAP would have had significantly better HWTT results but worse IDEAL-CT results than those containing the PMA and HP RAP because of the lack of "active" asphalt binder in the RAP; this trend, however, was not observed.

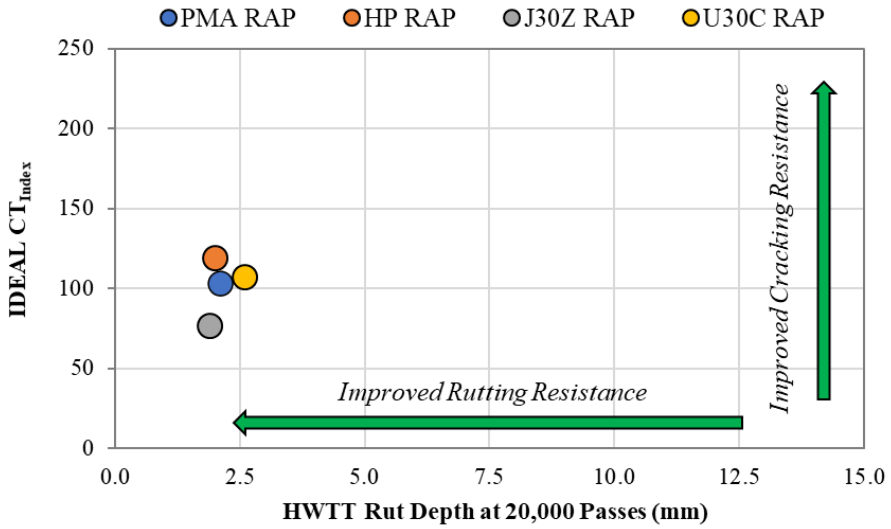

(a)

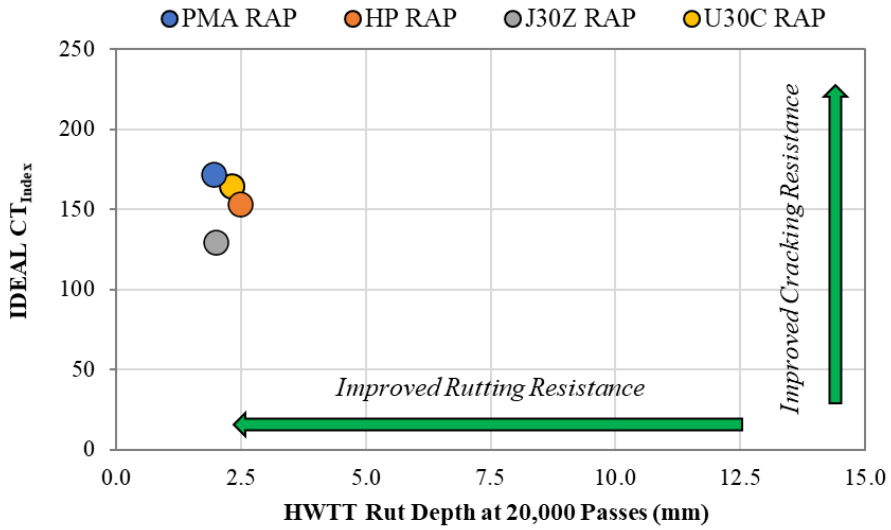

(b)

Figure 123. Performance Diagram of HWTT and IDEAL-CT Results: (a) FC-12.5 Mixtures, (b) SP-12.5 Mixtures

7.3 Summary of Findings

Solvent extraction using TCE was not effective in extracting asphalt binders from the artificial RAP prepared with OGFC mixtures containing EMA binders at 30% EDR. Especially for the U30C RAP, the asphalt binder content determined from solvent extraction was significantly lower than that used to prepare the OGFC RAP mixtures. The recovered asphalt binders from the PMA, J30Z, and U30C RAP were graded as PG 82-22, PG 94-16, and PG 46-34, respectively. However, these results should be interpreted with caution because the recovered EMA binders are not believed to be representative of those in the RAP because of the solvent extraction issues. FC-12.5 and SP-12.5 mixtures prepared with different types of artificial RAP materials had similar HWTT and IDEAL-CT results and thus, are expected to have similar rutting resistance and intermediate temperature cracking resistance. Overall, test results obtained in this experiment provide no conclusive evidence to reject the hypothesis that OGFC mixtures containing EMA binders, upon reaching their service lives, can be successfully recycled as RAP into new dense-graded asphalt mixtures.

CHAPTER 8. CONCLUSIONS AND RECOMMENDATIONS

8.1 Conclusions

This study sought to determine the viability of using epoxy-modified asphalt (EMA) to improve the durability and life span of open-graded friction course (OGFC) mixtures in Florida. To accomplish this objective, a comprehensive literature review was first conducted to synthesize existing studies on the state-of-the-practice on use of OGFC, OGFC mix design and performance testing, performance characterization of EMA binders and mixtures, and production and construction of EMA mixtures. Furthermore, informal communications with asphalt researchers, epoxy material suppliers, and international agency and industry representatives were made to gather information about their experiences with the design, production, and performance of OGFC mixtures containing EMA binders. Based on the information collected, a systematic experimental plan was developed and executed to explore the potential use of EMA binders for OGFC applications. The experimental plan consisted of five supplementary laboratory experiments. Experiment 1 was to select suitable asphalt binders for epoxy modification based on the chemical compatibility evaluation of EMA binders. Experiment 2 was to determine the optimum epoxy dosage rate (EDR) with respect to material cost and OGFC performance properties. Experiment 3 focused on developing a method of designing OGFC mixtures containing EMA binders. Experiment 4 was to characterize the performance properties of OGFC mixtures prepared with EMA *versus* PG 76-22 polymer-modified asphalt (PMA) and high polymer (HP) binders. Finally, Experiment 5 aimed at the recyclability evaluation of EMA OGFC mixtures for use as reclaimed asphalt pavements (RAP) in dense-graded asphalt mixtures. The major findings and conclusions of this study are summarized as follows.

Selection of Chemically Compatible EMA Binders

The laboratory test procedure combining the storage stability test with Soxhlet asphalt extraction was effective in discriminating the chemical compatibility of low-dosage EMA binders prepared with different sources of epoxy materials, base binders, and EDRs. Test results indicated that the PG 67-22 base binders A and Z with low resins content determined in the Saturates, Aromatics, Resins and Asphaltenes (SARA) analysis showed the best compatibility with the epoxy materials from a foreign source. On the other hand, the PG 67-22 base binders A and C with high saturates content in the SARA analysis were most compatible with the epoxy materials from a domestic source. Fluorescence microscopy was also found as an effective tool in qualitatively assessing the morphology of EMA binders. As EDR increased from 15% to 25%, the compatibility of EMA binders decreased as the network distribution of epoxy resins became less uniform. Image analysis of the fluorescence micrographs indicated that the base binder Z presented the best compatibility with the epoxy materials from a foreign source, while the base binder C was most compatible with the epoxy materials from a domestic source. This observation was consistent with those of the storage stability test and Soxhlet asphalt extraction results. Therefore, base binders Z and C were selected for epoxy modification using the epoxy materials from a foreign source and domestic source, respectively.

Determination of Optimum EDR

Binder Performance Testing

Rotational viscosity results indicated that as temperature increased, the viscosity of the EMA binders decreased, and shorter became the time required to achieve a fully cured stage at 15% and 25% EDR. At 15% EDR, the curing process of the foreign epoxy materials was faster than the domestic epoxy materials, while the opposite trend was observed at 25% EDR. At temperatures of 145, 165, and 190°C, the J25Z and U25C binders showed higher viscosity than both the PMA and HP binders. High-temperature and low-temperature true grade results showed that the epoxy materials stiffened the base asphalt binders. The HP binder showed the lowest intermediate pass/fail temperature and thus, is expected to have best fatigue resistance, followed by the EMA binders and then the PMA binder. When evaluating among the modified binders, the ranking from lower to higher ΔT_c was: J25Z = PMA < J15Z < U15C < HP. However, these rankings should be interpreted with caution because the applicability of ΔT_c to polymer-modified binders remains questionable.

The epoxy modification in the U25C binder led to a reduction in J_{nr} and an increase in %Recovery, as compared to the unmodified base asphalt C. However, the base binder softened rather than stiffened after the epoxy modification at 15% EDR. On the other hand, the epoxy modification was effective for J-EMA binders at both 15% and 25% EDR, resulting in a reduced J_{nr} associated with an increased %Recovery. However, as compared to U-EMA binders, the effect of epoxy modification in the J-EMA binders was less pronounced. The MSCR test results indicated that the PMA and HP binders provided the best balance of J_{nr} and %Recovery parameters.

LAS test results indicated that modification with both the domestic and foreign epoxy materials at 15% EDR did not improve the fatigue resistance of the base binders. Based on the MSCR results, this lack of improvement was likely due to the reduced material stiffness stemming from an incomplete curing reaction. Compared to the base and EMA binders, the PMA and HP binders had higher number of cycles to failure and thus, are expected to have better fatigue resistance.

The *G-R* parameter results in Black Space indicated that, with exception of the PMA binder, the evaluated binders are not likely to experience premature block cracking in the field. However, care should be taken when interpreting these results, since the applicability of the *G-R* parameter and its preliminary thresholds to polymer-modified asphalt binders is actively contested among the asphalt industry. When evaluating the *G-R* parameter results in the Black Space diagram, the PMA and HP binders presented smaller phase angle values (indicating increased elasticity, which is beneficial for fatigue and rutting resistance) than the base and EMA binders before and after PAV aging. Finally, the *G-R* Aging Index results indicated that the HP and EMA binders were the least susceptible to oxidative aging, followed by the PMA binder and then the unmodified binders.

Master curve analysis showed that epoxy and SBS modification of the asphalt binder can significantly affect the shape of the master curve, decreasing its slope and thus altering the time-dependency of the material response in a specific frequency range. Furthermore, |G*| and phase

angle master curves suggested that traditional parameters for performance characterization of unmodified binders may not be suitable to adequately characterize HP and EMA binders.

BBS test results demonstrated that the type and chemical characteristics of the aggregates greatly affected the bond strength of PMA, HP, and EMA binders. Moreover, the chemistry of the epoxy materials and EDR appeared to affect the degree of adhesion by allowing the development of bonds of different strength. The asphalt-aggregate systems with the least susceptibility to moisture damage were the "HP + GRN1" and "U15C + GRN2" combinations.

Lastly, it was observed that at 25% EDR, the EMA binder prepared with the epoxy materials from a domestic source became unworkable after long-term PAV aging, and the conventional Superpave asphalt binder tests were not applicable. Furthermore, the rheological characterization of EMA binders prepared with epoxy materials from a foreign source at 25% EDR was also challenging after PAV aging, especially when attempting to apply rheological models.

Mixture Performance Testing

As the EDR increased between 15% and 40%, most of the EMA mixtures had reduced Cantabro loss, increased indirect tensile (IDT) strength, and increased fracture energy (G_f) results, which indicate that epoxy modification of the asphalt binder has a positive impact on the raveling resistance, tensile strength, and fracture resistance of OGFC mixtures. The comparison in the Cantabro and IDT test results between the PMA and EMA mixtures was dependent on the EDR. Overall, the EMA mixtures at 30% and 40% EDRs performed better than the PMA and low-dosage EMA mixtures in the Cantabro and IDT tests. The differences among these mixtures were more pronounced after long-term aging, which is believed to be a more robust aging condition for evaluating the long-term raveling resistance and durability of OGFC mixtures. The Cantabro Aging Index (CAI) results indicated that the U-EMA mixtures (i.e., EMA mixtures prepared with base binder C and epoxy materials from a domestic source) have the best aging resistance, followed by the J-EMA mixtures (i.e., EMA mixtures prepared with base binder Z and epoxy materials from a foreign source), and then the PMA mixtures. Three evaluation criteria based on statistical comparisons of the Cantabro and IDT test results under various mix aging conditions were proposed to select the optimum EDR of EMA binders. The comparison results showed that 30% and 40% EDRs were able to consistently yield EMA OGFC mixtures with better performance properties than the PMA mixtures and thus, have the potential of extending the current life span of OGFC in Florida. Considering the high cost of epoxy materials, the lower EDR of 30% was selected as the final optimum EDR for both J-EMA and U-EMA binders. At this EDR, the estimated material cost of EMA OGFC mixtures is approximately 3.5 to 5 times higher than those containing a PMA binder.

Mix Design of EMA OGFC Mixtures

Using FDOT's current practice for mix design approval of OGFC mixtures containing PMA and HP binders as reference, a similar mix design procedure was developed for OGFC mixtures prepared with EMA binders at 30% EDR. This procedure consisted of determining a preliminary OBC based on the pie plate testing of OGFC mixtures with a PG 67-22 unmodified binder at various binder contents, verifying the asphalt draindown potential and raveling resistance of the EMA OGFC mixture at the preliminary OBC using the modified pie plate and Cantabro tests, respectively, and then if needed, adjusting the preliminary OBC to improve the pie plate and

Cantabro test results. This procedure was successfully validated with four FDOT approved FC-5 mix designs. All the OGFC mixtures prepared with EMA binders at 30% EDR showed less asphalt draindown in the pie plate test than those containing a PG 67-22 binder and had a Cantabro loss of less than 20% when tested at the short-term aging (i.e., unaged) condition. These results are consistent with FDOT's experience with the pie plate and Cantabro testing of OGFC mixtures with PMA and HP binders. Thus, the developed procedure has the potential of designing EMA OGFC mixtures with adequate raveling resistance before aging and minimal potential for asphalt draindown during production.

Performance Characterization of OGFC Mixtures

Overall, OGFC mixtures prepared with the HP binder had the lowest Cantabro loss results and are expected to have the best raveling resistance at the short-term aging and extended long-term aging (i.e., compacted specimen aging for 20 days at 85°C) conditions. At the short-term aging condition, the PMA mixtures performed similarly or better than the EMA mixtures at 30% EDR in the Cantabro test. However, after extended long-term aging, the EMA mixtures had significantly lower Cantabro loss results, indicating better long-term raveling resistance than the PMA mixtures. In most cases, the EMA mixtures at 30% EDR performed comparatively as the HP mixtures at the extended long-term aging condition. As mentioned previously, the Cantabro test results obtained after long-term aging are believed to provide more meaningful evaluations for the long-term raveling resistance and durability of OGFC mixtures than those obtained at the short-term aging (or unaged) condition because they consider the impact of asphalt aging on mix embrittlement.

In most cases, the J-EMA and U-EMA mixtures at 30% EDR had the highest IDT strength and G_f results at the short-term aging and extended long-term aging conditions, respectively. All the OGFC mixtures prepared with different types of asphalt binders except for one had a tensile strength ratio (TSR) of over 80%; therefore, they are not expected to be susceptible to moisture damage. Different from the OGFC mixtures containing PMA, HP, and J-EMA binders, the U-EMA mixtures at 30% EDR exhibited considerably higher wet strength than dry strength in the TSR test. This increase in the tensile strength is likely attributed to the accelerated curing of the EMA binder when the mixture was conditioned in a 60°C water bath for moisture conditioning as part of the TSR test.

The HWTT performance of OGFC mixtures was highly dependent on the mix design (i.e., aggregate source) and type of asphalt binder used. All mixtures prepared with the GRN1 and LMS mix designs had acceptable HWTT results with minimal rutting and no signs of stripping. Comparatively, the J-EMA and U-EMA mixtures at 30% EDR had similar or slightly better HWTT results than the HP and PMA mixtures. For both the GRN2 and GRN3 mix designs, the J-EMA mixtures had significantly better HWTT results than the other three mixtures. The PMA and HP mixtures prepared with the GRN2 mix design showed low to medium severity stripping failures, while the U-EMA mixtures prepared with both the GRN2 and GRN3 mix designs showed high severity stripping failures. It is speculated that the U-EMA mixtures exhibited early failure in HWTT because under the STA condition, the EMA binder was still at the early stage of its curing process and had not gained sufficient cohesive strength to resist the harsh condition of the HWTT.

Recyclability Evaluation of EMA OGFC Mixtures

Solvent extraction using TCE was not effective in extracting asphalt binders from the laboratory-aged artificial RAP prepared with OGFC mixtures containing EMA binders at 30% EDR. Most of the post-extraction aggregate residues of the U-EMA RAP were still coated with asphalt binder. As a result, the asphalt binder content determined from solvent extraction of this RAP was significantly lower than those of the PMA and J-EMA RAP. For the J-EMA RAP, only a small amount of asphalt-coated aggregate particles was observed after solvent extraction. The recovered asphalt binders from the J-EMA and U-EMA RAP were graded as PG 94-16 and PG 46-34, respectively. However, these results should be interpreted with caution because the recovered EMA binders are not believed to be representative of the asphalt binders in the RAP because of the solvent extraction issues. For both the FC-12.5 and SP-12.5 mix design, mixtures prepared with different types of artificial RAP materials had similar HWTT and IDEAL-CT results and thus, are expected to have equivalent rutting resistance and intermediate-temperature cracking resistance. Overall, test results obtained in this experiment seem to suggest that OGFC mixtures containing EMA binders, upon reaching their service lives, could be successfully recycled as RAP into new dense-graded asphalt mixtures. However, solvent extraction and recovery of asphalt binder from the EMA RAP are not feasible.

8.2 Recommendations

Based on the test results and findings of this study, the following future research and implementation activities are suggested:

- In this study, the two mix aging procedures of aging compacted specimens for 10 and 20 days at 85°C were used to simulate the long-term aging of OGFC mixtures for the evaluation of raveling resistance and durability. However, it remains unknown how these two aging procedures correlate to the field aging of OGFC pavements in Florida. Therefore, future research is suggested to review FDOT's pavement management system to determine the critical field aging conditions (in terms of aging time and climatic conditions) in Florida when the OGFC mixtures start to exhibit raveling issues. Furthermore, a laboratory aging study is needed to develop an implementable mix aging procedure that is representative of the critical field aging conditions for raveling evaluation of OGFC mixtures for mix design approval and product evaluation purposes.
- In Experiment 4 of the study, the U-EMA mixtures prepared with two granite-based FC-5 mix designs exhibited severe early failure in the HWTT when tested at the short-term aging condition, which raises a concern that the U-EMA mixtures may experience premature rutting, and possibly, shoving failures immediately after construction due to lack of cohesive strength. To address this concern, heavy vehicle simulator (HVS) testing of U-EMA mixtures is suggested to assess their post-compaction curing behavior and determine the time after construction when they can be allowed to open to traffic without causing premature surface failures.
- OGFC mixtures prepared with HP and EMA binders at 30% EDR had significantly lower Cantabro loss results at the extended long-term aging condition and thus, are expected to have better long-term raveling resistance than the corresponding mixtures containing PMA binders. Therefore, it is recommended that FDOT construct a field demonstration project to assess the long-term (i.e., up to 10 years or more) field performance of OGFC mixtures containing HP *versus* EMA binders. The field demonstration project would also

help FDOT identify any challenges associated with the production and construction of EMA OGFC mixtures.

- Life-cycle cost analysis is recommended for future research to compare the cost-effectiveness of OGFC mixtures prepared with PMA, HP, and EMA binders based on actual bid price and long-term field performance data.
- Future research is needed to explore mix design strategies to mitigate the HWTT stripping issues of PMA and HP OGFC mixtures prepared with the GRN2 mix design, as well as the U-EMA OGFC mixtures prepared with the GRN2 and GRN3 mix designs. Based on the recommendations of FDOT study BE555 (Gu et al., 2020; Gu et al., 2021), adding 0.5% liquid anti-strip additive or adding an additional 0.5% hydrated lime are potentially cost-effective ways to address these issues but their effectiveness should be verified with HWTT testing.

REFERENCES

Al-Qadi, I., Ozer, H., Lambros, J., Khatib, A., Singhvi, P., Khan, T., Rivera-Perez, J., and Doll, B. (2015). Testing Protocols to Ensure Performance of High Asphalt Binder Replacement Mixes Using RAP and RAS. Final Report No. FHWA-ICT-15-017, Illinois Center for Transportation, Urbana, Illinois.

Alvarez, A., Martin, E., Estakhri, C., Button, J., Glover, C., and Jung, S. (2006). Synthesis of Current Practice on the Design, Construction, and Maintenance of Porous Friction Courses. Report No. FHWA/TX-06/0-5262-1. Texas Department of Transportation, Austin, Texas.

Alvarez, A., Martin, A., and Estakhri, C. (2011). A Review of Mix Design and Evaluation Research for Permeable Friction Course Mixtures. Construction and Building Materials, Vol. 25, 1159-1166.

Apostolidis, P., Nahar, S. N., Liu, X., Lommerts, B., Erkens, S., and Scarpas, A. (2019). Insights into Polymerization-induced Phase Separation of Epoxy-Bitumen Systems and Strategies to Tailor High-Performance Bituminous Materials. Poster Session during the 99th Transportation Research Board (TRB) Annual Meeting, Washington, D.C.

Apostolidis, P., Pipintakos, G., Liu, X., Van de Ven, M., Erkens, S., and Scarpas, A. (2018). EMA Bitumen: Chemical Hardening and Its Interpretation. International Conference on Advances in Materials and Pavement Performance Prediction (AM3P 2018), Doha, Qatar.

Azari, H. (2010). Precision Estimates of AASHTO T283: Resistance of Compacted Hot Mix Asphalt (HMA) to Moisture-induced Damage. National Cooperative Highway Research Program, Transportation Research Board of the National Academies, Web-only Document 166, Washington, D.C.

Baginska, K., and Gawel, I. (2004). Effect of Origin and Technology on the Chemical Composition and Colloidal Stability of Bitumens. Fuel Processing Technology, 85(13), 1453-1462.

Barrett, M. (2008). Effects of a Permeable Friction Course on Highway Runoff. Journal of Irrigation and Drainage Engineering. Vol. 134, No. 5, 646-651.

Bernhard, R., Wayson, R., Haddock, J., Neithalath, N., El-Aassar, A., Olek, J., Pellinen, T., and Weiss, W. (2004). An Introduction to Tire/Pavement Noise of Asphalt Pavement. Institute of Safe, Quiet and Durable Highways, Purdue University, West Lafayette, Indiana.

Brewer, R.A. (1970). Epoxy-asphalt open-graded pavement as a skid-resistance treatment on the San Francisco Bay Bridge. Highway Research Board Special Report No. 116, Western Summer Meeting, Sacramento, California.

Buddhavarapu, P., Smit, A., and Prozzi, J. (2015). A Fully Bayesian Before-After Analysis of Permeable Friction Course Pavement Wet Weather Safety. Accident Analysis & Prevention, Vol. 80, 89-96.

ChemCo Systems. (2020). Epoxy Asphalt. Link at https://www.chemcosystems.com/epoxy_info/, accessed on April 1, 2019.

Chen, J., Tang, T., and Zhang, Y. (2017). Laboratory Characterization of Directional Dependence of Permeability for Porous Asphalt Mixtures. Materials and Structures, Vol. 50, Article No. 215.

Chen, J., Yin, X., Wang, H., and Ding, Y. (2018). Evaluation of Durability and Functional Performance of Porous Polyurethane Mixture in Porous Pavement. Journal of Cleaner Production, Vol. 188, 12-19.

Cong, P., Liu, N., Shang, S., and Zhao, H. (2015). Rheological and Fatigue Properties of Epoxy Asphalt Binder. International Journal of Pavement Research and Technology, Vol. 8, pp. 370-376.

Cong, P., Luo, W., Xu, P., and Zhang, Y. (2019). Chemical and Physical Properties of Hot Mixing Epoxy Asphalt Binders. Construction and Building Materials, Vol. 198, pp. 1-9.

Cong, P., Chen, S., Yu, J., and Chen, H. (2011). Compatibility and Mechanical Properties of Epoxy Resin Modified Asphalt Binders. International Journal of Pavement Research and Technology, Vol. 4, pp. 118-123.

Cong, P., Tian, Y., Liu, N., Xu, P. (2016). Investigation of Epoxy-Resin-Modified Asphalt Binder. Journal of Applied Polymer Science, Vol. 133.

Cooley, L., Brumfield, J., Wogawer, R., Partl, M., Poulikakos, L., and Hicks, G. (2009). Construction and Maintenance Practices for Permeable Friction Courses. NCHRP Report 640, The National Academies Press, Washington D.C.

D'Angelo, J. (2009). The Relationship of the MSCR Test to Rutting. Road Materials and Pavement Design, Vol. 10, Sup 1, pp. 61-80.

Dinnen, A. (1991). Epoxy Bitumen Binders for Critical Road Constructions. Proceedings of the 2nd Eurobitume Symposium, pp. 294-296.

Donavan, P. (2007). Exterior Noise of Vehicles. Handbook of Noise and Vibration Control. John Wiley & Sons Inc., Hoboken, New Jersey.

Elvik, R., and Greibe, P. (2005). Road Safety Effects of Porous Asphalt: A Systematic Review of Evaluation Studies. Accident Analysis & Prevention, Vol. 37, No. 3, 515-522.

Florida Department of Transportation (FDOT). (2020). Florida Method of Test for Determining the Optimum Asphalt Binder Content of an Open-graded Friction Course Mixture Using the Pie Plate Method. Link at https://fdotwww.blob.core.windows.net/sitefinity/docs/default-source/materials/administration/resources/library/publications/fstm/methods/fm5-588.pdf?sfvrsn=52e66086_2.

FHWA Asphalt Pavement Technology Program. (2011). The Multiple Stress Creep Recovery (MSCR) Procedure. Tech Brief, Federal Highway Administration, Washington, D.C.

Gaestel, C., Smajda, R., and Lamminan, K.A. (1971). Revue Générale des Routes et des Aérodromes 466, 85.

Geng, L., Ma, T., Zhang, J., Huang, X., and Hu, P. (2017). Research on Performance of a Dense Graded Ultra-Thin Wearing Course Mixture. Applied Sciences, Vol. 7, 800.

Gibson, N. (2009). Full-Scale Accelerated Performance Testing for Superpave & Structural Validation. Southeastern Asphalt User Producer Group, Hilton Head Island, South Carolina.

Gu, F., Moraes, R., Yin, F., Watson, D., Taylor, A., and Chen, C. (2020). Study of Anti-Strip Additives on Granite Based FC-5 Asphalt Mixtures. Florida Department of Transportation BE555 Final Report. Auburn, Alabama, 98 pp.

Gu, F., Moraes, R., Chen, C., Yin, F., Watson, D. and Taylor, A. (2021). Effects of Additional Antistrip Additives on Durability and Moisture Susceptibility of Granite-Based Open-Graded Friction Course. Journal of Materials in Civil Engineering, 33(9), p.04021245.

Gu, F., Watson, D., Moore, J., and Tran, N. (2018). Evaluation of the Benefits of Open Graded Friction Course: Case Study. Construction and Building Materials, Vol. 189, 131-143.

Hernandez-Saenz, M., Caro, S., Arambula-Mercado, E., Martin, A. (2016). Mix Design, Performance and Maintenance of Permeable Friction Courses in the United States: State of the Art. Construction and Building Materials, Vol. 111, 358-367.

Herrington, P.R., Alabaster, D., Arnold, G., Cook, S., Fussell, A., and Reilly, S. (2007). EMA open-graded porous asphalt. Land Transport New Zealand Research Report 321, Land Transport New Zealand, Wellington, New Zealand.

Herrington, P. (2010). Epoxy-modified porous asphalt. NZ Transport Agency Research Report 410, NZ Transport Agency, Wellington, New Zealand.

Herrington, P., and Alabaster, D. (2008). EMA Open-Graded Porous Asphalt. Road Materials and Pavement Design, Vol. 9(3), pp. 481-498.

Hintz, C., R. Velasquez, Z. Li, and Bahia, H. (2011a). Effect of Oxidative Aging on Binder Fatigue Performance. Journal of Association of Asphalt Paving Technologists, Vol. 80, pp. 527-548.

Hintz, C., Velasquez, R., Johnson, C., and Bahia, H. (2011b). Modification and Validation of Linear Amplitude Sweep Test for Binder Fatigue Specification. Transportation Research Record: Journal of the Transportation Research Board, Vol. 2207, pp. 99-106.

Hodd, K. (1989). Comprehensive Polymer Science and Supplements, Volume 5: Step Polymerization, Pergamon Press, Oxford, United Kingdom.

Holleran, G., Holleran, I., Bearsley, S., Dubois, C.J., and Wilson, D. (2017). Epoxy Asphalt for Durability of Open Graded Mixes: Part 1 Performance Approaches. AAPA International Flexible Pavements Conference, Melbourne, Victoria, Australia.

Jennings, P.W., Pribanic, P.W., Campbell, W., Dawson, K., Shane, S., and Taylor, R. (1980). High Pressure Liquid Chromatography as a Method of Measuring Asphalt Composition. FHWA-MT-79-30 Final Report, Department of Chemistry, Montana State University, Bozeman, Montana.

Kandhal, P., and Mallick, R. (1998). Open-Graded Asphalt Friction Course: State of the Practice. NCAT Report, 98-7, National Center for Asphalt Technology, Auburn, Alabama, 31 pp.

Kandhal, P., and Mallick, R. (1999). Design of New-Generation Open-Graded Friction Course. NCAT Report 99-03, National Center for Asphalt Technology, Auburn, Alabama.

Kandhal, P. (2002). Design, Construction, and Maintenance of Open-Graded Asphalt Friction Courses. National Asphalt Pavement Association Information Series 115, National Asphalt Pavement Association, Lanham, Maryland.

Kang, Y., Song, M., Pu, L., and Liu, T. (2015). Rheological Behaviors of Epoxy Asphalt Binder in Comparison of Base Asphalt Binder and SBS Modified Asphalt Binder. Construction and Building Materials, Vol. 76, pp. 343-350.

Li, Z.F. (1999). Epoxy Asphalt for Drainage Pavements. Foreign Updates on Municipal Engineering, vol. 3, Tianjin, China, p. 11–13.

Luo, S., Lu, Q., and Qian, Z. (2015). Performance evaluation of EMA open-graded porous asphalt concrete. Construction and Building Materials, 76, 97-102.

Marasteanu, M., Zofka, A., Turos, M., Li, X., Velasquez, R., Buttlar, W., Paulino, G., Braham, A., Dave, E., Ojo, J., Bahia, H., Williams, C., Bausano, J., Gallistel, A., and J. McGraw. (2007). Investigation of Low Temperature Cracking in Asphalt. Pavements National Pooled Fund Study 776: Report N. MN/RC 2007-43, Minnesota Department of Transportation, St. Paul, Minnesota.

Massingill Jr., J.L., and Bauer, R.S. (2000). Epoxy Resins. Applied Polymer Science: 21st Century, Pergamon Press, Oxford, United Kingdom.

McGraw, H. Chapter 16: Ethers, Epoxides and Sulfides. Link at https://slideplayer.com/slide/8922034/, accessed on April 11, 2018.

Moraes, R., Velasquez, R., and Bahia, H.U. (2011). Measuring the Effect of Moisture on Asphalt–aggregate Bond with the Bitumen Bond Strength Test. Transportation Research Record, 2209(1), 70-81.

Moraes, R., and Bahia, H. (2015). Effect of Mineral Fillers on the Oxidative Aging of Asphalt Binders: A Laboratory Study Using Mastics. Transportation Research Record: Journal of the Transportation Research Board, No. 2506, pp. 19-31.

Moraes, R., Swiertz, D., and Bahia, H. (2017). Comparison of New Test Methods and New Specifications for Rutting Resistance and Elasticity of Modified Binders. Proceedings of the 62nd Canadian Technical Asphalt Association (CTAA) Annual Conference, Halifax, Nova Scotia, Canada.

Moraes, R. and Yin, F. (2020). Evaluation of Epoxy Asphalt Binders for Open-Graded Friction Course (OGFC) Application. Proceedings of the RILEM International Symposium on Bituminous Materials – ISM Lyon 2020, Lyon, France.

Motamedi, M., Attar, M.M., and Rostami, M. (2017). Performance Enhancement of the Oxidized Bitumen Binder Using Epoxy Resin. Progress in Organic Coatings, Vol. 102, pp. 178-185, 2017.

OECD. (2008). Long-life surfaces for busy roads. OECD Transport Research Centre, Paris, France, 185 pp.

ONI. Retrieved from Fluorescence Microscopy a Simple Overview. Link at https://oni.bio/fluorescence-microscopy, accessed on April 27, 2021.

Partl, M., Pasquini, E., Canestrari, F., and Virgili, A. (2010). Analysis of Water and Thermal Sensitivity of Open Graded Asphalt Rubber Mixtures. Construction and Building Materials, Vol. 24, No. 3, 283-291.

Park, S.J. and Mansoori, G.A. (1988). Aggregation and Deposition of Heavy Organics in Petroleum Crudes. International Journal of Energy Research, Vol. 10, pp. 109-125.

Peng, W., and Riedl, B. (1995). Thermosetting Resins. Journal of Chemical Education, Vol. 72, pp. 587-592.

Pernia, Y., Metz, J., Gunaratne, M., Nash, T., and Musselman, J. (2016). Application of Image Analysis Techniques to Develop a Quality Control Tool for Automated Optimum Binder

Content Determination of Open-Graded Friction Course Mixtures. Transportation Research Record, No. 2575, 48-60.

Qian, Z., and Lu, Q. (2015). Design and laboratory evaluation of small particle porous epoxy asphalt surface mixture for roadway pavements. Construction and Building Materials, 77, 110-116.

Read, J., and Whiteoak, D. (2003). The Shell Bitumen Handbook, Fifth Edition, Institute of Civil Engineers Publishing, London, United Kingdom.

Roseen, R., Ballestero, T., Houle, J., and Briggs, J. (2012). Water Quality and Hydrologic Performance of a Porous Asphalt Pavement as a Storm-Water Treatment Strategy in a Cold Climate. Journal of Environmental Engineering, Vol. 138, No. 1, 81-89.

Rowe, G.M. (2011). Prepared Discussion for the AAPT paper by Anderson et al.: Evaluation of the Relationship between Asphalt Binder Properties and Non-Load Related Cracking. Journal of the Association of Asphalt Paving Technologists, Vol. 80, pp. 649-662.

Ruan, Y., Davidson, R., and Glover, C. (2003). Oxidation and Viscosity Hardening of Polymer Modified Asphalts. Energy & Fuels, Vol. 17, 2003, pp. 991-998.

Shimeno, S., and Tanaka, T. (2010). Evaluation and Further Development of Porous Asphalt Pavement with 10 Years Experience in Japanese Expressways. Proceedings of the 11th International Conference on Asphalt Pavements, Pp. 43-52, Nagoya, Japan.

Tabatabaee, H., Clopotel, C., Arshadi, A. and Bahia, H. (2013). Critical Problems with Using the Asphalt Ductility Test as a Performance Indicator. Transportation Research Record, Vol. 2370, pp. 84-91.

TAIYU Kensetsu Co., LTD. TAF-EPOXY & TAF-MIX. EP. Link at http://taiyuvn.com/en/epoxy-cho-ban-mat-cau-thep/, accessed on April 1, 2019.

Turner, T.F., and Branthaver, J.F. (1997). DSC Studies of Asphalts and Asphalt Components. Asphalt Science & Technology, Arthur Usmani: Editor, New York, Marcel Dekker.

van de Linda, A. (2019). Epoxy Asphalt – The New Zealand Experience. Washington, D.C.

Waters, J.C., Forrest, J.R., and Alabaster, D. (2018). Bitumen Extended EMA Open Graded Porous Asphalt (EMOGPA) from a Suppliers Perspective. 8th Symposium on Pavement Surface Characteristics: SURF 2018 – Vehicle to Road Connectivity, Brisbane, Queensland, Australia.

Watson, D., Gu, F., and Moore, J. (2018). Evaluation of the Benefits of Open-Graded Friction Course (OGFC) on NDOT Category-3 Roadways. Nevada Department of Transportation Report P 557-13-803, Carson City, Nevada.

Watson, D., Johnson, A., and Jared, D. (1998). Georgia DOT's Progress in Open-Graded Friction Course Development. Transportation Research Record No. 1616, Transportation Research Board, National Research Council, Washington, D.C., pp. 30-33.

Watson, D., Moore, K., Williams, K., and Cooley, A. (2003). Refinement of New-Generation Open-Graded Friction Course Mix Design. Transportation Research Record No. 1832, Transportation Research Board, National Research Council, Washington, D.C., pp. 78-85.

Watson, D., Tran, N., Rodezno, C., Taylor, A., and James, Jr, T. (2018). Performance-Based Mix Design of Porous Friction Courses. NCHRP Project 1-55. Transportation Research Board of the National Academies of Sciences, Engineering, and Medicine, In Press.

Wei, J., and Zhang, Y. (2012). Study on the Curing Process of Epoxy Asphalt. Journal of Testing and Evaluation, Vol. 40, No. 7, pp. 1169-1176.

Wu, J.P., Herrington, P.R., and Alabaster, D. (2017). Long-Term Durability of Epoxy-Modified Open-Graded Porous Asphalt Wearing Course. International Journal of Pavement Engineering, pp. 1-8.

Xin, J., Li, M., Li, R., Wolcott, M.P., and Zhang, J. (2016). Green Epoxy Resin System Based on Lignin and Tung Oil and Its Application in Epoxy Asphalt. ACS Sustainable Chemistry and Engineering, Vol. 4, pp. 2754-2761.

Xu, P., Zhu, X., Cong, P., Du, X., and Zhang, R. (2018). Modification of Alkyl Group Terminated Hyperbranched Polyester on Paving Epoxy Asphalt. Construction and Building Materials, Vol. 165, pp. 295-302.

Youtcheff, J., Elliot, R, and Hammoum, F. (2005). Epoxy Asphalt. Proceedings of the 42nd Petersen Asphalt Research Conference. Laramie, Wyoming.

Youtcheff, J., Gibson, N., Shenoy, A., and Al-Khateeb, G. (2006). Evaluation of Epoxy Asphalt and Epoxy Asphalt Mixtures. Proceedings of the 51st Annual Conference of the Canadian Technical Asphalt Association (CTAA), Polyscience Publications, Laval, Québec, Canada, pp. 351-367.

Zegard, A., Smal, L., Naus, R., Apostolidis, P., Liu, X., Van de Ven, M., Erkens, S., and Scarpas, A. (2019). Field Trials with Epoxy Asphalt for Surfacing Layers - Province of North Holland Case Study. Poster Session during the 99th Transportation Research Board (TRB) Annual Meeting, Transportation Research Board, Washington, D.C.

Zhou, F., Im, S., Sun, L., and Scullion, T. (2017). Development of an IDEAL Cracking Test for Asphalt Mix Design and QC/QA. Road Materials and Pavement Design, 18(sup4), 405-427.